



# **Synthesis of Uniquely Functionalised Tetrabenzotriazaporphyrins**

**Faeza Hamad Alkorbi**

This thesis is submitted in partial fulfilment of the requirements of the degree of  
Doctor of Philosophy at the University of East Anglia

**March 2020**

©This copy of the thesis has been supplied on condition that anyone who consults it, is understood to recognise that its copyright rests with the author and that no quotation from the thesis, nor any information derived therefrom, may be published without the author's prior written consent.

## **PREFACE**

The research described within this thesis is, to the best of my knowledge, original and my own work, except where due reference has been made.

**Faeza Alkorbi**

**2020**

## Abstract

Tetrabenzotriazaporphyrins (TBTAPs) are hybrid structures that lie between the omnipresent phthalocyanines and tetrabenzoporphyrins. These classes of materials are famous for their remarkable electronic and physical properties which result from the extensive delocalization of the  $\pi$ -electrons in their inner core. TBTAPs were found to share similar properties with these macrocyclic materials, however, the difficulties in their synthesis and purification made the interest in them rare and scarce unlike Pc and TBP. A brief review of the number of synthetic methods reported for their synthesis is described in Chapter 1, in addition to a summary of their distinctive properties and applications.

The synthesis of substituted derivatives is often driven by the desire to exploit and improve their performance. The research group at UEA has reported a straightforward, high-yielding synthesis of *meso*-aryl tetrabenzotriazaporphyrins, thus extending the access to these hybrids. Developing this synthetic procedure, from phthalonitrile and aminoisoindoline, the work in this thesis entails the synthesis of a range of novel and unique peripheral substituted MgTBTAPs bearing aryl substituent at their *meso*-position. The synthesis of the new compounds, which is described in Chapter 2, is based on employing aminoisoindoline and phthalonitrile derivatives to functionalize the benzo-units on the macrocycle and explanation of the conjugated system has been also described. In order to prepare these complexes, we have prepared a new series of substituted bromobenzamidine, aminoisoindoline and aza-dipyrromethene derivatives. Within this study a new synthesis has been uncovered whereby, for the first time, *meso*-aryl ABBA substituted TBTAPs are conveniently prepared.

## **Access Condition and Agreement**

Each deposit in UEA Digital Repository is protected by copyright and other intellectual property rights, and duplication or sale of all or part of any of the Data Collections is not permitted, except that material may be duplicated by you for your research use or for educational purposes in electronic or print form. You must obtain permission from the copyright holder, usually the author, for any other use. Exceptions only apply where a deposit may be explicitly provided under a stated licence, such as a Creative Commons licence or Open Government licence.

Electronic or print copies may not be offered, whether for sale or otherwise to anyone, unless explicitly stated under a Creative Commons or Open Government license. Unauthorised reproduction, editing or reformatting for resale purposes is explicitly prohibited (except where approved by the copyright holder themselves) and UEA reserves the right to take immediate 'take down' action on behalf of the copyright and/or rights holder if this Access condition of the UEA Digital Repository is breached. Any material in this database has been supplied on the understanding that it is copyright material and that no quotation from the material may be published without proper acknowledgement.



This thesis is dedicated to my precious son *Khalid*

Autism was a journey we hadn't planned, but it was made for us to share together and we walk it all hand in hand.

Autism is not a word to fear, it is a child to be loved.

## Acknowledgment

I firstly wish to acknowledge the guidance and support provided by my primary supervisor, Professor Andrew Cammidge, I appreciate everything he has done in the course of the supervision of this thesis. He provided a safe space for me to explore the new world of being a doctoral candidate, provided insightful feedback and he was a great support throughout. I thank him for his kindness and for the incredible encouragement and support. I would also like to express my gratitude to my second supervisor Dr Chris Richards and to Dr. Maria Paz Muñoz-Herranz and her group members for their cooperation and giving access to their equipment. I also thank Dr. David Hughes for X-Ray crystallography service. I would also thank the examiners Prof. Graeme Cooke (University of Glasgow) and Dr. Isabelle Fernandes (UEA) for their time.

I would also like to thank Saudi Culture Bureau and Najran University who provided full funding for this work.

A special and massive thank to my husband, Sulaiman, and my lovely children, Manal, Khalid, and Fahad for all their love, patience and encouragement. I am also forever grateful for my mother and father for all their sacrifices for us. Thanks are due to my brothers and sisters who are so supportive in whatever I do in my life.

I am forever thankful for former and present members of Cammidge's group for their support, and for creating a friendly working environment. I would especially like to thank Dr. Tahani Almutairi, Dr. Rhoda Beskine, and my best friends Ahad Alsahli and Norah Alsaiani. Lastly, I offer my regards to all of those who supported me in any respect during the completion of the project.

## Abbreviations

°C	Celsius
AcOH	acetic acid
aq	aqueous
Ar	aryl
Atm	atmosphere
b.p	boiling Point
BINAP	2,2'-bis(diphenylphosphino)-1,1'-binaphthyl
Bn	benzyl
Bu	butyl
Conc.	concentrated
d	doublet
DABCO	1,4-diazabicyclo [2.2.2] octane
DBU	1.8-diazabicyclo [5.4.0] undec-7-ene
DCM	dichloromethane
dd	doublet of dublets
DMF	N, N-dimethylformamide
DMSO	dimethylsulphoxide
eq.	equivalent
h	hour
HOMO	highest occupied molecular orbital
IR	Infrared
<i>J</i>	Coupling constant
LC	Liquid Crystal
LHMDS	Lithium hexamethyldisilazide
LUMO	lowest unoccupied molecule orbital
m	multiplet
m.p.	melting point
<i>m/z</i>	mass to charge ratio
MALDI-TOF	matrix-assisted laser desorption/ionisation-time-of-flight
max	maximum

Me	methyl
mmol	millimole
mol	mole
MS	mass spectrometry
MW	microwave
NMR	nuclear magnetic resonance
<i>np</i>	non- peripheral
OMe	methoxy
OPh	phenoxy
OTf	triflate, trifluoromethanesulfonate
<i>p</i>	Peripheral or para
PE	petroleum ether
Ph	phenyl
ppm	parts per million
R <sub>f</sub>	retention factor
rt	room temperature
s	singlet
t	triplet
<i>t</i> -Bu	tertiary butyl
THF	tetrahydrofuran
TLC	thin layer chromatography
UV/Vis	Ultraviolet/Visible spectroscopy
X	halid or hetero atom
δ	chemical shift in parts per million (ppm)
ε	molar extinction coefficient
λ	wavelength

# Table of Contents

<b>CHAPTER 1: INTRODUCTION AND LITERATURE REVIEW .....</b>	<b>1</b>
1.1 General introduction.....	2
1.2 Tetrabenzotriazaporphyrin (TBTAP).....	4
1.3 Nomenclature of Tetrabenzotriazaporphyrins (TBTAPs).....	4
1.4 Synthesis of Tetrabenzotriazaporphyrins .....	5
1.5 Properties of Tetrabenzotriazaporphyrins .....	35
1.5.1 Molecular properties .....	35
1.5.1.1 Electronic properties and UV-Vis spectroscopy .....	35
1.5.1.2 Magnetic circular dichroism (MCD).....	37
1.5.2 Solid State Properties.....	38
1.5.2.1 X-ray structure analyses.....	38
1.5.2.2 Mesophase behaviour (Liquid crystal properties).....	39
1.5.2.3 Electrical Properties and Thin film formation .....	41
1.6 Application of Tetrabenzotriazaporphyrins .....	43
1.7 Aim of the Project .....	44
<b>CHAPTER 2: RESULTS AND DISCUSSION .....</b>	<b>46</b>
2.1 Introduction .....	47
2.2 Synthesis of <i>meso</i> -substituted TBTAP <b>69a</b> .....	48
2.3 Synthesis of the first series of TBTAP hybrids.....	51
2.3.1 3,6-Di-substituted phthalonitrile derivatives.....	51
2.3.2 4,5-Disubstituted phthalonitrile derivatives.....	52
2.3.2.1 Synthesis of 4,5-di-substituted phthalonitrile .....	52
2.3.2.2 Synthesis of phthalonitrile <b>115</b> and its TBTAP complex <b>121</b> .....	57
2.3.2.3 Synthesis of phthalonitrile <b>116</b> and its TBTAP complex <b>127</b> .....	60

2.3.2.4 Synthesis of phthalonitrile <b>117</b> and its TBTAP complex <b>132</b> .....	63
2.3.2.5 Synthesis of 4,5-diphenyloxyphthalonitrile <b>118</b> and TBTAP <b>135</b> .....	67
2.3.2.6 Synthesis of phthalonitrile <b>119</b> and its TBTAP hybrids <b>142, 143</b> .....	69
2.3.3 Synthesis of naphtho-annulated TBTAP <b>147</b> .....	74
2.3.4 Synthesis of TBTAP from 4-t-Butylphthalonitrile <b>35</b> .....	78
2.4 Synthesis of the second series of TBTAP hybrids.....	80
2.4.1 General synthesis of the aminoisoindoline precursors.....	80
2.4.2 Synthesis of the TBTAP hybrid from aminoisoindoline <b>157</b> .....	85
2.4.3 Synthesis of TBTAP Hybrids <b>166</b> and <b>167</b> .....	89
2.4.4 Synthesis TBTAP Hybrids <b>173</b> and <b>172</b> .....	92
2.5 Electronic absorption spectra of newly synthesised Tetrabenzotriaza porphyrin complexes.....	96
2.6 Synthesis of aminoisoindoline dimers [Aza-(dibenzo)dipyrromethenes].....	99
2.7 Proposed mechanism of Tetrabenzotriazaporphyrin formation.....	106
2.8 Conclusion .....	108
2.9 Future Work .....	108
<b>CHAPTER 3: EXPERIMENTAL .....</b>	<b>109</b>
3.1 General Methods .....	110
3.2 MgTBTAP-(4-OMe-Ph) <b>69a</b> .....	112
3.3 Synthesis of the first series of <i>meso</i> -Ar-TBTAP hybrids .....	114
3.3.1 p-(OC <sub>6</sub> H <sub>13</sub> ) <sub>4</sub> -MgTBTAP-(4-MeO-Ph) <b>127</b> .....	118
3.3.2 p-(OC <sub>10</sub> H <sub>21</sub> ) <sub>4</sub> -MgTBTAP-(4-MeO-Ph) <b>132</b> .....	122
3.3.3 p-(OPh) <sub>4</sub> -MgTBTAP-(4-MeO-Ph) <b>135</b> .....	123
3.3.4 (Tetramethyl-tetralino) <sub>2</sub> -MgTBTAP-(4-OMe-Ph) <b>143</b> .....	128
3.3.5 (Tetramethyl-tetralino) <sub>3</sub> -MgTBTAP-(4-OMe-Ph) <b>142</b> .....	130
3.3.6 (Naphthalo) <sub>2</sub> -MgTBTAP-(4-OMe-Ph) <b>147</b> .....	131

3.4 Synthesis of the second series of <i>meso</i> -Ar-TBTAP hybrids.....	132
3.4.1 p-(OMe) <sub>4</sub> -MgTBTAP-(4-MeO-Ph) <b>161</b> .....	134
3.4.2 p-(OC <sub>6</sub> H <sub>13</sub> ) <sub>4</sub> -MgTBTAP-(4-MeO-Ph) <b>166</b> .....	137
3.4.3 p-(OC <sub>10</sub> H <sub>21</sub> ) <sub>4</sub> -MgTBTAP-(4-MeO-Ph) <b>167</b> .....	139
3.4.4 (Tetramethyl-tetralino) <sub>2</sub> -MgTBTAP-(4-OMe-Ph) <b>173</b> .....	142
3.4.5 (Tetramethyl-tetralino)-MgTBTAP-(4-OMe-Ph) <b>172</b> .....	144
3.5 Aza-dipyrromethene series (self-condensation dimers).....	145
<b>3.6 Bibliography .....</b>	<b>150</b>
<b>3.7 Appendix .....</b>	<b>161</b>

# **Chapter 1: Introduction and Literature review**

## 1.1 General introduction

Porphyrin (Pn) (**1**) has a macrocyclic structure; it consists of four pyrrole rings (five-membered closed structures containing one nitrogen and four carbon atoms) linked to each other by methine groups. Porphyrins are most well known for their essential roles within a number of biological processes. Some of the best-known examples are the iron-containing porphyrins found as heme (of haemoglobin) and the magnesium-containing reduced porphyrin found in chlorophyll<sup>1</sup>.

In porphyrins, when each of the pyrrole units is fused to a benzenoid ring it can form other macrocycles. One such group of macrocycles are Tetrabenzoporphyrins (TBP) (**2**). The four methine groups in the TBP structure can be replaced by four imine groups to form other system which is phthalocyanine (Pc) (**3**). In other words, phthalocyanine contains a ring system of four isoindole units linked by nitrogen atoms known as *aza*-bridges. It can also be named tetrabenzotetraazaporphyrin, (figure 1.1)<sup>2</sup>.

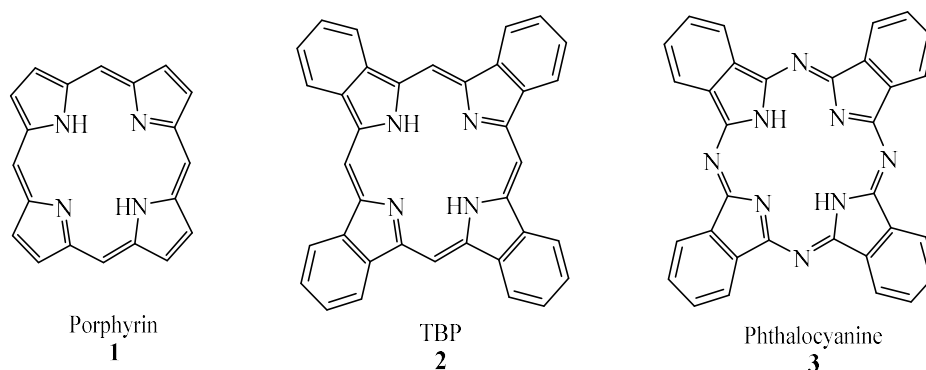


**Figure 1.1: Structures of porphyrin, Tetrabenzoporphyrins (TBP) and Phthalocyanine (Pc)**

Porphyrins and phthalocyanines have been studied for a long period of time and their properties and chemistry are well known. They are present in everyday life and their biological activities are one of the reasons for the great interest. They hold some advantages in comparison to other types of electro- and photoactive compounds which arise from their 18  $\pi$ -electron aromatic structure. These advantages are their high molar absorption coefficients and fast energy and/or electron transfer donor abilities to electron acceptor counterparts. Thus, porphyrins and phthalocyanines are widely used as molecular components in artificial photosynthetic systems, both for energy-

transfer and electron-transfer processes. Finally, porphyrins and phthalocyanines display complementary optical transitions<sup>3,4,5</sup>.

Phthalocyanines can be functionalized by two main methods, one is based on the introduction of substituents into the benzene rings, resulting in a substantial increase in the solubility of new compounds. Another suitable method for phthalocyanine modifications is to replace bridging nitrogen atoms by one or several methine moieties. This approach was employed to prepare structures **4-7**, which are tetrabenzotriaza porphyrin [ $H_2TBTAP$ , **4**], *cis*- and *trans*-tetrabenzodiazaporphyrins [ $H_2TBDAP$ , **5** and **6**, respectively] and tetrabenzomonoaza porphyrin [ $H_2TBMAP$ , **7**]<sup>2,6</sup>, (figure 1.2).

These set of hybrid macrocycles are structurally related to both phthalocyanine **3** and tetrabenzoporphyrin TBP **2**. They are rarely studied compared to the corresponding phthalocyanines and tetrabenzoporphyrins<sup>6</sup>. However, herein, a review of one of these macrocycles, tetrabenzotriazaporphyrin TBTAP **4**, is presented.

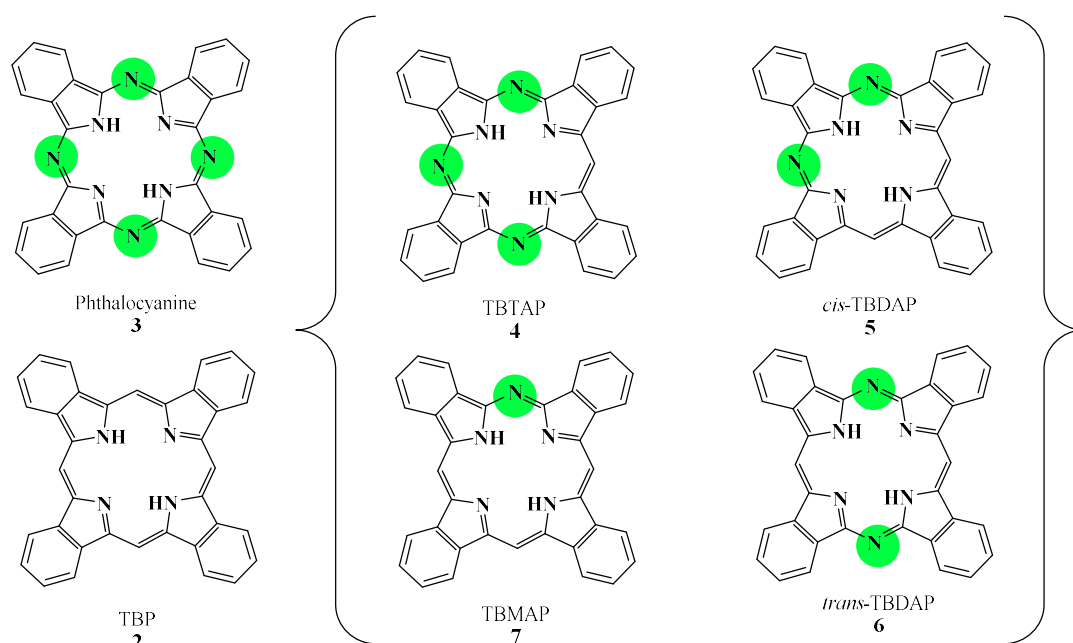


Figure 1.2: Molecular structures of Pc/TBP hybrid macrocycles

## 1.2 Tetrabenzotriazaporphyrin (TBTAP)

Tetrabenzotriazaporphyrins TBTAPs **4** are hybrid compounds related to the phthalocyanine **3** and tetrabenzoporphyrin **2** macrocycles. They differ only by the substitution of one *aza*-nitrogen of the Pc ring by a methine group. Data on tetrabenzotriazaporphyrin derivatives are scarce in the literature, and reviews focused on such macrocycles are absent. This is due both to a limited number of synthetic methods and difficulties of their isolation from a mixture of products. Indeed, the synthesis of these compounds can afford up to five structurally similar macrocycles which will be discussed later in this chapter.

## 1.3 Nomenclature of Tetrabenzotriazaporphyrins (TBTAPs)

Historically, there are two nomenclatures used to name tetrabenzotriazaporphyrin macrocyclic compounds, which are considered as either phthalocyanine or tetrabenzoporphyrin derivatives. However, the atomic numbering scheme of the phthalocyanine type is more commonly used. Therefore, the substituents on the benzenoid rings of the tetrabenzotriazaporphyrin system were numbered similarly to those of the phthalocyanine system, whereas the locations of the imino nitrogen atoms were termed based on those of fused tetrapyrroles. Letters are used for every side around the periphery of the porphyrin inner ring, the first letter of the alphabet was given to the side where the fusion happens. In other words, the lettering was beginning with "a" for the side (1,2), "b" for (2,3) and so forth. Thus letters *b*, *g*, *l* and *q* refer to the positions of the fused benzene rings on the pyrrole in the porphyrin ring<sup>7</sup>. The phthalocyanines and tetrabenzotriazaporphyrin hybrids both possess sixteen possible sites of substituents on the macrocycle. Substituents which are accommodated on the benzene rings at 2, 3, 9, 10, 16, 17, 23, 24 positions, are termed as the *peripheral* (*p*) sites, whereas those at positions 1, 4, 8, 11, 15, 18, 22, 25, are called the *non-peripheral* (*np*) sites. The structures and numbering of the atoms is illustrated in figure 1.3.

Much of the research undertaken on the hybrid compounds focused on the unsubstituted compounds as metal-free and as metalated derivatives. For clarity these will simply be referred to using the central ion or element before the abbreviations of the compound, e.g. H<sub>2</sub>TBTAP, *trans*-CuTBDAP. This style is extended for

compounds bearing substituents on the benzenoid rings which are included as a prefix in the compound abbreviation. For instance,  $(t\text{-Bu})_4\text{-ZnTBMAP}$  refers to a zinc metalated compound with a  $t\text{-Bu}$  group on each benzenoid ring, it does not indicate their locations. The compounds bearing eight substituents, two per benzenoid ring, located exclusively at the peripheral positions or at the non-peripheral sites are described by use of the letters  $p$  (peripheral) or  $np$  (non-peripheral), e.g.  $(np\text{-hexyl})_8\text{-ZnTBMAP}$ . On the other hand, compounds carrying substituents at the *meso*-positions the group identifier is at the end of the abbreviation e.g., a compound with two *meso*-phenyl groups on a metal-free TBDAP becomes  $\text{H}_2\text{TBDAP}(\text{Ph})_2$ <sup>8</sup>.

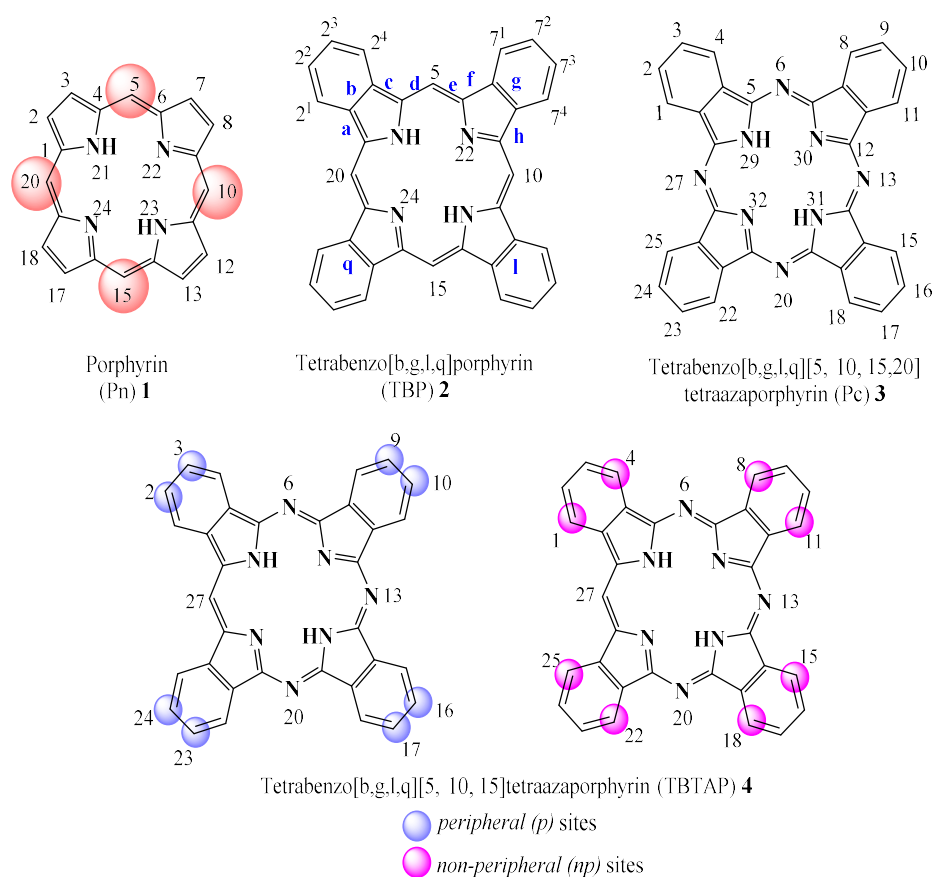


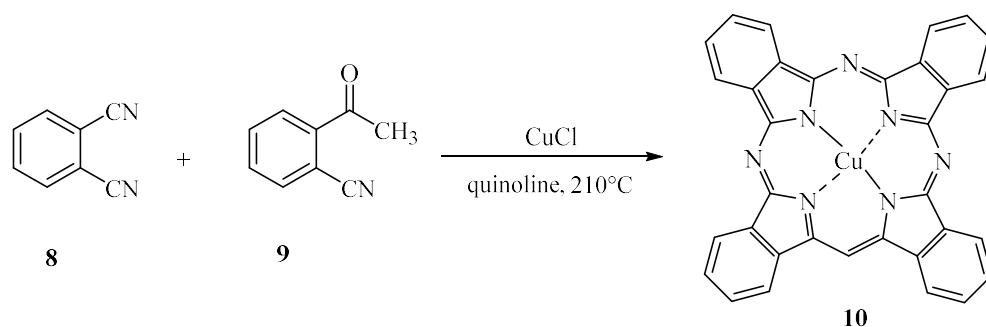
**Figure 1.3: Structures and numbering of the atoms for Tetrabenzotriazaporphyrins**

#### 1.4 Synthesis of Tetrabenzotriazaporphyrins

The discovery of tetrabenzotriazaporphyrin hybrid structures was by accident in 1934. Lowe and Linstead were studying the possibility of synthesis of  $N$ -alkyl

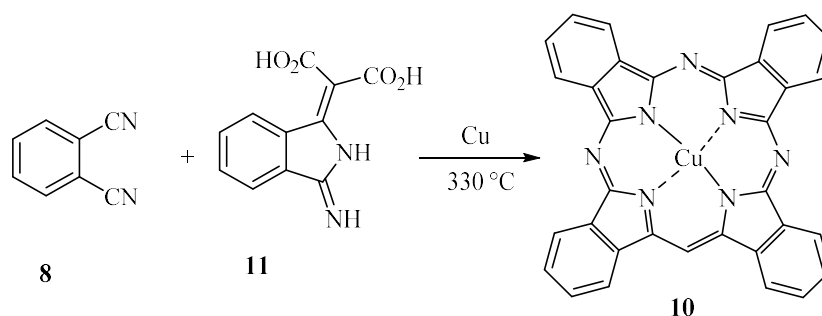
phthalocyanines from the reaction between methylmagnesium iodide and phthalonitrile. In their early experiments, the resulting materials consisted of a phthalocyanine and a poor yield of a green crystalline side-product. The use of benzyl magnesium chloride was also investigated, however, only the magnesium phthalocyanine material was recovered. As a result of the low yield of the unknown green product which was obtained from the MeMgI experiment, this reaction was not investigated further<sup>9,10</sup>. In 1936, Fischer *et al.* reported the synthesis of certain macrocyclic pigments containing four pyrrole rings joined together by both methine and aza links<sup>11,12</sup>. It was the first macrocyclic molecule that structurally related to phthalocyanines.

Soon afterwards, in 1937 Helberger<sup>13</sup> announced the description of copper derivatives of similar compounds containing a benzene ring fused to each of the four pyrrole rings. He was able to prepare the copper derivatives of TBMAP and TBDAP in 10 and 20% yields, respectively. CuTBMAP was obtained by heating an *o*-halogenoacetophenone with cuprous cyanide, whereas the CuTBDAP was prepared by reacting phthalonitrile with cuprous cyanide and in this case, the *o*-cyanoacetophenone was proposed as a key intermediate. In later studies carried out by Helberger and von Rebay, they declared similar results using this preformed intermediate, and published the first synthesis of tetrabenzotriazaporphyrin in 1937<sup>14</sup>. They performed the reaction of phthalonitrile (1,2-dicyanobenzene) **8** with *o*-cyanoacetophenone **9** in an equimolar ratio in the presence of copper(I)chloride (scheme 1.1). After the addition of pyridine to the reaction mixture, product **10** precipitated as violet crystals. A decrease in the amount of phthalonitrile with respect to *o*-cyanoacetophenone (the 1.0 :1.8 ratio) resulted in the isolation of the Cu complex of tetrabenzodiazaporphyrin (Cu-TBDAP). It was found that, in the absence of phthalonitrile, the reaction produces the Cu complex of tetrabenzomonoazaporphyrin (Cu-TBMAP).



**Scheme 1.1: The first synthesis of CuTBTAP by Helberger and von Rebay**

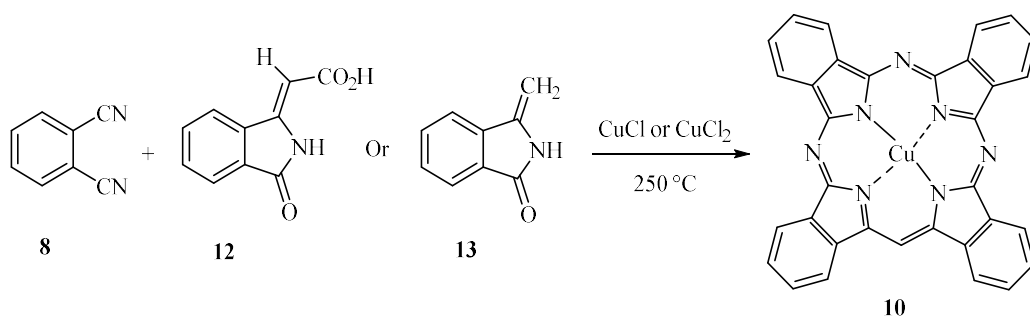
Similarly, Linstead *et al*<sup>15</sup>. carried out this reaction with the use of phthalonitrile **8** and o-cyanoacetophenone **9** in a ratio of 1.0: 1.77. They reported that a mixture of products obtained contains, in addition to (Cu-TBDAP), copper tetrabenzotriaza porphyrin (Cu-TBTAP) **10**. In Addition, they reported that the preparation of these pigments could also be achieved using malonate derivative, such as compound **11**, which is considered as another useful precursor in this synthesis (scheme 1.2).



**Scheme 1.2: Lindsted's synthesis of CuTBTAP using 11 as a precursor**

The combined use of synthetic methods used for the synthesis of phthalocyanines and porphyrins to produce the hybrid derivatives was investigated by Dent and various precursors and combinations were examined. In 1938, a method for the synthesis of (Cu-TBTAP) **10** was covered with a patent<sup>16</sup>. Phthalimidine acetic acid **12** or 3-methylene phthalimidine **13** (the latter can be easily prepared by heating acid **12** in water at 80 °C) served as a source of the methine bridge. The reaction was performed by condensation of an equimolar amount of phthalonitrile **8** and either **13** or its carboxylic derivative **12** at 250 °C, in the presence of a copper salt or by heating under reflux in 1-chloronaphthalene. Dent reported preparation of complex **10** in 30% yield (scheme 1.3). Dent was unable to prepare the other hybrid molecules with more than

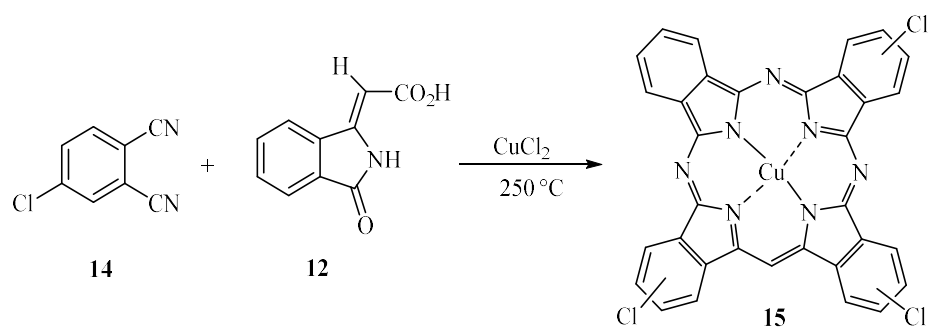
one methine group (e.g. CuTBDAPs or CuTBMAP) under the same reaction conditions.



**Scheme 1.3: Dent's synthesis of CuTBTAP using phthalimidine derivatives**

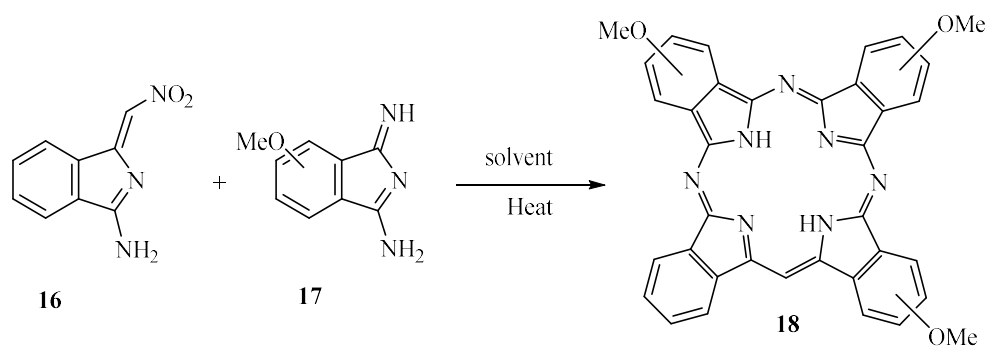
Moreover, the reaction stoichiometry was also examined; for example using 3 moles of phthalonitrile with 1 mole of phthalimidine acetic acid and 1 mole of cuprous chloride gave a reasonably good yield (70-80%) of the (CuTBTAP) **10** with a small impurity of copper phthalocyanine, whereas no green pigment was obtained when using a 1:3 ratio of phthalonitrile to phthalimidine acetic acid. Moreover, the formation of the (Cu-TBTAP) was not observed when the methyl-phthalimidine acetate or the corresponding copper salt was used instead of phthalimidine acetic acid **12** by itself.

It was shown that a similar reaction readily proceeds with the use of 4-chlorophthalonitrile **14** as precursor. The condensing of **14** with phthalimidine acetic acid **12** in the presence of cuprous chloride under the same previous conditions formed a Cl<sub>3</sub>-CuTBTAP **15**, which contains three phthalonitrile units and one methylene phthalimidine unit, (scheme 1.4). In addition to copper complexes, the synthesis of magnesium, tin and lead tetrabenzotriazaporphyrins was patented<sup>16</sup>.



**Scheme 1.4: Synthesis of Cl<sub>3</sub>-CuTBTAP from 4-chlorophthalonitrile**

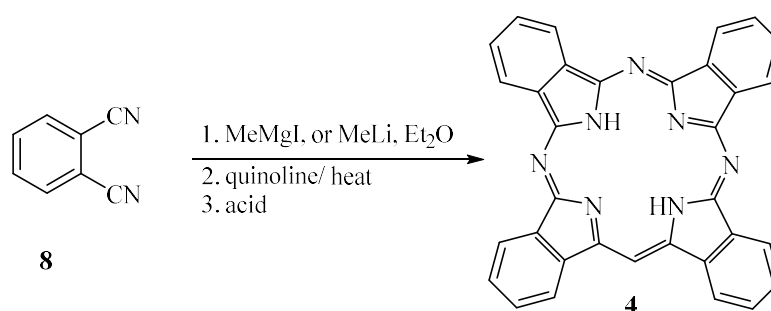
More recently, similar mixed condensation reaction using 1-amino-3-nitromethylideneisoindole **16** was suggested for the synthesis of tetrabenzotriaza porphyrin derivatives<sup>17,18</sup>. The compound **16** was prepared by the reaction of 1,3-diiminoisoindoline and nitro-methane in methanol on heating. A condensation reaction was performed between reactants **16** and **17** in preheated high-boiling solvents (xylene, nitrobenzene, o-dichlorobenzene, 1-methyl- or 1-chloro naphthalene). In addition, this reaction was carried out with unsubstituted isoindoline and the benzannulated derivative<sup>18</sup>. It should be noted that macrocycle **18** and its analogues are almost insoluble in organic solvents and, consequently, the purification by chromatography was not applicable, (scheme 1.5).



**Scheme 1.5: Mixed condensation reaction for synthesis of (OMe)<sub>3</sub>-H<sub>2</sub>TBTAP**

Linstead and co-workers<sup>10</sup> re-examined the reaction between phthalonitrile and organometallic reagents in the hope of obtaining and fully characterising the previously formed green side-product. This method is based primarily on using methylmagnesium iodide or MeLi, as the organometallic source. The synthesis of the unknown green product was found to be complicated but after a series of trial experiments a good synthetic procedure was developed. The reaction was carefully monitored and the isolation of intermediates aided an understanding of the mechanistic pathway. It is still not well defined but a general route has been put forward and has not been investigated or challenged further. The synthetic pathway was found to consist of two main steps, an initial reaction that occurs between phthalonitrile and either methyl lithium or methylmagnesium iodide in a low-boiling ethereal solvent generally at room temperature and then a full cyclisation taking place at a higher temperature using a high-boiling solvent. It was observed at this step, that quenching

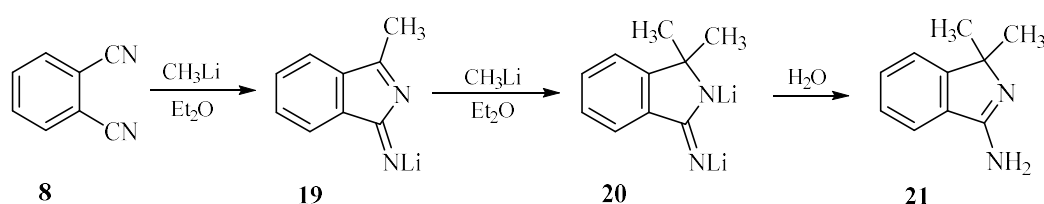
the reaction by acid in the ethereal solvent stage, a minimal amount of product was recovered due to decomposition. However, ethereal solvent was distilled off and further heating was applied to the solid residue after addition of a high boiling point solvent such as quinoline, cyclohexanol or  $\alpha$ -naphthyl methyl ether. This was followed by an acid work-up, and a green pigment was obtained in a pure crystalline form in a 40% yield. The crystalline material was analysed using X-ray diffraction and several quantitative oxidations, which identified it as metal-free tetrabenzotriazaporphyrin **4**, (scheme 1.6).



**Scheme 1.6: General synthetic route for metal-free TBTAP**

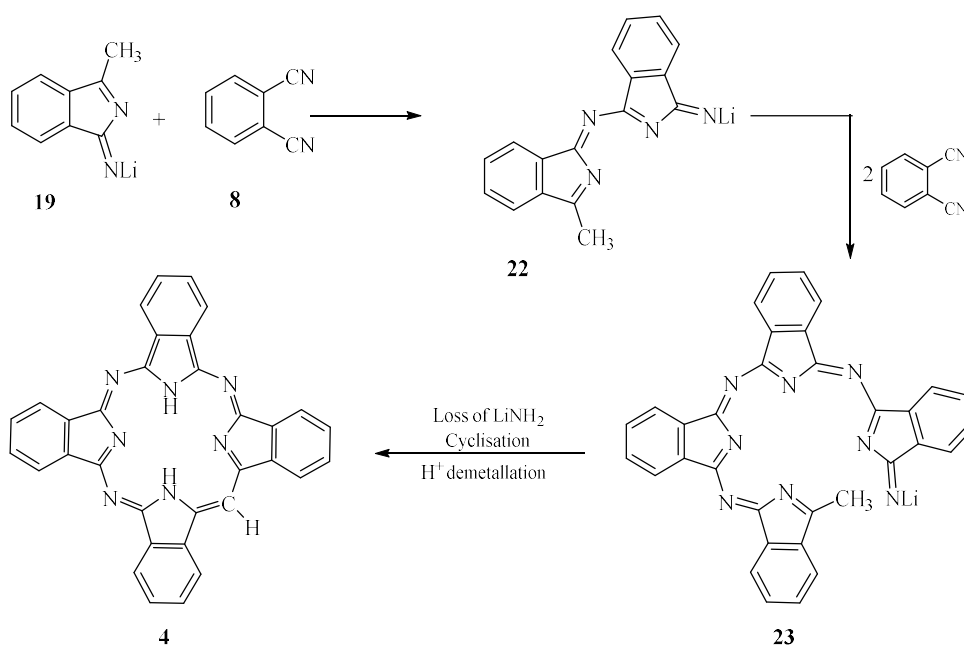
Linstead achieved a similar outcome by following the two-step procedure outlined above with a 15% yield of the tetrabenzotriazaporphyrin derivative. Nevertheless, other side products were also isolated which were thought to be other more carbon-rich analogues (tetrabenzodiazaporphyrin) together with a higher amount of Pc material. As mentioned above, the metal-free tetrabenzotriazaporphyrin was obtained when the magnesium was removed from the central cavity of TBTAP by means of an acid in the final step. Therefore, other elemental ions, such as lithium, nickel, copper, iron, or zinc can be accommodated. It should be noted that the metal complexes of TBTAP unsubstituted at the *meso*-carbon atom are poorly soluble in organic solvents. These compounds are purified mainly by recrystallization from 1-chloronaphthalene or quinoline. However, it was found that Mg and Cd complexes of tetrabenzotriazaporphyrins are fairly readily soluble in mixtures containing THF. This allowed the researchers to separate mixtures of reaction products by aluminium oxide column chromatography using a mixture of THF and trichloroethylene as the most efficient eluent. This method was employed to isolate Mg and Cd complexes of tetrabenzotriazaporphyrins in the pure form<sup>19</sup>.

An attempt was made to perform this reaction with methyllithium instead of methylmagnesium iodide. However, this reaction afforded a small amount of a mixture of products containing mainly diaza- and monoaza- macrocycles. This was explained as follows; phthalonitrile initially binds one methyllithium molecule to form lithium derivative **19**, and the latter rapidly reacts with the second MeLi molecule. The hydrolysis of dilithium derivative **20** gives a free base, 1-amino-3,3-dimethylisindole **21**, which cannot be involved in the formation of the macrocyclic system of tetrabenzotriazaporphyrin, (scheme 1.7).



**Scheme 1.7: Isolated intermediates in the mechanistic study of TBTAP formation**

The previous detailed study was carried out using an excess amount of methyllithium (2 equivalents), a series of experiments were performed using 1, 1.5 and 2 moles of the Grignard reagent in cold ether. It was observed from these trials, that the tetrabenzotriazaporphyrin was prepared from equimolecular quantities of phthalonitrile and methyllithium. At the end of the first reaction, an excess of the nitrile remained, that is thought to be responsible for the aza connections in the TBTAP material. However, intermediates **19** and **20** could be responsible for the introduction of the methine group at the *meso*-position. In the reaction mixture, phthalonitrile molecule reacts with intermediate **19** and it could give a dimeric compound **22**. The latter would eventually polymerise after further addition of two phthalonitrile molecules and gives a tetrameric complex **23**. The closure of the ring, which involves the elimination of either lithium amide or methylamine (depending on the organometallic source), would only then occur in the reaction when the high boiling point solvent is applied, (scheme 1.8). This reaction resembles a diene polymerisation as reported by Ziegler<sup>20</sup>. A complete understanding of this reaction mechanism for the hybrid macrocycle formation remains unclear due to the lack of adequate studies covering this area since investigations by Linstead and Barrett's<sup>10</sup>.

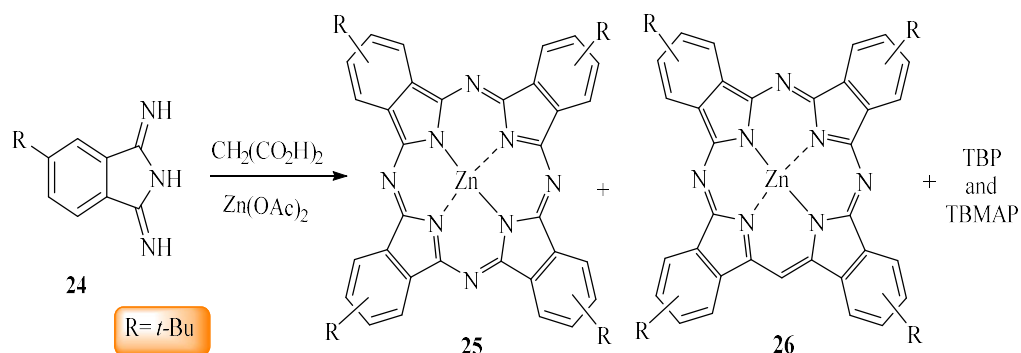


**Scheme 1.8: General proposed mechanism of TBTAP formation**

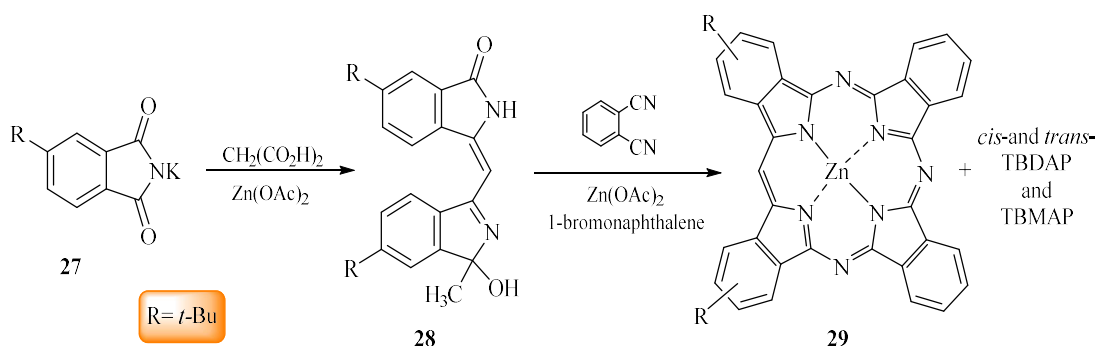
Other lithium reagents such as *n*-butyllithium were used to introduce a propyl group at the *meso*-position by Linstead. Unfortunately, this resulted in the recovery of mostly phthalocyanine product and pure TBTAP could not be isolated, which concurred with the earlier results obtained from the use of other bulky Grignard reagents. In other words, the tendency to obtain TBTAP and related macrocycles is greatest when methyl organometallic derivatives are used. Nevertheless, it is now known that it is indeed possible to use bulky Grignard reagents to yield TBTAPs and other analogues, but this was not examined until much later<sup>20</sup>. A demonstration introduced by Gilman *et al* explained the reactivities of organolithium and organomagnesium compounds toward certain aromatic nitriles. It was found that certain aromatic nitriles are more readily attacked by methyllithium than by methylmagnesium iodide<sup>21</sup>.

The low-yield of the reaction together with the poor solubility of these hybrid materials made it even more difficult to investigate further the properties and mechanism of formation. Therefore, Kopranenkov and co-workers<sup>22</sup> have investigated the preparation of these materials with much focus on the synthesis of substituted macrocycles to improve their solubility in a wide range of organic solvents. They described the synthesis of the Zn complex of (*t*-Bu)<sub>4</sub>-TBTAP **26** as an inseparable mixture with *t*-butyl-substituted analogues of zinc tetrabenzoporphyrin and

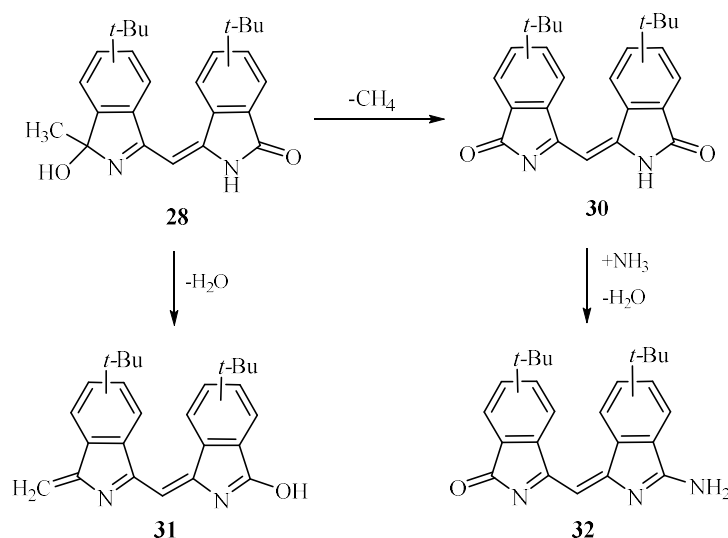
phthalocyanine **25**. The authors performed the mixed condensation of *t*-butyl-substituted isoindoline **24** with malonic acid in the presence of zinc acetate at 360 °C under an inert atmosphere, (scheme 1.9).



In similar manner, Zinc complex of (*t*-Bu)<sub>2</sub>-TBTAP **29** was synthesized starting from potassium 4-*t*-butylphthalimide **27** and malonic acid. It was isolated from a mixture of products by chromatography on aluminium oxide, (scheme 1.10). It also reported that the corresponding free ligand was produced in an insignificant amount<sup>23</sup>.



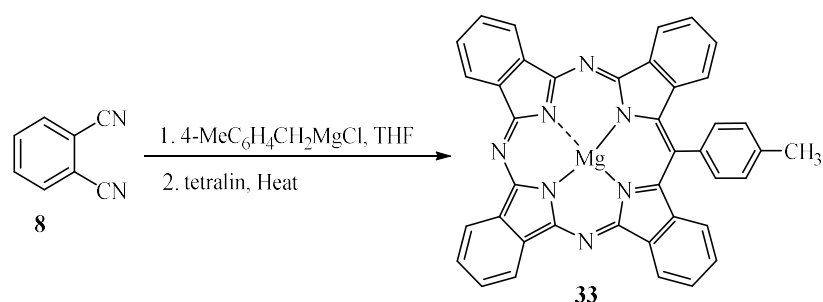
Compound **28** bears a resemblance to the intermediates isolated during Linstead and Barrett's mechanistic study and supports their proposed pathway<sup>10</sup>. An explanation is also given for the formation of the (*t*-Bu)<sub>2</sub>-tetrabenzotriazaporphyrin **29** and other aza-derivatives with the fragments of the dimer recombining with other dimeric species present as described in the scheme below<sup>23</sup>.



**Scheme 1.11: Dimeric species which explain formation of aza-derivatives**

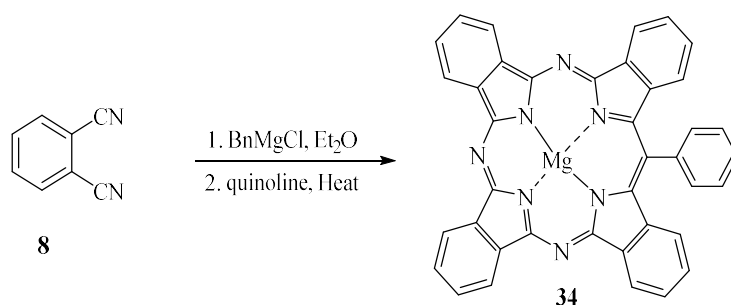
For several decades, these synthetic strategies have been used subsequently for the production of the tetrabenz(aza)porphyrins with very little variation. For example, Hoffman and co-workers<sup>24</sup> reported the synthesis of NiTBTAP and CuTBTAP by means of Linstead's strategies. Magnesium and cadmium derivatives were also generated from a mixture of phthalimidine acetic acid with either phthalonitrile or *o*-dicyanobenzamide. More recently, Antunes and Nyokong have prepared the metal-free tetrabenzotriazaporphyrin by this approach and converted it into the dihydroxy phosphorus derivative<sup>25</sup>.

Further investigations into the synthesis of tetrabenz(aza)porphyrins re-emerged, and a number of mixed cyclisation reactions using substituted precursors were reported to give a variety of substituted hybrid derivatives<sup>22,23</sup>. However, attempts to incorporate the substituent in the *meso*-position proved unsuccessful for various research groups which led to a low interest in investigating these hybrids at that time. Linstead and Barrett reported that the reaction of phthalonitrile with benzylmagnesium chloride instead of methylmagnesium iodide produces only unsubstituted phthalocyanine<sup>10</sup>. However, their procedure was modified later and resulted in producing the magnesium complex **33** of *meso*-(*p*-tolyl) TBTAP derivative, which was covered with a patent. The demetallation of **33** with concentrated HCl in dimethylformamide affords the TBTAP free ligand<sup>26,27</sup>, (scheme 1.12).



**Scheme 1.12: Synthesis of the MgTBTAP-(p-tolyl)**

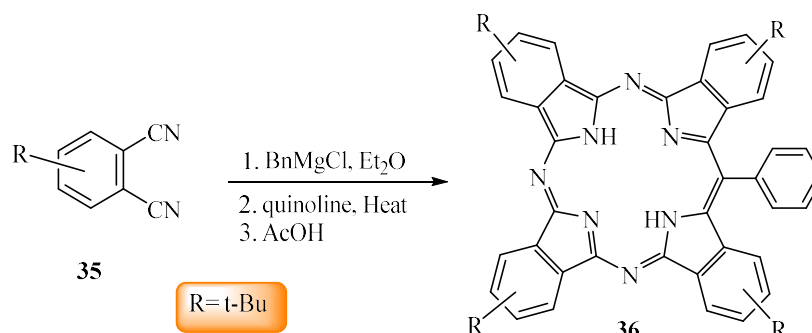
Leznoff and McKeown reinvestigated and described the preparation of a variety of *meso*-substituted TBTAPs from sterically hindered phthalonitriles with different Grignard reagents. The resulting materials consisted of a mixture of TBTAP, phthalocyanine and sometimes traces of TBDAP (*cis*- and *trans*- isomers). The reaction of phthalonitrile with benzylmagnesium chloride was examined and it was found that the heating in quinoline at 200 °C for 22 h resulted in the formation of magnesium *meso*-phenyl-tetrabenzotriazaporphyrin complex **34** in 15% yield<sup>28</sup>, (scheme 1.13).



**Scheme 1.13: Synthesis of MgTBTAP-Ph by Leznoff**

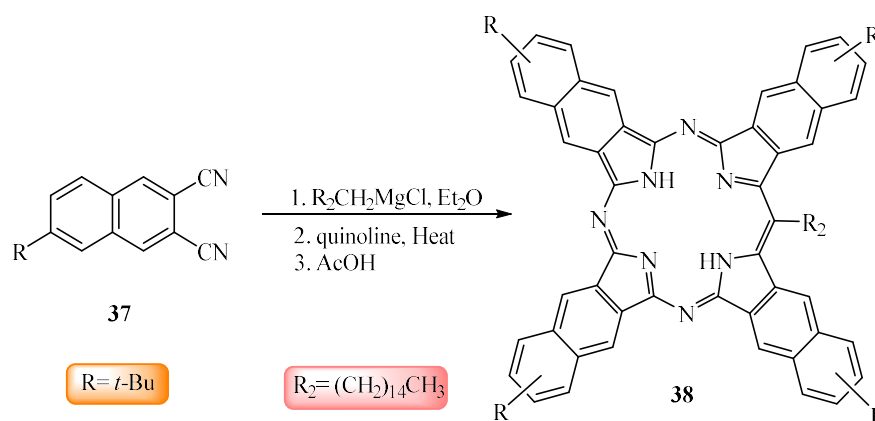
The authors also mentioned that the free macrocyclic ligand cannot be separated from unsubstituted phthalocyanine obtained as a by-product because of very low solubility of this ligand in organic solvents. On the contrary, Mg complex **34** is readily soluble in coordinating solvents; hence, it can be purified by chromatography. In addition, the formation of an inseparable mixture of *cis*- and *trans*-isomers of tetrabenzodiaza porphyrins as by-products was observed. The reaction with the 4-*t*-butyl derivative of phthalonitrile **35** instead of unsubstituted phthalonitrile affords products having higher solubility, which made it possible to separate these compounds by chromatography

and isolate tetra (*t*-Bu)-substituted tetrabenzotriazaporphyrin **36** as the free ligand. Mg complexes initially formed and subsequently were demetallized with acetic acid without isolation from the reaction mixture<sup>28</sup>, (scheme 1.14).



**Scheme 1.14: Synthesis of (*t*-Bu)<sub>4</sub>H<sub>2</sub>TBTAP-Ph**

Leznoff and McKeown<sup>28</sup> have also successfully used the same scheme to synthesize naphthalo-annulated triazaporphyrin based on 6-*t*-butyl-2,3-dicyanonaphthalene **37**. The yield of complex **38** was as low as 3% because it was difficult to separate the pure compound from the other reaction product, *t*-butyl-substituted naphthalocyanine. This was the only example of soluble naphtho-annulated triazaporphyrin, (scheme 1.15).

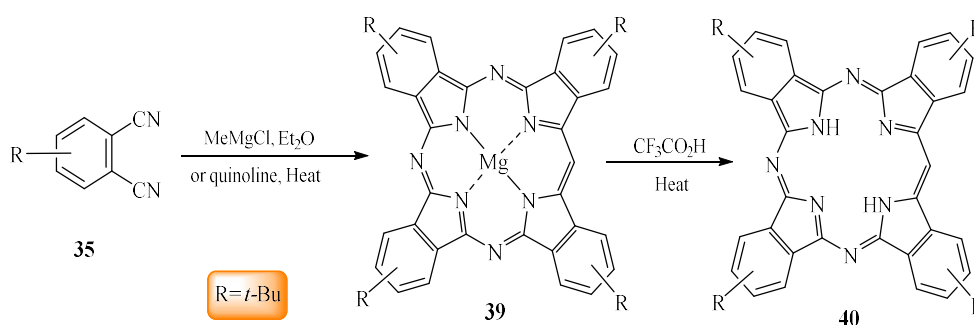


**Scheme 1.15: Synthesis of naphthalo-annulated triazaporphyrin complex**

Recently, Ivanova and co-workers<sup>29</sup> have prepared (*t*-Bu)-substituted tetrabenzotriazaporphyrins by treating *t*-Bu-phthalonitrile **35** with methylmagnesium iodide or chloride in quinoline. The (*t*-Bu)<sub>4</sub>MgTBTAP **39** and corresponding MgPc were separated by means of chromatography and the elimination of the metal achieved by

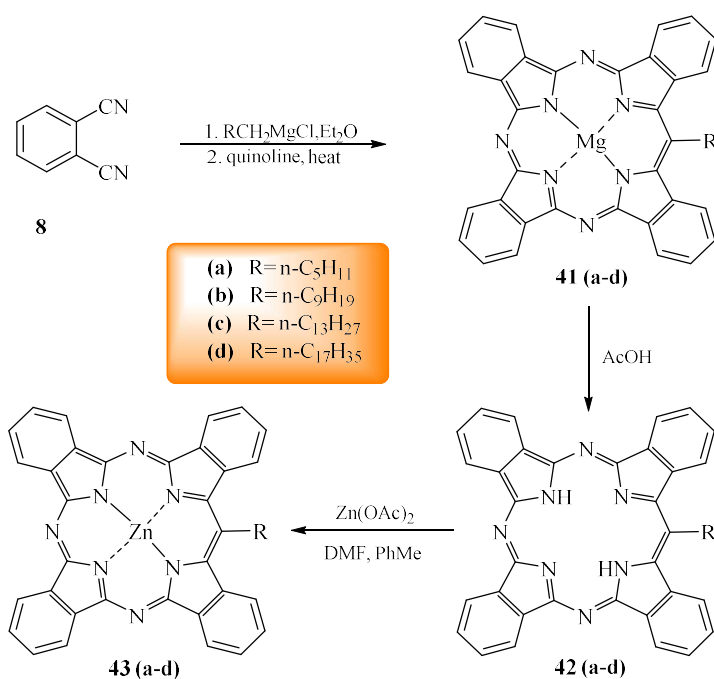
the reaction with trifluoroacetic acid to yield the free-metal TBTAP **40**, (scheme 1.16).

The macrocyclic ligand **40** is readily soluble in chloroform and was purified by aluminium oxide chromatography. The chromatographic separation of  $(t\text{-Bu})_4\text{-H}_2\text{TBTAP} **40** and  $(t\text{-Bu})_4\text{-H}_2\text{Pc}$  was described by Karasev *et al*<sup>30</sup>. It was suggested to use acidic aluminium oxide as the sorbent for column chromatography, resulting in a decrease in the content of phthalocyanine in the product to 1%.$



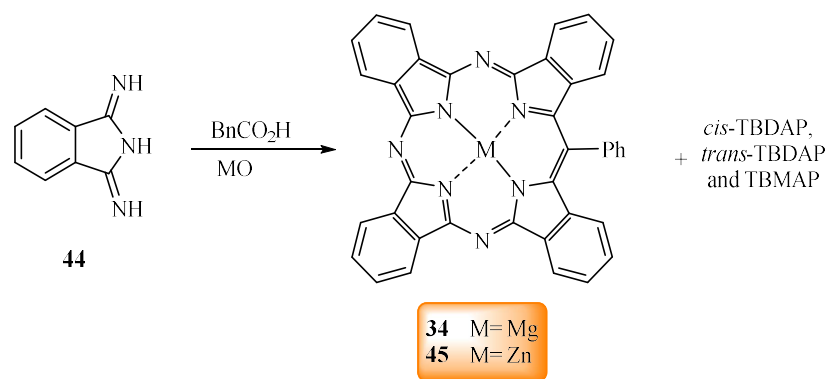
**Scheme 1.16: Synthesis of  $(t\text{-Bu})_4\text{MgTBTAP}$  and its free metal ligand**

For the purpose of increasing the solubility of tetrabenzotriazaporphyrin derivatives, Leznoff and co-worker<sup>31</sup> suggested also to introduce a substituent with a long hydrocarbon chain in *meso*-position of the macrocycle. The authors used a standard procedure based on the reaction of alkylmagnesium halides with unsubstituted phthalonitrile in diethyl ether at 20 °C followed by heating in quinoline at 120-185 °C. Magnesium complexes **41a-d** thus obtained were sufficiently soluble to be purified by chromatography on silica gel before transformation to the free ligands. The heating in acetic acid resulted in the formation of the demetallated *meso*-alkyltetrabenzotriazaporphyrins **42a-d**, which were recrystallized from toluene. The zinc complexes with these ligands **43a-d** were prepared by heating the corresponding macrocycles with a large excess of zinc acetate (10 equiv.), (scheme 1.17). All zinc complexes can be easily recrystallized from diethyl ether, the introduction of an alkyl substituent in *meso*-position leads to an increase in the solubility of both free macrocycles and their metal complexes.



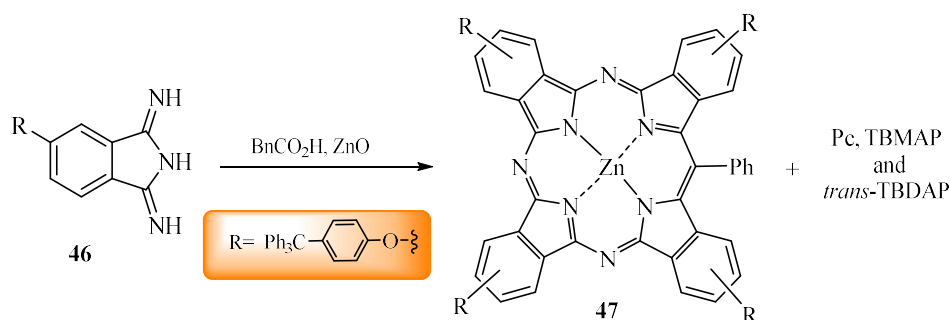
**Scheme 1.17: meso-position long alkyl chain substituent TBTAP derivatives**

The template synthesis has also been widely applied in recent years for the synthesis of azaporphyrin derivatives<sup>32,33,34,35</sup>. More recently, Galanin and co-workers described the preparation of a series of magnesium and zinc complexes of *meso*-substituted TBTAPs. Galanin *et al.* investigated the reactions of 1,3-diiminoisoindoline **44** together with carboxylic acids (containing a  $CH_2$  group adjacent to the carboxy group). Metal oxide was used as the template agent to yield a series of hybrid derivatives. During these investigations, they noted that increasing the ratio of carboxylic acid to diiminoisoindoline favoured the more porphyrin-like derivative. In addition, this reaction gave mixture of tetrabenzoporphyrin complexes which proved difficult to separate. The zinc complex with phenyl-substituted tetrabenzotriazaporphyrin **45** was also isolated from the reaction mixture; however, attempts to subject the latter compound to demetallation were unsuccessful due to its relative high stability. The yields of tetrabenzotriazaporphyrin derivatives **34** and **45** were 8.5% and 5%, respectively<sup>36,37</sup>, (scheme 1.18).

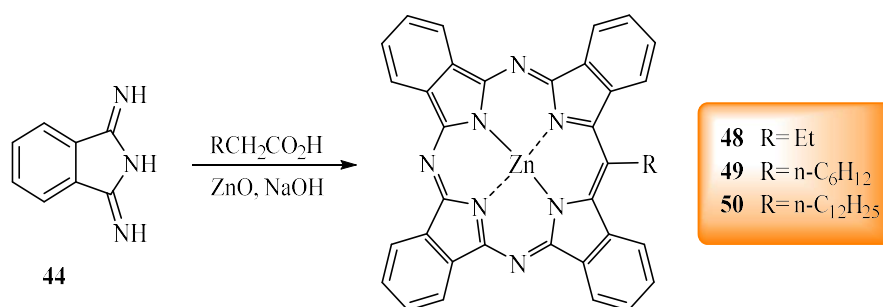


Scheme 1.18: Metal-TBTAP-Ph complexes reported by Galanin

The template condensation was performed also with the use of isoindoline containing the bulky 4-triphenylmethoxyphenoxy substituent **46**. The reaction of this compound with phenylacetic acid in the presence of zinc oxide afforded a mixture of products, from which Zn derivative of TBTAP **47** was isolated in 12% yield<sup>38</sup>, (scheme 1.19).

Scheme 1.19: Synthesis of (4-triphenylmethoxyphenoxy)<sub>4</sub>-ZnTBTAP-Ph complex

Similar reactions of 1,3-diiminoisoindoline **44** in the presence of zinc oxide as the template agent were performed also with other acids of the aliphatic series, such as butyric, caprylic and myristic. These reactions produced Zn complexes **48-50** and in all cases, *meso*-alkyl-tetrabenzotriazaporphyrin was isolated as the only product<sup>39</sup>, (scheme 1.20).

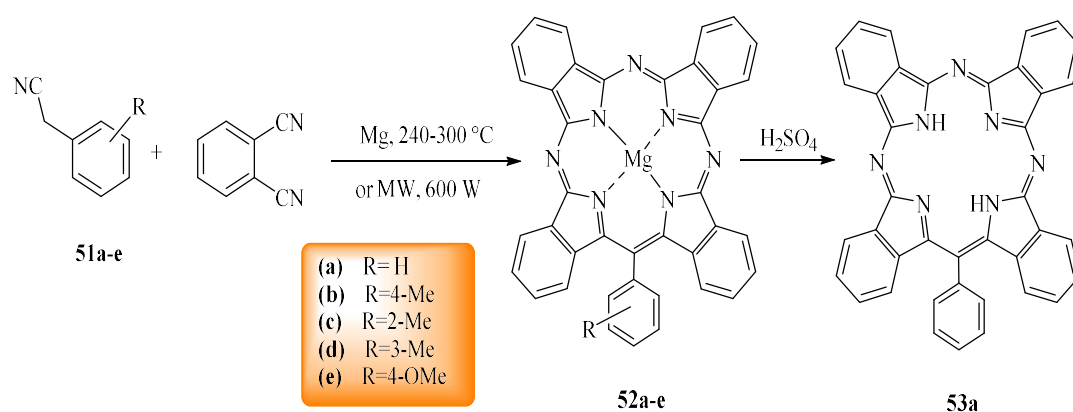


**Scheme 1.20: Galanin's synthesis of *meso*-alkyl-TBTAPs**

Galanin's route is generally faster than the other previous methods where a mixture of hybrid complexes including TBTAP, TBDAP and TBMAP are formed in an hour or sometimes less than one hour. In their investigation they observed that the resulting materials formed based on the ratios of the reactants used in these reactions where an excess of the carboxylic acids result in the formation of complexes with more methine bridges, whereas the more nitrogen bridges can be formed when decreasing the ratio of carboxylic acids to diiminoisoindolines<sup>36,38</sup>.

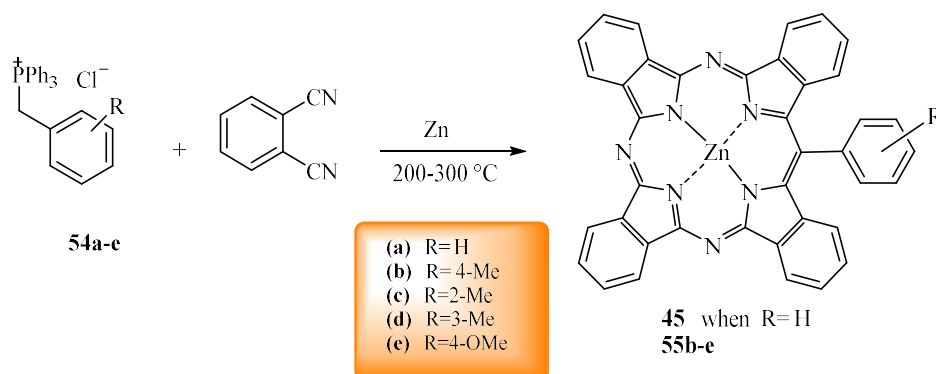
In the last few years, a series of single *meso*-substituted tetrabenzotriazaporphyrins have been reported; the authors studied the mixed condensation of arylacetonitriles with unsubstituted phthalonitrile in the presence of magnesium powder. Two different methods were investigated to prepare these complexes, and both showed the possibility of initiating the process by microwave radiation. As opposed to the fusion technique, these procedures give a higher yield in short period of time<sup>40,41</sup>.

The reaction between arylacetonitriles and phthalonitrile proceeded upon slow heating and gave Mg complexes of *meso*-aryl-substituted tetrabenzotriazaporphyrins **52a-e**. Only magnesium phthalocyanine was isolated as a by-product. No impurities of diaza- and monoaza- derivatives were found. Magnesium complexes **52a-e** are convenient compounds for subsequent modifications. They can be subjected to chromatographic purification and can be easily demetallated with sulfuric acid under mild conditions. This approach was used to prepare the corresponding free macrocycles, for instance, *meso*-phenyl-substituted TBTAP **53a**, in 98% yield<sup>40</sup>, (scheme 1.21).



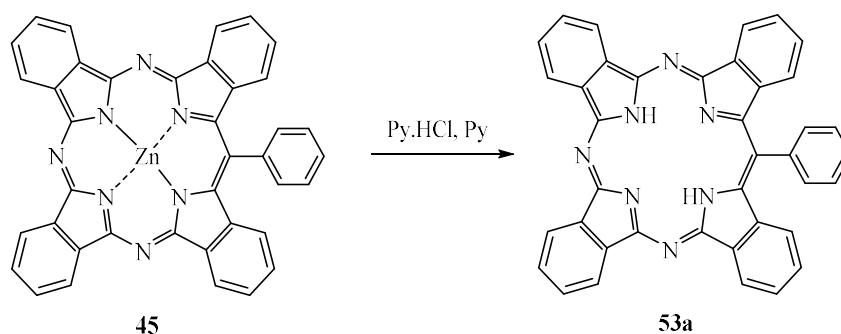
**Scheme 1.21: Aryl acetonitriles for the synthesis of *meso*-substituted TBTAPs**

Similarly, the gradual heating of unsubstituted phthalonitrile and benzyl triphenyl phosphonium salts **54a-e**, in the presence of zinc dust, afforded new zinc complexes **45**, **54b-e**. These compounds are readily soluble in organic solvents and can be easily separated by column chromatography on silica gel<sup>41</sup>, (scheme 1.22).



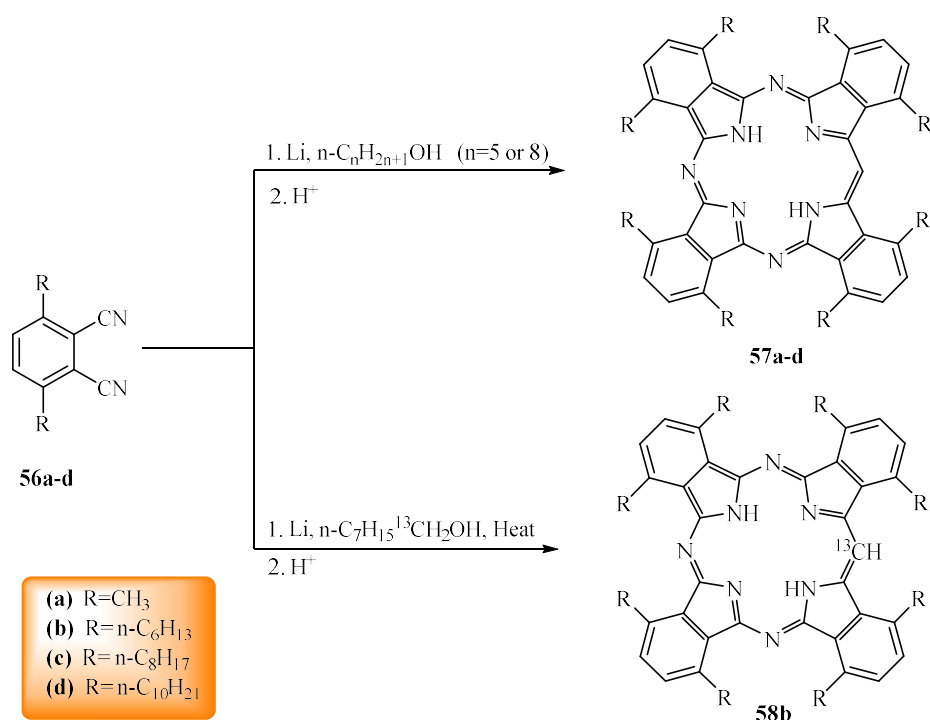
**Scheme 1.22: Benzyl phosphonium salts for synthesis of *meso*-substituted ZnTBTAPs**

It is difficult to produce a free macrocycle from tetrabenzotriazaporphyrin complexes containing Zn (II) as the central ion. Many authors reported that they failed to demetallate Zn complex **45**<sup>37,42</sup>. Nonetheless, Tomilova and co-worker were the first to perform the quantitative demetallation of this compound under non-traditional conditions on heating in an ionic liquid (pyridinium hydrochloride)<sup>43</sup>, (scheme 1.23).

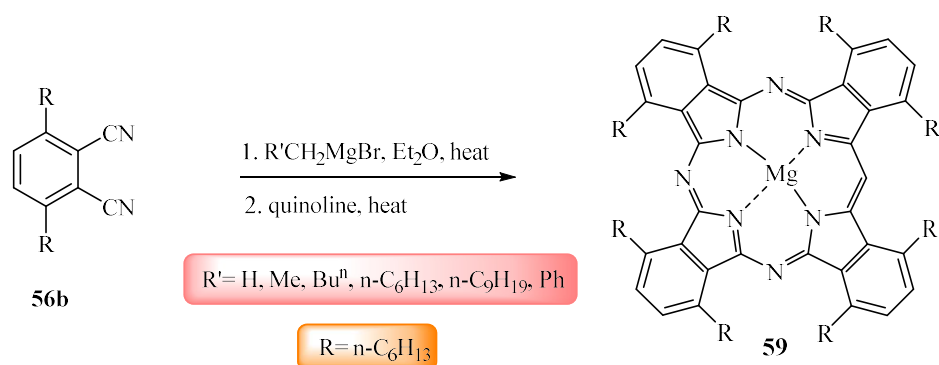


**Scheme 1.23: Non-traditional conditions for ZnTBTAP-Ph demetallation**

In 2005, Cammidge and co-workers<sup>44</sup> studied the tetramerization of 3,6-di(*n*-hexyl)phthalonitrile in *n*-pentanol or *n*-octanol with metallic lithium for the preparation of non-peripherally substituted octaalkyl-phthalocyanine. They isolated a dark green by-product in addition to the desired phthalocyanine. The products were isolated in a ratio of (95:5) (Pc/TBTAP). The isolated by-product identified later as *np*-(*n*-hexyl)<sub>8</sub>H<sub>2</sub>TBTAP **57b**, which was the first single-isomer of tetrabenzotriaza porphyrin with substituents located on the benzenoid rings. It was noted that the reaction with the use of the lithium *n*-pentoxide prepared beforehand affords only octa-substituted phthalocyanine. The use of excess of lithium metal (19 equivalents) in pentanol gave a (77:23) ratio of (Pc/TBTAP), and using a solvent with a higher boiling point such as *n*-octanol results in decrease of the ratio to (53:47). It was also reported that the configuration of the reaction products depends on the substituents in the starting phthalonitrile. 3,6-Disubstituted phthalonitriles, **56a**, **c** and **d** respectively, were shown to form mixtures of phthalocyanine and tetrabenzotriazaporphyrin, whereas 4-*t*-butylphthalonitrile and 4,5-di(*n*-hexyl) phthalonitrile give only the corresponding phthalocyanines. The source of the *meso*-carbon in the reactions was unclear, it was initially suggested that it might originate from the  $\alpha$ -carbon of dialkyl-phthalonitrile. However, upon the failure of two phthalonitriles to yield TBTAP, further investigations were made using <sup>13</sup>C labelling experiments to test this hypothesis which was proved to be wrong. Instead, it appeared that the alcohol used in the reaction serves as a source of the methine group at *meso*-position. Thus, a study of the reaction with *n*-octanol <sup>13</sup>C isotope-labelled at the  $\alpha$ -position gave tetrabenzotriazaporphyrin with the <sup>13</sup>C label at the *meso*-site in 87%. Evidently, the incorporation of the <sup>13</sup>C-label from octanol involves a remarkable cleavage of the alkyl chain<sup>44</sup>, (scheme 1.24).

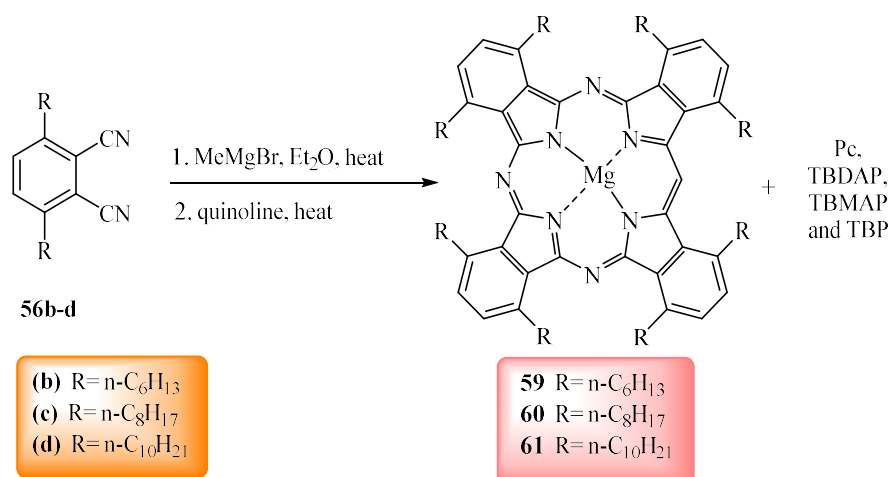
Scheme 1.24: Synthesis of *np*-(alkyl)<sub>8</sub>H<sub>2</sub>TBTAB complexes

In 2011, Cammidge group used Leznoff's procedure to introduce bulky substituents at the *meso*-position of TBTAP macrocycles. The ease of forming non-peripherally substituted (n-C<sub>6</sub>H<sub>13</sub>)<sub>8</sub>-TBTAP **57b** from 3,6-dihexyl phthalonitrile **56b**, intrigued the group to extend their investigation into various organomagnesium with the same precursor for the synthesis of other tetrabenzo(aza)porphyrin derivatives. However, the same product **59** was isolated from all trials, which was unsubstituted on the *meso*-position. This led to conclude that the Grignard reagents can't be used to introduce a phenyl or alkyl substituent at the *meso* position due to the steric crowding when 3,6-disubstituted phthalonitriles are used<sup>45</sup>, (scheme 1.25).



**Scheme 1.25: Attempts to introduce bulky substituents at the *meso*-position of *np*-TBTAP macrocycles from various Grignard reagents**

Moreover, the group described controlled synthetic strategies and successfully prepared novel derivatives of the metal-free as well as magnesium and copper derivatives of tetrabenzoporphyrin hybrids. In light of the previous studies by Linstead<sup>10</sup> and Galanin<sup>36,37</sup> that showed that slight differences in the amounts of Grignard reagents/carboxylic acids affected the outcome of reactions it was decided to analyse systematically the effect of the stoichiometric ratios of methyl magnesium bromide to 3,6-dihexylphthalonitrile on the product(s) formed. Thus, studies using a series of stoichiometric ratios were undertaken commencing with 1:4 equivalents (MeMgBr/phthalonitrile) and increased to 5:1 (MeMgBr/ phthalonitrile) in whole unit as regular increase (1.0, 2.0, 3.0, 4.0 and 5.0). Reactions were carried out following the two-step synthetic protocol developed by Linstead and Barrett<sup>10</sup>. Treatment of a solution of 3,6-dialkylphthalonitriles **56b-d** in ether or THF with different amounts of the Grignard reagent followed by exchanging the solvent to quinoline and heating the mixture at high temperature in order to obtain the tetrabenzoporphyrin magnesium derivatives<sup>45</sup> **59-61**, (scheme 1.26).



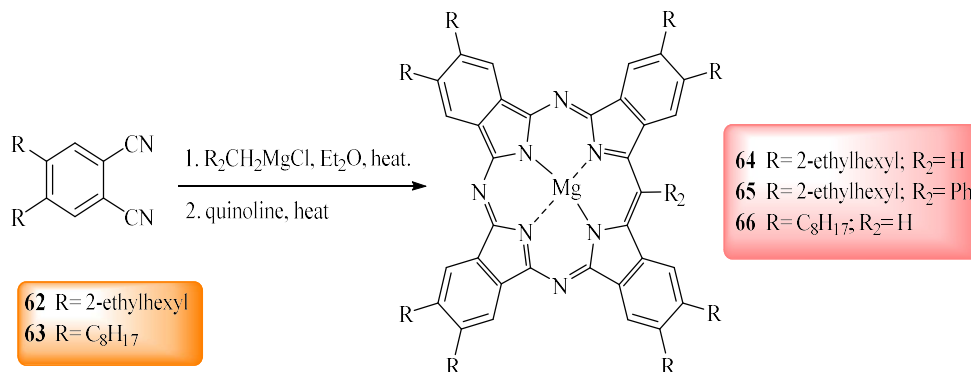
**Scheme 1.26: Controlled procedure for the synthesis of tetrabenzoporphyrin derivatives**

It was notable that the possibility to obtain the full series of tetrabenzoporphyrins as their magnesium analogues increased when more equivalents of Grignard reagent are used. In other words, each stoichiometric ratio of MeMgBr/phthalonitrile used affected the product distribution in a controlled manner. In more details, the reaction of 1:4 equivalents of MeMgBr to phthalonitrile failed to produce any hybrid molecule, whereas changing the equivalents to a 1:1 ratio gave a mixture of TBTAP and TBDAP. Significant amounts of TBTAP, TBDAP and TBMAP were observed when the equivalents of MeMgBr: phthalonitrile increased to a 2:1 ratio with traces of Pc and TBP. Further increase in the ratio led to a reduction in the formation of phthalocyanine-like hybrids, whereas the formation of benzoporphyrin-like macrocyclic products was increased. The various magnesium tetrabenzoporphyrinato species were successfully isolated excluding the (*cis* and *trans*) TBDAP hybrids. The demetallation on heating in acetic acid affords free ligands, which, in turn, form the corresponding copper complexes after heating with copper (II) acetate in n-pentanol after isolations. Generally, this controlled procedure provides a particularly convenient synthesis of a full range of tetrabenzoporphyrin derivatives (i.e. TBTAB, *cis*- and *trans*-TBDAP, TBMAP, TBP, Pc)<sup>45</sup>.

More recently, the synthesis of non-peripherally octaalkyltetrabenzotriazaporphyrin macrocycles has been investigated by another research group with the aim to improve the reaction yield. The modified procedure using a stable solvent was significantly

effective for the scale-up of the reaction system as well as the yield enhancement. For example, *np*-(C<sub>6</sub>H<sub>13</sub>)<sub>8</sub>-H<sub>2</sub>TBTAP yield was improved from 27% to 35% in comparison between conventional and improved method respectively. The improved yield and stability of the reaction were accomplished by using MeLi and cyclohexanol for the series of *np*-octaalkyltetrabenzotriazaporphyrins<sup>46</sup>.

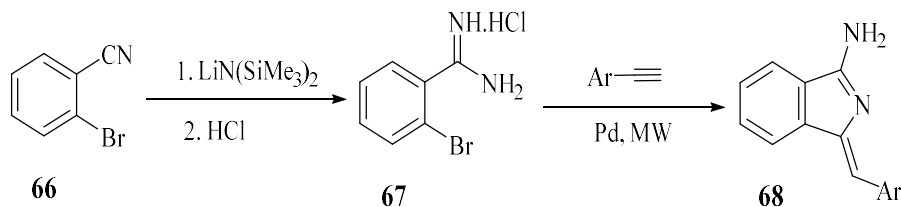
Cambridge-Cook groups also investigated using 4,5-dialkylphthalonitriles **62** and Grignard reagent MeMgBr, the reactions gave a predominate mixture of TBTAP and Pc. In contrast to 3,6-dialkylphthalonitriles, introducing a phenyl or alkyl group at the *meso*-position of the TBTAP can be achieved when the 4,5-dialkylphthalonitriles are used. For instance, the reaction of 4,5-bis(2-ethylhexyl)-phthalonitrile **62** with benzylmagnesium chloride performed under similar previous conditions produced the substituted magnesium complex **65**. The formation of a product containing the unsubstituted methine bridge was not observed in this reaction<sup>45</sup>, (scheme 1.27).



#### Scheme 1.27: *meso*-Substituted MgTBTAP complexes using 4,5-dialkylphthalonitriles

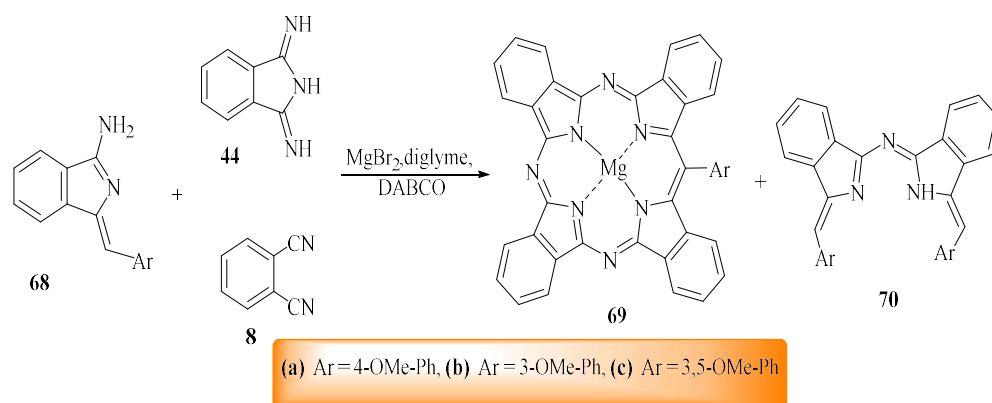
In recent years, considerable attention has been focused on the preparation of TBTAPs using more precise methods. Cambridge's group<sup>47</sup> reported a modern approach for the preparation of substituted *meso*-phenyl TBTAP as a single product of hybrid macrocycles. This method proved to give a significant yield of TBTAP and avoided the formation of further hybrid complexes. The synthetic strategy involves the preparation of the aminoisoindoline or its derivatives by applying the procedure demonstrated by Hellal *et al.* The aminoisoindoline **68** was synthesised from a copper-free Sonogashira coupling between terminal arylacetylenes and 2-bromo benzimidamide hydrochloride **67** under microwave irradiation<sup>48</sup>. The latter was

formed from treatment of a solution of 4-bromobenzonitrile **66** with a solution of lithium bis(trimethylsilyl)amide (LiHMDS) in THF followed by quenching with isopropanol/HCl<sup>49</sup>, (scheme 1.28).



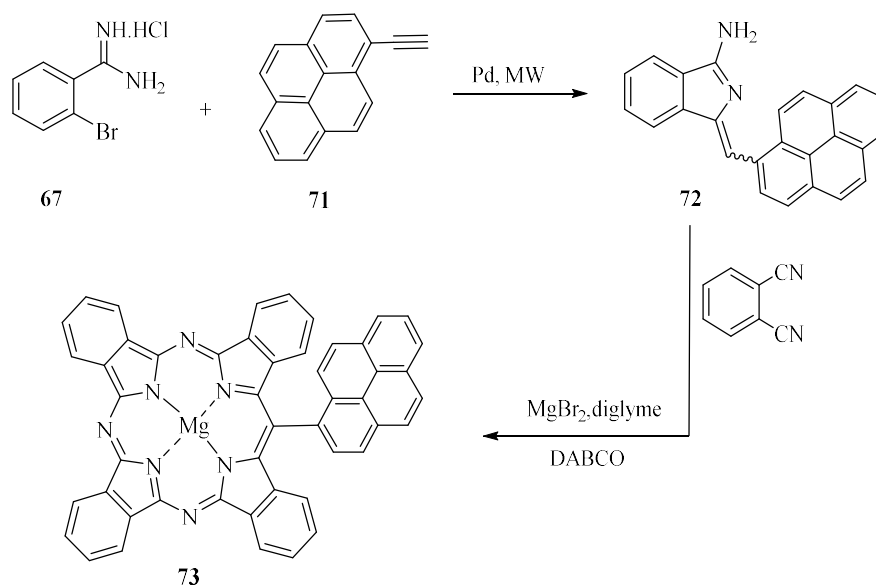
**Scheme 1.28: General synthesis of aminoisoindoline**

The first attempts to synthesise TBTAP began with heating a solution of diiminoisoindoline **44** and aminoisoindoline **68** in high boiling organic solvents (starting with quinoline, DMEA, DMF, and finally diglyme) in the presence of magnesium bromide as a template agent. The reaction mixture was found to contain the desired *meso*-phenyl TBTAP **69a** along with Pc and a self-condensation product of aminoisoindoline **70**. However, due to the unsatisfactory outcomes and side-products formation, the reaction was modified to use phthalonitrile **8** as a less reactive precursor instead of diiminoisoindoline **44**. The group successfully reported a versatile and high yielding synthesis of *meso*-aryl substituted TBTAP derivatives **69a-c**. Additionally, the group demonstrated the synthesis of *meso*-phenol substituted TBTAPs from the corresponding methoxy substituted complexes using Magnesium iodide (MgI<sub>2</sub>)<sup>47</sup> or Boron tribromide (BBr<sub>3</sub>)<sup>50</sup>. Further functionalising was employed which include alkylation and acylation of the phenol group, the demetallation and transmetallation of the Mg in the centre core of the TBTAPs was also achieved<sup>47</sup>, (scheme 1.29).



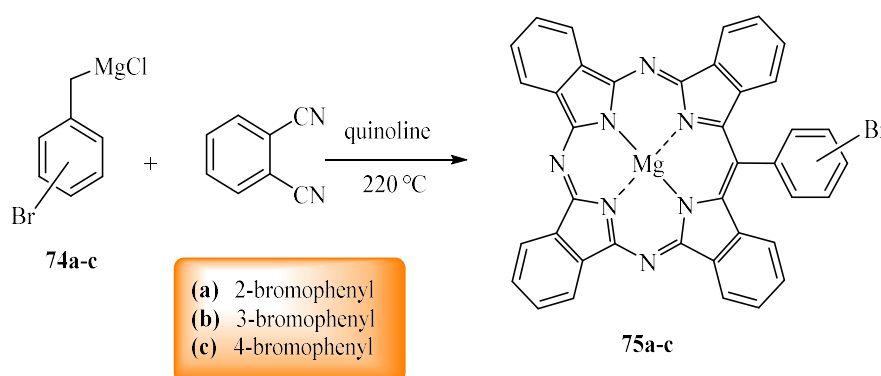
**Scheme 1.29: Improved protocol for the synthesis of meso-aryl TBTAPs**

The new synthetic route therefore opens the way for the design and synthesis of new families of *meso*-aryl TBTAPs, and their further elaboration into functional molecular materials. To illustrate the potential of the new synthetic protocol Cammidge and co-workers selected pyrene as complementary aromatic unit. Thus, 1-ethynylpyrene **71** was reacted with 2-bromoamidine **67** to give the corresponding aminoisoindoline **72**. In this case the product was isolated as a mixture of stereoisomers. The mixture was cyclised with phthalonitrile using their previously developed conditions and the reaction proceeded smoothly resulting in the isolation of *meso*-(1-pyrenyl) TBTAP **73**<sup>50</sup>, (scheme 1.30).



**Scheme 1.30: Synthesis of MgTBTAP-(1-pyrenyl) 73**

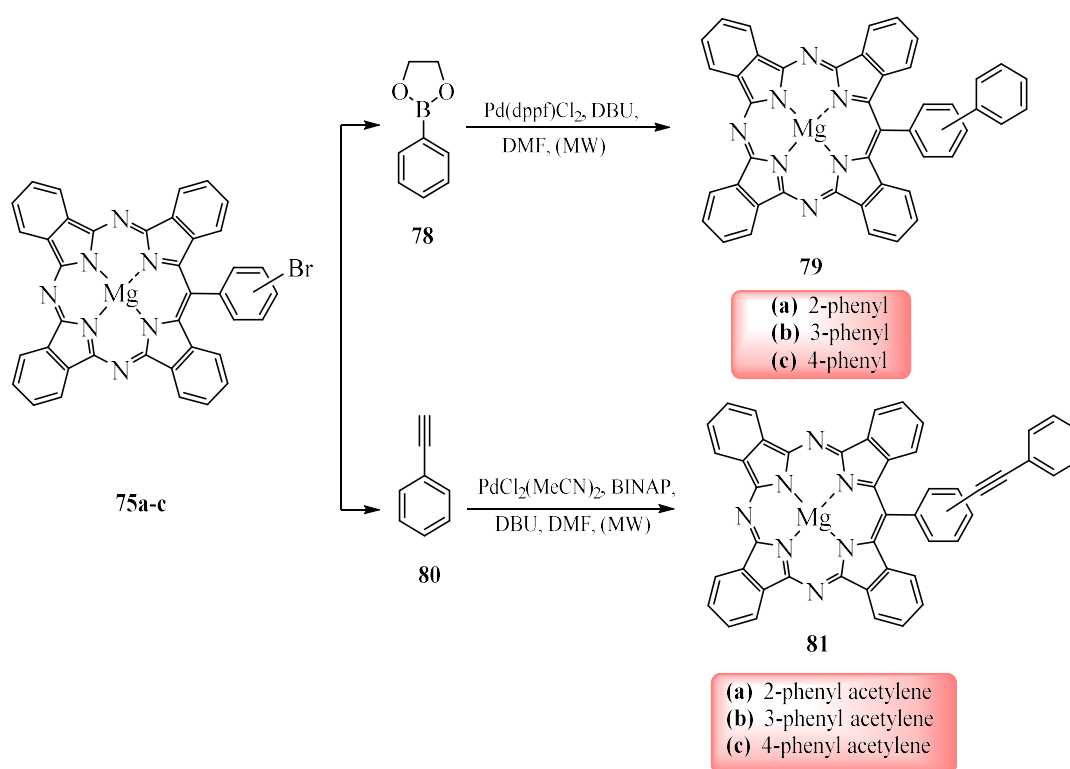
Cambridge's group have been interested in novel TBTAPs bearing aryl substituents at the *meso*-position, therefore, they extended their research and used new and improved synthetic strategies. In particular, they focused on the known protocol employing Grignard reagents which was reported by Leznoff<sup>28</sup>. A series of functionalised *meso*-phenyl substituted TBTAPs **75a-c** were prepared by reaction between phthalonitrile and the isomeric series of 2-, 3- and 4-bromobenzyl magnesium chlorides **74a-c**. The procedure was later improved further by using diglyme as the only solvent, resulting in a cleaner, more convenient transformation and isolation, (scheme 1.31). Furthermore, to enhance the solubility and prevent aggregation, the group investigated the use of 4,5-disubstituted phthalonitriles with 2-bromobenzyl magnesium chloride **74a**. Two phthalonitriles were chosen, one with branched (chiral) chains and the other with high symmetry and heavily branched. Despite the fact that the formation of the TBTAPs from these phthalonitrile derivatives was straightforward, they were isolated in relatively low yields<sup>50</sup>.



**Scheme 1.31: Synthesis of MgTBTAP complexes from the isomeric series of bromobenzyl magnesium chlorides**

Soon after that, Cambridge's group demonstrated, for the first time, the functionalisation of TBTAP hybrids using cross-coupling chemistry on parent *meso*-bromophenyl TBTAPs **75a-c** using microwave irradiation<sup>51</sup>. The treatment of bromide derivatives **75a-c** with phenyl or 4- methoxyphenyl boronic acid under standard Suzuki Miyaura conditions led to de-bromination of the starting materials. However, the boronic acid was replaced with its corresponding boronate ester **78** and it was indeed successfully employed in cross-coupling reactions and gave corresponding TBTAPs **79a-c**. It should be noted that the isomeric products were isolated in low

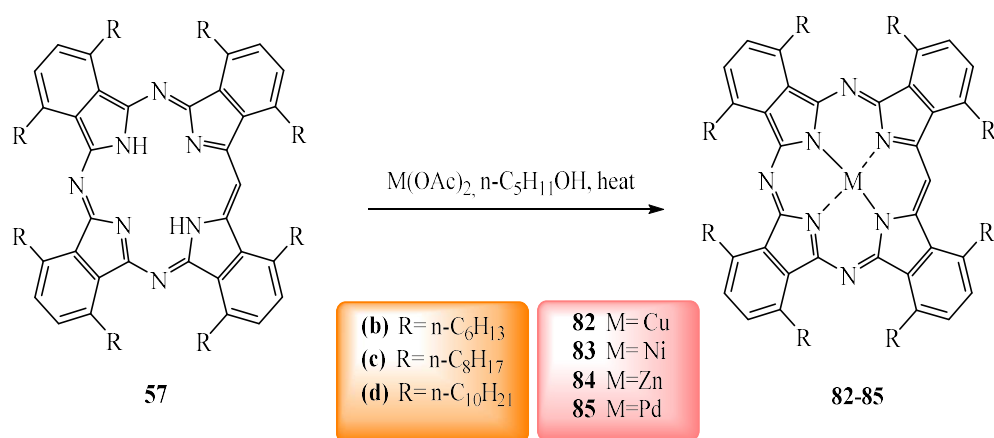
yields (9-11%). The Sonagashira cross-coupling was the second functionalisation strategy to be employed on **75a-c** using phenylacetylene **80** as a reactant. However, copper-free conditions were employed to avoid the possibility of the copper incorporation into the macrocyclic ligand (displace the labile magnesium). The reaction was carried out under microwave heating similar to Suzuki Miyaura cross-coupling and gave MgTBTAP complexes **81a-c**. In contrast, the TBTAP derivatives **81a-c**, from copper free Sonagashira cross-coupling, were isolated in good yields (40-73%), (scheme 1.32). Both strategies demonstrate the potential for engineering multifunctional systems with predictable and fixed relative positioning of the individual components<sup>51</sup>.



**Scheme 1.32: Synthesis of *meso*-phenyl substituted TBTAPs by coupling reactions**

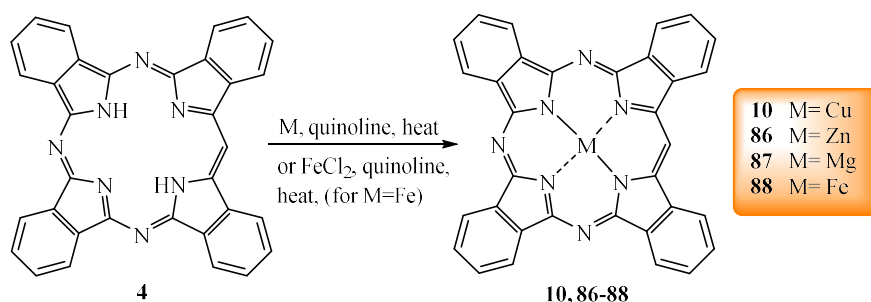
In addition to the most well-studied Mg and Zn complexes with tetrabenzotriaza porphyrin, metal complexes of such ligands with other metal ions (for example, Ni, Pd, Cu and Fe) were also described. Since tetrabenzotriazaporphyrins are structurally similar to classical phthalocyanines, these compounds can be synthesized using methods developed for the preparation of phthalocyanines. For example, complexes **82-85** were synthesized by heating free ligand **57** with an excess of metal acetate in

pentyl alcohol. After the chromatographic purification on silica gel, the metal complexes were obtained in yields up to 97%<sup>45,52,6</sup>, (scheme 1.33).



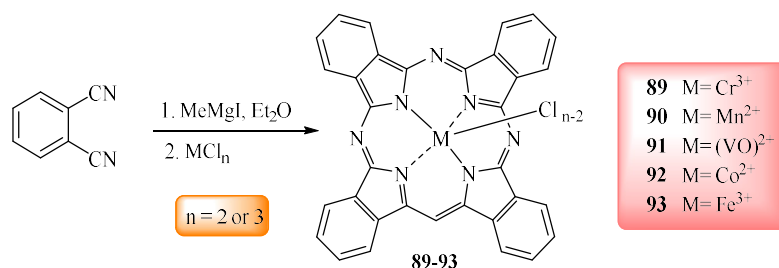
**Scheme 1.33: Synthesis of various metal-TBTAP complexes.**

In the case of poorly soluble free ligands, such as unsubstituted tetrabenzotriazaporphyrin, dimethylformamide or pyridine can be used as the solvent. The reaction was performed by heating the reactants under reflux in DMF or pyridine<sup>53</sup>, the metal complex precipitated after the dilution of the reaction mixture with an equal volume of water. The complexation of tetrabenzotriazaporphyrin with metals was carried out in higher alcohols and also in other high-boiling solvents, in quinoline or 1-chloronaphthalene, in which the free ligand is readily soluble at high temperatures. This method was applied to prepare complexes **10**, **86** and **87**, with the use of metals copper, zinc and magnesium respectively. However, the synthesis of iron complex **88** was performed in the presence of iron (II) chloride as the source of the central ion<sup>10</sup>, (scheme 1.34). Aluminium metal complex was synthesized according to a similar scheme by using AlCl<sub>3</sub> in quinoline, the product was isolated by diluting the reaction mixture with a large amount of dichloromethane. In some cases, AlMe<sub>3</sub> in dichloromethane is employed to give the metal complex<sup>54,55</sup>.



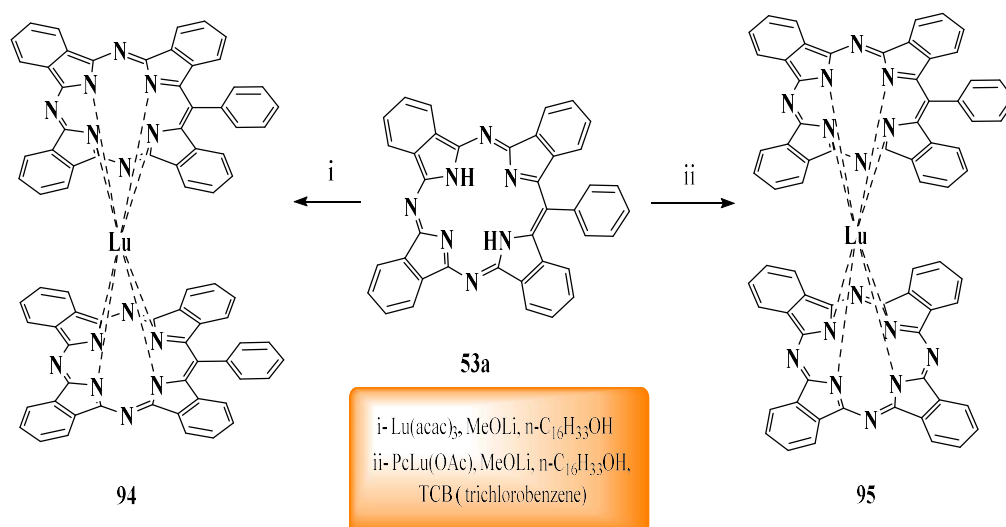
**Scheme 1.34: Synthesis of Metal-TBTAP complexes from free ligands**

Tetrabenzotriazaporphyrin complexes of chromium **89**, manganese **90**, vanadyl **91**, cobalt **92** and iron (III) **93** were synthesized according to the procedure described by Barrett and Linstead<sup>10</sup>, a salt of the required metal is introduced into the reaction after the addition of an organomagnesium reagent to the phthalonitrile<sup>56,57</sup>, (scheme 1.35).



**Scheme 1.35: Synthesis of various metal TBTAP complexes**

It should be noted that attempts to use this approach for the preparation of sandwich-type complexes containing the tetrabenzotriazaporphyrin ligand were unsuccessful<sup>58</sup>. Although, Pushkarev *et al.* reported<sup>43</sup> the preparation of the first homo- and heteroleptic rare-earth double-decker complexes based on meso-phenyl-tetrabenzotriazaporphyrin **53a**. Lutetium complex **94** was prepared according to a procedure developed for the selective synthesis of double-decker complexes with phthalocyanine ligands. The reaction of free ligand **53a** with lutetium acetylacetonate [Lu(acac)<sub>3</sub>] proceeds on heating under reflux in hexadecyl alcohol in the presence of lithium methoxide to give green homoleptic complex **94** in good yield (81%). Heteroleptic complex **95** containing tetrabenzotriazaporphyrin and phthalocyanine ligands was generated under similar conditions with the participation of lutetium phthalocyanine in 72% yield<sup>43</sup>, (scheme 1.36).



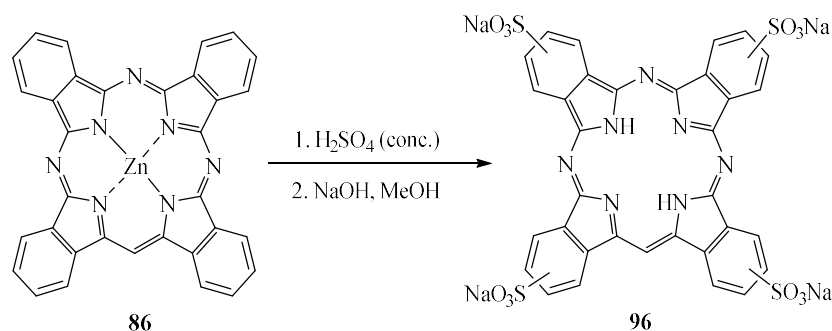
**Scheme 1.36: Homo- and heteroleptic lutetium double-decker complexes based on *meso*-phenyl-tetrabenzotriazaporphyrin**

It was observed that cadmium complexes with TBTAP ligand exhibit unusual properties<sup>59</sup>. The addition of an excess of a copper or zinc salt to a solution of cadmium derivative in dimethyl sulfoxide at 25 °C leads to transmetallation, whereas rather severe conditions are required for complexes of most other metals.

The reactions of the phthalocyanine series with trivalent phosphorus proceed in a different way than those with pentavalent phosphorus, and they can be used to synthesize a new macrocyclic system directly from phthalocyanine<sup>60</sup>. However, the reactions of free tetrabenzotriazaporphyrin with trivalent and pentavalent phosphorus compounds (PBr<sub>3</sub> and POBr<sub>3</sub>) gave the same product<sup>25</sup>.

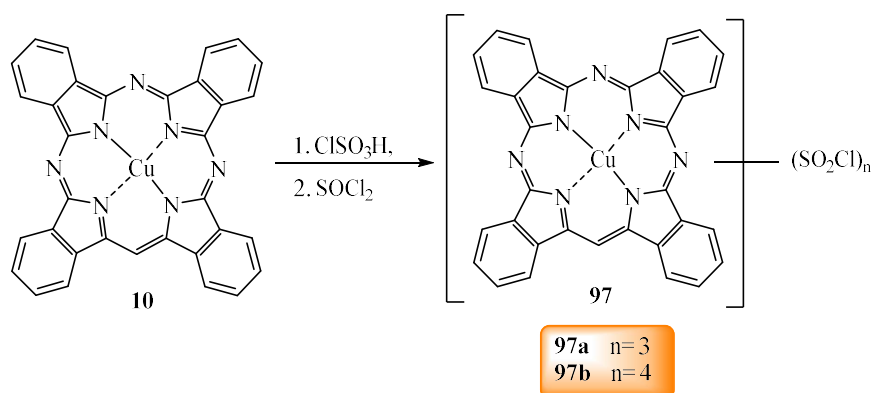
Free tetrabenzotriazaporphyrins and their complexes with metals are insoluble in water. However, for some practical application it is very important to prepare water-soluble derivatives. The main method used for that is based on the sulfonation of the macrocycle on the benzene rings. The synthesis of first sulfonated derivatives of tetrabenzotriazaporphyrin was covered with a patent in 1938<sup>61</sup>. These compounds are produced by heating the copper complex of TBTAP **10** in the presence of 5% oleum (solution of sulfur trioxide in sulfuric acid) at 100 °C. It was shown that concentrated sulfuric acid can be used as the sulfonating agent<sup>62</sup>. For example, the reaction with Zn complex **86** also proceeds at 100 °C. This reaction produced tetra-sulfonated compound **96** readily soluble in water, which can be isolated as a green powder upon

the addition of acetone to an aqueous solution of the mixture, (scheme 1.37). This reaction leads to the elimination of the zinc ion to form the free macrocycle. To some extent, this was an unexpected result, because many authors mentioned the stability of Zn complexes to acids, including sulfuric acid<sup>22,37,42</sup>. Seemingly, this could be attributed to the reaction conditions, which was carried out at high temperature, and the long action of the corrosive reagent.



**Scheme 1.37: Water-soluble tetra-sulfonated TBTAP complex**

More recently, the sulfonation of the Cu complex of tetrabenzotriazaporphyrin **10** with chlorosulfonic acid was described in a patent<sup>63</sup>. It was noted that the reaction performed at 127- 135 °C results in the introduction of three sulfonyl chloride groups per macrocycle **97a**, whereas, at 143 - 145 °C, four sulfonyl chloride groups are introduced **97b**. The latter reaction was accompanied by partial hydrolysis of sulfonyl chloride groups because it was isolated by the treatment of the reaction mixture with ice, (scheme 1.38). Macrocyclic sulfochlorides **97a** and **97b** were introduced into the reactions with various amines with the aim of preparing dyes.



**Scheme 1.38: Sulfochloride complexes of copper TBTAP**

## 1.5 Properties of Tetrabenzotriazaporphyrins

Phthalocyanines are widely known for their intense blue-green colour as a result of the aromatic  $18\pi$ -electron aromatic core which is the principal contributor to their electronic absorption behaviour<sup>2</sup>. Tetrabenzotriazaporphyrins were first differentiated from the Pc materials through their green colour. Tetrabenzotriazaporphyrins TBTAPs and phthalocyanines possess comparable physicochemical properties (optical, electronic and chemical properties) due to their structural similarity. This is why tetrabenzotriazaporphyrins are often used in the same fields as phthalocyanine derivatives. The first patent on the application of tetrabenzotriazaporphyrins was granted one year after their discovery in 1937<sup>61</sup>. Due to one of the main features of this class of compounds, their deep blue or green colour, they were covered with a patent as dyes<sup>61</sup>. More detailed description of the properties of tetrabenzotriazaporphyrins will be discussed in the following sections.

### 1.5.1 Molecular properties

#### 1.5.1.1 Electronic properties and UV-Vis spectroscopy

As with the phthalocyanines, the extended conjugation in the ring produces low energy  $\pi$ - $\pi^*$  transitions which are detected in two main regions of the UV-Vis spectrum. Metallated phthalocyanines (MPcs) exhibit a characteristic single strong absorption band (*Q*-band), which appears in the red/ near-infrared region of the spectrum (670-720 nm) giving the phthalocyanines their characteristic blue/green colour. On the other hand, metal-free phthalocyanines ( $H_2Pc$ s) are usually characterised by a split *Q*-band signal, arising from the reduced symmetry in the molecular structure compared to the metallated phthalocyanines ( $D_{2h}$  for  $H_2Pc$  and  $D_{4h}$  for the MPc). Both MPcs and  $H_2Pc$ s show a weaker absorption in the blue region of the UV-Vis spectrum called *B*-band or Soret-band at about 320-370 nm. As opposed to the symmetric phthalocyanine molecule, tetrabenzotriazaporphyrins have lower symmetry ( $C_{2v}$ ) due to the presence of the methine bridge instead of the nitrogen atom in the meso position. This is reflected in the spectral characteristics. Thus, the absorption spectra of MgTBTAPs and MgPcs are very similar, the main pronounced difference is that the *Q*-band of the TBTAP complex is split into two components<sup>8</sup>.

The interpretation of the *Q*- and *B*-bands in tetrabenzotriazaporphyrins can be understood by Gouterman's four-orbital<sup>64</sup> linear combination of atomic orbital model (LCAO). This approach was initially developed to explain the electronic transitions of tetrapyrroles. The *Q*- and *B*-band absorptions are assigned to the allowed  $\pi \rightarrow \pi^*$  electronic transitions from the HOMO [highest occupied molecular orbital/the second highest energy occupied orbital ( $a_{2u}, a_{1u}$ )], to the LUMO [lowest unoccupied molecular orbital (eg)].

A previously available literature data has been produced to calculate the energy levels of molecular orbitals (MO) of the tetrabenzotriazaporphyrins by using different method such as LCAO-MO method<sup>65</sup> and the most thorough investigation was undertaken using the Pariser-Parr-Pople (PPP)<sup>66</sup>. Further calculations have been achieved by Kobayashi and co-workers using the ZINDO (Zerner's Intermediate Neglect of Differential Overlap) program<sup>67</sup>. These predictions and calculations were agreed with Linstead's investigations on a series of Pc, TBTAP, TBDAPs TBMAP, and TBP. It was observed that the *Q* band shifts to shorter wavelength and lower intensity as the aza-links are replaced by methine units and the extinction coefficients of the Soret band decrease, while those of the *Q*-band increase<sup>15</sup>.

Recently, Cammidge-Cook research group reported a set of data of absorption spectra for non-peripherally substituted hybrid derivatives, as metal-free, magnesium and copper tetrabenzotriazaporphyrins. As the number of *meso*-nitrogen atoms increases from zero to four,  $\lambda_{\max}$  of the *Q* band absorption peak becomes red-shifted by almost 100 nm, and extinction coefficients increased at least threefold. Simultaneously the blue-shifted Soret band substantially decreased in intensity<sup>45,6</sup>, their data is consistent with the results of the earlier studies<sup>15</sup>. The EAS strongly depends on the nature of the central metal ion in metal complexes which was noted by Solov'ev and co-worker<sup>68</sup>. Thus, the general tendency for a long-wavelength shift is retained in going from magnesium to copper. For example, inserting the copper metal in the central cavity of tetrabenzotriazaporphyrin derivatives led to a hypsochromic shift<sup>45,6</sup>. In earlier study, it was observed that the introduction of substituents into both the aromatic system of the macrocycle and the *meso* position of the ring has only a slight effect on the character of the absorption spectrum<sup>69</sup>.

In a later study in 2015, a further investigation was undertaken on tetrabenzoporphyrin derivatives and showed that the changes in the Q band absorption when aza-linkages increased could be related to the relative electron-density of each macrocycle expressed as the sum of electronegativity of all meso N and CH atom groups,  $\Sigma\chi_R$ . X-ray photoelectron spectroscopy was used to differentiate between the three different types of macrocyclic nitrogen atoms (the  $N_{\text{inner}}$ ,  $(\text{NH})_{\text{inner}}$ , and  $N_{\text{meso}}$ ) in the metal-free complexes<sup>70</sup>. X-ray photoelectron spectroscopy was previously utilized to probe aspects of the bonding of the N-H protons in the centre of H<sub>2</sub>TBMAP and H<sub>2</sub>TBTAP. The spectra of the compounds were interpreted to reveal that each internal ‘N-H’ proton is localized at a pyrrole nitrogen with no interaction with the aza bridging nitrogens<sup>71</sup>.

### 1.5.1.2 Magnetic circular dichroism (MCD)

MCD is a spectroscopic technique which usually complements UV-visible spectroscopy. It is used to measure the differential absorption of left and right polarised light. This technique, combined with UV-Vis spectroscopy is used to investigate electronic transitions. Although mainly used for chiral molecules, achiral compounds still exhibit MCD (Faraday effect)<sup>72</sup>. MCD spectroscopy has previously been used to identify the main electronic bands of tetrabenzotriazaporphyrins and a tetranaphthotriazaporphyrin<sup>67</sup>.

MCD spectra of the copper-metallated macrocycles and time dependent density functional theory (TD-DFT) calculations are reported for the unsubstituted copper-metallated ligands. In the paper, the MCD spectral data are used to validate theoretical descriptions of the electronic structures provided by calculated TD-DFT and ZINDO/s spectra<sup>6</sup>. Michl’s perimeter model is used to analyse and predict the results observed in the experimental and calculated optical spectra, which provides a readily accessible conceptual framework<sup>73</sup>. TDDFT calculations have been employed to interpret the photophysical properties of a *meso*-substituted tetrabenzotriazaporphyrin and its magnesium and zinc complexes for further characterization of the UV-vis spectrum<sup>74,75</sup>. Moreover, DFT calculations were used to better understand the electrochemical redox process. The influence of the different number of meso-

nitrogen atoms on the redox properties of the macrocyclic copper derivatives was also investigated by cyclic voltammetry, square wave voltammetry (SW), and linear sweep voltammetry (LSV)<sup>70</sup>.

## 1.5.2 Solid State Properties

### 1.5.2.1 X-ray structure analyses

X-ray studies of tetrabenz(aza)porphyrins were carried out in 1939 of the metal-free and copper tetrabenzotriazaporphyrin crystals obtained by sublimation<sup>10</sup>. The main characteristic of the crystal lattice is that the molecules possessed a ‘pseudo’ centre of symmetry, which was attributed to the homogenous statistical distribution of the meso-carbon bridge<sup>76</sup>. Cammidge-Cook group at UEA were able to obtain single crystals of metal-free and magnesium *np*-(*n*-C<sub>6</sub>H<sub>13</sub>)<sub>8</sub> -TBTAP as well as crystals of the corresponding Mg-metallated TBMAP and TBP. These were the first reported examples of X-ray structures of ring-substituted hybrids and TBP. Replacement of two or three of the aza-linking atoms with methine groups leads to a quite different solid-state conformation.

The crystal structure of the compounds is isostructural, and the molecules have very similar dimensions, conformations, orientations and packing arrangements. The whole molecule of TBMAP and TBP was approximately planar in the crystal with greatest departure from planarity exhibited by TBTAP. The cores of the TBTAP molecules are parallel and each molecule is coplanar with the four molecules around it. More importantly, data were presented to show a comparison of the Mg-N distances which indicate an increase in the size of the central cavity as the series progresses towards less-nitrogenated compounds<sup>45</sup>.

A recently developed synthetic procedure afforded *meso*-aryl substituted tetrabenzotriaza porphyrin complexes and their structures were confirmed by X-ray<sup>47,50,77</sup>. It was shown that the presence of the *meso*-aryl substituent in the TBTAP molecule results in considerable and even unexpected structural effects<sup>77</sup>.

### 1.5.2.2 Mesophase behaviour (Liquid crystal properties)

The atoms or molecules in crystals exist in a highly ordered arrangement while no such order is present in liquids. An additional phase that can occur between isotropic liquid and crystalline solid and shares some of their properties is termed as liquid crystalline phase, mesophase or mesomorphic phase, (figure 1.4).

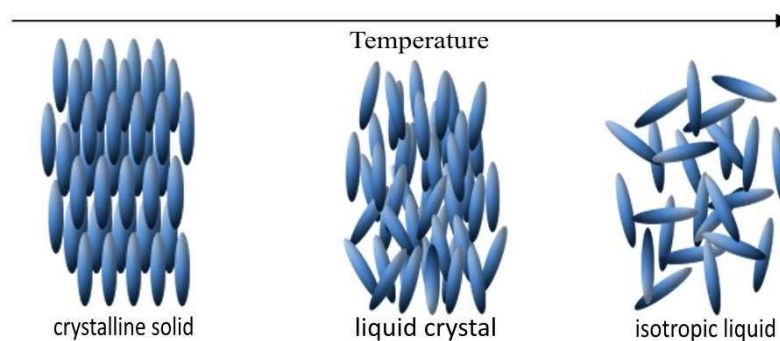


**Figure 1.4: Simplified diagrams of states of matter<sup>78</sup>**

Liquid crystalline phases can be formed *via* two different ways. For example, they can be obtained by heating or cooling the materials and these are called thermotropic liquid crystals, whereas the liquid crystals that are obtained by dissolving the materials in controlled amount of solvents, are named lyotropic liquid crystals. Depending on the molecular shapes, the thermotropic liquid crystals are classified as *calamitic* (rodlike) and *discotic* (disc-like) liquid crystals<sup>79</sup>.

Phthalocyanines typically belong to thermotropic, discotic liquid crystals. It is expected that tetrabenzotriaza porphyrin derivatives will exhibit the same mesophase behaviour as the parent phthalocyanine molecule due to their structural similarity<sup>80,81</sup>. (figure 1.5).

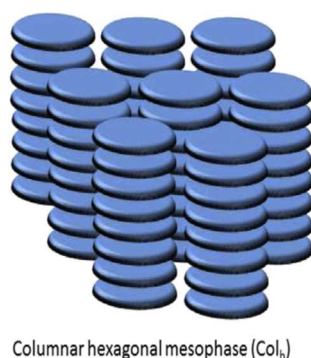


**Figure 1.5: Molecular arrangements in the (discotic) columnar mesophase<sup>82</sup>**

The thermotropic mesophase behaviour of an asymmetrically shaped and highly substituted tetrabenzotriazaporphyrin (TBTAP) derivative has been studied by optical microscopy, DSC and X-ray diffraction. In contrast to an earlier study of this system which described the structure of the mesophase as discotic lamellar<sup>83</sup>, detailed X-ray diffraction study indicates that the TBTAP derivative forms a disordered hexagonal columnar mesophase (Col<sub>h</sub>), with a weak tendency towards antiparallel orientation of neighbouring molecules observed in the form of a weak pseudo-centred rectangular packing<sup>84</sup>.

In 2011, a new set of mesophase data of *np*-octahexyl substituted TBTAP, TBDAP, TBMAP and TBP compounds was reported by Cammidge and Cook group. The data were obtained by means of differential scanning calorimetry (DSC) and polarising optical microscopy (POM). In regards to the clearing temperatures (mesophase to isotropic liquid), it was found that the metal-free series follow the trends set by the parent phthalocyanine analogues, whereas, the Cu-metallated series showed marked differences with clearing temperatures reducing significantly across the series. The mesophase behaviour of magnesium derivatives were complicated. However, it was reported that all the compounds display a columnar hexagonal phase (Col<sub>h</sub>)<sup>45</sup>.

A recent and detailed study discussed the mesophase behaviour of liquid crystalline mixture<sup>85</sup> and thin-films<sup>86</sup> of non-peripherally octa-hexyl-substituted phthalocyanine analogues. It is known that the origin of the favourable electrical properties of PcH<sub>2</sub> is strongly associated with their molecular packing structure. The crystal-to-crystal thermal phase transition and the selective crystal growth of C<sub>6</sub>PcH<sub>2</sub>, C<sub>5</sub>PcH<sub>2</sub>, and

C<sub>6</sub>TBTAPH<sub>2</sub> have been investigated by DSC and temperature-controlled XRD measurements<sup>87</sup>.

### 1.5.2.3 Electrical Properties and Thin film formation

Organic semiconductors have attracted much interest owing to their light weight and flexibility. In particular, some of these materials are applicable to “printed electronics” based on solution processing and are promising for realizing low-cost thin-film devices, such as organic field-effect transistors and organic photovoltaics. The high-performance devices utilising organic semiconductors require several characteristics such as high solubility in organic solvents, high carrier mobility, and a self-organized molecular orientation. Liquid crystalline (LC) organic semiconductors can potentially satisfy these requirements. In particular, discotic LC materials tend to self-assemble into a highly ordered columnar mesophase, and charge carriers are efficiently transported via the overlap of  $\pi$  orbitals along the axis of molecular stacking<sup>88</sup>.

Substituted phthalocyanine-based thin films are being used as the conductive layers in a wide range of optoelectronic devices, such as organic light-emitting diodes (OLEDs)<sup>89</sup>, organic solar cells<sup>90</sup> and organic field-effect transistors (OFETs)<sup>91</sup>. However, the challenging synthesis of the tetrabenzotriazaporphyrins has limited the thin film studies of the hybrid derivatives. In 1994, the effect of stearic acid molecules was investigated on the molecular orientation of Langmuir-Blodgett (LB) monolayers of (*t*-Bu)<sub>4</sub>-H<sub>2</sub>TBTAP-*n*-C<sub>15</sub>H<sub>31</sub><sup>69</sup>. Similar studies were carried out of its copper complex and (*t*-Bu)-substituted copper phthalocyanine. The data of comparative analysis of Langmuir layer were presented by Valkova and co-worker<sup>92</sup>. The structure of floating layers was estimated qualitatively, then followed by quantitative study later<sup>93</sup>.

The LB deposition technique appears to have received less attention over recent years and the spin-coating deposition provides a convenient and general method to formulate thin films due to the ease and quick preparation time. Cammidge and Cook group used this method in depositing films of *np*-octaalkyl substituted hybrid derivatives, which showed broader band UV-visible spectra in comparison to solution-phase spectra of the same materials<sup>8</sup>.

Additionally, spin-coated films had been reported of non-peripherally substituted nickel tetrabenzotriazaporphyrin molecules and their phthalocyanine analogues. The (hexyl)<sub>8</sub>-NiTBTAP transistor exhibits superior performance and both compounds can be utilized in printable electronics for large area roll-to-roll deposition on flexible substrates<sup>94</sup>. A comparative study of the electrical performance of two other organic thin-film transistors (OTFTs) fabricated with octadecyl substituted copper TBTAP and copper phthalocyanine analogue was performed with the aim of finding the best performance<sup>95</sup>.

Recently, bulk heterojunction (BHJ) organic solar cells (OSCs) have been the subject of much academic and industrial interest because of their potential to serve as a flexible, low-cost, and scalable source of electrical power. Discotic liquid crystalline (DLC) materials have been demonstrated as a novel type of small-molecule donors for bulk heterojunction (BHJ) OSCs which included phthalocyanine–tetrabenzoporphyrin hybrid macrocycles C<sub>6</sub>PcH<sub>2</sub> to C<sub>6</sub>TBPH<sub>2</sub> and C<sub>6</sub>TBTAPH<sub>2</sub><sup>96,97</sup>.

The search for renewable and environmentally friendly energy sources has become a current topic of interest due to the continuous depletion of fossil fuels and serious environmental issues. With the potential of becoming a clean and renewable energy source, dye-sensitized solar cells (DSSC) have drawn much attention because of their relatively high photoelectronic absorption efficiencies and lower production cost<sup>98</sup>.

## 1.6 Application of Tetrabenzotriazaporphyrins

Tetrabenzotriazaporphyrins were used as dyes due to their main features, their deep blue or green colour, as well as their analogues which contain various chromophore groups<sup>99,61,63</sup>. The needs of industry for compounds soluble in aqueous media gave rise to a class of water-soluble dyes, sulfonated derivatives of TBTAB have been utilised as reactive colorants and photoactivators<sup>62</sup>. Moreover, in the area of biological and medicinal chemistry, TBTAP derivatives, which are compatible with aqueous solutions and free of aggregation, have found use as fluorescent markers. These marker components are useful in applications such as fluorescence immunoassays, *in vivo* imaging and *in vivo* tumor therapy<sup>55,100</sup>.

Iron and manganese tetrabenzotriazaporphyrin complexes can serve as photo-oxidation catalysts in similar way that TBMAP and TBDAPs have been employed in oxidation of the o-cresols<sup>101</sup>. Complexes of unsubstituted tetrabenzotriazaporphyrin with certain transition metals (chromium, iron, manganese, cobalt and vanadium) are described for the possibility of their application as sensors for gases<sup>56,57</sup>. Tetrabenzotriazaporphyrin hybrid compounds are used also as optical data carriers as in electrographic recording materials and rewritable optical information recording medium<sup>102,103</sup>. Furthermore, free tetrabenzotriazaporphyrins are employed in electron diffraction devices as light-sensitive layers<sup>104</sup>. In recent years, azaporphyrin macrocycles, TBTAP included, have found use in various electro-optic devices. These include photo-absorbing (solar- and photo-sensitive devices), photo-emitting devices [organic light emitting diodes (OLEDs)] or devices capable of both photo-absorption and emission<sup>105,106</sup>.

## 1.7 Aim of the Project

In the past two decades, a growth in the number of publications on the synthesis and application of tetrabenzotriazaporphyrins is evidence that this is a promising field of investigation. The development of new methods for the synthesis of tetrabenzotriazaporphyrins and their complexes is an important aspect since the synthetic approaches to such compounds are not well developed. However, in the recent years our group in UEA has developed a straightforward and versatile synthesis of *meso*-substituted tetrabenzotriazaporphyrins (TBTAPs), thus, giving access to a range of new materials of functionalized TBTAPs. The improvement stemmed from using aminoisindoline as precursor which acts as initiator for macrocyclization. The UEA research group reported functionalized TBTAPs which are obtained from the parent TBTAP **69**, which is isolated in a good yield (40%) (scheme 1.28) and (scheme 1.29). The breakthrough new approach of the synthesis of TBTAP hybrids has the potential to stimulate further modification to functionalize the *meso*-phenyl TBTAP derivatives. Our approach is to synthesise new TBTAP derivatives by introducing various substituent to the benzene rings of the TBTAP macrocycle.

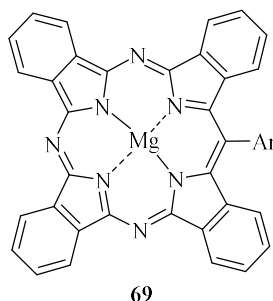


**Figure 1.6:** *meso*-Aryl-substituted tetrabenzotriazaporphyrin parent compound

The present project aimed to synthesise two series of functionalised *meso*-aryl TBTAPs with two main methods. In the first series, we aimed to investigate using various phthalonitrile derivatives with the same aminoisindoline precursor. However, the second series of TBTAPs employed derivatives of aminoisindoline to functionalise the macrocycles. To achieve that, we introduced substituent to the aminoisindoline benzene ring using various 2-bromobenzonitrile derivatives, (figure 1.7).

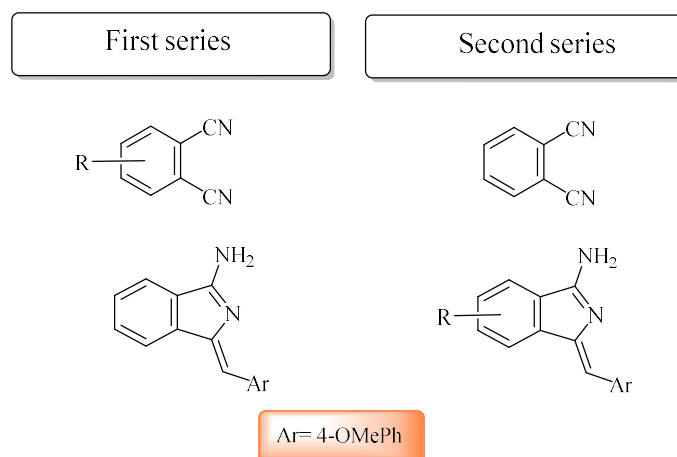


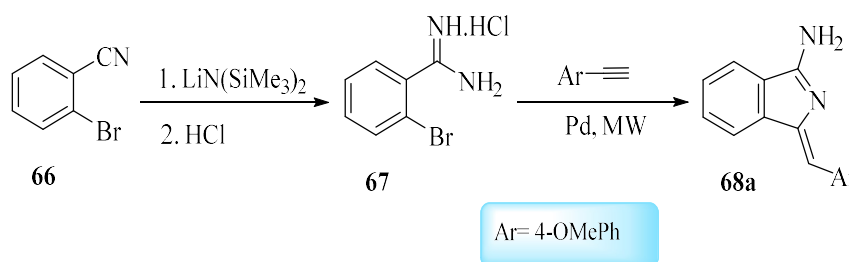
**Figure 1.7: The targeted precursors to functionalise the *meso*-aryl TBTAP**

The proposed formation of *meso*-substituted TBTAPs was believed to be initiated by the reaction between phthalonitrile and aminoisoindoline in the presence of magnesium ion and further addition of phthalonitrile lead to oligomer formation<sup>47</sup>. However, this project gave a strong indication that more complex reaction sequence operates. It was anticipated that working with the chosen precursors would provide mechanistic insight, and importantly lead to unprecedented new hybrids, while these compounds find ever increasing practical application in contemporary technologies.

## **Chapter 2: Results and discussion**

## 2.1 Introduction

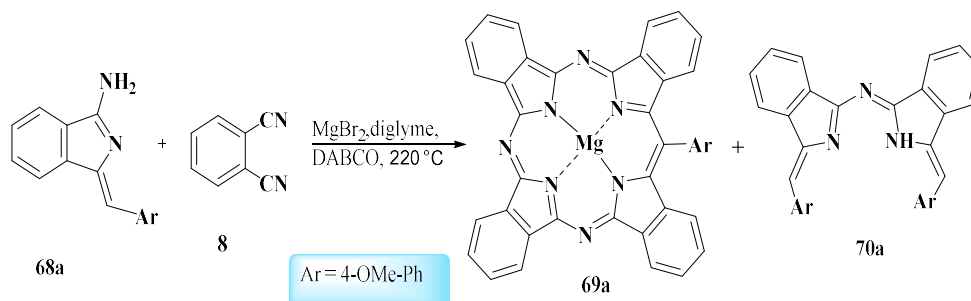
As the Tetrabenzotriazaporphyrin hybrids are related to both phthalocyanine and porphyrin, they have similar properties and potential applications. However, the difficulties and the challenges associated with their synthesis have led to reduce the interest and there has been a lack of their investigation. Recently, UEA group has increased their interest in synthesis of the TBTAP hybrids after they introduced the first example of a single isomer TBTAP synthesis from a serendipitous finding<sup>44</sup>. After the early encouraging results, the group has been working to develop a modern synthetic methodology to synthesize the TBTAPs. With greater success, the group reported a straightforward, versatile, high yielding synthesis of *meso*-substituted tetrabenzo triazaporphyrins TBTAPs<sup>47,50,51</sup>. The key in the new approach of synthesis was using an aminoisoindoline as an intermediate. They are themselves easily accessed following methodology shown in scheme 2.1.



**Scheme 2.1: Synthesis of aminoisoindoline 68a**

The reaction between aminoisoindoline precursor **68a** and phthalonitrile at 220°C was initiated in presence of magnesium ion as metal template. After the initiation, further phthalonitrile was added to complete the oligomer formation. The group reported a functionalized TBTAPs **69a**, which was isolated in a good yield (40%), (scheme 2.2). The complexes reported by the group mostly focused on functionalising the phenyl group on the *meso*-carbon linkage which would undergo additional reactions. However, in the present work our interest was to functionalise the TBTAP parent **69a** by introducing various substituents to the benzene rings on the macrocycle<sup>47,50,51</sup>. Herein, we used this synthesis and explored the effect of using various phthalonitrile and aminoisoindoline derivatives on TBTAP oligomer formation. It was anticipated that the study would allow some further mechanistic information to be obtained on the

TBTAP reaction. Thus, much of this research focuses on the synthesis and characterisation a new sets of peripherally substituted magnesium TBTAP complexes. The results are promising and encouraging for more future work and potential projects in tetrabenzo(aza)porphyrin hybrids.



**Scheme 2.2:** The general synthesis of *meso*-substituted TBTAB **69a**

Before commencing work on the synthesis of substituted-MgTBTAP derivatives we deemed it necessary to follow the procedure reported by Cammidge's group<sup>47</sup> to synthesize the TBTAP **69a**. This reported synthesis was carefully investigated to determine the factors controlling overall efficiency.

## 2.2 Synthesis of *meso*-substituted TBTAP **69a**

The synthesis of *meso*-substituted TBTAP **69a** was carried out as reported by the group to establish the reproducibility of the reaction conditions<sup>47</sup>, (scheme 2.2). According to the procedure, 3 eq of phthalonitrile with MgBr<sub>2</sub> in diglyme in a preheated mantle was heated for 10 min at 220°C under Argon atmosphere. A solution containing phthalonitrile **8** and aminoisoindoline **68a**, (1eq each), in dry diglyme was added to the heated mixture using a syringe pump over 1h. Once the addition was completed, another solution of phthalonitrile (1eq) and DABCO in diglyme was added also over 1h and with the syringe pump. The solvent was removed under a stream of Argon, the reaction mixture allowed to cool, then (1:1) of (DCM:MeOH) was added. The crude was purified using two flash column chromatography separations. The first column was carried out using DCM which eluted the red fraction, which was the aminoisoindoline dimer **70a**. Then a mixture of DCM:Et<sub>3</sub>N (20:1), and

DCM:THF:Et<sub>3</sub>N (10:1:4) was used to separate the green-blue fraction. The green-blue material was subjected to a second column, and a mixture of PE:THF:MeOH (10:3:1) was used as an eluent.

Our first attempts to synthesise the TBTAP **69a** followed the same procedure as reported. There were visible colour changes, from colorless to deep green/blue colour, in the reaction mixture after heating for a few minutes. The colour got deeper green with continuous addition of the other solutions. The reaction mixture was analysed by thin layer chromatography (TLC) and showed a blue spot corresponding to the expected Mg-Pc, the red aminoisoindoline “dimer” **70a** and MgTBTAP **69a**. Mg-phthalocyanine was the dominant product, and the TBTAP was isolated with a very low yield and with impurity. It had previously been established that heating above 220°C caused Pc formation from reaction of phthalonitrile and MgBr<sub>2</sub>. The high and uncontrolled temperature from the mantle was causing this problem. After several unsuccessful attempts to get pure TBTAP, we decided to replace the heating source from mantle to an oil bath to ensure an even and controlled temperature. The reaction was monitored as we heated the reaction mixture; we observed that at a lower temperature (140-180°C) the aminoisoindoline dimer was easily formed and the precursor was mostly consumed. By the end of the reaction, the dimer and Mg-Pc were the major products, and we were having the same issues with TBTAP yield and impurity. Thus, we preheated the oil bath to the desired temperature and placed the reaction mixture to minimise the red dimer formation and ensure that aminoisoindoline participate in TBTAP cyclisation. After separation, we finally obtain a pure sample of TBTAP **69a** after it had been recrystallised from a mixture of acetone and EtOH. Since the oil bath was not easy to handle, especially when we have the syringe pump, we tried to use the more popular DrySyn<sup>®</sup> heating block instead. The yield was slightly lower than the oil bath but it was much better than mantle, which provided more fluctuating heating. The table (2.1) summarises the effect of the heating source on the yield of the TBTAP. In addition to that, we have to consider that the phthalonitrile needed to be recycled from hot xylene before it was used as precursor in this reaction. Furthermore, Mg-Pc impurity in TBTAP was the biggest issue in the second separation by chromatography column. The Mg-Pc impurity is not easy to detect in TLC especially if it is diluted, thus we often discarded any fraction that we

suspected to include Pc or we frequently checked the fractions with MALDI-TOF MS before mixing the fraction together.

Heating source	observations
Heating mantle	Dimer <b>70a</b> was dominant product with gradual increase of the temperature, and Pc in higher temperature and low yield of TBTAP (less than 10%)
Oil bath	In preheated oil bath a mixture of dimer <b>70a</b> and MgPc with average 20% yield of TBTAP
DrySyn <sup>®</sup> block	Same observation from oil bath and lower yield (average 17%)

**Table 2.1: Influence of the heating source on TBTAP **69a** yield**

<sup>1</sup>H NMR spectroscopy in deuterated acetone for **69a** give similar spectra to the reported compound in deuterated tetrahydrofuran. As shown in figure 2.1, there are two protons as doublet at 9.62 ppm with coupling constant ( $J = 7.6$  Hz), and four protons as multiplet in range from 9.59 – 9.49 ppm. The figure also shows a peak at 8.26 ppm which appeared as doublet of doublet with four protons integration ( $J = 6.0, 2.6$  Hz). The four protons of the aromatic ring in the meso position appeared as doublet at 8.06 and 7.58 ppm with coupling constant ( $J = 8.5$  Hz). Two peaks are triplets with two protons integration each at 8.00 and 7.69 ppm, and the last two protons in the aromatic range were a doublet at 7.25 ppm ( $J = 8.2$  Hz). At 4.23 ppm the peak of the methoxy group appears as a singlet. The data is consistent with the values in the reference compound<sup>47</sup>.

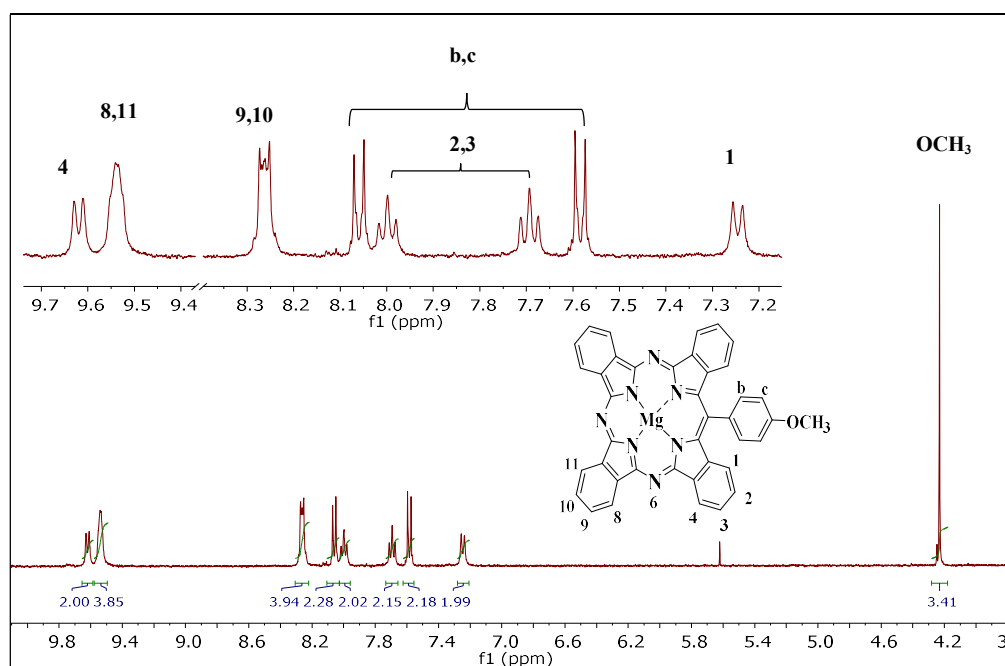


**Figure 2.1:**  $^1\text{H}$  NMR spectrum of TBTAP 69a

After we successfully found reproducible reaction conditions to give the TBTAP with average 20% yield, we moved to investigate the synthesis of functionalised *meso*-substituted TBTAPs and we classified them to two main series.

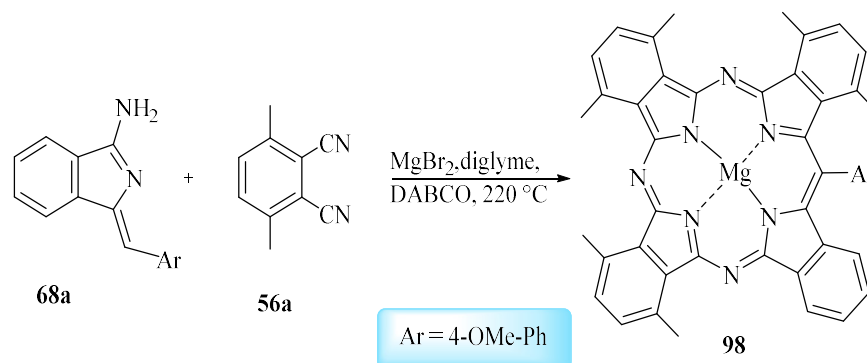
As mentioned in the section 1.6, we aimed to use substituted phthalonitriles for the first series, with consistent use of the aminoisoindoline **68a** as precursor for the whole series. On the other hand, the second series of TBTAP hybrids, various aminoisoindoline derivatives will be used with unsubstituted phthalonitrile **8**, (figure 1.7).

## 2.3 Synthesis of the first series of TBTAP hybrids

### 2.3.1 3,6-Di-substituted phthalonitrile derivatives

Non-peripherally substituted phthalocyanines appear to present less aggregation and improved solubility<sup>80</sup>. Using 3,6-di-substituted phthalonitriles for TBTAP synthesis indicated the problem of steric hindrance when the *meso*-position is occupied by a substituent. With use of the Cambridge group's prior knowledge regarding the synthesis of non-peripherally substituted tetrabenzotriazaporphyrins<sup>45</sup>, we have chosen a precursor with small substituents as in 3,6-dimethylphthalonitrile **56a**, which

was prepared by a former lab member and available to use for a TBTAP synthesis<sup>107</sup>. The reaction was performed as described in the last section and the reaction mixture turned to dark green colour product which indicates formation of Pc/TBTAP, (scheme 2.3).



**Scheme 2.3: Attempt to synthesise MgTBTAP from 56a**

The work up and separation proceeded as normal and we isolated the green fraction from other impurities. However, the isolated compound decomposed when left in the fridge to crystallise. We made several attempts to repeat the reaction with more precautions to avoid the decomposition but with no success. The product either decomposed during the separation or when it was left to crystallise. The instability of 3,6-disubstituted TBTAPs, even when there was a small group such as the methyl group, agreed with the prior studies<sup>45</sup>, which led us to eliminate this group of phthalonitriles from consideration in this present research.

### 2.3.2 4,5-Disubstituted phthalonitrile derivatives

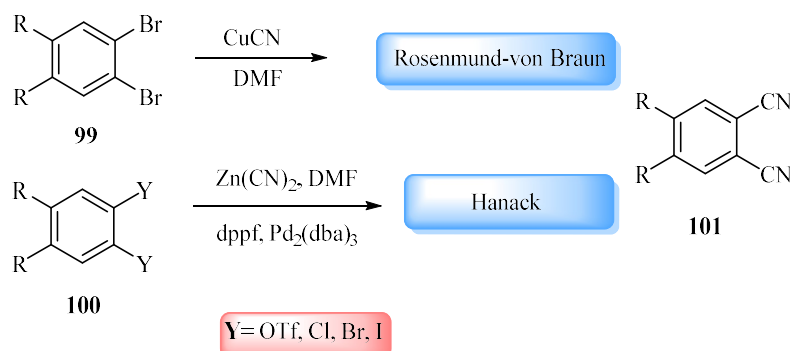
The 4,5-disubstituted phthalonitrile certainly seemed the most suitable materials to use in our investigation. Several synthetic routes to synthesize 4,5-di-substituted phthalonitriles are briefly discussed in the next section.

#### 2.3.2.1 Synthesis of 4,5-di-substituted phthalonitrile

##### 1. Classic approaches

The Rosenmund-von Braun cyanation<sup>108</sup> is widely used when preparing 4,5-disubstituted phthalonitriles **101**. A mixture of dibrominated derivative **99** and copper

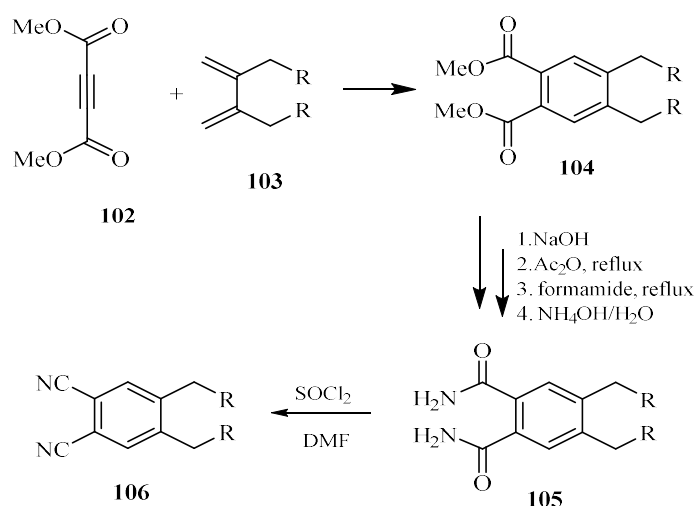
cyanide in dry DMF is refluxed in the traditional conditions for this reaction. Alternative cyanation was developed by Hanack<sup>109</sup> which used zinc cyanide as the cyanide source and palladium as a catalyst to convert aryl triflate or halides **100** into nitriles **101**, (scheme 2.4).



**Scheme 2.4: Classic cyanation reactions**

## 2. Diels-Alder cycloaddition

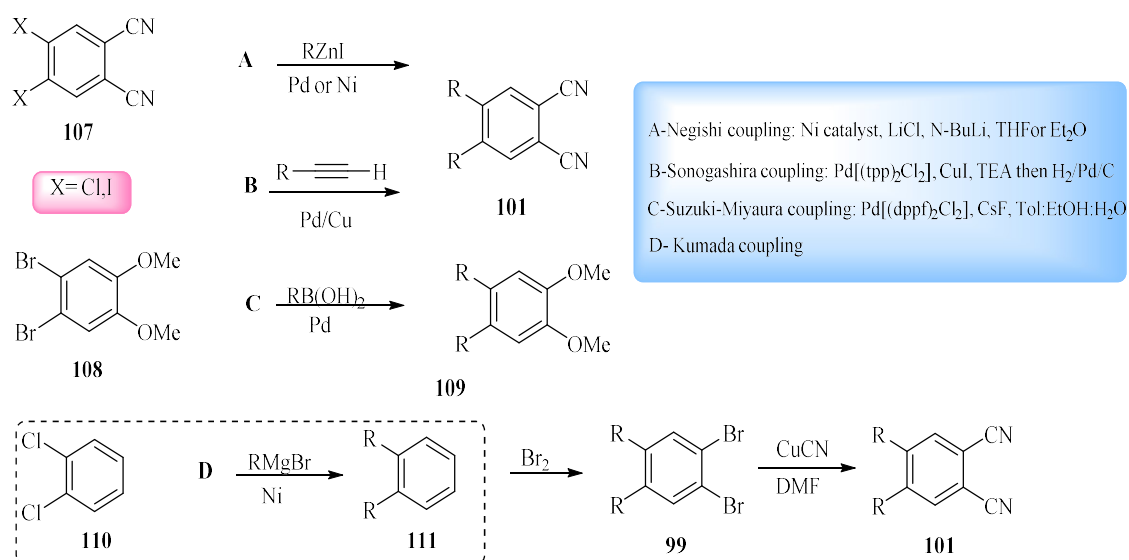
The Diels-Alder cycloaddition has been successfully applied to prepare 4,5-disubstituted phthalonitriles **106**, usually *via* multiple steps<sup>110,111,112</sup>. The scheme (scheme 2.5) shows a typical synthesis which involves the 4+2 addition using a commercially available dimethylacetylenedicarboxylate (DMAD) **102**, then followed by demethylation of the product and it continues with multi steps to finally reaches the dehydration step using thionyl chloride to afford the targeted 4,5-substituted phthalonitrile **106**. Phthalonitrile with substituent such as alkyl, phenyl, ester, silyl or amines have been prepared by Diels Alder addition. Moreover, other dienes and dienophiles can be used for the synthesis of substituted phthalonitrile<sup>107</sup>.



Scheme 2.5: Diels-Alder synthesis of 4,5- disubstituted phthalonitriles

### 3. Cross-coupling reactions

Metal catalysed coupling reactions are routinely employed to generate C-C and C-heteroatom bonds. Cross-couplings such as Negishi<sup>113</sup>, Sonogashira<sup>114</sup>, Suzuki-Miyaura<sup>115</sup> and Kumada<sup>116</sup> reactions are powerful and widely used for preparing 4,5-disubstituted phthalonitrile **101**. A brief description of how these cross-coupling reactions are employed to synthesize 4,5-di-substituted phthalonitrile is given below, (scheme 2.6).



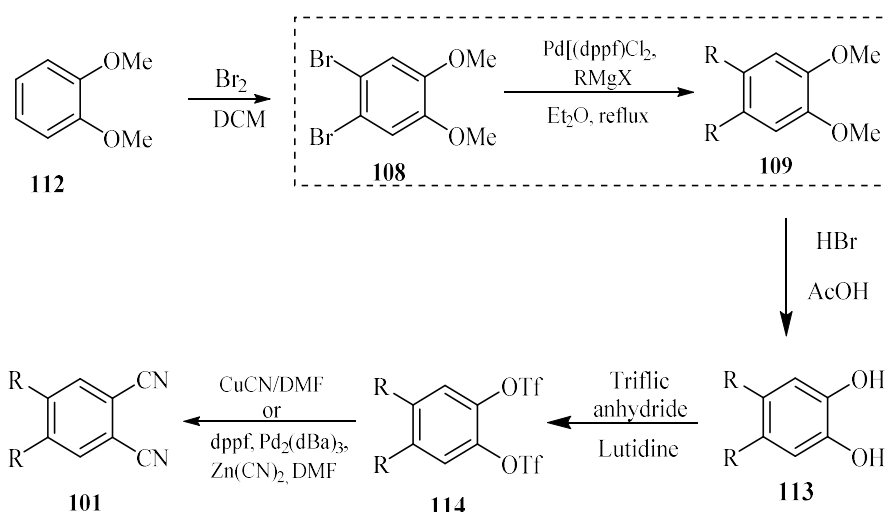
Scheme 2.6: Cross-coupling reactions to synthesise 4,5-di-substituted phthalonitriles

Negishi cross-coupling reactions<sup>113</sup> are straightforward and powerful strategies to prepare 4,5-di-substituted phthalonitriles **101** in a single step. The Negishi coupling reaction involves reaction between aryl halides **107** and organozinc reagents using nickel or palladium as catalysts. 4,5-Dichlorophthalonitrile was used with alkylzinc iodide reagent to attempt to prepare the 4,5-dialkylphthalonitrile by a previous member from our lab. However, the purification of this compound proved to be difficult due to the mixture of the side products which was obtained from the reaction. Similarly, when 4,5-dibromoveratrole **108** was used as substrate, the observed result was mostly starting material, mono-alkylsubstituted and alkyl-alkyl coupling with only traces of 4,5-di-substituted veratrole<sup>78</sup>.

Sonogashira cross-coupling reaction<sup>114</sup> was reported by Leznoff's group<sup>117</sup> as a synthetic route for preparing 4,5-disubstituted phthalonitrile **101**. A terminal alkyne, in excess, reacts with 4,5-diiodophthalonitrile in triethylamine (TEA) at 110°C in presence of Pd and CuI as catalysts to give the 4,5-dialkynylphthalonitrile. Then, the desired 4,5-dialkylphthalonitrile was achieved by hydrogenation of 4,5-dialkynyl phthalonitrile. As with Negishi coupling, this approach has been investigated by our lab members and the synthesis of the 4,5-diiodophthalonitrile proved to be impractical due to difficulties in the synthesis of the starting material for this reaction in good yield. A mixture of a wide range of iodinated products were obtained and attempts were made to separate the mixture with no success<sup>78</sup>.

Third cross-coupling reaction is Suzuki-Miyaura coupling<sup>115</sup>, which is one of the convenient reactions for C-C bond formation. In this coupling, organoboron reagents are used which exhibit stability toward air, moisture and thermal treatment. A suitable organic halide or related electrophiles were used as the coupling partner. The general method for Suzuki coupling involves treatment of aryl halide **108** with arylboronic acids in presence of a Pd[(dppf)<sub>2</sub>Cl<sub>2</sub>] catalyst with CsF as a base. Unfortunately, the Suzuki approach also failed to produce the desired products as major products when it was investigated by other members in our group. The Suzuki coupling was applied to both 4,5-dichlorophthalonitrile **107** and 4,5-dibromoveratrole **108** and gave unwanted coupling products in many cases<sup>78</sup>.

Finally, the Kumada cross-coupling reaction<sup>116</sup> as another option can be used for preparing the 4,5-disubstituted phthalonitriles **101**. Dichlorobenzene **110** is treated with a freshly prepared alkylmagnesium bromide and Nickel catalyst to give di-substituted alkylbenzene **111**. Bromination and cyanation gives the target phthalonitrile **101**. This route has proved to be difficult to apply and needs to be modified in some cases. Previous work in our lab developed a new synthetic route by optimizing Kumada cross-coupling reactions, where 4,5-dibromoveratrole **108** was used. The new synthetic procedure proved to be reliable and feasible for synthesis of 4,5-disubstituted phthalonitrile **101**, with strict and careful conditions in terms of temperature and reagents portions, (scheme 2.7). Cook-Cammidge group reported synthesis of 4,5-disubstituted phthalonitriles with various alkyl groups<sup>118</sup> (R= n-C<sub>6</sub>H<sub>13</sub>, n-C<sub>7</sub>H<sub>15</sub>, n-C<sub>9</sub>H<sub>19</sub>). However, this route is not pursued in this project for reasons that will be discussed in next section.



**Scheme 2.7: Controlled synthetic route for the synthesis of 4,5-disubstituted phthalonitriles**

After exploring the possible substituted phthalonitriles and together with the aim of this project, a decision was made to employ 4,5- alkoxy and phenoxy phthalonitrile derivatives **115-118** and heavily branched group **119** for our new TBTAP reactions using the classic Rosenmund-von Braun reaction<sup>119</sup>, (figure 2.2). In addition, we explored the synthesis of naphtho-annulated tetrabenzotriazaporphyrins by using the

commercially available 1,2-naphthalenedicarbonitrile. The Rosenmund–von Braun reaction<sup>108</sup> was used throughout this project to convert the dibromo derivatives **99** into their corresponding dinitrile derivatives **101**. Despite the problematic synthesis and low-yield of this approach, it was preferable for several reasons. First of all, the ease of synthesis of the dibromo derivatives **99** from commercial and affordable sources in simple reactions and in big scale suitable for the synthesis. Also, some of the dialkyloxy derivatives synthesis was developed by our group for other projects<sup>120,121</sup>. In addition, the side product from the reaction was isolated and used for our next series of TBTAP hybrids as will be discussed later in this chapter.

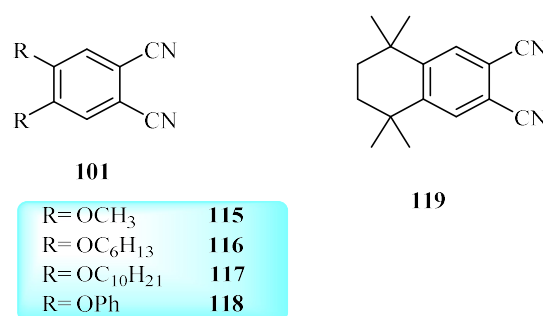
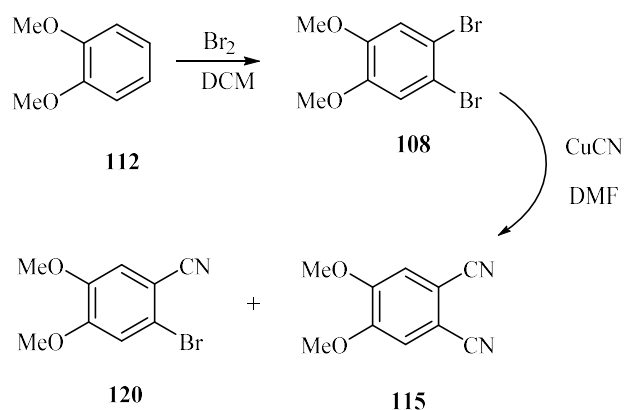


**Figure 2.2: Targeted 4,5-disubstituted phthalonitrile precursors**

### 2.3.2.2 Synthesis of phthalonitrile **115** and its TBTAP complex **121**

4,5-Dimethoxyphthalonitrile **115** was easily synthesised by the Rosemund-von Braun cyanation<sup>108</sup> which used CuCN as a cyanide source, (scheme 2.8). Despite the toxicity of the reaction and the messy work up and formation of several side products in this reaction, it was to our benefit to separate one of them. The monosubstituted product **120** in this reaction was used as starting material in the second series of TBTAP hybrids as will be discussed later in this chapter. Dibromoveratrole **108** was synthesised using simple bromination of commercially available veratrole **112**. The bromination was achieved by dropwise addition of bromine to a solution of veratrole in DCM at 0°C. Then, the mixture was left to warm to room temperature and left to stir overnight. After work up, the crude product was dried, and the solvent was removed under reduced pressure then recrystallised using 2-propanol to afford the

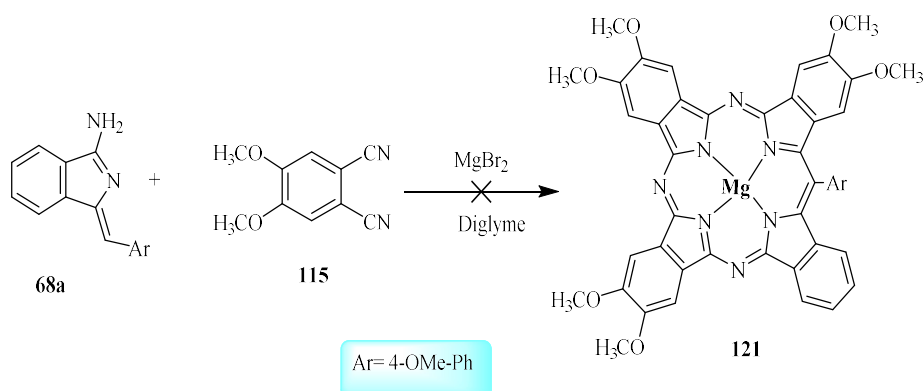
dibromoveratrole **108** with 98% yield<sup>122</sup>. Cyanation of dibromoveratrole using CuCN in dry DMF at 150-153°C gave **115**<sup>123</sup>.



**Scheme 2.8: Synthesis of dimethoxy phthalonitrile 115**

However, the cyanation reaction was challenging in some aspects as expected, at higher temperature the formation of copper phthalocyanine was obvious. Thus, controlling the temperature was important and it must be avoided to raise the temperature above 153°C. The reaction was monitored by TLC every hour, and as we needed the monosubstituted product **120** from this reaction, the starting material wasn't completely consumed. The reaction was left to reflux for maximum 3 hours and upon cooling DCM was added to the mixture then filtered to remove the copper salts. The filtrate was then washed with  $\text{NH}_4\text{OH}$  until no blue colour was obtained. The crude product was purified using column chromatography. Since the dibromoveratrole **108** was not completely consumed the TLC showed three spots with the first spot corresponding to the starting material **108**. The second spot was isolated as the monosubstituted nitrile **120** and third spot was our targeted dimethoxy phthalonitrile **115**. The difference in  $R_f$  of the starting material **108** and monosubstituted nitrile **120** was very small on the TLC so separating them was achieved by gradient solvent system. First PE:DCM (3:1) to remove starting material then PE:DCM (2:1) which eluted the remaining starting material mixed with mono product **120** and finally the pure mono product in later fractions. Under these conditions copper phthalocyanine formation was not observed in most of the cases. Controlling the temperature and the time in this reaction was crucial to avoid Cu-Pc formation and to get acceptable yield.

With our 4,5-dimethoxyphthalonitrile **115** in hand, we performed the TBTAP synthesis with aminoisoindoline **68a** using the same conditions that we optimised previously. A mixture of 3eq of 4,5-dimethoxy phthalonitrile **115** and  $\text{MgBr}_2$  in diglyme was heated at  $220^\circ\text{C}$  under Argon using preheated oil bath. A second solution from 1eq of 4,5-dimethoxy phthalonitrile **115** and 1eq of aminoisoindoline **68a** in dry diglyme was added to the heated mixture using a syringe pump over 1h. When the addition was completed, another 1eq of **115** and DABCO in diglyme was added over 1h. Surprisingly, we observed that no TBTAP or Pc was formed at all; it usually takes a few minutes to observe the green colour after heating the mixture. The reaction was completed as normal and when it finished the crude mixture was mostly red fraction (dimer **70a**), unreacted starting material and a brown fraction. We also observed a very weak green spot on TLC near the baseline. Repeating the same reaction in lower and higher temperature gave the same result with no change and no formation of either Pc or TBTAP **121** under these conditions. The fact that MgPc was formed from phthalonitrile under similar conditions suggest that the low reactivity of dimethoxy phthalonitrile may affect formation of both Pc and TBTAP, (scheme 2.9).



**Scheme 2.9: Attempted synthesis of methoxy substituted TBTAP 121**

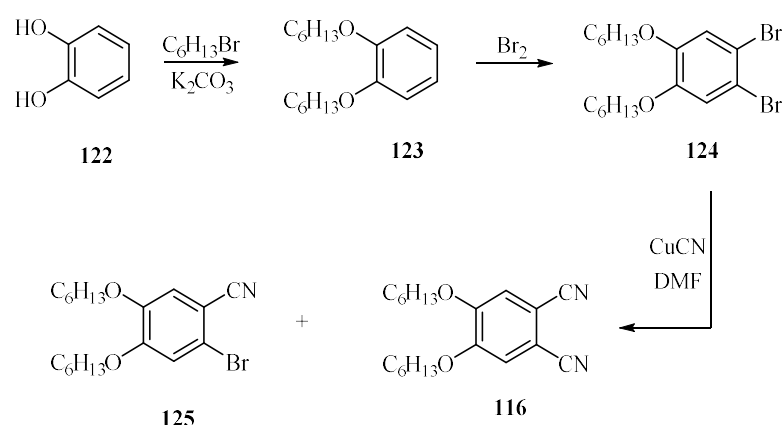
4,5-Dimethoxyphthalonitrile **115** was used as a precursor to prepare the metal-free octamethoxyphthalocyanine and metallo-octamethoxyphthalocyanines  $[(\text{OMe})_8\text{MPc}]$  ( $\text{M} = \text{Zn}, \text{Cu}, \text{Ni}, \text{Mg}, \text{Co}, \text{Fe}, \text{Ru}, \text{TiCl}$  and  $\text{RhCl}$ )<sup>124</sup>. However, these reactions were carried out with presence of DBU as a strong base catalyst by conventional thermal treatment and by using green energy techniques such as exposure to UV-irradiation as well as microwave irradiation<sup>124,125,126</sup>. In the literature, no TBTAP ligands or complexes were reported bearing methoxy-substituents on benzo-subunits, thus, no

further investigation was undertaken and we moved to the second targeted compound in this section.

### 2.3.2.3 Synthesis of phthalonitrile 116 and its TBTAP complex 127

The nature of the substituents not only affects the solubility of the TBTAPs but also their physical and chemical behaviour. Thus, attention was switched to long-chain 4,5-dialkoxy phthalonitrile, which could aid formation and isolation of TBTAPs unlike methoxy phthalonitrile.

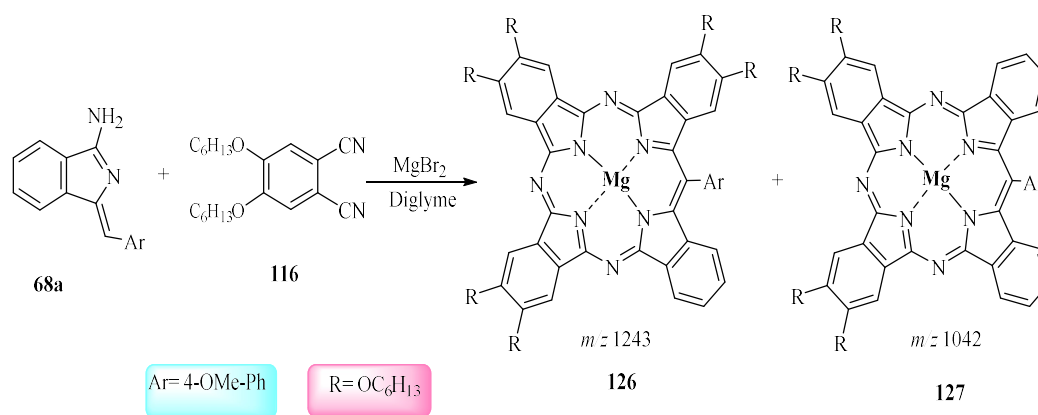
Generally, 4,5-alkoxysubstituted phthalonitriles were prepared by simple alkylation of commercially available catechol **122** followed by bromination reaction to form 1,2-dibromo-4,5-dialkoxybenzene. Following the procedure developed by our group, catechol **122** and 1-bromohexane were stirred with potassium carbonate in ethanol at reflux to yield the dihexyloxybenzene<sup>120</sup> **123**. Subsequent bromination gave 1,2-dibromo-4,5-di-hexyloxybenzene **124**. It was a straightforward synthesis of 1,2-dibromo-4,5-dihexyloxybenzene **124** and gave good yields in large scale synthesis<sup>121</sup>. The cyanation reaction<sup>127</sup> was similar to that described previously [in synthesis of dimethoxy phthalonitrile **115**], (scheme 2.10). Conditions, temperature and time, were carefully controlled to minimize CuPc formation and also gave access to 2-bromobenzonitrile **125**. The structure of the compounds was confirmed by NMR spectroscopy.



Scheme 2.10: Synthesis of 4,5-dihexyloxy phthalonitrile 116

The synthesis of TBTAP was attempted using 4,5-dihexyloxy phthalonitrile **116**. In contrary to what we observed when dimethoxy phthalonitrile **115** was used, green colour was observed after a few minutes of the addition of the aminoisoindoline solution which indicated formation of TBTAP and/or Pc. However, the poor solubility of **116** in diglyme caused blockage in the syringe and the pump stopped. The reaction was performed again as a one pot reaction with the same quantities to the original reaction for maximum two hours and worked up as usual. The crude mixture was separated using two column chromatography. First, we used DCM as an eluent to remove the red fraction, then DCM:Et<sub>3</sub>N (20:1) → DCM:THF: Et<sub>3</sub>N (10:4:1) to isolate the other fractions depending on their colour. The green fraction was only subject to the second column, and we used PE:THF (5:1) mixture as eluent.

It was found that the green fraction consisted of multiple spots on TLC, analysing the spots by MALDI-TOF MS gave some indication of the products in the green fraction. First spot was easily identified as (OC<sub>6</sub>H<sub>13</sub>)<sub>8</sub>-MgPc derivative, but was very weak. The second spot corresponded to our expected TBTAP **126** which gave *m/z* 1243 in addition to an unknown green fraction with *m/z* 1042. Several attempts were made to separate the mixture with different solvents using column chromatography, separation was really challenging. The spots were very close and one spot was very sensitive to the light more than the others, however, we successfully separated one compound in pure state. The main fraction isolated was analysed by MALDI-TOF mass spectrum and gave a molecular ion peak (*m/z* 1042) which identified as (OC<sub>6</sub>H<sub>13</sub>)<sub>4</sub>-MgTBTAP **127**, (figure 2.3), (scheme 2.11). This unexpected result is the first example of a ABBA-Ar TBTAP.



Scheme 2.11: Synthesis of TBTAP hybrid 126 and 127

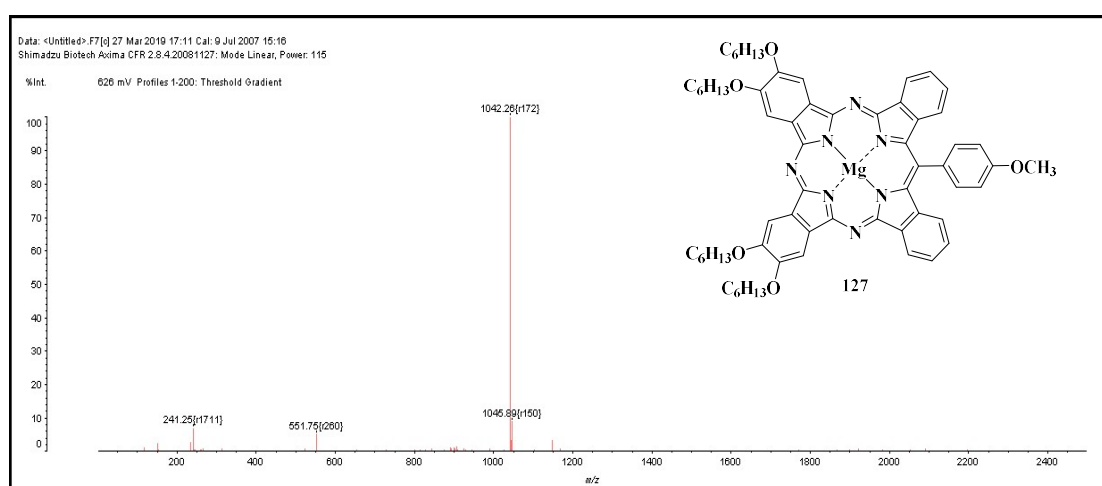


Figure 2.3: MALDI-TOF MS for TBTAP complex 127

The isolated compound was pure and characterised by NMR to correspond to the *p*-(OC<sub>6</sub>H<sub>13</sub>)<sub>4</sub>TBTAP-(OMe-Ph) hybrid **127**. The <sup>1</sup>H NMR spectrum in deuterated tetrahydrofuran gave all signals corresponding to all protons on the compound, (figure 2.4). All signals for sixteen aromatic protons from 9.56-7.22 ppm range are observed. Four aromatic protons were from the phenyl group at meso-position, eight protons were on the peripheral positions and four protons on non-peripheral positions of the tetrabenzotriazaporphyrin macrocycle. Also, the peaks at 4.62-4.58 ppm range corresponded to the methylene group from the alkyloxy group and the protons from methoxy group at the *meso*-position were found at 4.19 ppm. The protons of the alkoxy chains were at 2.12-1.04 ppm range as expected. The product was analysed by UV-Vis spectroscopy and showed the distinctive split Q-band at 670 and 648 nm.

Compound **127** failed to provide a suitable crystal for X-Ray diffraction analysis after several attempts.

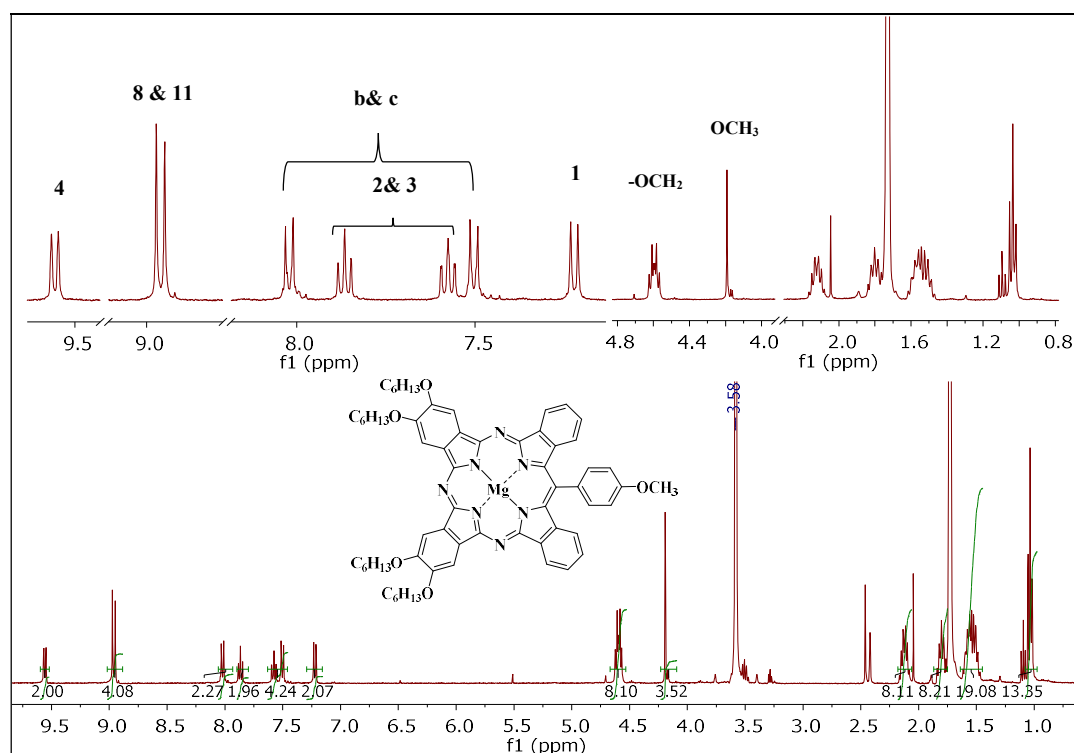


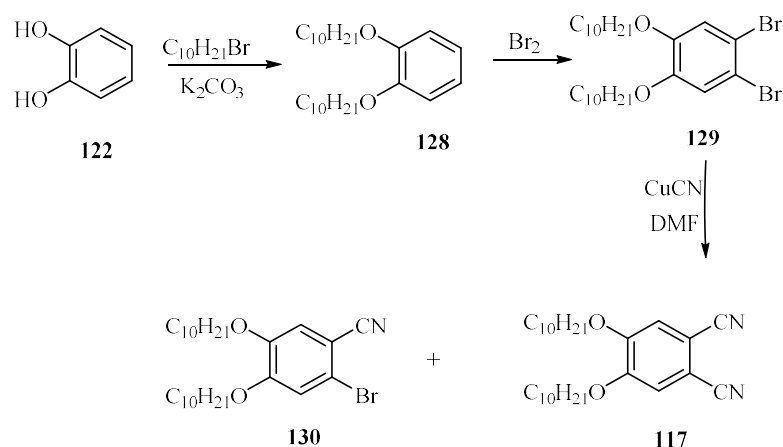
Figure 2.4:  $^1\text{H}$  NMR spectrum of TBTAP **127**

Given these unexpected results, the reaction was repeated and gave the same outcomes and demonstrating reproducibility. We expected TBTAP **126** to be the major and only hybrid beside MgPc, so this was a remarkable result. The complex **126** was formed in this reaction as a side product, however, it was very sensitive to the light and some difficulties associating with its purification due to both MgPc and **127** impurities. Thus, from this point, we moved to the next phthalonitrile for further investigation and verification of this result.

#### 2.3.2.4 Synthesis of phthalonitrile **117** and its TBTAP complex **132**

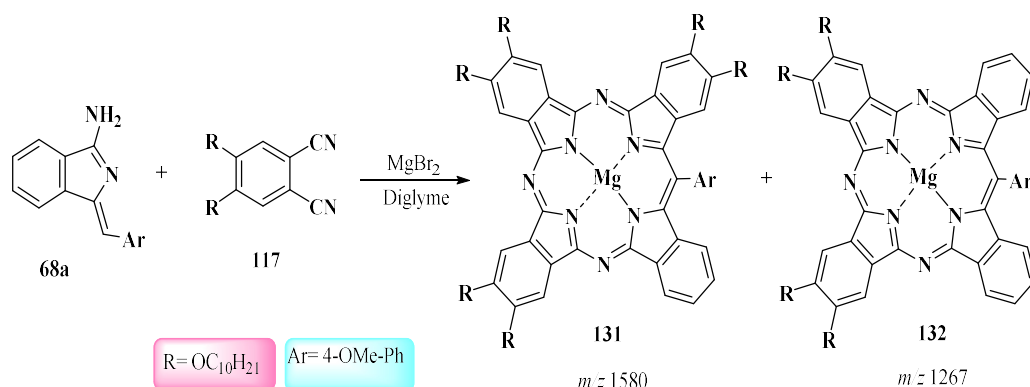
4,5-Didecyloxy phthalonitrile **117** was chosen to be the next phthalonitrile in this series, its synthesis was similar to 4,5-dihexyloxy phthalonitrile **116**. Starting from 1-bromodecane with catechol to produce **128**<sup>120</sup> and followed by bromination<sup>121</sup> and

cyanation reaction<sup>127</sup> as we described earlier to give **129**, **117** and **130** as shown in the scheme 2.12.



**Scheme 2.12: Synthesis of 4,5-dialkoxyphthalonitrile 117**

Performing TBTAP reaction using phthalonitrile **117** faced the same solubility issue as we faced previously with dihexyloxy phthalonitrile **116**. Due to the poor solubility of the substituted phthalonitrile **117** in diglyme at room temperature, this reaction was also performed without the slow addition and without the syringe pump. After completion of the reaction, the crude mixture showed several spots on the TLC for the green fraction. In similar way to the previous reaction, the analysis of the spots by MALDI-TOF MS showed similar formation of several hybrids, (scheme 2.13). The spots were found to be corresponding to  $(OC_{10}H_{21})_8$ -MgPc ( $m/z$  1786) and two MgTBTAP hybrids **131** and **132** ( $m/z$  1580, 1267 respectively) as shown in figure 2.5.



**Scheme 2.13: Synthesis of decyloxy TBTAP hybrid 132**

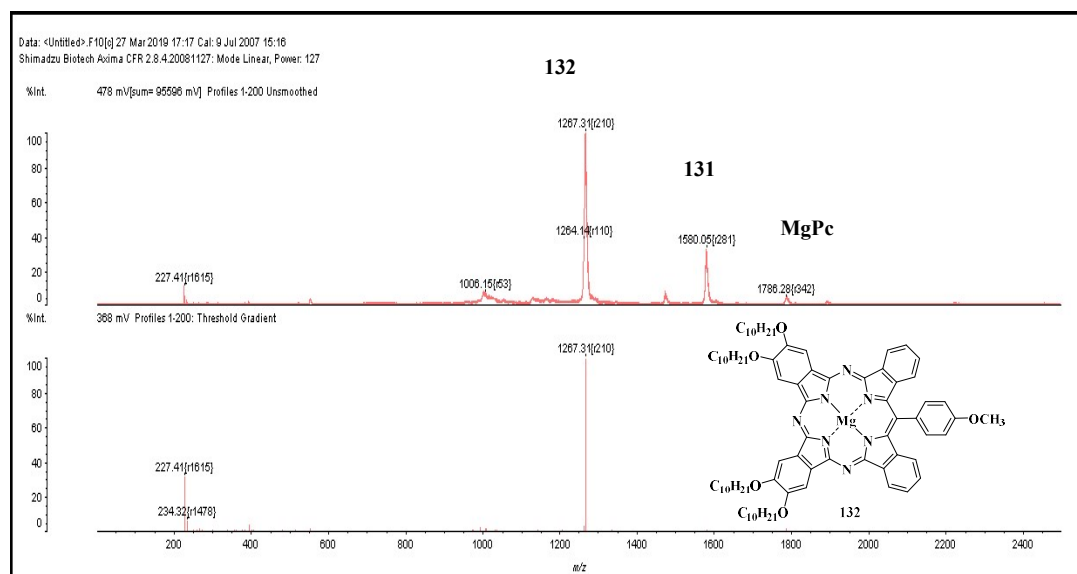


**Figure 2.5: MALDI-TOF Ms of (OC<sub>10</sub>H<sub>21</sub>)<sub>n</sub>-MgTBTAP hybrids in a mixture**

So far, using substituted phthalonitrile proved to give *p*-(alkoxy)<sub>4</sub>MgTBTAP-(OMe-Ph) hybrid as a major product and traces of hexa-substituted hybrid and Pc. The isolated compound **132** gave exact molecular ion peak in the MALDI-TOF mass spectrum ( $m/z$  1267). The product was analysed by UV-Vis spectroscopy and showed the distinctive split Q-band at 673 and 649 nm as shown in the figure 2.6.

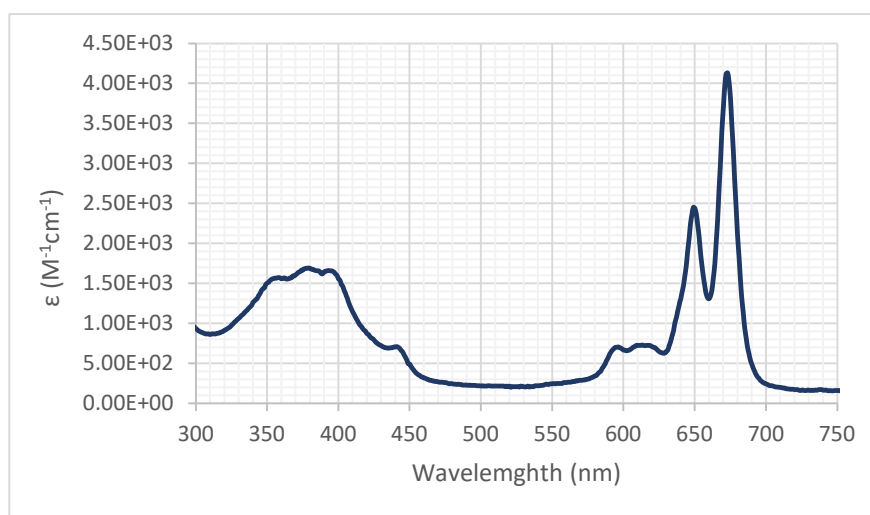


**Figure 2.6: UV-Vis spectrum of 132**

We can see the similarity of <sup>1</sup>H NMR spectra for both compounds **132**, (figure 2.7) and compound **127** in deuterated tetrahydrofuran (figure 2.4). (OC<sub>10</sub>H<sub>21</sub>)<sub>4</sub>-MgTBTAP-(OMe-Ph) hybrid **132** gave all signals corresponding to its structure. A total of sixteen

aromatic protons from 9.68-7.34 ppm range were assigned to the protons from benzene units in the macrocycle. The peaks at 4.68-4.31 ppm range corresponded to the methylene groups from the alkyloxy groups and methoxy group at the *meso*-position. The decyloxy chain protons appeared at 2.24-1.05 ppm range as expected.

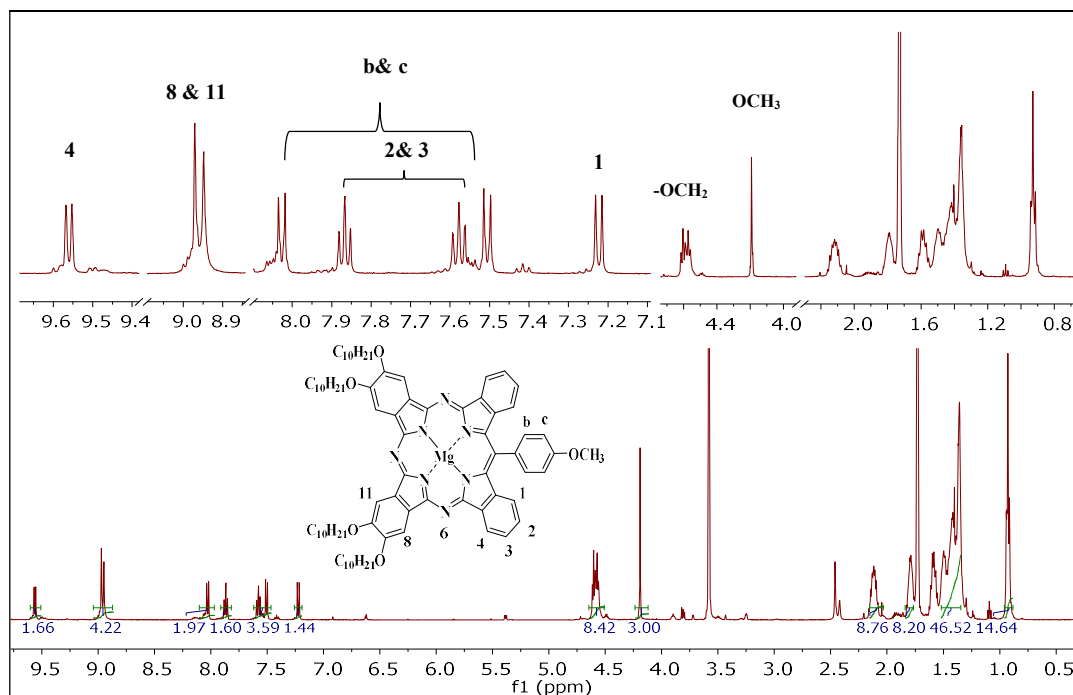


**Figure 2.7:**  $^1\text{H}$  NMR spectrum of TBTAP hybrid 132

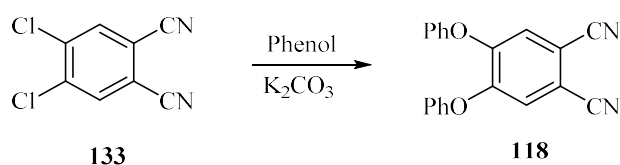
As we keep facing issues with separating the hybrids mixture, we tried to replace the magnesium in the hybrids core with zinc in attempt for better separation. The zinc acetate  $\text{Zn}(\text{OAc})_2$  was added to the green fraction in DMF and stirred at 150 °C for 2h. The crude mixture was analysed by TLC and compared with Mg-complexes. Replacing the metal made no difference to the separation and the movement of the compounds in the silica.

The previous results obtained from using both phthalonitriles **116** and **117** were relatively unexpected in terms of formation of two TBTAP hybrids. Both phthalonitriles have poor solubility in diglyme which prevented the slow addition of the reagents. Therefore, we expect that to be the main factor in the complexity of the reaction and forming other hybrids. Phthalonitriles derivatives which are soluble in diglyme may give us different results, if that is the only reason.

### 2.3.2.5 Synthesis of 4,5-diphenyloxyphthalonitrile **118** and TBTAP **135**

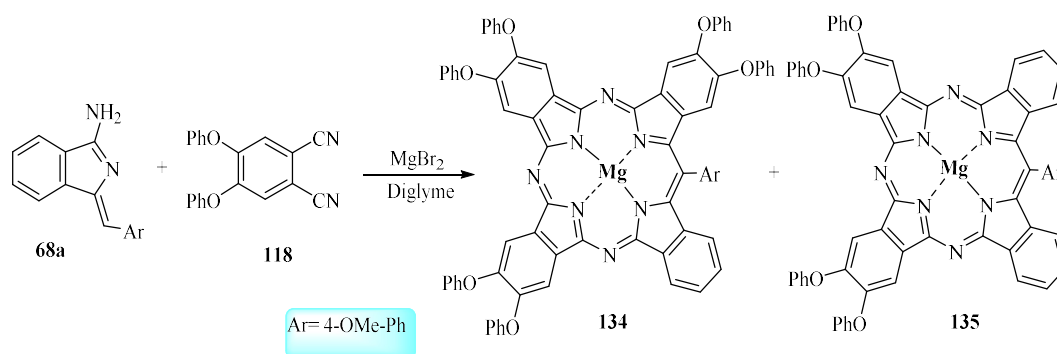
Diphenoxy-phthalonitrile **118** was reported to be readily soluble in benzene, chloroform, and DMF and moderately soluble in alcohols<sup>128,129</sup>, additionally, it was found to be soluble in diglyme.

Synthesis of diphenoxy-phthalonitrile **118** was achieved by using dichlorophthalonitrile and phenol in DMF at 110 °C in presence of potassium carbonate<sup>128</sup>, (scheme 2.14). Dichlorophthalonitrile **133** was synthesised by a former lab member from Cammidge group<sup>78</sup> and it is also available commercially. The purification of compound **118** was achieved by crystallisation from methanol in 81% yield. The compound was pure and characterised using <sup>1</sup>H NMR and <sup>13</sup>C NMR spectroscopy and showed all signals as in the reference<sup>128</sup> which confirm the structure.



**Scheme 2.14: Synthesis of 4,5-diphenyloxyphthalonitrile **118****

Then, we applied the normal conditions for TBTAP reaction; diphenoxy phthalonitrile **118** was soluble in diglyme as mentioned, therefore, we were able to perform the slow addition using the syringe pump. Upon completion, the reaction was worked up as usual and the green fraction was separated from first column. TLC of the green fraction showed multiple spots similar to the two previous reactions. The spots were identified by MALDI-TOF MS as follows; (OPh)<sub>8</sub>MgPc with (*m/z* 1274), (OPh)<sub>6</sub>-MgTBTAP-(OMe-Ph) **134** (*m/z* 1194) and (OPh)<sub>4</sub>-MgTBTAP-(OMe-Ph) **135** with molecular ion peak (*m/z*1009), (figure 2.8). This is consistent with previous observations from alkyloxy substituted phthalonitrile **116** and **117**. (OPh)<sub>6</sub>-MgTBTAP-(OMe-Ph) hybrid **134** showed stability toward the light unlike corresponding alkyloxy derivatives, however, its separation proved to be challenging as well, (scheme 2.15). As we stated, tetra-substituted TBTAP hybrid **135** was successfully isolated and it was characterised by NMR and UV-Vis spectroscopy. The UV-Vis spectrum showed the Q band split at 675 and 652 nm.



Scheme 2.15: Synthesis of phenoxy TBTAP hybrid 135

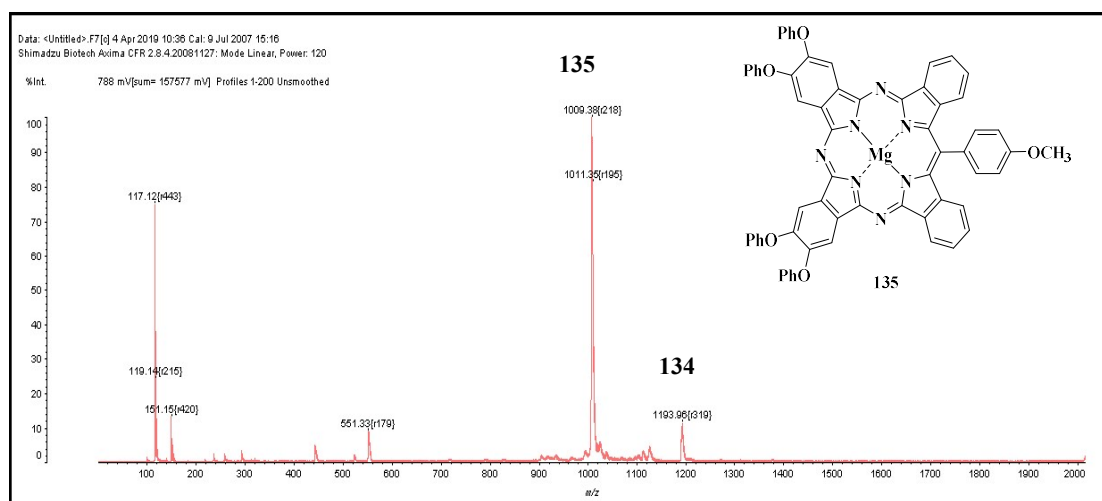
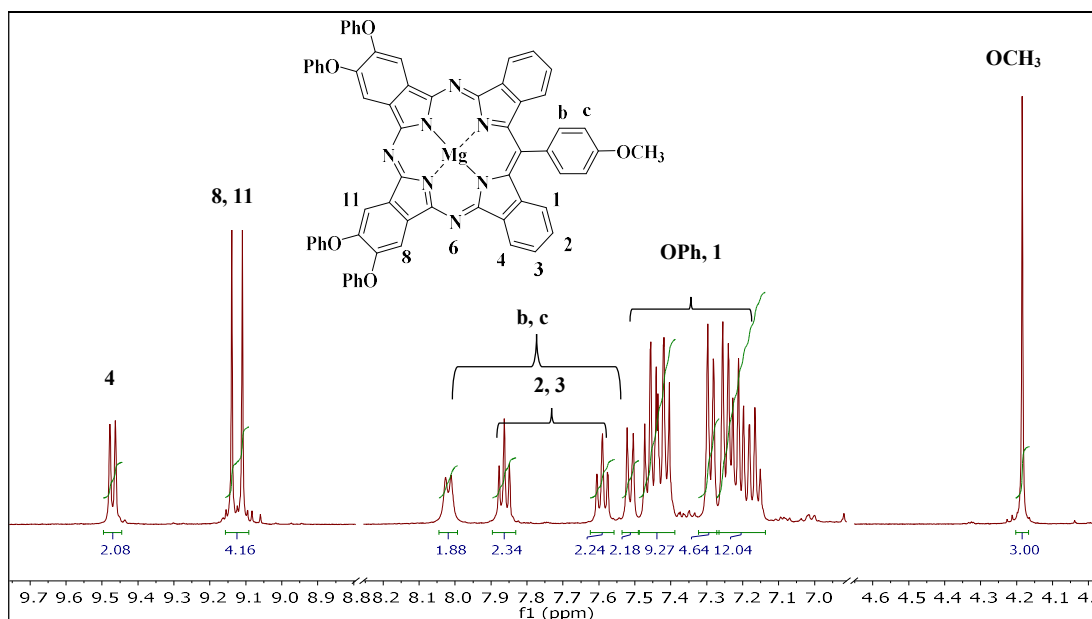


Figure 2.8: MALDI-TOF MS of TBTAP hybrids 134 and 135

The  $^1\text{H}$  NMR spectrum in deuterated tetrahydrofuran for **135** gave all signals corresponding to all protons, (figure 2.9). Six protons were found in the highly deshielded range from 9.48- 9.11 ppm from the non-peripheral sites of the complex. The splitting of the peaks at the range 8.02-7.51 ppm clearly indicate the eight protons from both phenyl group at *meso*-position, and peripheral position of the tetrabenzotriazaporphyrin macrocycle. The shielded protons and phenoxy protons appeared in the range from 7.47-7.15 ppm with integration of twenty-two protons in total. The methoxy group protons at the *meso*-position were found at 4.19 ppm.

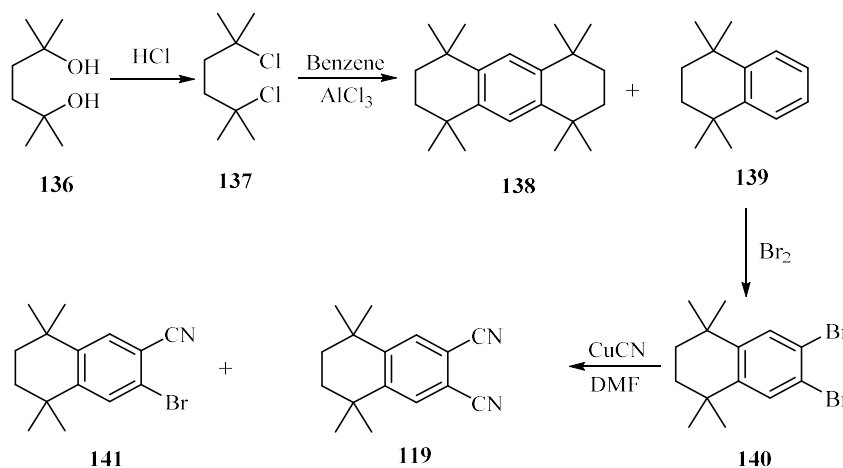


**Figure 2.9:**  $^1\text{H}$  NMR spectrum of tetra-phenoxy TBTAP hybrid 135

Up to this point, we observed that the tetra-substituted TBTAPs were the main products that we could isolate. It seems that the slow addition does not favour the formation of hexa-substituted phenoxy TBTAP as we were expecting. In fact, the slow addition still gives tetra-substituted TBTAP as major product with other hybrids.

### 2.3.2.6 Synthesis of phthalonitrile 119 and its TBTAP hybrids 142, 143

The next phthalonitrile in this series was the 6,7-dicyano-1,1,4,4-tetramethyl-tetralin **119**. This derivative was chosen for a number of reasons. It is relatively easily prepared, and we expect all products to be soluble and stable due to the bulk of the system and NMR spectra are expected to be simple. The synthetic route for this phthalonitrile<sup>119</sup> is illustrated in scheme 2.16.

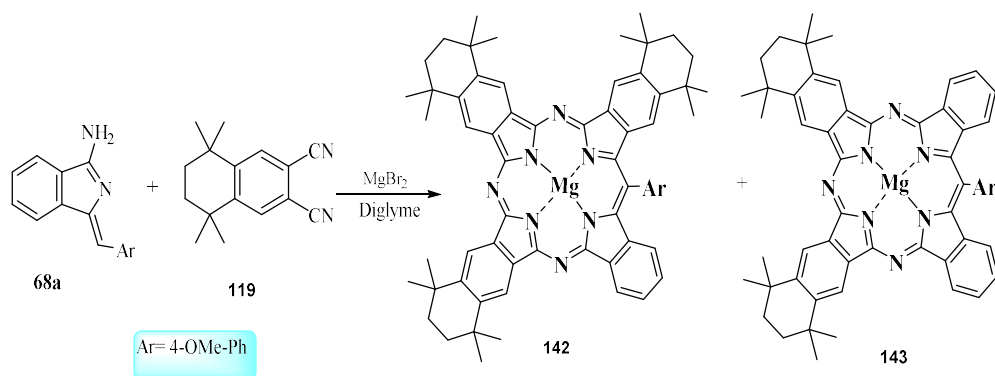


Scheme 2.16: Synthesis of phthalonitrile 119

As we can see this route starts with a simple reaction to convert the 2,5-dimethylhexane-2,5-diol **136** into its corresponding dichloride **137** using a concentrated solution of hydrochloric acid<sup>130</sup>. The acid was added to the diol and cooled with an ice bath then left to stir at room temperature overnight, then the mixture was washed with water and extracted with DCM. The organic material was concentrated and crystallisation from methanol gave the 2,5-dichloro-2,5-dimethylhexane **137** in a good yield. The second step was achieved using Brunson's procedure *via* Friedel-Crafts reaction<sup>131</sup>. 2,5-Dichloro-2,5-dimethylhexane **137** was reacted with benzene in the presence of aluminium chloride at 50°C, but gave di-cycloalkylation product **138** as the major product and the mono product in lower yield. Therefore, we performed the reaction again at 60°C, and the mono product yield was increased and the di product was easily removed by methanol after work up. Thus, the temperature should be at 60°C in order to avoid the unwanted di addition. This reaction was carried out on a large scale and the desired product **139** was purified after work up by vacuum distillation. We also explored using the column chromatography and PE or hexane as an eluent solvent. The yield was slightly higher when distillation was used as purification method compared with the column chromatography (64%, 61% respectively). 1,1,4,4-Tetramethyl-1,2,3,4-tetrahydronaphthalene **139** underwent bromination reaction using Ashton's procedure<sup>132,133</sup>. A mixture of the compound **139** with iodine and iron powder was dissolved in DCM and the mixture was cooled to 0°C. Bromine was added dropwise to the cooled mixture over 30 min, and the mixture then left to stir at room temperature overnight. The reaction could not be easily

followed by TLC to check the completion of the reaction due to the similar  $R_f$  values of the starting material and product in all solvents. Thus, the reaction was checked continuously by  $^1\text{H}$  NMR spectroscopy to ensure the total consumption of the starting material. The product **140** was easily identified by its two aromatic protons at 7.50 ppm (singlet), whereas, the starting material give different splitting pattern. As we mentioned previously, all cyanation reactions in this project followed the Rosenmund–von Braun synthesis<sup>108</sup>. A mixture of 6,7-dibromo-1,1,4,4-tetramethyl-1,2,3,4-tetrahydronaphthalene **140** and copper cyanide in dry DMF was heated to 153-155°C under an argon atmosphere and the reaction was monitored by TLC. The reaction was stopped after 3 hours to avoid formation of copper phthalocyanine and after cooling the reaction was worked up as usual. Analysis of the crude mixture by TLC showed three spots, the two first spots were corresponding to the starting material **140** and the mono nitrile product **141**, the third spot was the dinitrile product **119**. The crude mixture was purified by careful column chromatography using a gradient solvent mixture and we were able to isolate both products (di and mono nitrile) and recover unreacted starting material successfully.  $^1\text{H}$  NMR spectroscopy analysis of 6,7-dicyano-1,1,4,4-tetramethyl-1,2,3,4-tetrahydro-naphthalene **119** showed a signal at 7.71 ppm as a singlet with integration of two protons which correspond to the aromatic protons.

A reasonable amount of phthalonitrile **119** had been accumulated and it was found to be soluble in diglyme. Thus, the TBTAP reaction was carried out in the normal conditions and with use of the syringe pump as a means of addition to achieve slow addition. In the typical reaction, a mixture of **119** and  $\text{MgBr}_2$  in diglyme was heated in oil bath. Two mixtures of **119** were added slowly, first with aminoisoindoline **68a** and the other with DABCO, both in diglyme and over an 1h. After cooling, DCM: MeOH mixture was added to the resulting material and sonicated. The crude mixture was analysed by TLC and showed three spots which agreed with the previous results from alkyloxy and phenoxy phthalonitriles (**116**, **117** and **118**). The green fraction was separated from other fractions and first spot was identified by MALDI-TOF MS as MgPc and it was very weak. The other spots gave molecular ion peaks at ( $m/z$  971) and ( $m/z$  861) which indicated the formation of hexa-substituted hybrid **142** and tetra-substituted TBTAP hybrid **143**, (scheme 2.17).



**Scheme 2.17: Synthesis of TBTAP hybrids 142 and 143**

Regarding the separation of the TBTAP hybrids **142** and **143**, it was relatively easy unlike alkyloxy and phenoxy complexes. They were isolated and successfully characterised by NMR spectroscopy to confirm their structure.

Figure 2.10 shows stacked  $^1\text{H}$  NMR spectra of both **142** and **143**, and the most noticeable difference is the chemical shifts and peak splitting for both shielded and deshielded protons. The protons on non-peripheral sites and close to the *meso*-phenyl group were shielded and have the same environment in **143**, whereas, in **142** their environments differ due to the addition of the substituent to the third benzene unit. As a result, in **143**, two integrated protons appeared as doublet which was changed in **142** to give one proton as singlet and the other as doublet. The same applies to the deshielded protons on non-peripheral sites. However, the sum of protons on peripheral site was changed from four protons in **143** to two protons in **142**. In both compounds the methoxy protons peak appeared at 4.20 ppm and the methyl and methylene protons appeared as expected between 2.09-1.36 ppm.

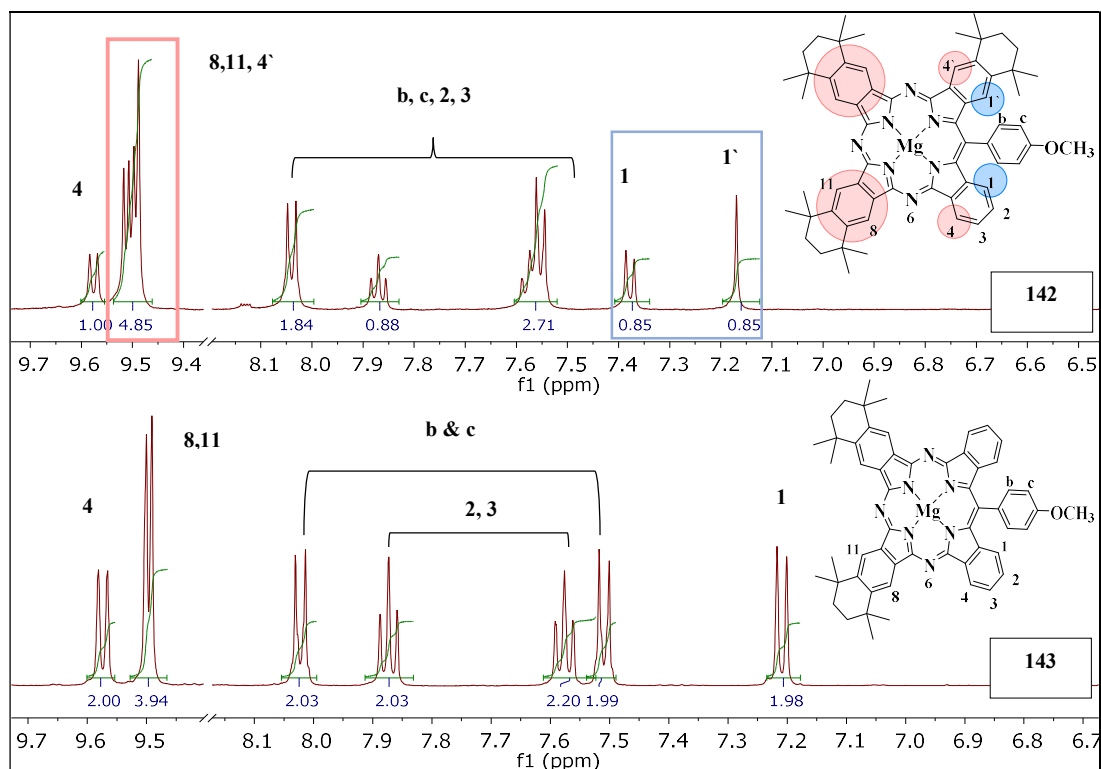


**Figure 2.10:**  $^1\text{H}$  NMR spectra of MgTBTAP hybrids **143** and **142**

It should be noted that hybrid **143** was more stable than **142** towards the light, but the latter shows more stability in contrast to the equivalent complexes obtained from alkyloxy phthalonitriles. The branched substituent could be the key factor to facilitate the separation and to stabilize hybrid **142**.

Hence the reaction with phthalonitrile **119** gave satisfactory results, and we were able to isolate the two hybrids. We decided to study the impact of using the syringe pump (slow addition) in this reaction. We performed the reaction again with the same quantities and exact conditions all together in one pot reaction. Similarly, analysing the green fraction from the reaction mixture by TLC gave three spots corresponding to the three hybrids as previously stated. However, hexa-substituted hybrid **142** was so dilute comparing with the first method using the syringe pump, which made its separation difficult beside its light sensitivity. As a result, tetra-substituted TBTAP **143**, was the major product and gave 22% yield which was higher in this case comparing with the slow addition of reagents (14% yield), (table 2.2). Figure 2.11 illustrates the UV-Vis absorption spectra of the two hybrids **142** and **143**.

	<b>142</b>	<b>143</b>
Yield -slow addition	1%	14%
Yield- one pot reaction	traces	22%

**Table 2.2: The effect of the addition method on 142 and 143 yield**

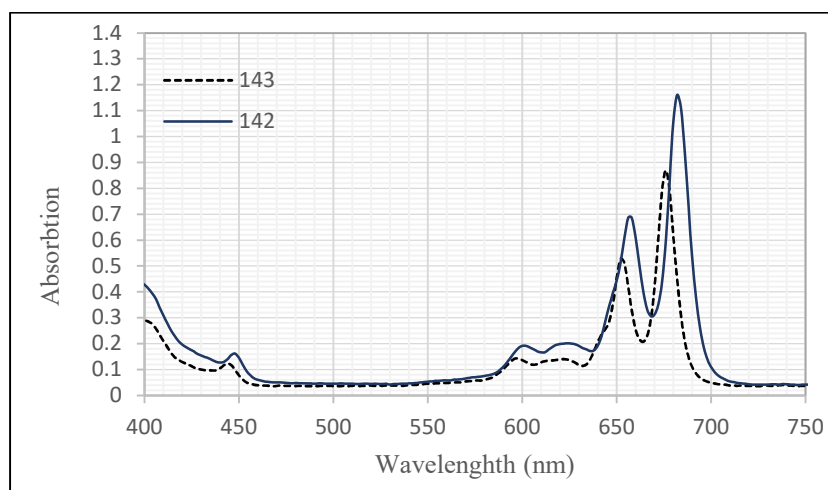


**Figure 2.11: The UV-Vis spectra of 142 and 143**

### 2.3.3 Synthesis of naphtho-annulated TBTAP 147

Phthalocyanines that contain four benzo units fused to the ring are termed naphthalocyanines (Nc). The extension of the molecule's  $\pi$ -system in naphthalocyanines results in a bathochromic shift of the Q-band in the absorption spectrum of  $\sim 100$  nm as compared to phthalocyanine<sup>2</sup>. Similar to the phthalocyanine, TBTAP showed the similar behaviour, Lezznoff reported synthesis of a series of *meso*-substituted alkyl-TBTAP and corresponding naphtho-triazaporphrin derivative (NTAP): it was shown that the electronic absorption of naphtho-annulated compound **38** showed dramatic red-shift as compared to its analogue **144**<sup>28</sup>, (figure 2.12).

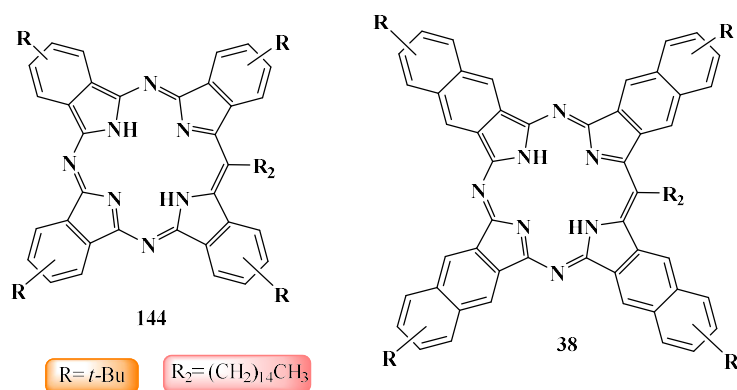
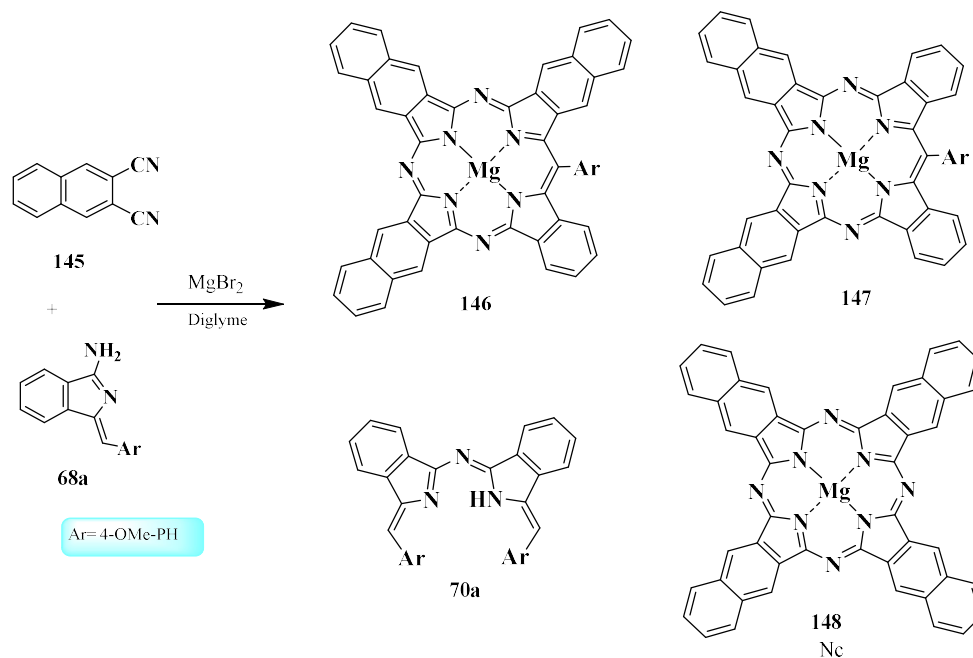


**Figure 2.12: TBTAP compounds synthesised by Lezcnoff**

Naphthalene-1,2-dicarbonitrile **145** was proposed to be applied in mixed condensation with aminoisoindoline **68a** under the normal reaction conditions, (scheme 2.18).

Naphthalene-1,2-dicarbonitrile **145** was found to be soluble in diglyme, thus, we used the syringe pump for slower addition. TBTAP reaction was employed in normal conditions and mixture of 3 eq naphthalene-1,2-dicarbonitrile **145** was heated in diglyme with MgBr<sub>2</sub>. Further quantities of naphthalene-1,2-dicarbonitrile were added over 1h, first with aminoisoindoline **68a** and with DABCO later. The reaction proceeded as normal and the crude mixture was analysed by TLC and there were four green spots. The most certain product was identified using MALDI-TOF as MgNc **148** ( $m/z$  737) and as from our previous results, the two spots with ion peaks ( $m/z$  792) and ( $m/z$  740) were assigned as NTAP derivatives **146** and **147** (with three and two benzene units fused to the macrocycle, respectively). The last spot gave molecular ion peak at ( $m/z$  687) which indicate forming unknown hybrid or intermediate during the reaction, (figure 2.13).



Scheme 2.18: Synthesis of Naphthalene TBTAP 147

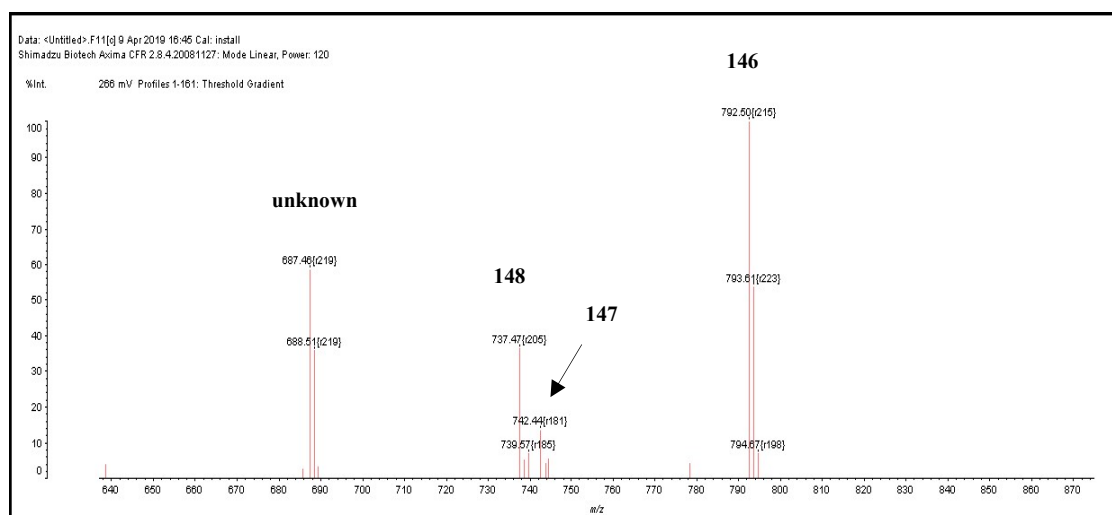


Figure 2.13: MALDI-TOF MS of the hybrids in the inseparable green fraction

Forming the new hybrid increased the separation challenges in the reaction. Chromatography separation with various solvents was performed to find the most appropriate eluent. However, only hybrid **147** was isolated from the green mixture with 4% yield. NTAP **147** shows the distinct split for the Q band at 709 and 680 nm which was a shift to a longer wavelength due to the extension of the molecule's  $\pi$ -system comparing with the parent TBTAP **69a**.



complexes **15** and **29** bear structural similarity to the MgTBTAPs obtained in this research. A  $\text{Cl}_3\text{-CuTBTAP}$  **15** was synthesised by condensing 4-chlorophthalonitrile with phthalimidine acetic acid in the presence of cuprous chloride<sup>16</sup>, whereas, (*t*-Bu)<sub>2</sub>-ZnTBTAP **29** was synthesized from phthalonitrile and dimeric compound **28**<sup>23</sup>, (figure 2.15).

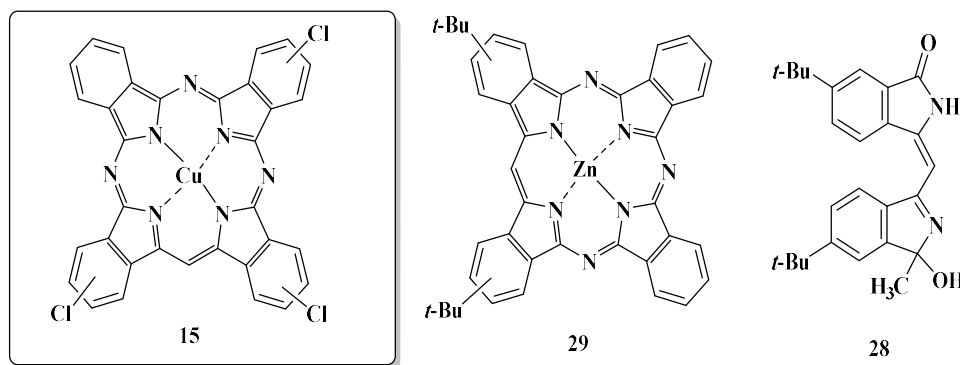


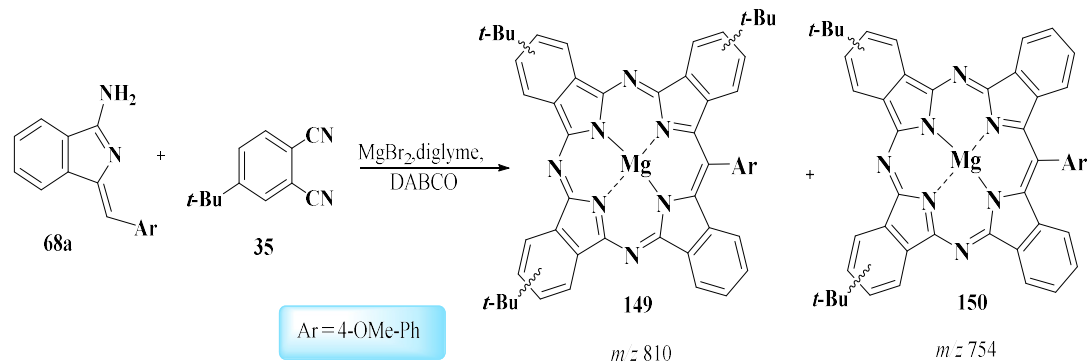
Figure 2.15: Examples of similar reported TBTAP complexes or ligand

### 2.3.4 Synthesis of TBTAP from 4-*t*-Butylphthalonitrile **35**

4-*t*-Butylphthalonitrile **35** is widely used in tetrabenzotriazaporphyrins synthesis<sup>23,22,29</sup> and it is commercially available. Therefore, we decided to employ this derivative as the last substituted phthalonitrile precursor and to explore the outcomes. We performed a similar synthesis under our previous conditions for synthesis of TBTAP complex. 4-*t*-Butylphthalonitrile was soluble in diglyme, thus the reaction was carried out using the syringe pump for slow addition. The addition was completed and the reaction mixture allowed to cool then worked up normally. The dimer **70a** and (*t*-Bu)<sub>4</sub>MgPc impurities were isolated by column chromatography. The other green fraction was isolated and analysed by TLC to give several spots which, with further analysis with MALDI TOF MS, give two main ion peaks *m/z* 810 for **149** and *m/z* 754 for **150**, (figure 2.16). The molecular ion peaks clearly show formation of two TBTAP hybrids in line with our previous result, (scheme 2.19).

However, more careful TLC revealed more spots overlapped with each other, which may indicate forming different isomers. Separation proved to be challenging with most

of the solvent mixtures that we tried. MALDI TOF-MS enables rapid and easy detection of an analyte in a mixture, although, the separate identification of compounds having the same molecular weight is not possible.



Scheme 2.19: Synthesis of 149 and 150 from 4-t-butylphthalonitrile 35

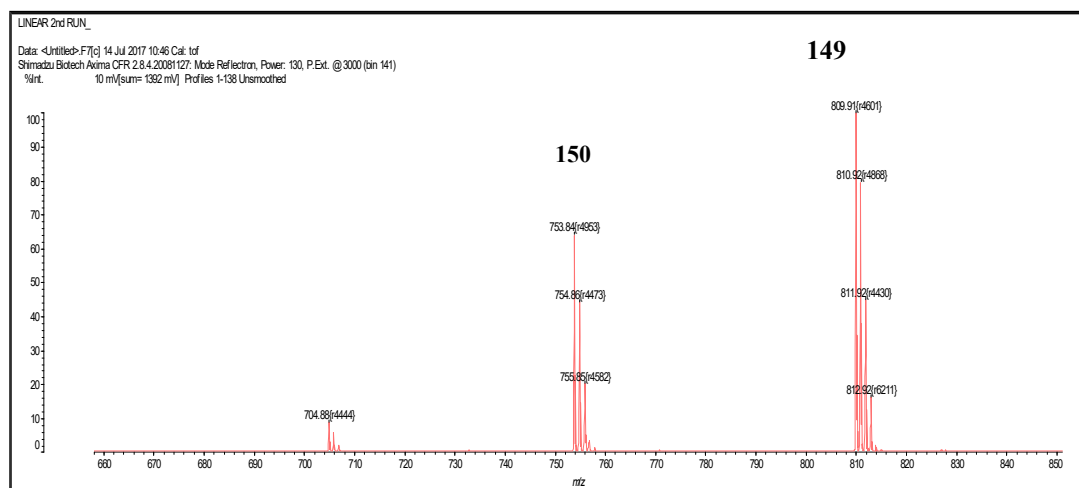


Figure 2.16: (*t*-Bu)-MgTBTAP hybrids 149 and 150 in a mixture

In summary, for this part of the research, the synthesis of tetrabenzotriazaporphyrins (TBTAPs) using the improved methodology proved to give the targeted compound **69a** in good yield (20%) by mixed reaction between aminoisoindoline **68a** and phthalonitrile **8**. However, replacing the phthalonitrile **8** with different phthalonitrile derivatives proved to be more complex and resulted in the formation of other unexpected macrocyclic structures. In fact, in these reactions it appears that the ABBA-Ar TBTAP structures are the dominant products. This is a rarely investigated class of hybrids, and the method opens the way for further investigation. The electronic

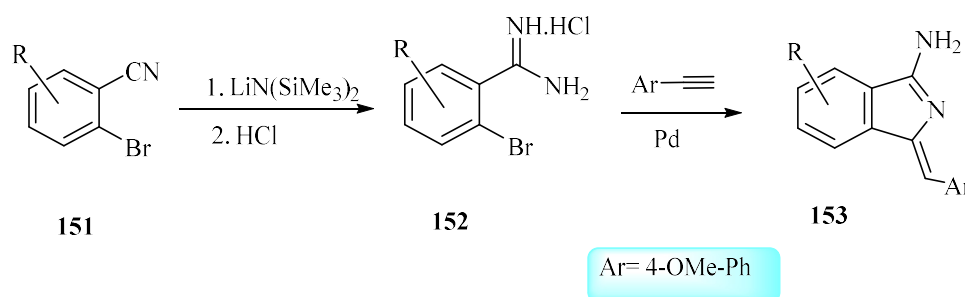
absorption spectra of the compounds from this series will be briefly discussed later in this chapter after the synthesis of the next series.

## 2.4 Synthesis of the second series of TBTAP hybrids

In the first part of the project, newly functionalised TBTAP hybrids were prepared using substituted phthalonitriles. In an alternative approach, the introduction of substituents on the aminoisoindoline ring would complete the control possible in these syntheses and was investigated next.

### 2.4.1 General synthesis of the aminoisoindoline precursors

The general synthetic route to aminoisoindoline derivatives is shown in scheme 2.20. It starts with 2-bromobenzonitrile derivatives **151** to convert them to the corresponding 2-bromobenzamide hydrochlorides<sup>49</sup> **152**. A solution of  $\text{LiN}(\text{SiMe}_3)_2$  in THF is usually added to a solution of 2-bromobenzonitriles **151** in dry THF, and the mixture left to stir for four hours under nitrogen inert gas. A mixture of 1:1 hydrochloric acid and isopropanol is added to the reaction to give 2-bromobenzamide hydrochlorides **152**. The second step involves a coupling reaction between amidines **152** and 4-ethynylanisole in the presence of palladium catalyst and performed in microwave reactor<sup>48</sup>.

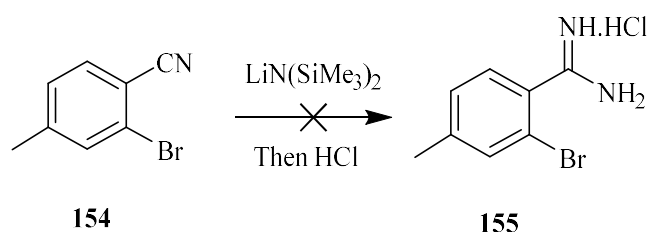


**Scheme 2.20: General synthesis of Aminoisoindoline derivatives**

Other members in our group previously synthesised the aminoisoindoline derivatives using various number of phenylacetylenes by the coupling reaction in the second step<sup>50</sup>. However, in this project we prepared the aminoisoindoline derivatives using 2-

bromobenzonitrile derivatives to give the corresponding amidines substituted in their benzene ring. Sequentially, the coupling reaction was applied between the resulting amidine hydrochloride and 4-ethynylanisole to give the targeted aminoisindolines.

This synthesis sequence started with a commercially available 4-methyl-2-bromo benzonitrile **154**. A solution of  $\text{LiN}(\text{SiMe}_3)_2$  in THF was added to the 4-methyl-2-bromo benzonitrile **154** solution. The solution colour changed from yellow to red-maroon colour by adding  $\text{LiN}(\text{SiMe}_3)_2$  solution. This was not observed with the earlier reactions. It was found that the colour change may indicate the deprotonating of the methyl group<sup>134</sup> and the desired product not formed in this reaction, (scheme 2.21), despite several attempts.



**Scheme 2.21: Attempt to synthesise 2-bromo-4-methyl amidine 155**

It was difficult to find suitable 2-bromobenzonitrile derivatives **151** from commercial sources. Thus, all 2-bromobenzonitrile derivatives **151** in this section were isolated as side products from Rosenmund–von Braun cyanation reactions as we previously discussed in the synthesis of phthalonitrile precursors. In the Rosenmund–von Braun cyanation reactions from corresponding 1,2-dibromobenzene derivatives, the reaction conditions, time and temperature, were slightly modified to favour the mono cyanide product (2-bromobenzonitrile). The separation of mono product was often difficult, due to the similar movement with starting materials on the silica. However, the separation was achieved by using a gradual solvent system mixture of PE:DCM starting from less polar ratio mixture and increasing the polarity of the mixture throughout the separation. We successfully separated the 2-Bromobenzonitrile compounds in this section which are illustrated in figure 2.17. 2-bromobenzonitriles were characterised by  $^1\text{H}$  NMR and  $^{13}\text{C}$  NMR spectroscopy to confirm their structures.

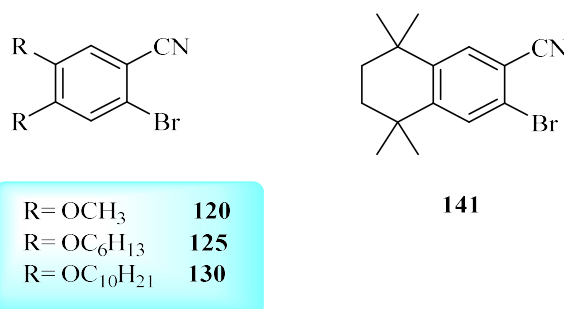
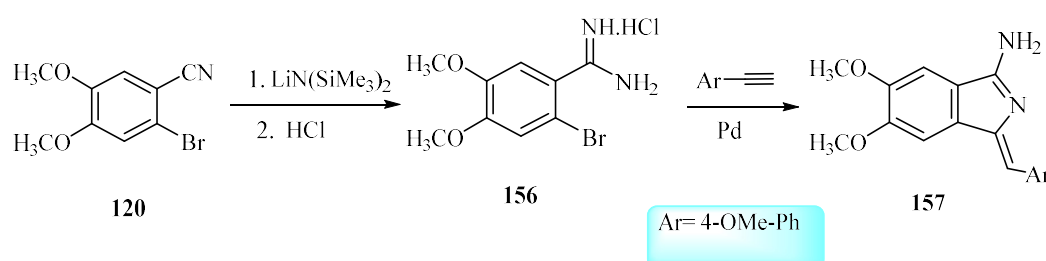


Figure 2.17: Targeted 2-bromobenzonitriles

Once a reasonable amount of 2-bromobenzonitriles had been accumulated we moved on to start the synthesis of aminoisoindolines following the synthesis illustrated in scheme 2.22. Bromobenzonitriles were converted into the corresponding amidine derivatives<sup>49</sup> by a solution of  $\text{LiN}(\text{SiMe}_3)_2$ , the colour changing to red was not observed in any of the reactions as in methyl-substituted benzonitrile. Thus, the reaction was stirred for 4h under inert atmosphere and upon the completion, hydrochloric acid was added to the mixture resulting in hydrolysis of the product and formation of 2-bromobenzamidine hydrochloride derivatives. The compounds were purified by simple crystallisation and their structures were confirmed by NMR spectroscopy. The 2-bromobenzamidine hydrochloride derivatives underwent a coupling reaction with 4-ethynylanisole in presence of a palladium catalyst to give crude mixtures which were purified by column chromatography<sup>48</sup>. Pure aminoisoindolines were characterised by NMR spectroscopy and showed all peaks as expected. All reactions were performed similarly without any alteration to the original and typical conditions. Therefore, dimethoxy substituted-aminoisoindoline **157** synthesis will be discussed as an example in more detail, (scheme 2.22).



Scheme 2.22: Synthesis of aminoisoindoline 157

2-Bromo-4,5-dimethoxybenzonitrile **120** was isolated from cyanation reaction as we explained and characterised by  $^1\text{H}$  NMR spectroscopy in deuterated chloroform. The spectrum showed two singlet peaks with one proton integration each in the aromatic range (7.07 and 7.05 ppm). Methoxy protons appeared as two singlet peaks at 3.93 and 3.89 ppm with three protons integration each. For the next step, 2-bromo-4,5-dimethoxy benzonitrile **120** was dissolved in dry THF and  $\text{LiN}(\text{SiMe}_3)_2$  was added to the mixture and left to stir under nitrogen at room temperature for 4h. The mixture was then cooled using an ice bath and a 1:1 mixture of concentrated hydrochloric acid and isopropanol was added dropwise and the mixture left to stir overnight. The resulting precipitate was filtered off and washed several times with diethyl ether, then recrystallised from methanol. The  $^1\text{H}$  NMR spectra for the pure compound **156** (in deuterated methanol) showed two aromatic protons as singlets at 7.31 and 7.20 ppm and methoxy protons were at 3.90, 3.88 ppm, (figure 2.18). The product gave suitable crystals for X-ray diffraction analysis as shown in figure 2.19.

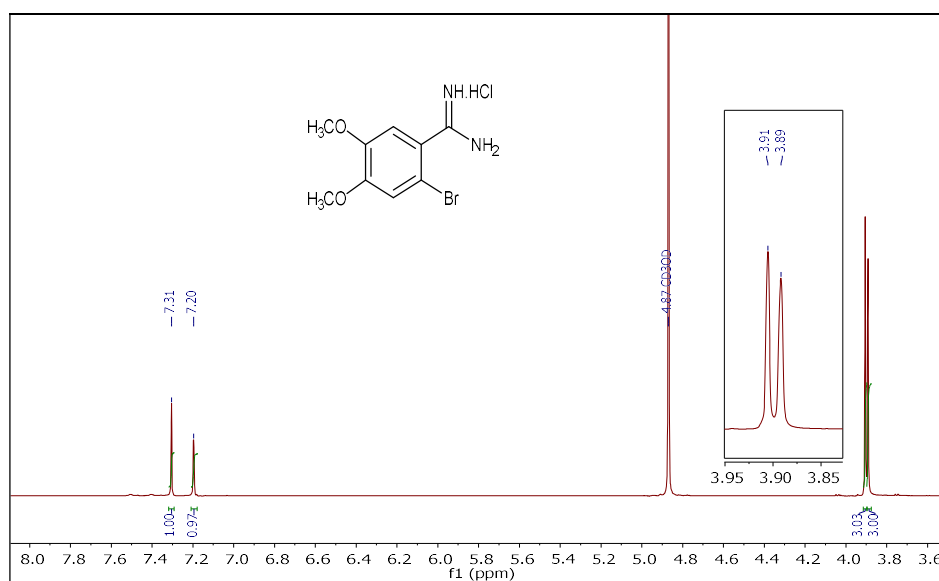


Figure 2.18:  $^1\text{H}$  NMR spectrum of OMe-amidine **156**

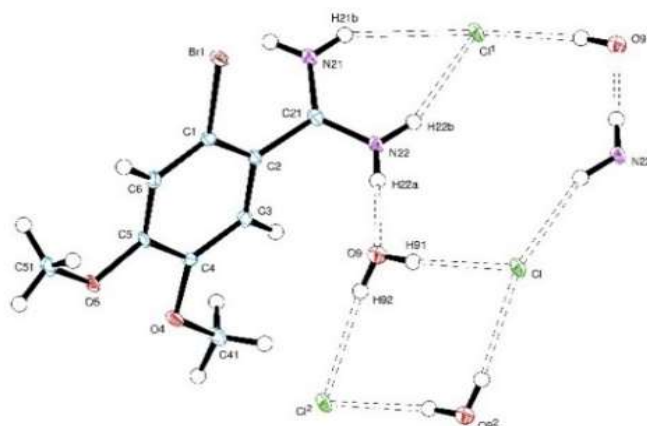


Figure 2.19: X-ray structure of OMe-amidine **156**

The coupling reaction was performed between the amidine **156** and 4-ethynyl anisole using  $\text{PdCl}_2(\text{MeCN})_2$  as a catalyst in the microwave reactor at  $120^\circ\text{C}$  for 1h. After work up, the crude was purified by column chromatography. The pure fractions were collected, and the solvent was removed to leave a semisolid material which was then recrystallised using a mixture of PE and DCM. The aminoisoindoline product **157** gave molecular ion peak at ( $m/z$  311) on MALDI-TOF MS and its structure was confirmed by NMR spectroscopy and X-ray diffraction analysis, (figure 2.20).

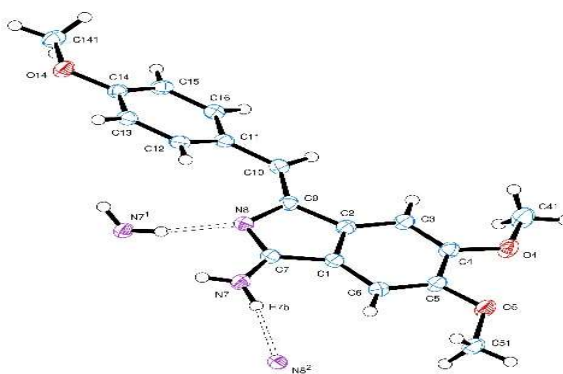
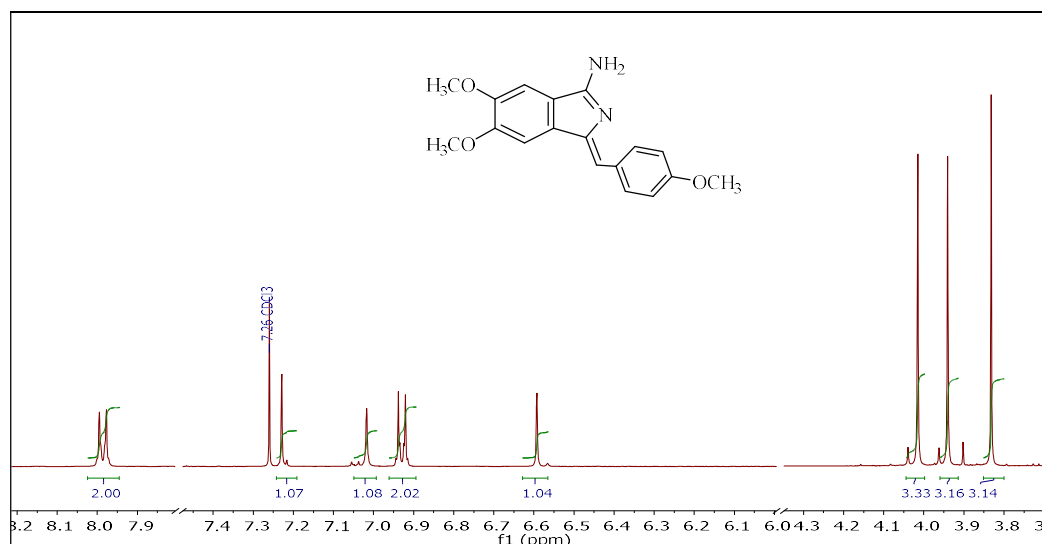


Figure 2.20: X-ray structure of OMe-aminoisoindoline **157**

Figure 2.21 shows the  $^1\text{H}$  NMR spectrum of the compound **157**. It shows three singlets in the range at 7.23, 7.02 and 6.59 ppm. Four protons showed AA'BB' system appeared as doublet with a coupling constant 8.8 Hz at 7.99 and 6.93 ppm. Methoxy groups protons were at 4.02, 3.94 and 3.83 ppm. The UV-Vis spectrum shows a broad band with  $\lambda_{\text{max}}$  at 362 nm.



**Figure 2.21:** <sup>1</sup>H NMR spectrum of **157**

The aminoisoindoline precursor **157** was prepared successfully with good quantities, therefore, general synthesis of TBTAP was performed using this precursor and phthalonitrile.

#### 2.4.2 Synthesis of the TBTAP hybrid from aminoisoindoline **157**

In the first series, dimethoxy phthalonitrile failed to give any hybrids under the conditions of the TBTAP improved procedure, in fact it failed to form any green materials at all. However, the dimethoxy-substituted aminoisoindoline **157** showed the opposite behaviour and even gave an impressive result in condensation reaction with phthalonitrile **8** as we will discuss below.

Initially, the solubility of the aminoisoindoline **157** in diglyme was poor at room temperature and the mixture was blocking the syringe pump and preventing the addition. Thus, the reaction was carried out as one pot reaction without the use of the pump to add the reagents, this was very similar to previous reactions of the phthalonitriles from the first series.

According to the procedure, a solution of 5 eq of phthalonitrile **8**, aminoisoindoline **157** (1 eq), MgBr<sub>2</sub> and DABCO in diglyme was stirred for 1.5h in preheated oil bath at 220°C under Argon atmosphere. The solvent was removed under a stream of Argon,

the reaction mixture allowed to cool, then (1:1) of (DCM:MeOH) was added. The crude was purified using two flash column chromatography separations.

The first column was performed and we isolated the expected red fraction which was the dimethoxy-aminoisoindoline dimer **159**. Then another eluent mixture was used to separate the green-blue fraction which was subjected to a second column. A mixture of PE:THF:MeOH was used as an eluent. Before that, the green fraction was analysed by TLC and showed multiple spots as expected. The spots were analysed by MALDI-TOF MS and showed the two molecular ion peaks at ( $m/z$  702) and ( $m/z$  762) and traces of MgPc **160**, (figure 2.22).

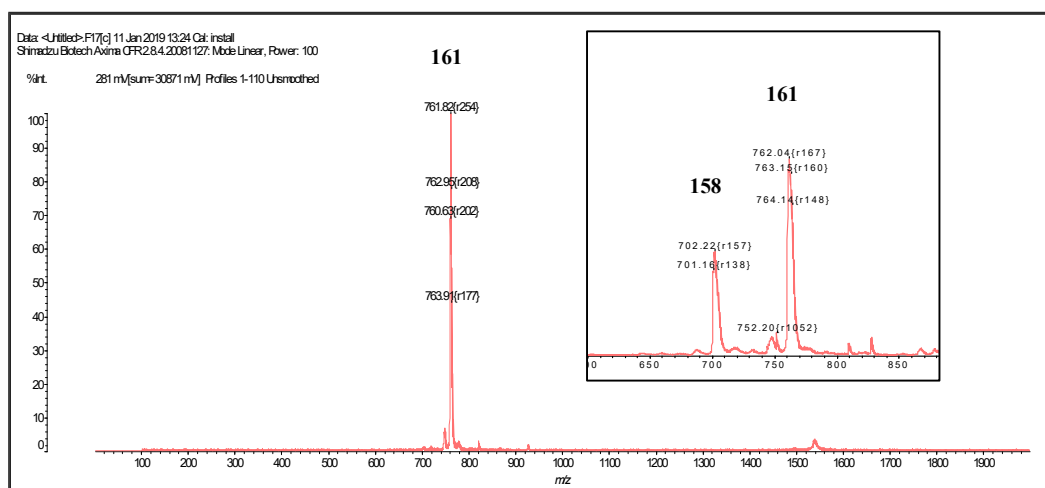
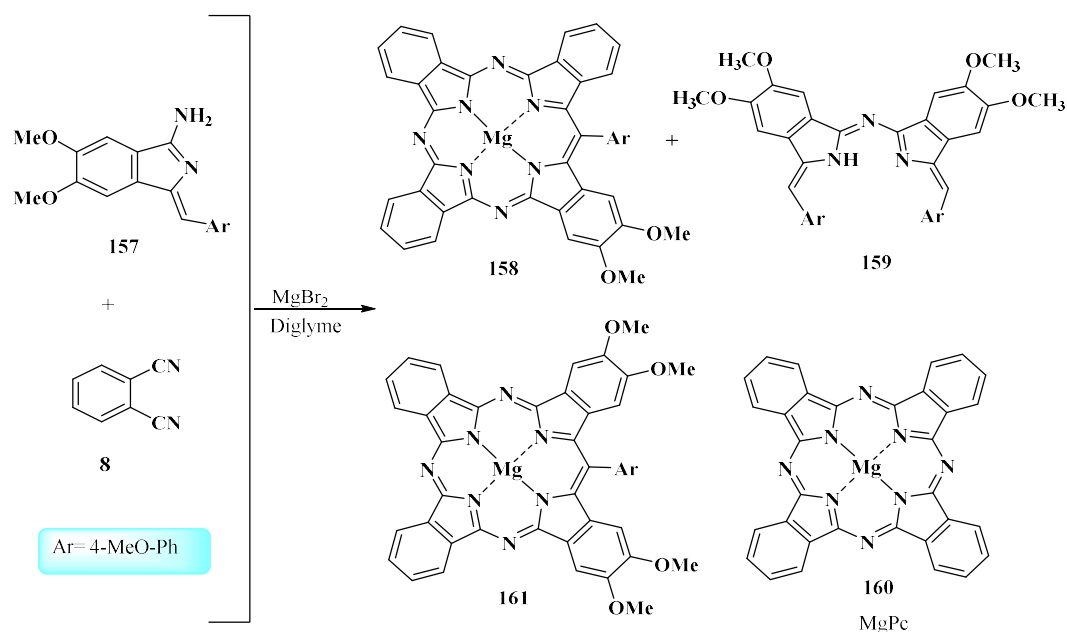


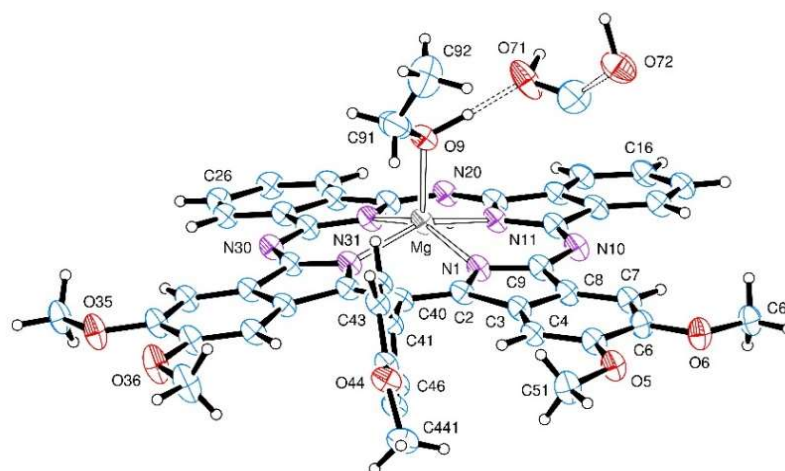
Figure 2.22: MALDI-TOF MS of TB-TAP hybrids **158** and **161**(pure and in a mixture)

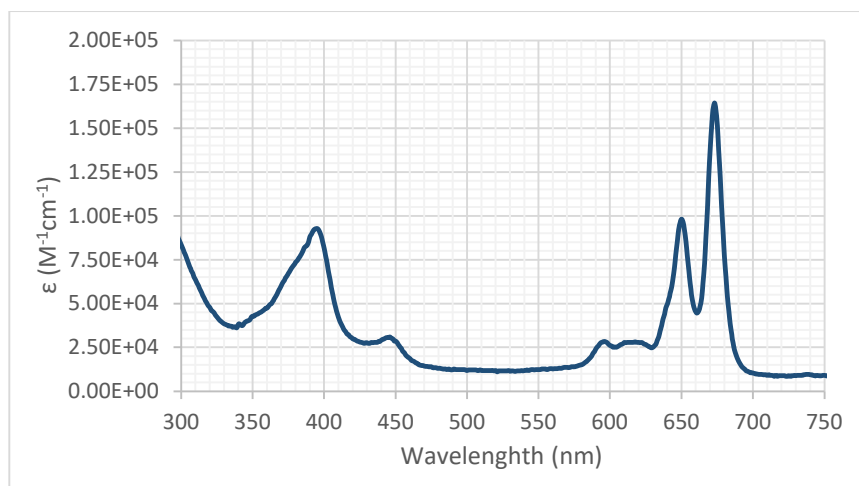
As we discussed previously, the phthalonitriles derivatives condensed with aminoisoindoline **68a** have the tendency to form tetra substituted TB-TAPs as major products across all the derivatives we explored. In a similar way, it seems that methoxy aminoisoindoline reaction with phthalonitrile **8** tend to give tetra substituted TB-TAP as major products, (scheme 2.23).



Scheme 2.23: Synthesis of OMe TBTAP 161

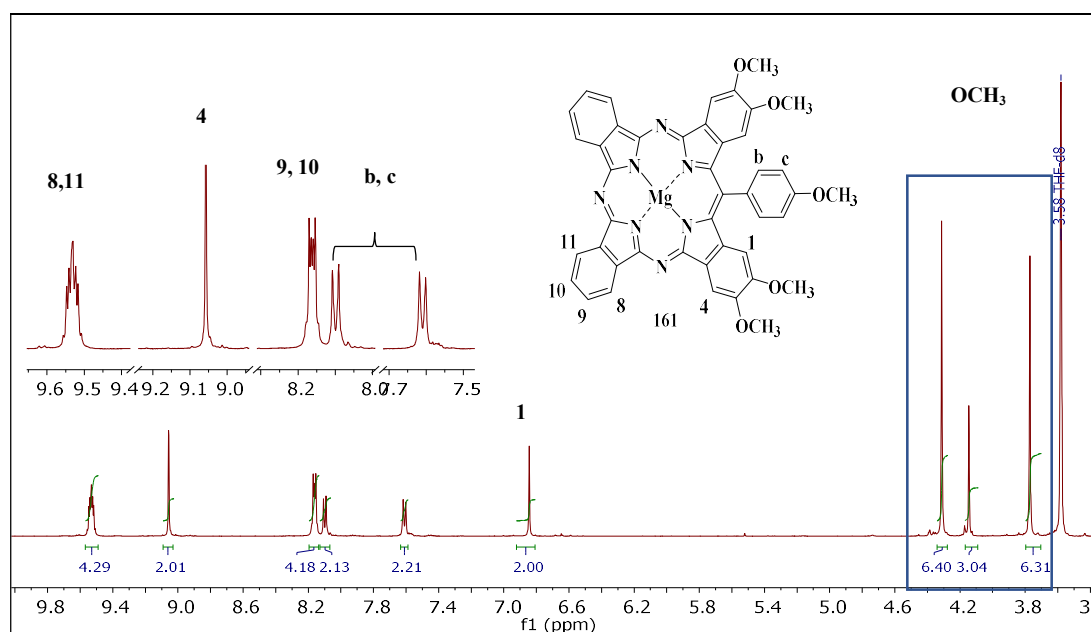
The hybrid **158** was contaminated with impurities of MgPc **160** and hybrid **161** and it was difficult to isolate the compound in a pure state. On the other hand, the major product **161** was successfully isolated and characterised by NMR spectroscopy. It was also possible to grow crystals suitable for analysis by X-ray, (figure 2.23). The electronic absorption spectrum for the resulting compound gave the characteristic Q band of metallated- TBTAPs at 673 and 650 nm, (figure 2.24).

Figure 2.23: X-ray structure of (OMe)<sub>4</sub>-MgTBTAP-(4-OMe-Ph) hybrid 161



**Figure 2.24: UV-Vis spectrum of 161**

Figure 2.25 shows the  $^1\text{H}$  NMR analysis of the compound **161** with sixteen protons in the range from 9.55 to 6.84 ppm corresponding to all the aromatic protons in the TBTAP macrocycle and the *meso*-substituted phenyl. From left to right in the spectrum clearly shows four protons as multiplet and two protons as single peaks. The range from 8.2 to 7.5 ppm shows four protons on the peripheral site appear as multiplet and the *meso*-phenyl protons appearing as doublet in the similar range with coupling constant ( $J=8.1$  Hz). The two protons adjacent to the *meso*-phenyl ring give shielded peak at 6.84 ppm, also the peaks of the methoxy groups were at 4.31, 4.14 and 3.77 ppm.



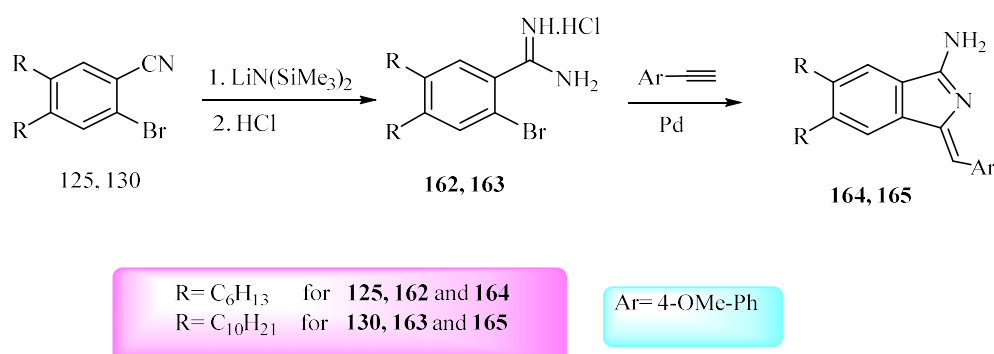
**Figure 2.25:**  $^1\text{H}$  NMR spectrum of TBTAP hybrid **161**

Synthesis of  $(\text{OMe})_4\text{-MgTBTAP}$  **161** from substituted aminoisoindoline **157** gave promising result, thus, we expect similar or rather better results when the methoxy group is replaced with longer alkoxy chains. Aminoisoindolines substituted with hexyloxy **164** and decyloxy **165** chain were explored to demonstrate the effect of the chain length on the synthesis of TBTAP hybrids.

### 2.4.3 Synthesis of TBTAP Hybrids **166** and **167**

Aminoisoindolines **164** and **165** were synthesised by following the general synthesis of aminoisoindoline derivatives<sup>48</sup>, (scheme 2.24). The first step was converting 2-bromo benzonitrile derivatives **125/130** into amidine derivatives.  $\text{LiN}(\text{SiMe}_3)_2$  solution in THF was added to 2-bromobenzonitriles **125/130** and followed by hydrolysis using solution of hydrochloric acid in 2-propanol to give the amidine hydrochlorides<sup>49</sup> **162/ 163**. Both compounds were pure and their structures were confirmed by NMR spectroscopy. In deuterated methanol, both compounds gave two singlet peaks with one proton integration in aromatic range. Peaks appeared at (7.27, 7.14 ppm) and (7.27, 7.15 ppm) corresponding to the benzene ring protons for **162** and **163** respectively. The alkyloxy chains protons appeared at range from 4.05- 0.90 ppm as expected for both.

The second step was coupling reaction between amidine derivatives and 4-methoxyphenylacetylene using microwave radiation for 1h in presence of Pd catalyst to give the aminoisindolines **164/165**. The compounds were characterised and their structures were confirmed by NMR spectroscopy. The  $^1\text{H}$  NMR spectra for both **164** and **165** were similar to a previously discussed aminoisindoline derivative **157**. It showed three protons as singlets in the aromatic range. Four protons showed AA'BB' system as doublet. Methoxy group protons and alkyloxy chains protons also were in the expected range.

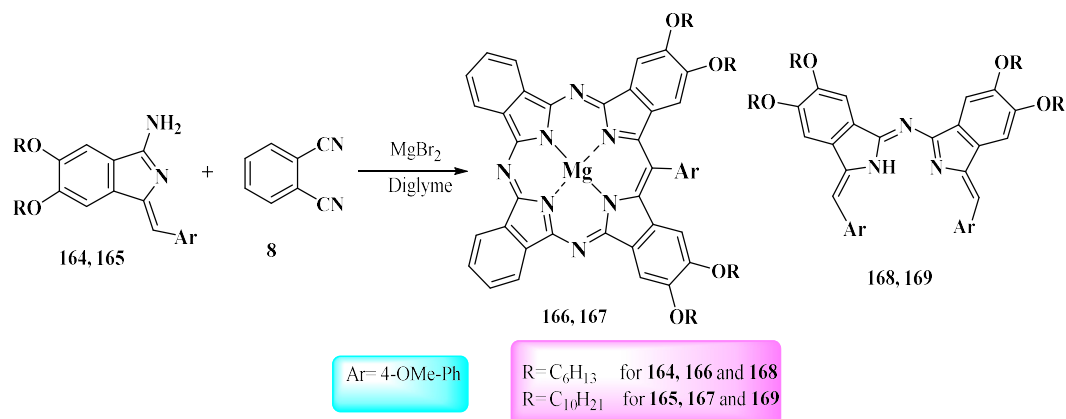


**Scheme 2.24: Synthesis of aminoisindoline derivatives 164 and 165**

The resulting aminoisindoline derivatives **164** and **165** showed poor solubility in diglyme at room temperature. As a result, the general synthesis of TBTAP was employed without the syringe pump and one-pot reaction was performed.

A solution of 5eq of phthalonitrile **8**, aminoisindoline **164/165** (1eq),  $\text{MgBr}_2$  and DABCO in diglyme was stirred for 1.5h in preheated oil bath at  $220^\circ\text{C}$  under Argon atmosphere. The solvent was removed under a stream of Argon, the reaction mixture allowed to cool, then (1:1) of (DCM:MeOH) was added. The crude was purified using two flash column chromatography separations. We isolated the fractions according to their colours, only the green-blue fraction was subjected to a second column. The green fraction was analysed by the TLC and showed multiple spots, which seems to be the general tendency for this synthesis. It gave a mixture of compounds, two TBTAP hybrids and unsubstituted phthalocyanine in addition to the aminoisindoline dimers **168** and **169**.

Likewise, we faced difficulties in separating the hybrids in the green fraction and we were only able to isolate one hybrid. For both reactions the isolated compound is tetrasubstituted -TBTAP hybrid **166/ 167**, (scheme 2.25).



**Scheme 2.25: Synthesis of alkyloxy TBTAP hybrids 166 and 167**

The hybrids from this series **166** and **167** have the same molecular formula and therefore, same molecular ion peak on the MALDI-TOF MS to TBTAP hybrids from the first series **127** and **132** respectively. However, the chemical environments of the protons in the isomeric structures differ, as clearly observed in the <sup>1</sup>H NMR spectra. Both **166** and **167** showed similarities in their NMR spectra, the only difference was the alkyloxy chains protons in terms of their integration and number. We have the chance here to compare the compounds from both series. The comparison between the isomers **132** and **167** will only be discussed here to clarify the differences and they apply to the other isomers **127** and **166**. The protons on the peripheral and non-peripheral sites of the TBTAP macrocycle show different splitting, and chemical shifts in some cases, due to the change of the alkyloxy chains positions, (figure 2.26).

Starting with the protons of the two compounds **132** and **167** which are nearest to the *meso*-phenyl group, both shielded and de-shielded non-peripheral protons changed from doublet in **132** spectra to singlet in **167**, whereas, the peripheral protons are not observed in the **167** spectra. On the other side, four non-peripheral protons appear as singlet in **132** and become multiplet and more de-shielded in **167**, in addition to the peripheral protons peak. The change of the alkyloxy chains positions has impact on

the protons directly bound to an oxygen and adjusting protons (OCH<sub>2</sub>-CH<sub>2</sub> groups) in the chains which cause noticeable difference of the chemical shifts in **167**.

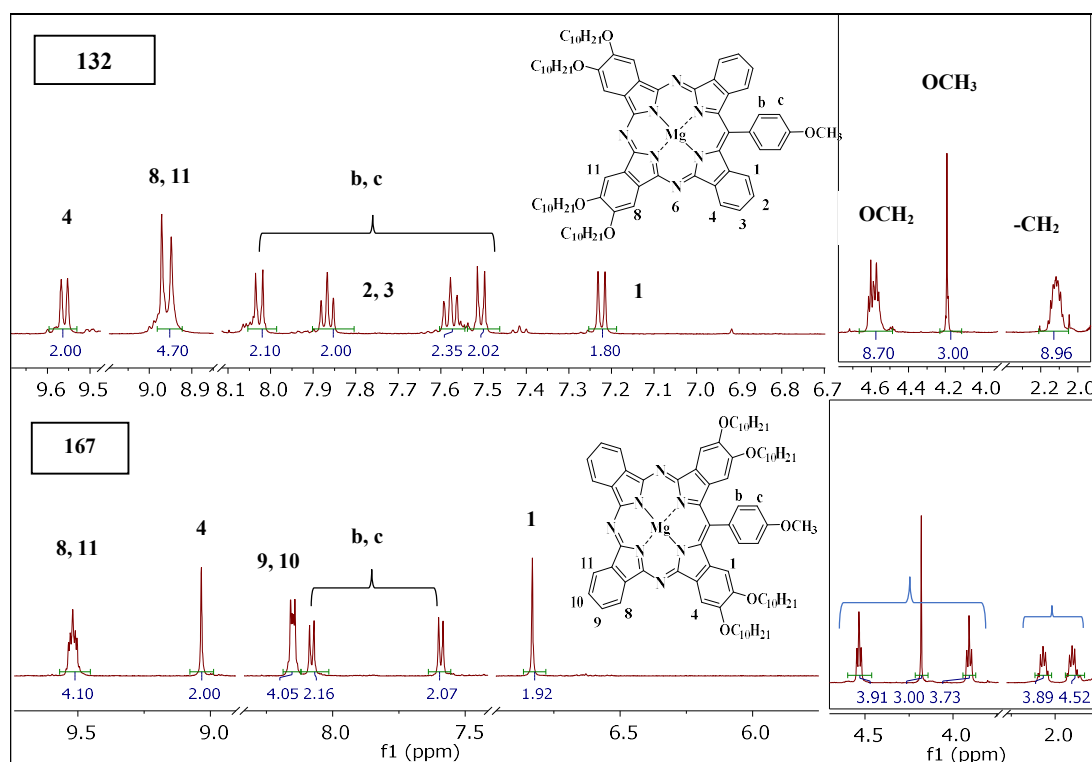


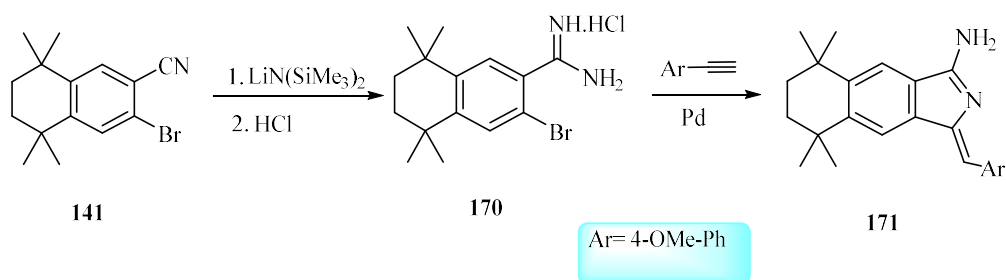
**Figure 2.26:** <sup>1</sup>H NMR spectra of isomeric TBTAP hybrids **132** and **167**

We have therefore demonstrated the controlled synthesis of complex TBTAP hybrids, giving a single regioisomer in each case. Our experiments show that the ABBA-AR hybrids are the major products in these reactions. Possible mechanism is discussed later in this chapter.

#### 2.4.4 Synthesis TBTAP Hybrids **173** and **172**

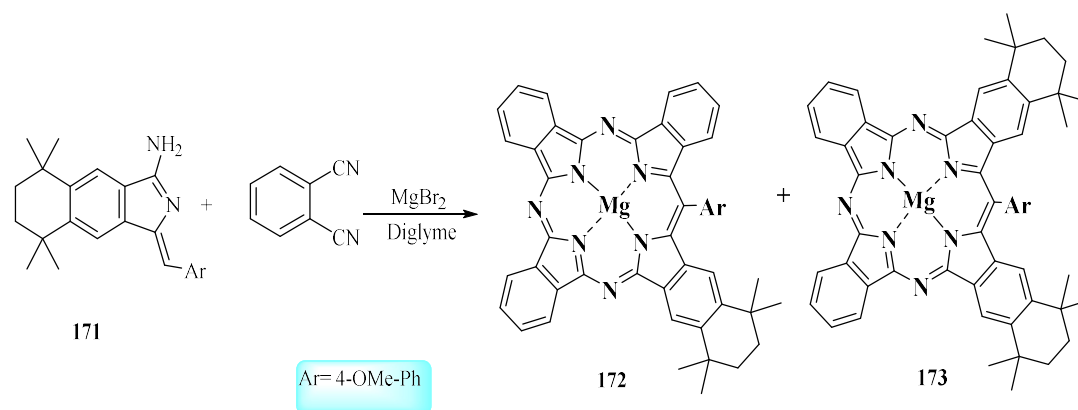
The use of branched groups in the synthesis of the TBTAP **142** and **143** from the first series made their separation relatively straightforward compared with alkyloxy and phenoxy groups in synthesis of **127**, **132**, and **135**. We therefore reasoned that using similar group here would also ease the separation issue and we could be separating two hybrids.

The synthesis of aminoisoindoline **171** started from 2-bromobenzonitrile **141**, which was isolated during the cyanation reaction, as side product, from the corresponding dinitrile **119**. 2-Bromobenzonitrile **141** was converted into the corresponding amidine<sup>49</sup> **170**, which was subsequently subjected to a coupling reaction<sup>48</sup> to finally prepare the targeted precursor **171**, (scheme 2.26). The compounds were characterised by NMR spectroscopy to confirm their structures.



**Scheme 2.26: Synthesis of aminoisoindoline 171**

The TBTAP general reaction was performed with syringe pump since the **171** was soluble in diglyme. In the typical reaction, a mixture of phthalonitrile **8** and  $\text{MgBr}_2$  in diglyme was heated in oil bath. A mixture of phthalonitrile with aminoisoindoline **171** was added slowly, and another mixture of **8** with DABCO was subsequently added, both in diglyme and over an 1h. After cooling, (DCM: MeOH) mixture was added to the resulting material and sonicated. The crude mixture was analysed by TLC and showed three spots which agreed with the previous results from alkyloxy and phenoxy phthalonitrile. The green fraction was separated from other fractions and first spot was identified by MALDI-TOF MS. These results were similar to the previous observations from alkyloxy aminoisoindoline derivatives. However, in this situation we isolated the two TBTAP hybrids **172** and **173** (in 2% and 10% yield respectively), which we may expect due to the heavily branched substituents, (scheme 2.27).



**Scheme 2.27: Synthesis of TBTAP hybrids 172 and 173**

The molecular ion peak of **172** on MALDI-TOF mass spectroscopy was ( $m/z$  751) and the Q band in the UV-Vis spectrum were at 677 and 653 nm. On the other hand, the ion peak of **173** was at ( $m/z$  862) and the Q band were at 680 and 656 nm.

TBTAP complex **173** is an isomeric structure of the hybrid **143**, and the differences and changes in their  $^1\text{H}$  NMR spectra were found compatible and in agreement with the previously discussed comparison between **132** and **167**. However, the TBTAP complex **172**  $^1\text{H}$  NMR spectrum showed that the non-peripheral sites of the macrocycle have different chemical environments resulting from the addition of the bulky substituent. The shielded protons, by the phenyl group on the *meso*-position, appeared as two different peaks one singlet and the other was doublet. In a similar way, the de-shielded protons appeared at 9.60-9.57 ppm. The remaining aromatic protons appeared as expected at the range from 9.54-7.57 ppm. Methoxy protons were at 4.21 ppm and the aliphatic protons appeared at the expected range as well, (figure 2.27).

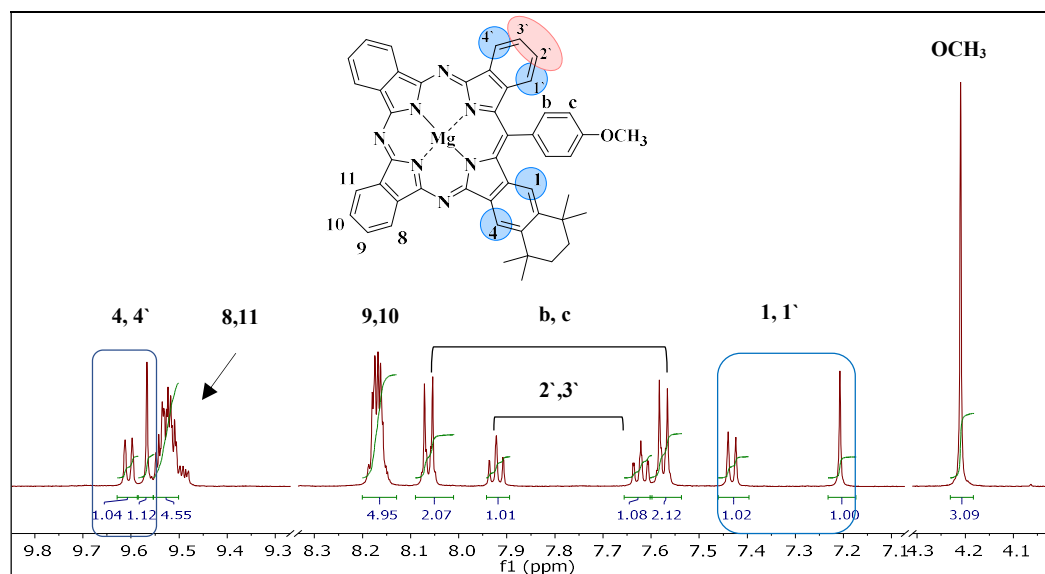


**Figure 2.27:** <sup>1</sup>H NMR spectrum of **172**

With compound **172** we have reached the last TBTAP complex prepared in this series using aminoisoindoline derivatives. All the TBTAPs prepared in this project, in both series, have different molecular structures and this could affect their physical properties. In the next section we will highlight the Electronic absorption spectrum (EAS) of the newly and uniquely functionalised tetrabenzotriazaporphyrins.

## 2.5 Electronic absorption spectra of newly synthesised Tetrabenzotriaza porphyrin complexes

In general trend, the Q band shifts to shorter wavelength and lower intensity as the aza-links are replaced by methine units<sup>45</sup>. Therefore, maxima of the most intense Q band of TBTAPs appears at shorter wavelength compared with corresponding phthalocyanine. The characteristic single strong absorption Q-band of Metallated phthalocyanines (MPcs) appears in the red/ near-infrared region of the spectrum (670-720 nm). In many studies, it was noted that the maxima of the most intense bands of phthalocyanines and the corresponding TBTAPs are similar<sup>30</sup>.

In this section we will compare the effect of introducing substituents into the aromatic system of the macrocycle and the impact of their molecular structure differences on the maximum absorption of the Q-band. It was reported that the electronic absorption spectra strongly depend on the nature of the central metal ion in metal complexes<sup>45,68</sup>. The complexes under the study herein all have magnesium as central metal, which means only the substituents effect is shown in the spectra. Also, the comparison will be against the parent TBTAP complex **69a** for more accuracy. The table 2.3 shows the TBTAP complexes newly synthesised in this project and the maximum absorption of their characteristic Q-band, (figure 2.28).

In terms of the nature of the substituents, the alkyloxy chain caused slight shift to the longer wavelength, (2-5 nm), with the increase in the length of the alkyloxy chain for both series. For example, the  $\lambda_{\text{max}}$  of the most intense bands of the complex **132** shifted to longer wavelength, by (3nm), as the chain length increased compared with **127**. However, the bulky substituents phenoxy groups as in complex **135** caused red shifted by only 5nm, whereas, the other cyclic branched group showed shift up to 12 nm for the complex **142** with three of these groups. In comparison between the isomeric complexes with alkyloxy substituents their molecular structure difference has nearly no effect, although, a shift by 4 nm was shown in the isomeric hybrids **143** and **173**.

Maximum absorption of the Q bands of the parent MgTBTAP <b>69a</b>			
670, 648 nm			
First Series complexes		Second Series complexes	
Complex	$\lambda_{\max}$ , (nm)	Complex	$\lambda_{\max}$ , (nm)
<b>127</b>	670, 648	<b>166</b>	675, 652
<b>132</b>	673, 649	<b>167</b>	675, 652
<b>135</b>	675, 652	<b>161</b>	673, 650
<b>142</b>	682, 658	<b>172</b>	677, 653
<b>143</b>	676, 652	<b>173</b>	680, 656
<b>147</b>	709, 681		

Table 2.3: Maximum absorption of the Q-bands of Mg-TBTAP complexes

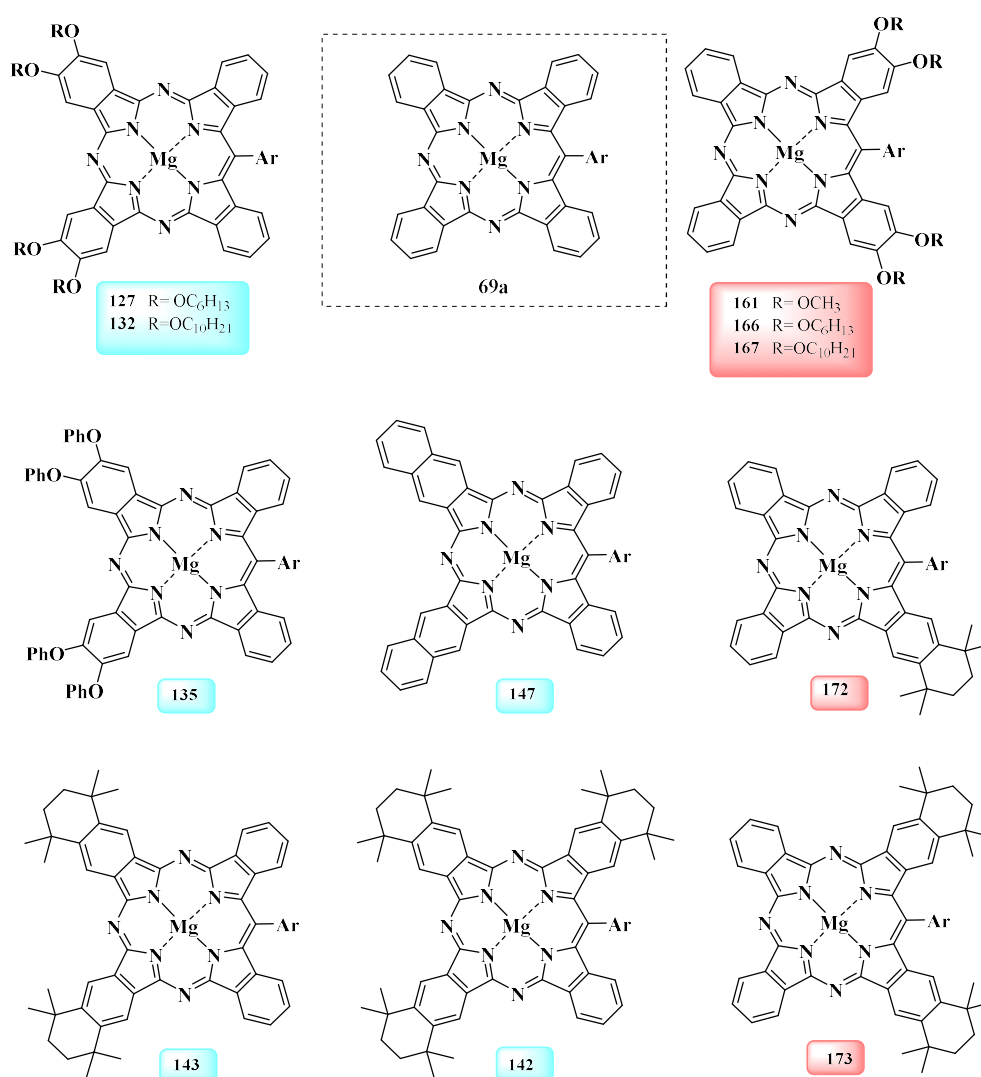
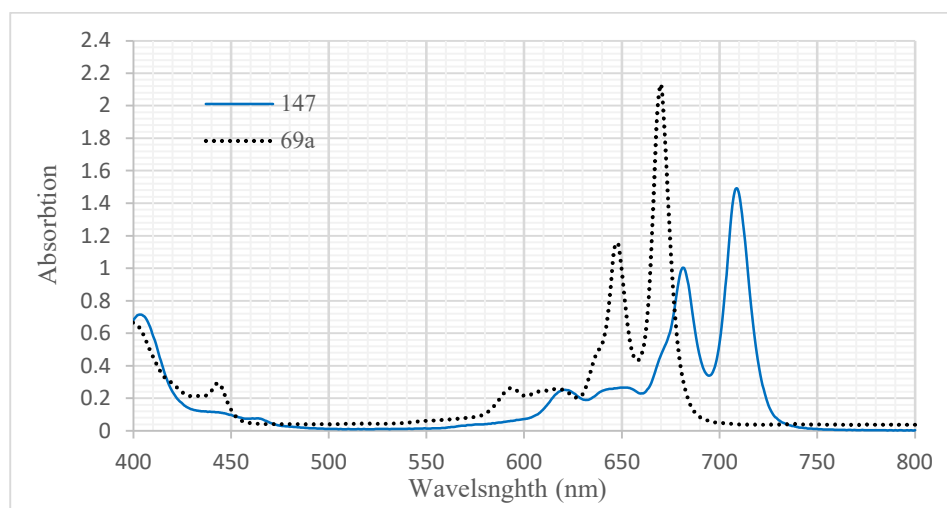


Figure 2.28: The newly synthesised TBTAP complexes

Lastly, the naphtho-annulated complex **147** showed a significant red shift to the longer wavelength by 39 nm which was expected due to the extension of the molecule's  $\pi$ -system, (figure 2.29). The increase of benzene units fused to the TBTAP macrocycle in naphthyl annulated TBTAP has had bathochromic shift by 90 nm in Leznoff's isolated compounds<sup>28</sup> **38** and **144**, whereas herein the shift by only 39 nm.



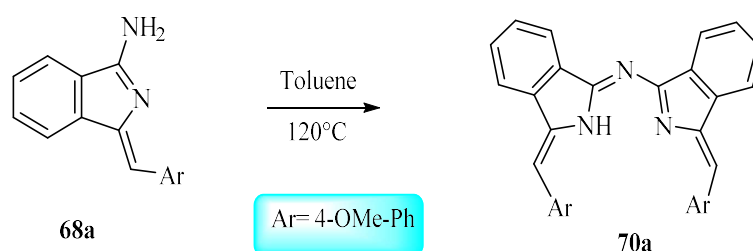
**Figure 2.29: The bathochromic shift of naphtho-annulated TBTAP 147**

It was reported that the introduction of substituents both onto the *meso*-position of the ring and in the aromatic system of the macrocycle has only a slight effect on the character of the absorption spectrum<sup>69</sup>. Our results on this aspect were consistent with the literature, additionally, it was shown that the number of substituents on the macrocycle could slightly affect their spectrum.

## 2.6 Synthesis of aminoisindoline dimers [Aza-(dibenzo)dipyrromethenes]

Dipyrromethenes are widely used as intermediates for the synthesis of porphyrins, fluorescent dyes, electronic materials and other coordination compounds<sup>135</sup>. The syntheses of such compounds are generally based on the acid-catalysed condensation of pyrrole with aldehydes or ketones in an organic solvent. A direct application of these methods towards benzo-annulated derivatives has been impossible because the respective isindolic precursors are unstable and therefore unavailable. The current synthesis is limited to treating a phthalonitrile-based electrophile with a Grignard reagent followed by reduction with formamide at high temperature<sup>136</sup>. Nevertheless, a different class of aza-(dibenzo)dipyrromethenes compounds were previously reported by our group and converted to boron derivatives (BODIPYs), developing into an increasingly important class of stable organic dyes<sup>137</sup>. Aza-dipyrromethenes have also seen promising applications outside of their boron-coordinated complexes, especially as complexes of Zn (II), which have successfully been incorporated as active components in organic photovoltaics (OPVs)<sup>138,139</sup>.

The mixed condensation of phthalonitrile and aminoisindoline in diglyme for all the reactions we performed gave the dimeric products resulting from self-condensation of the aminoisindolines and called aza-(dibenzo)dipyrromethenes. Aza-(dibenzo)dipyrromethene **70a** was synthesised by heating a mixture of aminoisindoline **68a** in toluene to 120°C under inert gas according to the procedure reported by Cammidge's group<sup>137</sup>, (scheme 2.28).

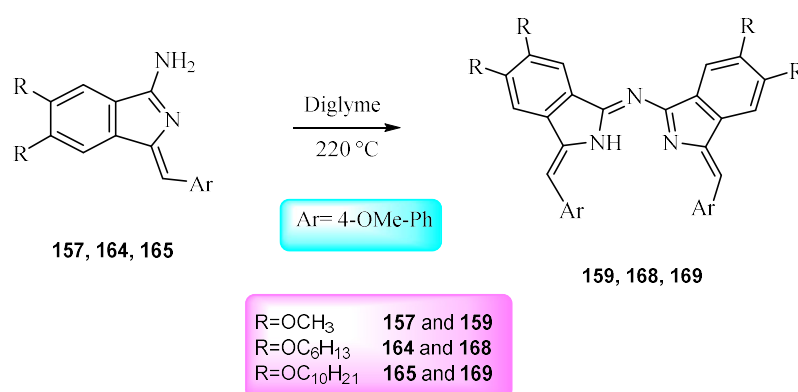


**Scheme 2.28: Synthesis of aza-(dibenzo) dipyrromethene 70a**

Similarly, attempts were made to synthesise the other dimeric derivatives **159**, **168**, **169** and **174**. The reactions were monitored by TLC and showed no signs of completion after 24-48 hours. A great amount of the starting materials still unreacted

with traces of red coloured material formed, indicates the slow formation of the dimers. Increasing the temperature had no effect either. Thus, the solvent was changed to diglyme at 220 °C and the reaction monitored by TLC which resulted in the formation of the corresponding dimers and consuming of the starting materials in average of 1h to 4h.

Alkyloxy derivatives dimers **159**, **168** and **169** were synthesised using same approach, (scheme 2.29), and also characterised by NMR spectroscopy and MALDI-TOF mass spectroscopy to confirm their structures.



**Scheme 2.29: General synthesis of alkyloxy dimers**

Aza-(dibenzo) dipyrromethene **174** was synthesised by self- condensation of the aminoisoindoline **171** in diglyme at 220 °C for 3h under inert gas, (scheme 2.30). The reaction mixture was allowed to cool, then water was added and stirred for 15 min. The crude was purified using column chromatography and DCM as eluent solvent then the polarity was increased and mixture of DCM:Methanol (50:1) was used to give compound **174**. The compound gave suitable crystals for X-Ray diffraction analysis which confirm its molecular structure with *Z/Z* configuration, (figure 2.30), The MALDI-TOF analysis confirm the structure with ion peak (*m/z* 704).

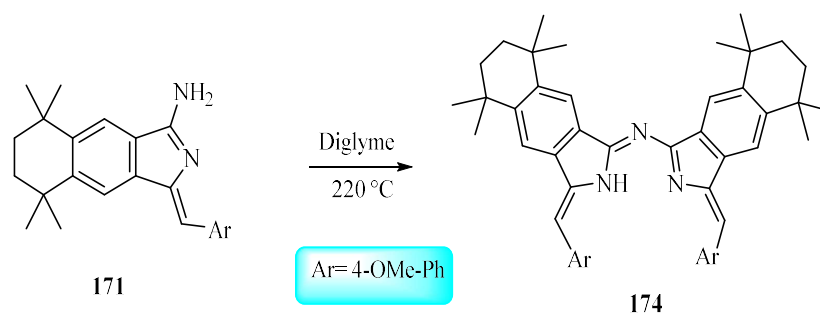
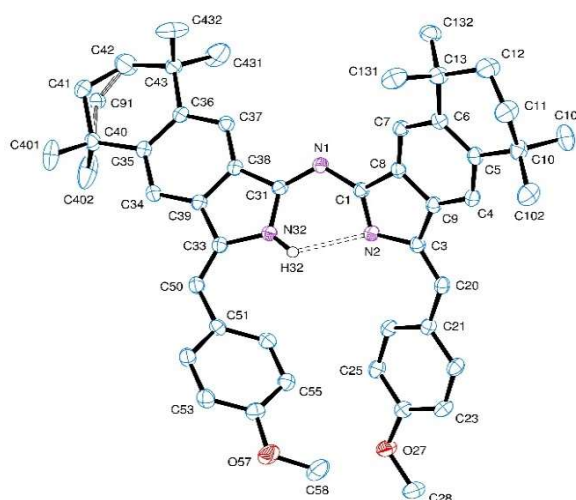
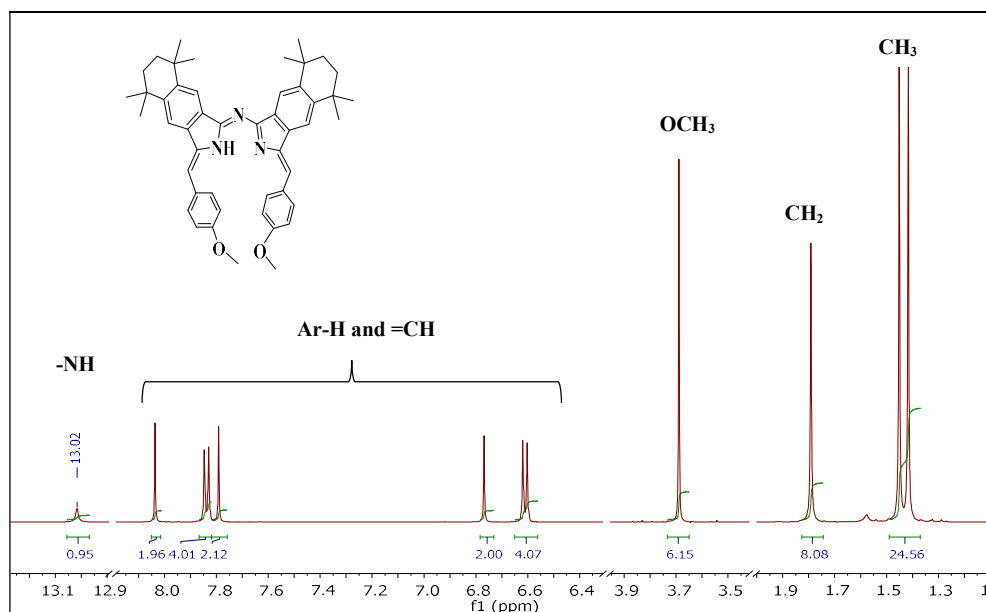
**Scheme 2.30: Synthesis of aza-(dibenzo) dipyrromethene 174****Figure 2.30: X-Ray structures of the dimer 174**

Figure 2.31 displays all the protons signals of the dimer **174** as follows; the N-H proton appeared at 13.02 ppm. The aromatic protons of the isoindoline benzene rings and the vinyl protons (C=C-H) were at 8.04, 7.79 and 6.77 ppm. Two doublet peaks at 7.84 and 6.61 ppm, with four protons each and coupling constant ( $J = 8.7$  Hz), show the distinct AA'BB' aromatic pattern. Methoxy groups protons were at 3.69 ppm, and in the range from 1.79-1.42 ppm, methyl and methylene protons appeared as expected.



**Figure 2.31:**  $^1\text{H}$  NMR spectrum of the dimer **174**

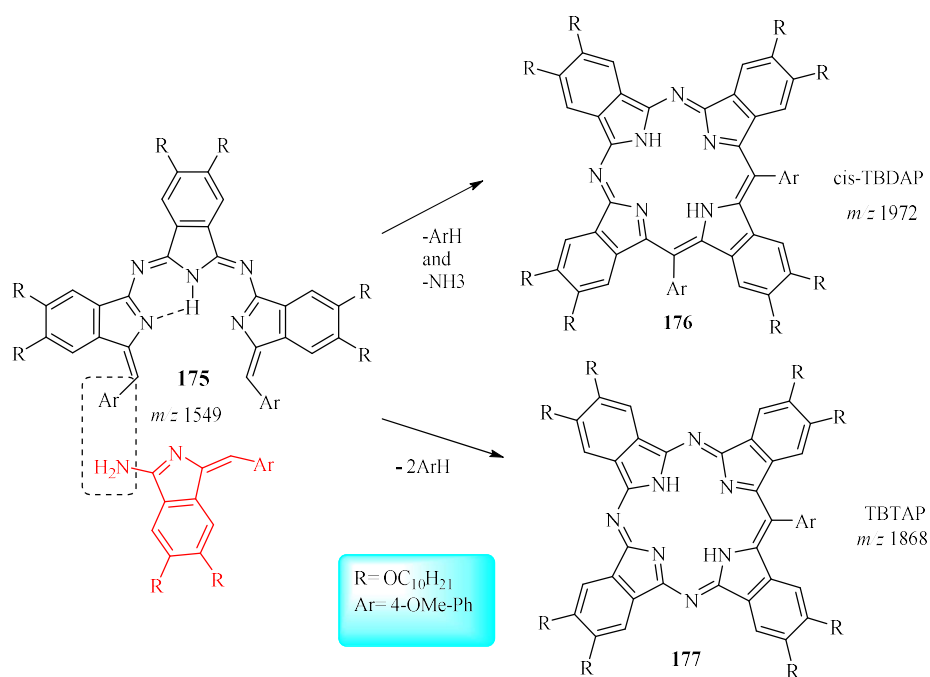
Alkyloxy derivatives dimers **159**, **168** and **169** were synthesised using same approach and also characterised by NMR spectroscopy and MALDI-TOF mass spectroscopy to confirm their structures. However, a green fraction was noticeable in these derivatives during the separation. The fraction was very dilute and not detected by the MALDI to identify it. The reaction was repeated for all the derivatives for 24 hours, and the intensity of the green fraction was only observed with the synthesis of dimer **169**.

The green fraction was isolated by preparative thin layer chromatography and analysed by MALDI-TOF mass spectroscopy to give ion peak at ( $m/z$  1973). The reaction was containing one reactant; thus, it only suggests the structure of tetrabenzodiazaporphyrin ligand  $(\text{OC}_{10}\text{H}_{21})_8\text{H}_2\text{TBDAP}-(4\text{-OMe-Ph})_2$ .

We took a closer look to explain the formation of the green material from condensation reaction of aminoisoindoline **165**. The aminoisoindoline dimer **169** was formed by self-condensation through elimination of  $\text{NH}_3$  molecule. The reaction is favorable and proceed spontaneously at lower temperature, as previously mentioned in the synthesis of parent TBTAP **69a**. Therefore, the only suggestion here is that the aminoisoindoline molecules could have condensed by different ways, with the high temperature of the solution for long period of time. It is important but it is still hard to explain the mechanism of formation of either *cis* or *trans*-TBDAP or mixture of them which

involves elimination of benzyl ring and  $\text{NH}_3$  (and changing the configuration of the molecule from *Z* to *E*).

For *trans*-TBDAP, it only could be obtained from the self-condensation of the dimer **169**, through reduction and loss of two benzyl rings. However, previous experiments were carried out in our group re-subjecting the unsubstituted dimer **70a** as precursor in the synthesis of TBTAP, to the same reaction conditions and no formation of hybrid macrocycles was observed<sup>47</sup>. Thus, we assumed that the unreacted aminoisindoline molecules might have formed an intermediate compound **175** through their active nitrogen atoms. This could be the impact of several factors such as high temperature, time and the long alkyloxy chains, with no clear explanation of its formation. Scheme 2.31 illustrates the proposed formation of *cis*-TBDAP supported with MALDI TOF-MS.



**Scheme 2.31: The proposed formation of the TBDAP from the condensation reaction of aminoisindoline 165**

MALDI-TOF Mass spectrum of the green fraction showed three ion peaks, the main peak corresponding to the suggested *cis*-( $\text{OC}_{10}$ )<sub>8</sub>TBDAP-(4-MeO-Ph)<sub>2</sub> **176** and two additional peaks for the trimer **175** and for the corresponding ( $\text{OC}_{10}$ )<sub>8</sub>TBTAP-(4-MeO-Ph) **177**, (figure 2.32).

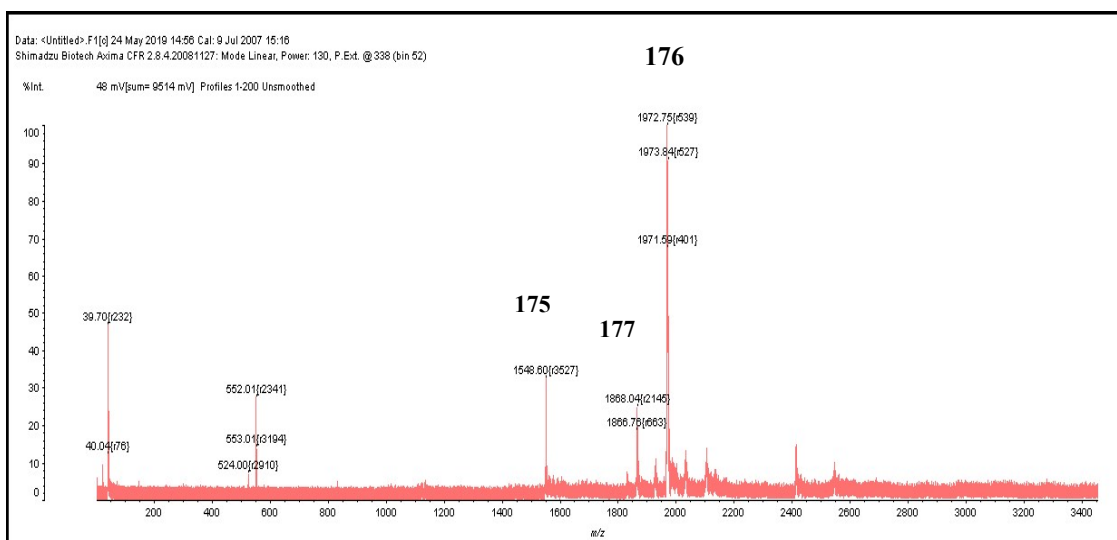
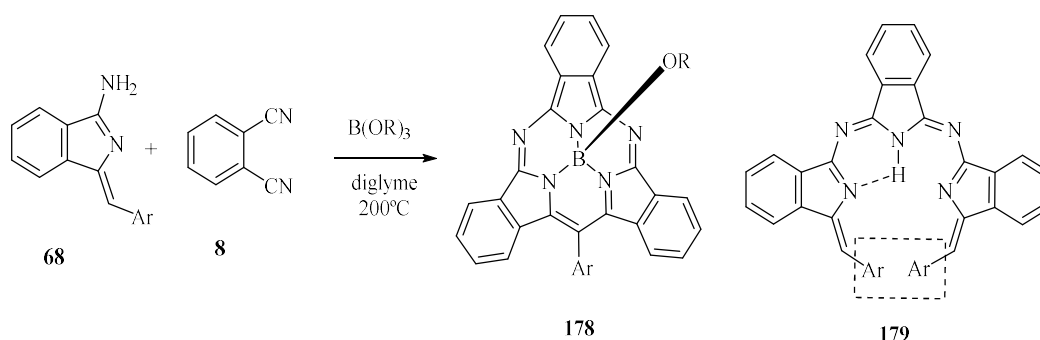


**Figure 2.32: MALDI-TOF of the green fraction isolated from synthesis of 169**

Our proposal for this formation of TBDAP and TBTAP is based on an observation that a similar intermediate was isolated during mechanistic investigation of SubTBDAP formation using phthalonitrile, aminoisoindoline and tributyl borate at 200°C in diglyme<sup>140</sup>, (scheme 2.32).



**Scheme 2.32: Synthesis of Sub-TBDAP and the isolated intermediate 179**

The intermediate **179** was characterised by mass spectrometry and NMR spectroscopy and gave a trimer helical-like conformation structure stabilised with a hydrogen bond. The chirality of the trimer in the crystal was analysed and gave left-handed (M-configuration)<sup>141</sup>, (figure 2.33).

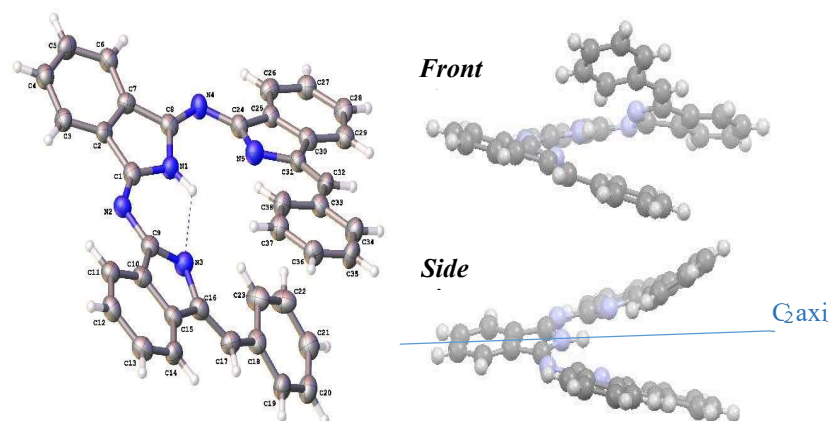


**Figure 2.33: The isolated trimer 179 during mechanistic investigation of SubTBDAP<sup>141</sup>**

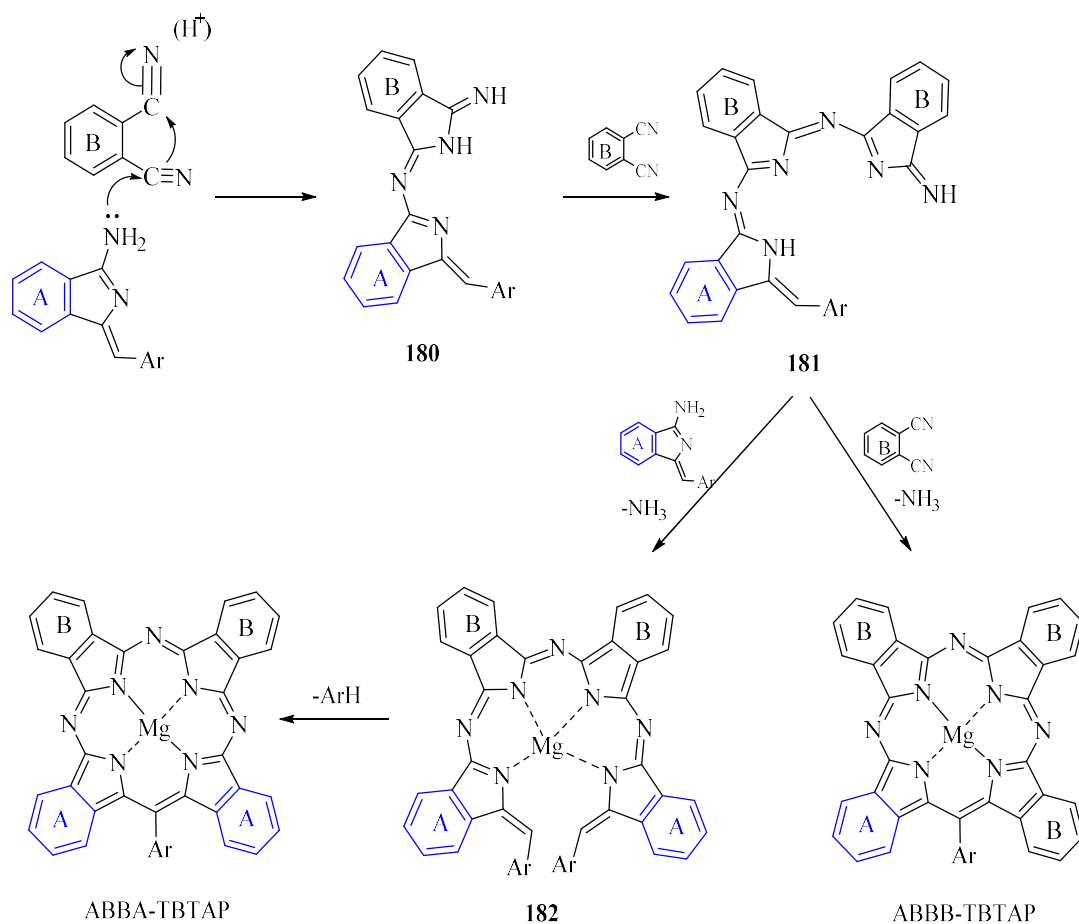
Helicenes are notable for having chirality despite lacking both asymmetric carbons and chiral centres. They are *ortho*-condensed polycyclic aromatic compounds, due to the steric effect between the terminal benzene rings, these aromatic systems adopt a nonplanar distorted structure. The helix winds around a central axis either with right-handed (P-configuration) or left-handed (M-configuration) helicity<sup>141</sup>.

The mechanism of formation of the hybrid materials (TBTAPs and SubTBDAPs) still remains unclear, and the isolated trimer obtained from reaction between the aminoisoindolines and phthalonitrile in sub-TBDAP synthesis could give a clue to our possible pathway.

## 2.7 Proposed mechanism of Tetrabenzotriazaporphyrin formation

The proposed mechanism of the formation of metallophthalocyanine from phthalonitrile involves cyclotetramerization process under basic conditions. Alcohol is assumed to be firstly deprotonated by some basic promoters such as DBU or DBN leading to strong nucleophilic alkoxide species. An alkoxide ion attacks the nitrile of phthalonitrile to obtain the monomeric alkoxyiminoisoindolenine intermediates. Subsequently, the dimeric intermediates can react with further phthalonitrile molecule to form the tetramer and the reduction of the intermediates occur by loss of aldehyde in the last step. The stability of the 18- $\pi$  electron aromatic system can be considered the key for the phthalocyanine formation<sup>142,143</sup>. However, under the conditions of the reaction of TBTAP synthesis, MgBr<sub>2</sub> can promote formation of MgPc from phthalonitrile. Before the present work the primary mechanism for TBTAP formation was explained as that the aminoisoindoline acts as nucleophile and attacks a molecule of phthalonitrile and gives a dimeric intermediate **180**. The intermediate **180** add further phthalonitrile until build a chain, four units long, then cyclisation occurs (promoted by the magnesium bromide) to give the Ar-TBTAP<sup>10,47</sup>. However, from our work it is clear that the mechanisms operating are more complicated. In the original reaction, formation of the parent TBTAP **69a**, no substituents were present on either the phthalonitrile or aminoisoindoline. Thus, the different mechanistic pathways in this case lead to identical TBTAP structures.

Introducing substituents revealed that the dominant product in these reactions is a TBTAP hybrid that incorporates two aryl rings from aminoisoindoline (A), plus two from phthalonitrile (B). The hybrid has specific regiochemistry-ABBA. Possible mechanism pathways are shown in scheme 2.33. The first step is likely to be the same as originally proposed, in which the aminoisoindoline attacks phthalonitrile and leads to a chain growth followed by reaction with aminoisoindoline give the intermediate **182** (analogue of **175** and **179**) which can cyclise to obtain the observed ABBA-Ar TBTAP. Dimeric condensation of the initial intermediate **180** is also possible.



**Scheme 2.33: Possible pathways leading to Formation of TBTAPs**

## 2.8 Conclusion

The detailed investigation of TBTAP formation using the reaction of aminoisoindolines and phthalonitriles, using magnesium ion as template, has been performed. The use of substituted derivatives shows that the dominant pathway leads to the surprising formation of novel ABBA-Ar TBTAP hybrids as single regioisomer. This novel chemistry has been expanded to give isomeric substituted TBTAPs. The synthesis of two series of peripheral *meso*-aryl substituted TBTAP complexes bearing different functional groups has been successfully achieved. In addition, a series of novel amidine, aminoisoindoline and aza-(dibenzo)dipyrromethene derivatives were synthesised throughout this work to achieve the main aim of this work. These functionalised complexes may develop the understanding of the mechanism of their synthesis for future investigating work.

## 2.9 Future Work

Work in the immediate future should focus on the stoichiometric ratios of phthalonitrile and aminoisoindoline. We would hope by optimising the ratio, the selectivity could be controlled. Moreover, further investigations are recommended in regarding the TBDAP formation from aminoisoindoline. Optimising this reaction would allow ready access to a variety of analogues of tetrabenzo(aza)porphyrins. The new synthesised aza-(dibenzo) dipyrromethene derivatives could be converted into the corresponding aza-(dibenzo) BODIPY analogues by straightforward reaction with Boron trifluoride etherate ( $\text{BF}_3 \cdot \text{OEt}_2$ ). Boron dipyrromethenes (BODIPYs) considered as important class of stable organic dyes. They have proved to be highly fluorescent and sensitive to their environment, leading to potential applications in areas such as sensing and imaging.

## **Chapter 3: Experimental**

### 3.1 General Methods

Reagents and solvents were obtained from commercial sources and used without further purification unless otherwise stated. Phthalonitrile was recrystallised from hot xylene. THF was freshly distilled from sodium and benzophenone. Reactions and distillation were carried out under an inert atmosphere (argon or nitrogen gas), in most air-sensitive reactions argon was preferred. Brine is a saturated aqueous solution of sodium chloride. Organic layers were dried using anhydrous magnesium sulphate. Evaporating of solvent was performed using a Buchi rotary evaporator at reduced pressure.

$^1\text{H}$  NMR spectra were recorded either at 400 MHz on Ultrashield Plus<sup>TM</sup> 400 spectrometer or 500 MHz on a Bruker Ascend<sup>TM</sup> 500 spectrometer in 5 mm diameter tubes. Signals are quoted in ppm as  $\delta$  downfield from tetramethylsilane ( $\delta=0.00$ ) and coupling constants  $J$  given in Hertz.  $^{13}\text{C}$  spectra were recorded at 101 MHz or 126 MHz on the same spectrometers. NMR spectra were performed in solution using deuterated chloroform, methanol, dichloromethane or tetrahydrofuran at room temperature unless otherwise stated.

Ultraviolet-Visible absorption spectra were recorded on Hitachi U-3310 Spectrophotometer in solvent as stated. MALDI-TOF mass spectra were carried out using a Shimadzu Biotech Axima instrument. IR spectra were recorded using a Perkin-Elmer Spectrum BX FT-IR spectrometer. Thin layer chromatography (TLC) was performed using aluminium sheets coated with Alugram<sup>®</sup> Sil G/UV254 (Macherey-Nagel), and the compounds were visualised by viewing under short-wavelength UV-light at 245 nm or 366 nm. Column chromatography was carried out using silica gel 60Å mesh 70 – 230 (63 – 200  $\mu\text{m}$ ) under regular conditions (at ambient temperature and atmospheric pressure or at moderate pressure occasionally). Solvent ratios are given as v: v. Melting points were taken on a Reichart Thermovar microscope with a thermopar based temperature control. Reactions using microwave irradiation were carried out in Biotage Initiator+ Microwave system.

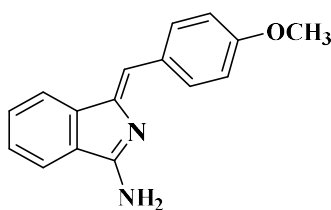
**2-Bromobenzamidine hydrochloride 67**

Following the method reported by Dalai<sup>49</sup>, a solution of 2-bromobenzonitrile **66** (3.7g, 20.33 mmol) in dry THF (3 ml) was added to a solution of  $\text{LiN}(\text{SiMe}_3)_2$  in anhydrous THF (1 M, 22 ml, 22 mmol, 1.1eq). The reaction mixture was stirred at room temperature for 4 h. A 5N HCl solution in isopropanol (15 ml) was added to the cooled mixture. The crude reaction mixture was left to stir at room temperature overnight. The precipitate was filtered off and washed with diethyl ether to give the title compound as colourless crystals (4.2 g, 88 %).

**Mp** > 250°C (lit. > 250 °C)<sup>49</sup>

**<sup>1</sup>H NMR** (500 MHz, Methanol-*d*<sub>4</sub>)  $\delta$  7.81 (dd,  $J = 7.4, 1.5$  Hz, 1H), 7.64 – 7.54 (m, 3H).

**<sup>13</sup>C NMR** (126 MHz, Methanol-*d*<sub>4</sub>)  $\delta$  168.0, 134.73, 134.51, 132.93, 130.70, 129.26, 120.78.

**(Z)-1-[(4-methoxy)benzylidene]-1H-indol-3-amine 68a**

A mixture of 2-bromobenzamidine hydrochloride **67** (706.5 mg, 3 mmol), BINAP (102 mg, 0.165 mmol, 0.055eq) and  $\text{PdCl}_2(\text{MeCN})_2$  (39 mg, 0.15 mmol, 0.05eq) was sealed in a microwave vessel with a magnetic bar and then purged and refilled with  $\text{N}_2$  thrice. Then, 4-ethynylanisole (0.467 ml, 0.476 g, 3.6 mmol, 1.2eq) and DBU (1.12 ml, 1.14 g, 7.5 mmol, 2.5eq) in dry DMF (12 ml) was added. The mixture was stirred under  $\text{N}_2$  for 5 min to give a clear yellow solution with a white solid<sup>48</sup>. Finally, the

mixture was irradiated in a microwave reactor at 120°C for 1 h. After cooling, ethyl acetate (50 ml) was added and the mixture washed with a saturated solution of NaHCO<sub>3</sub> (3x75 ml). The organic layer was dried with MgSO<sub>4</sub>, filtered and concentrated. The residue was finally purified by column chromatography using PE:AcOEt (1:1) then AcOEt as solvent gradient to afford a yellow semisolid that was recrystallized from a DCM:Petroleum ether (1:1) to yield the title compound as yellow needles (620 mg, 83%).

**Chemical Formula:** C<sub>16</sub>H<sub>14</sub>N<sub>2</sub>O

**Mp** 150°C (lit. 156- 157 °C)<sup>47</sup>

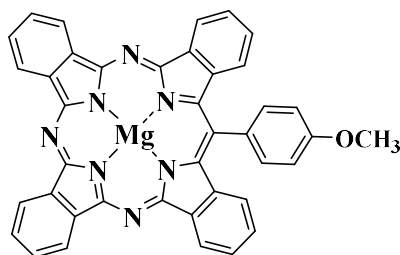
**<sup>1</sup>H-NMR** (400 MHz, Chloroform-d) δ 7.99 (d, *J* = 8.7 Hz, 2H), 7.77 (d, *J* = 7.8 Hz, 1H), 7.68 (d, *J* = 7.7 Hz, 1H), 7.50 (td, *J* = 7.5, 1.0 Hz, 1H), 7.38 (td, *J* = 7.5, 0.9 Hz, 1H), 6.94 (d, *J* = 8.7 Hz, 2H), 6.76 (s, 1H), 3.83 (s, 3H).

**<sup>13</sup>C-NMR** (101 MHz, Chloroform-d) δ (ppm)= 164.05, 159.56, 142.60, 142.07, 132.00, 130.11, 129.51, 128.77, 127.43, 120.26, 119.78, 115.60, 114.36, 55.46.

**MS** (MALDI-TOF): *m/z* = 250.1 [M]<sup>+</sup> (100%)

**UV-vis** (DCM): λ<sub>max</sub> (nm) (ε (dm<sup>3</sup>.mol<sup>-1</sup>.cm<sup>-1</sup>)) = 372 (3.33·10<sup>4</sup>)

### 3.2 MgTBTAP-(4-OMe-Ph) 69a



A suspension of phthalonitrile **8** (154 mg, 1.2 mmol, 3eq) and MgBr<sub>2</sub> (110 mg, 0.6 mmol, 1.5eq) in dry diglyme (0.5 ml) was stirred for 10 min at 220°C, in an oil bath, under an argon atmosphere. A solution of aminoisoindoline **68a** (100 mg, 0.4 mmol, 1eq) and phthalonitrile (51 mg, 0.4 mmol, 1eq) in dry diglyme (1 ml) was added dropwise over 1 hour using a syringe pump. Finally, a third solution of DABCO (67.5

mg, 0.6 mmol, 1.5eq) and phthalonitrile (51 mg, 0.4 mmol, 1eq) in dry diglyme (0.5 ml) was added dropwise over 1 hour. The reaction was heated for 0.5 h at 220°C under an argon atmosphere. Then, the solvent was removed under an argon stream while cooling. A 1:1 mixture of DCM:MeOH (20 ml) was added and the mixture sonicated. The solvents were removed under vacuum and the crude mixture purified by two consecutive flash chromatography columns. First, using DCM→DCM:Et<sub>3</sub>N (20:1)→DCM:THF:Et<sub>3</sub>N (10:4:1) as eluent, the fractions were collected according to their colours. Only the green fraction was subjected to the second column using PE:THF:MeOH (10:3:1) as eluent. Recrystallisation from acetone and EtOH gave the title compound as purple crystals<sup>47</sup> (51 mg, 20%).

**Chemical Formula:** C<sub>40</sub>H<sub>23</sub>MgN<sub>7</sub>O

**Mp** > 300°C (lit. > 300°C)<sup>47</sup>

**<sup>1</sup>H-NMR** (400 MHz, Acetone-*d*<sub>6</sub>) δ 9.61 (d, *J* = 7.7 Hz, 2H), 9.53 (s, 4H), 8.31 – 8.21 (m, 4H), 8.06 (d, *J* = 8.3 Hz, 2H), 7.99 (t, *J* = 7.3 Hz, 2H), 7.69 (t, *J* = 7.6, 2H), 7.58 (d, *J* = 8.3 Hz, 2H), 7.24 (d, *J* = 8.2 Hz, 2H), 4.23 (s, 3H, OCH<sub>3</sub>).

**<sup>1</sup>H-NMR** (500 MHz, THF-*d*<sub>8</sub>) δ 9.60 (d, *J* = 7.3 Hz, 2H), 9.53-9.50 (m, 4H), 8.22 – 8.13 (m, 4H), 8.05 (d, *J* = 8.5 Hz), 7.92 (t, *J* = 7.2 Hz, 2H), 7.62 (t, *J* = 7.4, 2H), 7.52 (d, *J* = 8.5 Hz, 2H), 7.25 (d, *J* = 8.3 Hz, 2H), 4.20 (s, 3H, OCH<sub>3</sub>).

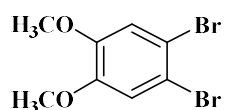
**<sup>13</sup>C-NMR** (126 MHz, THF) δ 162.01, 156.56, 153.51, 152.60, 143.53, 141.32, 141.21, 140.99, 140.24, 135.98, 134.16, 130.08, 129.79, 128.24, 127.39, 126.76, 125.89, 123.91, 123.70, 123.63, 115.30, 56.14.

**MS** (MALDI-TOF): *m/z* = 641.72 [M]<sup>+</sup> (100%)

**UV-vis** (dist. THF) λ<sub>max</sub> (nm) (ε (dm<sup>3</sup>.mol<sup>-1</sup>.cm<sup>-1</sup>)) = 670 (2.74·10<sup>5</sup>), 648 (1.48·10<sup>5</sup>), 594 (3.38·10<sup>4</sup>), 444 (3.74·10<sup>4</sup>), 398 (8.65·10<sup>4</sup>).

### 3.3 Synthesis of the first series of *meso*-Ar-TBTAP hybrids

#### 1,2-Dibromo-4,5-dimethoxybenzene **108**<sup>122</sup>



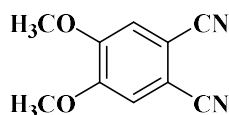
Veratrole **112** (1,2-dimethoxybenzene) (40.0 g, 0.29 mol) was stirred in dichloromethane (300 ml) at 0°C. Bromine (32.8 ml, 0.64 mol, 102.3g) was added dropwise while stirring for 2 h. The mixture was further allowed to stir 1 h at room temperature. The reaction mixture was washed with sodium thiosulphate, brine and water. The aqueous layer was extracted with DCM (3x100 ml). The organic extract was dried with magnesium sulphate (MgSO<sub>4</sub>) and the solvent was evaporated. The residue was recrystallised from isopropanol to give colorless crystals (80 g, 95%).

**Mp** 88-90°C (lit. 97-98 °C)<sup>129</sup>

<sup>1</sup>H-NMR (500 MHz, Chloroform-*d*) δ 7.06 (s, 2H), 3.85 (s, 6H, OCH<sub>3</sub>).

<sup>13</sup>C-NMR (126 MHz, CDCl<sub>3</sub>) δ 149.05, 116.10, 114.92, 56.42 (OCH<sub>3</sub>).

#### 1,2-Dicyano-4,5-dimethoxybenzene<sup>123</sup> **115**



A mixture of 1,2-dibromo-4,5-dimethoxybenzene **108** (1.3 g, 4.39 mmol) and CuCN (1.97 g, 21.99 mmol) was heated to reflux in dry DMF (15 mL) under an argon atmosphere and the reaction monitored by TLC every hour. After 3 hours, the reaction mixture was cooled to room temperature and 20 ml of DCM was added. The solid then filtrated off to remove the copper salts. The filtrate was washed with water (3 x 50 mL) and with an aqueous solution of ammonia until no blue colour was obtained in the aqueous layer. Finally, the organic layer was washed with a saturated solution of NaHCO<sub>3</sub>, dried over MgSO<sub>4</sub> and filtered. The filtrate was evaporated under reduced pressure to give the crude product. The crude material was purified by column

chromatography using (1:2) DCM:PE → (1:1) DCM:PE → DCM to yield the product **115** as a colorless solid (0.26 g, 32%).

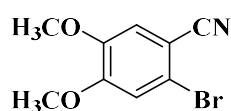
**Mp** 182-184°C (lit. 179-181°C)<sup>123</sup>

**<sup>1</sup>H-NMR** (500 MHz, CDCl<sub>3</sub>) δ 7.15 (s, 2H), 3.97 (s, 6H, OCH<sub>3</sub>).

**<sup>13</sup>C-NMR** (101 MHz, CDCl<sub>3</sub>) δ 152.73, 115.86, 114.90, 109.12, 56.79 (OCH<sub>3</sub>).

**FT-IR** (NaCl), ν (cm<sup>-1</sup>): 2225 (C≡N).

### 2-Bromo-4,5-dimethoxybenzonitrile **120**



This compound was isolated as side product from the cyanation reaction of **108** (0.45 g, 42%).

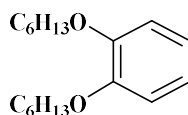
**Mp** 118-120°C (lit. 113)<sup>144</sup>

**<sup>1</sup>H-NMR** <sup>1</sup>H NMR (400 MHz, Chloroform-*d*) δ 7.07 (s, 1H), 7.05 (s, 1H), 3.93 (s, 3H), 3.89 (s, 3H).

**<sup>13</sup>C-NMR** <sup>13</sup>C NMR (101 MHz, CDCl<sub>3</sub>) δ 153.33, 148.65, 117.76, 117.73, 115.63, 115.39, 107.03, 56.62, 56.50.

**FT-IR** (NaCl), ν (cm<sup>-1</sup>): 2230 (C≡N).

### 1,2-Bis(hexyloxy)benzene **123**<sup>120</sup>



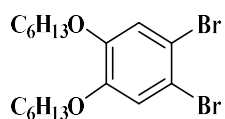
1,2-Dihexyloxybenzene **123** was synthesised according to conditions used by Cammidge group. Pyrocatechol (20 g, 0.18 mol), 1-bromohexane (89.4 g, 0.54 mol) and potassium carbonate (74.6 g, 0.54 mol) were stirred in ethanol (300 ml) at 80°C

for 2 days. The mixture was allowed to cool to room temperature, filtered, washed with distilled water and extracted with dichloromethane (3x50 ml). The organic layer was evaporated in vacuo giving orange oily compound, which was distilled under vacuum. The pure product was collected at 185 °C as a colourless oil.

$^1\text{H-NMR}$  (500 MHz, Chloroform-*d*)  $\delta$  6.97 (s, 4H), 4.08 (t,  $J= 7.1$ , 4H), 1.994-1.87 (m, 4H), 1.60-1.56 (m, 4H), 1.46- 1.43 (m, 8H), 1.03- 1.00 (m, 6H).

$^{13}\text{C-NMR}$  (126 MHz,  $\text{CDCl}_3$ )  $\delta$  149.28, 120.97, 114.06, 69.17, 31.64, 29.37, 25.77, 22.64, 14.00.

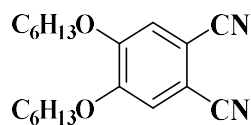
### 1,2-Dibromo-4,5-bis(hexyloxy)benzene **124**<sup>121</sup>



1,2-Bis(hexyloxy)benzene **123** (36.13 g, 0.130 mol) was stirred in dichloromethane (300 mL) at -10°C. Bromine (17.53 mL, 54.4 g, 0.340 mol) was added dropwise via syringe, and the mixture was stirred at 0 °C for 1 hour. On completion, the mixture was washed with sodium metabisulphite solution ( $\text{Na}_2\text{S}_2\text{O}_5$ ) (20%, 200 mL). The organics were extracted with dichloromethane and dried over  $\text{MgSO}_4$ . The solvent was removed under reduced pressure, and the pure product obtained as an orange oil.

$^1\text{H-NMR}$  (500 MHz, Chloroform-*d*)  $\delta$  7.06 (s, 2H), 3.94 (t,  $J= 7.0$ , 4H), 1.82-1.77 (m, 4H), 1.48-1.42 (m, 4H), 1.35-1.32 (m, 8H), 0.92-0.89 (m, 6H).

$^{13}\text{C-NMR}$  (101 MHz,  $\text{CDCl}_3$ )  $\delta$  149.17, 118.13, 114.78, 69.73, 31.63, 29.14, 25.73, 22.70, 14.12.

**1,2-Dicyano-4,5-bis(hexyloxy)benzene 116**

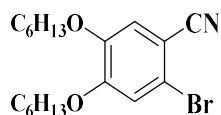
A mixture of 1,2-Dibromo-4,5-bis(hexyloxy)benzene **124** (3.83 g, 8.78 mmol) and CuCN (3.93 g, 43.9 mmol) was heated to reflux in dry DMF (15 mL) under an argon atmosphere and the reaction monitored by TLC every hour. After 3 hours, the reaction mixture was cooled to room temperature and DCM (20 ml) was added. The solid then filtrated off to remove the copper salts. The filtrate was then washed with water (3 x 50 mL) and with an aqueous solution of ammonia until no blue colour was obtained in the aqueous layer. Finally, the organic layer washed with a saturated solution of NaHCO<sub>3</sub>, dried over MgSO<sub>4</sub> and filtered. The filtrate was evaporated under reduced pressure to give the crude product. The crude material was purified by column chromatography using (1:2) DCM:PE → (1:1) DCM:PE → DCM to yield the product as a colorless solid (1.05 g, 36%).

**Mp** 104.6- 106 °C (lit. 100.3 °C)<sup>130</sup>.

**<sup>1</sup>H-NMR** (500 MHz, Chloroform-*d*) δ 7.11 (s, 2H), 4.05 (t, 4H), 1.87- 1.82 (m, 4H), 1.50- 1.44 (m, 4H), 1.38- 1.30 (m, 8H), 0.92- 0.89 (m, 6H).

**<sup>13</sup>C-NMR** (126 MHz, CDCl<sub>3</sub>) δ 152.60, 116.10, 115.91, 108.50, 69.85, 31.51, 28.79, 25.61, 22.65, 14.08.

**FT-IR** (NaCl), ν (cm<sup>-1</sup>): 2228 (C≡N).

**2-Bromo-4,5-bis(hexyloxy)benzonitrile 125**

This compound was isolated as side product from cyanation reaction **124** (1.94 g, 58%).

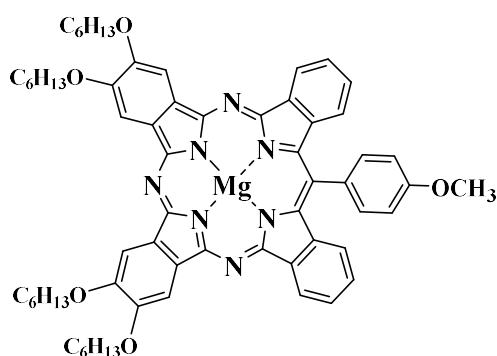
**Mp** 52.6 °C.

**<sup>1</sup>H-NMR** (500 MHz, Chloroform-*d*)  $\delta$  7.04 (s, 1H), 7.03 (s, 1H), 4.01 (t, 2H), 3.96 (t, 2H) 1.86-1.78 (m, 4H), 1.49-1.43 (m, 4H), 1.36-1.32 (m, 8H), 0.93-0.88 (m, 6H).

**<sup>13</sup>C-NMR** (126 MHz, CDCl<sub>3</sub>)  $\delta$  153.57, 148.43, 117.98, 117.42, 117.24, 116.75, 106.57, 69.80, 69.64, 31.61, 31.56, 29.02, 28.90, 25.70, 25.67, 22.70, 22.68, 14.13, 14.11.

**FT-IR** (NaCl),  $\nu$  (cm<sup>-1</sup>): 2231 (C≡N).

### 3.3.1 p-(OC<sub>6</sub>H<sub>13</sub>)<sub>4</sub>-MgTBTAP-(4-MeO-Ph) 127



A suspension of 4,5-dihexyloxyphthalonitrile **116** (657 mg, 2 mmol), MgBr<sub>2</sub> (110 mg, 0.6 mmol, 1.5 eq), DABCO (67.5 mg, 0.6 mmol, 1.5eq) and aminoisoindoline **68a** (100 mg, 0.4 mmol) in dry diglyme (2 ml) was heated at 220°C, in an oil bath for 1.5 h under an argon atmosphere. Then, the solvent was removed under an argon stream while cooling. A 1:1 mixture of DCM:MeOH (20 ml) was added and the mixture sonicated. The solvents were removed under vacuum and the crude purified by two consecutive flash chromatography columns. First, using DCM→DCM:Et<sub>3</sub>N (20:1)→DCM:THF:Et<sub>3</sub>N (10:4:1) as eluent, the fractions collected according to their colours. Only the green fraction was subjected to the second column using PE:THF:MeOH (10:3:1) as eluent. Recrystallisation from acetone and Ethanol gave the title compound as green crystals (6.6 mg, 4%).

**Chemical Formula:** C<sub>64</sub>H<sub>71</sub>MgN<sub>7</sub>O<sub>5</sub>

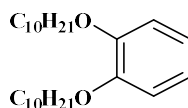
**Mp** 222 °C.

**<sup>1</sup>H-NMR** (400 MHz, THF-*d*<sub>8</sub>) δ 9.56 (d, *J* = 7.4 Hz, 2H), 8.97 (s, 2H), 8.95 (s, 2H), 8.02 (d, *J* = 8.5 Hz, 2H), 7.87 (t, *J* = 7.4 Hz, 2H), 7.58 (ddd, *J* = 8.1, 6.9, 1.2 Hz, 2H), 7.50 (d, *J* = 8.5 Hz, 2H), 7.22 (d, *J* = 8.1 Hz, 2H), 4.62-4.57 (m, 8H), 4.19 (s, 3H, OCH<sub>3</sub>), 2.17-2.05 (m, 8H), 1.84-1.76 (m, 8H), 1.62-1.47 (m, 16H), 1.11-1.62 (m, 12H).

**MS** (MALDI-TOF): *m/z* = 1042.26 [M]<sup>+</sup> (100%).

**UV-vis** λ<sub>max</sub> (nm) (ε (dm<sup>3</sup>·mol<sup>-1</sup>·cm<sup>-1</sup>)) = 670 (7.55·10<sup>4</sup>), 648 (5.31·10<sup>4</sup>), 594 (2.14·10<sup>4</sup>), 416 (1.17·10<sup>5</sup>).

**1,2-Bis(decyloxy)benzene 128**<sup>145</sup>

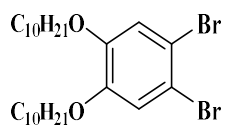


Catechol **122** (20.00 g, 0.182 mol), 1-bromodecane (100.43 g, 0.454 mol) and potassium carbonate (75.31 g, 0.545 mol) were dissolved in ethanol (250 mL). The reaction mixture was stirred and heated at reflux for 48 hours under nitrogen. On completion the mixture was filtered under suction and washed with dichloromethane. The filtrate was collected and the solvent removed in vacuo. The crude product was purified using vacuum distillation, collecting the fraction at 185°C. giving the pure product as an oil that crystallised on standing to give a cream solid (64.8 g, 91%).

**Mp** 37.7°C (lit. 41°C)<sup>146</sup>

**<sup>1</sup>H-NMR** (400 MHz, Chloroform-*d*) δ 6.89 (s, 4H), 3.99 (t, *J* = 6.7 Hz), 1.86- 1.75 (m, 4H), 1.51-1.41 (m, 4H), 1.37- 1.25 (s, 24H), 0.92- 0.83 (m, 6H).

**<sup>13</sup>C-NMR** (101 MHz, CDCl<sub>3</sub>) δ 149.40, 121.15, 114.29, 69.44, 32.07, 29.79, 29.74, 29.60, 29.51, 26.21, 22.84, 14.26.

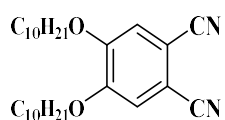
**1,2-Dibromo-4,5-bis(decyloxy)benzene 129**<sup>127</sup>

1,2-Bis(decyloxy)benzene **128** (36.13 g, 0.130 mol) was stirred in dichloromethane (300 ml) at  $-10^{\circ}\text{C}$ . Bromine (17.53 ml, 54.4 g, 0.340 mol) was added dropwise via syringe, and the mixture was stirred at  $0^{\circ}\text{C}$  for 1 hour. On completion, the mixture was washed with sodium metabisulphite solution ( $\text{Na}_2\text{S}_2\text{O}_5$ ) (20%, 200 ml). The organics were extracted with dichloromethane and dried over  $\text{MgSO}_4$ . The solvent was removed in vacuo, and the pure product was obtained as an orange oil that crystallised on standing to give a colourless solid (68.3g, 96%).

**Mp**  $41.5^{\circ}\text{C}$  (lit.  $42^{\circ}\text{C}$ )<sup>146</sup>

**$^1\text{H-NMR}$**  (500 MHz, Chloroform-*d*)  $\delta$  7.06 (s, 2H), 3.94 (t,  $J = 6.6$  Hz), 1.86 – 1.74 (m, 4H), 1.47 – 1.41 (m, 4H), 1.38 – 1.22 (m, 24H), 0.91 – 0.85 (m, 6H).

**$^{13}\text{C-NMR}$**  (126 MHz,  $\text{CDCl}_3$ )  $\delta$  149.19, 118.17, 114.80, 69.77, 32.06, 29.74, 29.71, 29.49, 29.19, 26.07, 22.84, 14.26.

**1,2-Dicyano-4,5-Bis(decyloxy)benzene 117**

A mixture of 1,2-Dibromo-4,5-bis(decyloxy)benzene **129** (3.59 g, 6.55 mmol) and  $\text{CuCN}$  (2.93 g, 32.75 mmol) was refluxed in dry DMF (15 mL) under an argon atmosphere and the reaction monitored by TLC every hour. After 3 hours, the reaction mixture was cooled to room temperature and 20 ml of DCM was added. The solid then filtrated off to remove the copper salts. The filtrate was washed with water (3 x 50 ml) and with an aqueous solution of ammonia until no blue colour was obtained in the aqueous layer. Finally, the organic layer washed with a saturated solution of  $\text{NaHCO}_3$ , dried over  $\text{MgSO}_4$  and filtered. The filtrate was evaporated under reduced pressure to

give the crude product. The crude material was purified by column chromatography using (1:2) DCM:PE → (1:1) DCM:PE → DCM to yield the product as a colorless solid (1.1 g, 38%).

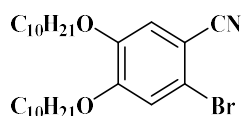
**Mp** 100-102 °C (lit. 106 °C)<sup>146</sup>

**<sup>1</sup>H-NMR** (500 MHz, Chloroform-*d*) δ 7.11 (s, 2H), 4.04 (t, *J* = 6.5 Hz, 4H), 1.84 (m, 4H), 1.52- 1.42 (m, 4H), 1.39 – 1.16 (m, 24H), 0.88 (t, *J* = 6.8 Hz, 6H).

**<sup>13</sup>C-NMR** <sup>13</sup>C NMR (126 MHz, CDCl<sub>3</sub>) δ 152.61, 116.10, 115.93, 108.53, 69.87, 32.03, 29.68, 29.66, 29.46, 29.38, 28.85, 25.96, 22.82, 14.25.

**FT-IR** (NaCl), ν (cm<sup>-1</sup>): 2229 (C≡N).

### 2-Bromo-4,5-bis(decyloxy)benzonitrile **130**



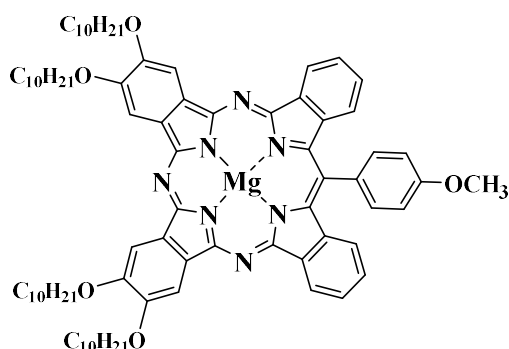
This compound was isolated as side product from cyanation reaction of **129** (1.85 g, 57%).

**Mp** 80-81°C

**<sup>1</sup>H-NMR** (500 MHz, Chloroform-*d*) δ 7.03 (s, 2H), 4.01 (t, *J* = 6.6 Hz, 2H), 3.96 (t, *J* = 6.5 Hz, 2H), 1.86- 1.78 (m, 4H), 1.53 – 1.46 (m, 4H), 1.40 – 1.19 (m, 24H), 0.89- 0.86 (m, 6H).

**<sup>13</sup>C-NMR** (101 MHz, CDCl<sub>3</sub>) δ 153.59, 148.45, 117.98, 117.42, 117.29, 116.79, 106.58, 69.82, 69.65, 32.05, 29.72, 29.69, 29.47, 29.46, 29.42, 29.07, 28.95, 26.04, 26.00, 22.83, 14.26.

**FT-IR** (NaCl), ν (cm<sup>-1</sup>): 2230 (C≡N).

3.3.2 p-(OC<sub>10</sub>H<sub>21</sub>)<sub>4</sub>-MgTBTAP-(4-MeO-Ph) 132

A suspension of 4,5-bis(decyloxy)benzene-1,2-dicarbonitrile **117** (881 mg, 2 mmol), MgBr<sub>2</sub> (110 mg, 0.6 mmol, 1.5eq), aminoisoindoline **68a** (100 mg, 0.4 mmol) and DABCO (67.5 mg, 0.6 mmol, 1.5eq) in dry diglyme (2 ml) was heated at 220°C, in an oil bath for 1.5 h under an argon atmosphere. Then, the solvent was removed under an argon stream while cooling. A 1:1 mixture of DCM:MeOH (20 ml) was added and the mixture sonicated. The solvents were removed under vacuum and the crude purified by two consecutive flash chromatography columns. First, using DCM→DCM:Et<sub>3</sub>N (20:1)→DCM:THF:Et<sub>3</sub>N (10:4:1) as eluent, the fractions collected according to their colours. Only the green fraction was subjected to the second column using PE:THF:MeOH (10:3:1) as eluent. Recrystallisation from acetone and Ethanol gave the title compound as green crystals (73 mg, 28%).

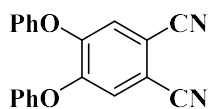
**Chemical Formula:** C<sub>80</sub>H<sub>103</sub>MgN<sub>7</sub>O<sub>5</sub>

**Mp** 173 °C

**<sup>1</sup>H-NMR** (500 MHz, THF-*d*<sub>8</sub>) δ 9.68 (d, *J* = 7.5 Hz, 2H), 9.09 (s, 2H), 9.06 (s, 2H), 8.14 (d, *J* = 8.4 Hz, 2H), 7.98 (t, *J* = 7.2 Hz, 2H), 7.69 (t, *J* = 7.9 Hz, 2H), 7.62 (d, *J* = 8.4 Hz, 2H), 7.34 (d, *J* = 8.1 Hz, 2H), 4.73- 4.68 (m, 8H), 4.31 (s, 3H, OCH<sub>3</sub>), 2.26- 2.21 (m, 8H), 1.92- 1.89 (m, 8H), 1.68- 1.46 (m, 48H), 1.06- 1.03 (m, 12H).

**MS** (MALDI-TOF): *m/z* = 1267.31[M]<sup>+</sup> (100%)

**UV-vis** λ<sub>max</sub> (nm) (ε (dm<sup>3</sup>·mol<sup>-1</sup>·cm<sup>-1</sup>)) = 673 (4.13·10<sup>3</sup>), 649 (2.45·10<sup>3</sup>), 596 (7.06·10<sup>2</sup>), 441 (7.11·10<sup>2</sup>), 380 (1.69·10<sup>3</sup>).

**4,5-Diphenoxybenzene-1,2-dicarbonitrile 118** <sup>128</sup>

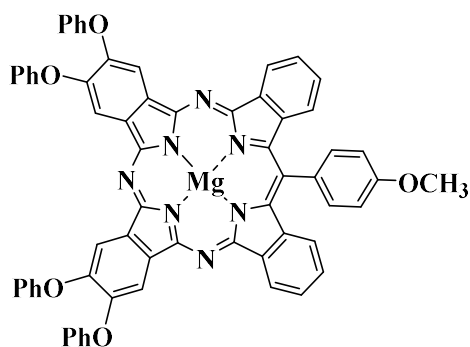
A mixture of 1.0 g (5.1 mmol) of 4,5-dichlorophthalonitrile **133**, 1.4 g (15.3 mmol) of phenol, 3.0 g (22 mmol) of  $K_2CO_3$ , and 30 mL of anhydrous DMF was stirred at  $110^\circ C$  during 8 h, cooled, and diluted with 100 mL of water. The precipitate was filtered off, washed with 5% aqueous KOH and with water to pH 7, and dried at  $70^\circ C$ . The solid then recrystallised from Methanol to afford the product as green crystals (1.3 g, 81%).

**Mp** 140-145 °C (lit. 148-150°C)<sup>129</sup>

**<sup>1</sup>H-NMR** (500 MHz, Chloroform-*d*)  $\delta$  7.46 (t,  $J = 7.9$  Hz, 4H), 7.30 (t,  $J = 7.4$  Hz, 2H), 7.17 (s, 2H), 7.09 (d,  $J = 8.0$  Hz, 4H).

**<sup>13</sup>C-NMR** (126 MHz,  $CDCl_3$ )  $\delta$  154.23, 152.08, 130.71, 126.10, 122.09, 120.04, 115.14, 110.48.

**FT-IR** (NaCl),  $\nu$  ( $cm^{-1}$ ): 2236 (C $\equiv$ N)

**3.3.3 p-(OPh)<sub>4</sub>-MgTBTAP-(4-MeO-Ph) 135**

A suspension of 4,5-diphenoxyphthalonitrile **118** (378 mg, 1.2 mmol, 3eq) and  $MgBr_2$  (110 mg, 0.6 mmol, 1.5eq) in dry diglyme (0.5 ml) was stirred for 10 min at  $220^\circ C$ , in an oil bath, under an argon atmosphere. A solution of aminoisoindoline **68a** (100 mg, 0.4 mmol, 1eq) and 4,5-diphenoxy-phthalonitrile **118** (125 mg, 0.4 mmol, 1eq) in dry diglyme (1 ml) was added dropwise over 1 hour using a syringe pump. Finally, a third

solution of DABCO (67.5 mg, 0.6 mmol, 1.5eq) and 4,5-diphenoxyphthalonitrile **118** (125 mg, 0.4 mmol, 1eq) in dry diglyme (0.5 ml) was added dropwise over 1 hour. The reaction was heated for 0.5 h at 220°C under an argon atmosphere. Then, the solvent was removed under an argon stream while cooling. A 1:1 mixture of DCM:MeOH (20 ml) was added and the mixture sonicated. The solvents were removed under vacuum and the mixture purified by two consecutive flash chromatography columns. First, using DCM→DCM:Et<sub>3</sub>N (20:1) →DCM:THF:Et<sub>3</sub>N (10:4:1) as eluent, the fractions were collected according to their colours. Only the green fraction was subjected to the second column using PE:THF:MeOH (10:3:1) as eluent. Recrystallisation from acetone and EtOH gave the title compound as green powder (105 mg, 52%).

**Chemical Formula:** C<sub>64</sub>H<sub>39</sub>MgN<sub>7</sub>O<sub>5</sub>

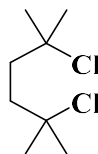
**Mp** > 300 °C

**<sup>1</sup>H-NMR** (500 MHz, THF-*d*<sub>8</sub>) δ 9.47 (d, *J* = 7.6 Hz, 2H), 9.14 (s, 2H), 9.11 (s, 2H), 8.02 (d, *J* = 8.6 Hz, 2H), 7.86 (t, *J* = 7.3 Hz, 2H), 7.59 (t, *J* = 7.4 Hz, 2H), 7.51 (d, *J* = 8.6 Hz, 2H), 7.47- 7.40 (m, 6H), 7.30- 7.15 (m, 16H), 4.18 (s, 3H, OCH<sub>3</sub>).

**<sup>13</sup>C-NMR** (101 MHz, THF) δ 162.03, 159.40, 159.16, 155.32, 152.72, 152.56, 151.30, 150.54, 144.05, 141.30, 140.18, 137.65, 137.09, 135.84, 134.14, 130.82, 130.73, 128.37, 127.56, 126.70, 125.92, 124.27, 124.04, 123.66, 119.22, 118.80, 116.36, 115.61, 115.33, 56.15.

**MS** (MALDI-TOF): *m/z* = 1009.38 [M]<sup>+</sup> (100%)

**UV-vis** λ<sub>max</sub> (nm) (ε (dm<sup>3</sup>.mol<sup>-1</sup>.cm<sup>-1</sup>)) = 675 (1.45·10<sup>5</sup>), 652 (9.12·10<sup>4</sup>), 597 (2.65·10<sup>4</sup>), 446 (2.95·10<sup>4</sup>), 399 (5.61·10<sup>4</sup>).

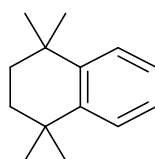
**2,5-Dichloro-2,5-dimethylhexane 137**

Following a known procedure reported by Lamei and co-worker<sup>130</sup>, a solution of 2,5-dimethylhexane-2,5-diol **136** (5.0 g, 34.24 mmol) in concentrated hydrochloric acid (50 ml) was stirred at 0°C for 30 min. The mixture was left to warm to room temperature and completed stirring overnight. The light pink solid was filtered off and washed thoroughly with water. The solid was then dissolved in DCM, washed again with water and extracted with DCM (3x50 mL). The organic extracts were dried using (MgSO<sub>4</sub>) and the solvent removed under reduced pressure to afford the product as a white solid which was recrystallised in methanol to give compound as colorless crystals (5.3 g, 85%).

**Mp** 63.5°C (lit. 59-60 °C)<sup>130</sup>

<sup>1</sup>H-NMR (500 MHz, CDCl<sub>3</sub>, 298 K):  $\delta$  (ppm) = 1.95 (s, 4H), 1.60 (s, 12H).

<sup>13</sup>C-NMR (125.7 MHz, CDCl<sub>3</sub>, 298 K):  $\delta$  (ppm) = 70.49, 41.31, 32.68.

**1,1,4,4-Tetramethyl-1,2,3,4-tetrahydronaphthalene<sup>147</sup> 139**

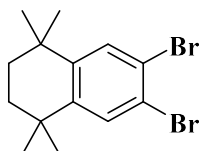
Following Bruson's procedure *via* Friedel-Crafts reaction, a solution of 2,5-dichloro-2,5-dimethylhexane **137** (1.0 g, 5.46 mmol) in benzene (50 mL, 0.56 mol) was stirred for 10 min at 60°C. Anhydrous Aluminium trichloride AlCl<sub>3</sub> (0.29 g, 2.18 mmol) was added in small portions over 30 min. The thick suspension was then stirred at 60°C for 24 h. The resulting material was cooled to room temperature, poured into dilute hydrochloric acid and extracted with DCM (3x50 mL). The organics were washed with water, diluted sodium carbonate solution, dried (Na<sub>2</sub>SO<sub>4</sub>), filtered and the solvent

removed under reduced pressure. The resulting material was washed several times by methanol to remove the side-products. The orange oil was removed under reduced pressure to give the product as a colourless liquid (0.90 g, 87%). For large scale synthesis the orange oil was purified by vacuum distillation or column chromatography using PE or hexane as eluent solvent.

$^1\text{H-NMR}$  (500 MHz, Chloroform- $d$ )  $\delta$  7.32 (dd,  $J = 5.9, 3.4$  Hz, 2H), 7.14 (dd,  $J = 6.0, 3.4$  Hz, 2H), 1.70 (s, 4H), 1.30 (s, 12H).

$^{13}\text{C-NMR}$  (126 MHz,  $\text{CDCl}_3$ ) 144.93, 126.61, 125.66, 35.25, 34.35, 32.03.

### 6,7-Dibromo-1,2,3,4-tetrahydro-1,1,4,4-tetramethylnaphthalene 140



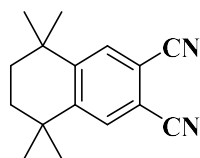
The bromination was achieved using the method described by Ashton and co-workers<sup>132,133</sup>. 1,1,4,4-Tetramethyl-1,2,3,4-tetrahydronaphthalene **139** (0.96 g, 5.11 mmol) was dissolved in DCM (15 mL). Iron powder (34.0 mg, 0.61 mmol) and iodine (12.95 mg, 0.051 mmol) were added to the mixture and cooled to 0°C. Bromine (0.53 mL, 10.19 mmol) was added dropwise *via* syringe to the stirring mixture over 30 min. After complete addition, the reaction mixture was allowed to warm up to room temperature and stirred for 24 h. The resulting mixture was washed with an aqueous solution of sodium metabisulfite and sodium bicarbonate to remove the excess bromine. Water and brine were added and the mixture extracted with DCM (3×50 mL). The organic extracts were dried over  $\text{MgSO}_4$ , filtered and the solvent removed under reduced pressure to give brownish solid. The product was purified by column chromatography over silica gel using PE/DCM (3:2) as eluents to give the title compound as a yellow solid (1.6 g, 90%).

**Mp** 114- 117 °C (lit. 111-112 °C)<sup>148</sup>

$^1\text{H-NMR}$  (500 MHz,  $\text{CDCl}_3$ , 298 K):  $\delta$  7.50 (s, 2H), 1.65 (s, 4H), 1.25 (s, 12H).

$^{13}\text{C}$ -NMR (125.7 MHz,  $\text{CDCl}_3$ , 298 K):  $\delta$  (ppm) = 146.54, 131.95, 121.58, 34.78, 34.40, 31.76.

**6,7-Dicyano-1,2,3,4-tetrahydro-1,1,4,4-tetramethylnaphthalene 119**



A mixture of 6,7-dibromo-1,1,4,4-tetramethyl-1,2,3,4-tetrahydronaphthalene **140** (1.52 g, 4.39 mmol) and  $\text{CuCN}$  (1.97 g, 21.99 mmol) was refluxed in dry DMF (15 ml) under an argon atmosphere and the reaction was monitored by TLC. After 3 hours, the reaction mixture was cooled to room temperature and 20 ml of DCM was added. The solid then filtrated of to remove the copper salts. The filtrate washed with water (3 x 50 mL) and with an aqueous solution of ammonia until no blue colour was obtained in the aqueous layer<sup>127</sup>. Finally, the organic layer washed with saturated solution of  $\text{NaHCO}_3$ , dried over  $\text{MgSO}_4$  and filtered. The filtrate was evaporated under reduced pressure to give the crude product. The crude material was purified by column chromatography (silica: (1:2) DCM:PE  $\rightarrow$  (1:1) DCM:PE  $\rightarrow$  DCM) to yield the product as a yellow solid (0.34 g, 33%).

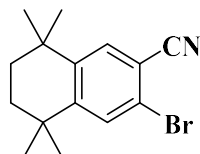
**Mp** 204- 205 °C (lit. 206-208 °C)<sup>149</sup>

$^1\text{H}$ -NMR (500 MHz,  $\text{CDCl}_3$ , 298 K):  $\delta$  7.71 (s, 2H), 1.72 (s, 4H), 1.30 (s, 12H).

$^{13}\text{C}$ -NMR (125.7 MHz,  $\text{CDCl}_3$ )  $\delta$  151.80, 132.62, 116.05, 112.58, 35.13, 34.10, 31.45.

**FT-IR** (NaCl),  $\nu$  ( $\text{cm}^{-1}$ ): 2232 ( $\text{C}\equiv\text{N}$ ).

### 6-Bromo-7-cyano-1,2,3,4-tetrahydro-1,1,4,4-tetramethylnaphthalene 141



This compound was isolated as side product from cyanation reaction **140** (0.57 g, 45%).

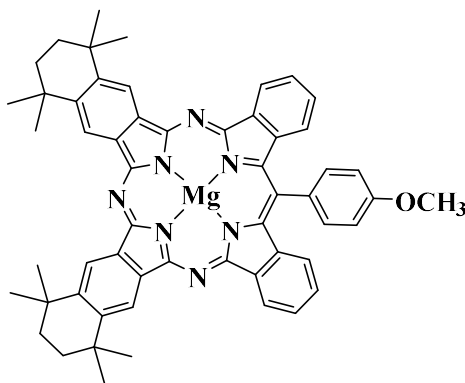
**Mp** 158-159°C

**<sup>1</sup>H-NMR** (500 MHz, CDCl<sub>3</sub>) δ 7.57 (s, 1H), 7.55 (s, 1H), 1.68 (s, 4H), 1.27 (s, 6H), 1.27 (s, 6H).

**<sup>13</sup>C-NMR** (125.7 MHz, CDCl<sub>3</sub>) δ 152.82, 145.53, 133.29, 131.41, 121.53, 117.87, 112.96, 35.13, 34.45, 34.41, 31.67, 31.54.

**FT-IR** (NaCl), ν (cm<sup>-1</sup>): 2232 (C≡N).

### 3.3.4 (Tetramethyl-tetralino)<sub>2</sub>-MgTBTAP-(4-OMe-Ph) 143



#### Slow addition Method:

A suspension of 6,7-dicyano-1,1,4,4-tetramethyl-1,2,3,4-tetrahydronaphthalene **119** (286 mg, 1.2 mmol, 3eq) and MgBr<sub>2</sub> (110 mg, 0.6 mmol, 1.5eq) in dry diglyme (0.5 ml) was stirred for 10 min at 220°C, in an oil bath, under an argon atmosphere. A solution of aminoisoindoline **68a** (100 mg, 0.4 mmol, 1eq) and 6,7-dicyano-1,1,4,4-

tetramethyl-1,2,3,4-tetrahydronaphthalene **119** (95 mg, 0.4 mmol, 1eq) in dry diglyme (1 ml) was added dropwise over 1 hour using a syringe pump. Finally, a third solution of DABCO (67.5 mg, 0.6 mmol, 1.5eq) and 6,7-dicyano-1,1,4,4-tetramethyl-1,2,3,4-tetrahydronaphthalene **119** (95 mg, 0.4 mmol, 1eq) in dry diglyme (0.5 ml) was added dropwise over 1 hour. The reaction was heated for 0.5 h at 220°C under an argon atmosphere. Then, the solvent was removed under an argon stream while cooling. A 1:1 mixture of DCM:MeOH (20 ml) was added and the mixture sonicated. The solvents were removed under vacuum and the mixture purified by two consecutive flash chromatography columns. First, using DCM → DCM:Et<sub>3</sub>N (20:1) → DCM:THF:Et<sub>3</sub>N (10:4:1) as eluent, the fractions were collected according to their colours. Only the green fraction was subjected to the second column using PE:THF:MeOH (10:3:1) as eluent. Recrystallisation from acetone and Ethanol gave the title compound as green crystals (25 mg, 14%).

**One-pot Method:**

A suspension of 6,7-dicyano-1,1,4,4-tetramethyl-1,2,3,4-tetrahydronaphthalene **119** (476 mg, 2 mmol, 5 eq) and MgBr<sub>2</sub> (110 mg, 0.6 mmol, 1.5eq), of aminoisoindoline **68a** (100 mg, 0.4 mmol, 1eq) and of DABCO (67.5 mg, 0.6 mmol, 1.5eq) in dry diglyme (2 ml) was stirred for 1.5 h at 220°C, in an oil bath, under an argon atmosphere. Then, the solvent was removed under an argon stream while cooling and worked up and separated as previously mentioned. (39 mg, 22%).

**Chemical Formula:** C<sub>56</sub>H<sub>51</sub>MgN<sub>7</sub>O

**Mp** > 300 °C

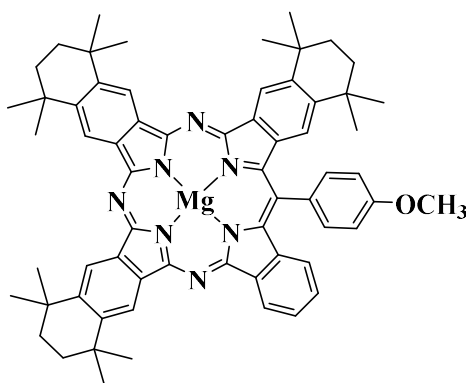
**<sup>1</sup>H-NMR** (500 MHz, THF-*d*<sub>8</sub>) δ 9.57 (d, *J* = 7.4 Hz, 2H), 9.50 (s, 2H), 9.49 (s, 2H), 8.02 (d, *J* = 8.4 Hz, 2H), 7.87 (t, *J* = 7.2 Hz, 2H), 7.58 (t, *J* = 7.2 Hz, 2H), 7.51 (d, *J* = 8.4 Hz, 2H), 7.21 (d, *J* = 8.1 Hz, 2H), 4.20 (s, 3H, OCH<sub>3</sub>), 2.10 (s, 8H, CH<sub>2</sub>), 1.82 (s, 24H).

**<sup>13</sup>C-NMR** (126 MHz, THF) δ 161.91, 157.78, 154.02, 152.17, 147.87, 147.49, 142.08, 141.13, 139.84, 139.19, 138.89, 136.19, 134.12, 127.89, 127.06, 126.82, 125.63, 123.62, 121.91, 121.65, 115.20, 56.12, 36.68, 36.63, 36.59, 33.32.

**MS** (MALDI-TOF):  $m/z = 861.31 [M]^+$  (100%).

**UV-vis**  $\lambda_{\max}$  (nm) ( $\epsilon$  ( $\text{dm}^3 \cdot \text{mol}^{-1} \cdot \text{cm}^{-1}$ )) = 676 ( $1.88 \cdot 10^5$ ), 652 ( $1.14 \cdot 10^5$ ), 598 ( $3.08 \cdot 10^4$ ), 444 ( $2.67 \cdot 10^4$ ), 398 ( $6.44 \cdot 10^4$ ).

### 3.3.5 (Tetramethyl-tetralino)<sub>3</sub>-MgTBTAP-(4-OMe-Ph) 142



This compound was isolated from the previous reaction as side product (5.3 mg, 1%).

**Chemical Formula:**  $\text{C}_{64}\text{H}_{65}\text{MgN}_7\text{O}$

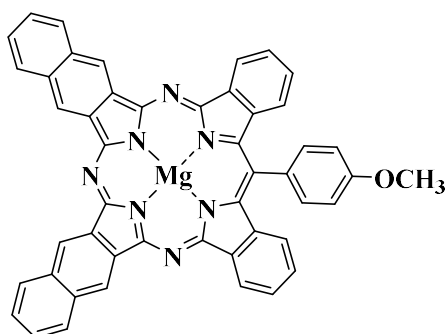
**Mp** > 300 °C

**<sup>1</sup>H-NMR** (500 MHz, THF-*d*<sub>8</sub>)  $\delta$  9.58 (d,  $J = 7.5$  Hz, 1H), 9.57- 9.49 (m, 5H), 8.04 (d,  $J = 8.3$  Hz, 2H), 7.87 (t,  $J = 7.2$  Hz, 1H), 7.59- 7.54 (m, 3H), 7.38 (d,  $J = 8.0$  Hz, 1H), 7.17 (s, 1H), 4.20 (s, 3H, OCH<sub>3</sub>), 2.09 (s, 12H), 1.82 (s, 24H), 1.36 (s, 12H).

**<sup>13</sup>C-NMR** (126 MHz, THF)  $\delta$  161.88, 153.96, 153.27, 152.94, 147.56, 147.25, 147.17, 145.14, 144.85, 142.96, 142.02, 140.96, 139.91, 139.36, 139.10, 138.89, 138.20, 136.50, 134.33, 127.65, 126.74, 125.67, 124.53, 123.58, 121.80, 121.73, 121.58, 120.80, 115.48, 56.22, 36.67, 36.60, 36.31, 36.11, 33.34, 33.19, 33.17.

**MS** (MALDI-TOF):  $m/z = 971.92 [M]^+$  (100%)

**UV-vis**  $\lambda_{\max}$  (nm) ( $\epsilon$  ( $\text{dm}^3 \cdot \text{mol}^{-1} \cdot \text{cm}^{-1}$ )) = 682 ( $5.89 \cdot 10^3$ ), 658 ( $3.49 \cdot 10^3$ ), 602 ( $9.75 \cdot 10^2$ ), 448 ( $8.22 \cdot 10^2$ ), 398 ( $2.21 \cdot 10^3$ ).

3.3.6 (Naphthalo)<sub>2</sub>-MgTBTAP-(4-OMe-Ph) **147**

A suspension of 2,3-naphthalenedicarbonitrile **145** (214 mg, 1.2 mmol, 3eq) and MgBr<sub>2</sub> (110 mg, 0.6 mmol, 1.5eq) in dry diglyme (0.5 ml) was stirred for 10 min at 220°C, in an oil bath, under an argon atmosphere. A solution of aminoisoindoline **68a** (100 mg, 0.4 mmol, 1eq) and 2,3-naphthalenedicarbonitrile **145** (71 mg, 0.4 mmol, 1eq) in dry diglyme (1 ml) was added dropwise over 1 hour using a syringe pump. Finally, a third solution of DABCO (67.5 mg, 0.6 mmol, 1.5eq) and 2,3-naphthalenedicarbonitrile **145** (71 mg, 0.4 mmol, 1eq) in dry diglyme (0.5 ml) was added dropwise over 1 hour. The reaction was heated for 0.5 h at 220°C under an argon atmosphere. Then, the solvent was removed under an argon stream while cooling. A 1:1 mixture of DCM:MeOH (20 ml) was added and the mixture sonicated. The solvents were removed under vacuum and the mixture purified by two consecutive flash chromatography columns. First, using DCM→DCM:Et<sub>3</sub>N (20:1) → DCM:THF:Et<sub>3</sub>N (10:4:1) as eluent, the fractions were collected according to their colours. Only the green fraction was subjected to the second column using PE:THF:MeOH (10:3:1) as eluent. Recrystallisation from acetone and Ethanol gave the title compound as purple crystals (11.1 mg, 8%).

**Chemical Formula:** C<sub>48</sub>H<sub>27</sub>MgN<sub>7</sub>O

**Mp** > 300 °C

**<sup>1</sup>H-NMR** (500 MHz, THF-*d*<sub>8</sub>) δ 9.99 (s, 2H), 9.91 (s, 2H), 9.54 (d, *J* = 7.5 Hz, 2H), 8.64 (ddd, *J* = 14.5, 6.1, 3.2 Hz, 4H), 8.01 (d, *J* = 8.4 Hz, 2H), 7.86 (m, 6H), 7.56 (ddd, *J* = 8.0, 6.8, 1.2 Hz, 2H), 7.51 (d, *J* = 8.4 Hz, 2H), 7.16 (d, *J* = 8.0 Hz, 2H), 4.19 (s, 3H, OCH<sub>3</sub>).

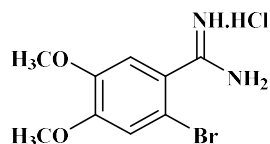
**<sup>13</sup>C-NMR** <sup>13</sup>C NMR (126 MHz, THF)  $\delta$  161.91, 158.71, 154.28, 152.29, 141.62, 141.00, 139.49, 138.56, 138.50, 136.04, 135.60, 135.33, 134.01, 130.93, 130.84, 128.04, 127.91, 127.89, 127.68, 126.75, 125.56, 123.54, 123.44, 123.06, 115.29, 56.12.

**MS** (MALDI-TOF):  $m/z = 740.35 [M]^+$  (100%)

**UV-vis**  $\lambda_{\max}$  (nm) ( $\epsilon$  (dm<sup>3</sup>.mol<sup>-1</sup>.cm<sup>-1</sup>)) = 709 (8.02·10<sup>3</sup>), 681 (5.39·10<sup>3</sup>), 621 (1.36·10<sup>3</sup>), 404 (3.84·10<sup>3</sup>).

### 3.4 Synthesis of the second series of *meso*-Ar-TBTAP hybrids

#### 2-Bromo-4,5-dimethoxybenzamidinium hydrochloride **156**

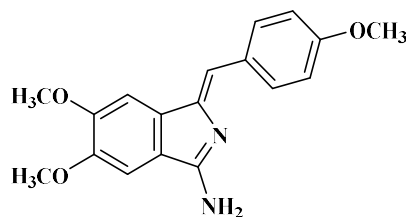


Following the method reported by Dalai<sup>49</sup>, a solution of 2-bromo-4,5-dimethoxy benzonitrile **120** (2.33 g, 9.5 mmol) in dry THF (1 ml) was added to a solution of LiN(SiMe<sub>3</sub>)<sub>2</sub> in anhydrous THF (1 M, 10.5 ml, 10.45 mmol, 1.1eq). The reaction mixture was stirred at room temperature for 4 h. A 5N HCl solution in isopropanol (15 ml) was added to the cooled mixture. The crude reaction mixture was left to stir at room temperature overnight. The precipitate was filtered off and washed with diethyl ether to give the title compound as colorless crystals (2.5 g, 89%).

**Mp** 148-150°C

**<sup>1</sup>H-NMR** (500 MHz, MeOH-*d*<sub>4</sub>)  $\delta$  7.30 (s, 1H), 7.19 (s, 1H), 3.90 (s, 3H, OCH<sub>3</sub>), 3.88 (s, 3H, OCH<sub>3</sub>).

**<sup>13</sup>C-NMR** (126 MHz, MeOH-*d*<sub>4</sub>)  $\delta$  167.97, 153.86, 150.28, 124.3, 117.42, 113.64, 112.03, 57.0, 56.97.

**(Z)-5,6-dimethoxy-1-[(4-methoxy)benzylidene]-1H-isindol-3-amine 157**

A mixture of 2-bromo-4,5-dimethoxybenzamidinium hydrochloride **156** (882.0 mg, 3 mmol), BINAP (102 mg, 0.165 mmol, 0.055eq) and PdCl<sub>2</sub>(MeCN)<sub>2</sub> (39 mg, 0.15 mmol, 0.05eq) was sealed in a microwave vessel with a magnetic bar and then purged and refilled with N<sub>2</sub> thrice. Then, 4-ethynylanisole (0.467 ml, 0.476 g, 3.6 mmol, 1.2eq) and DBU (1.12 ml, 1.14 g, 7.5 mmol, 2.5eq) in dry DMF (12 ml) was added. The mixture was stirred under N<sub>2</sub> for 5 min to give a clear yellow solution with a white solid. Finally, the mixture was irradiated in a microwave reactor at 120°C for 1 h. After cooling, ethyl acetate (50 ml) was added and the mixture washed with a saturated solution of NaHCO<sub>3</sub> (3x75 ml). The organic layer was dried with MgSO<sub>4</sub>, filtered and concentrated<sup>48</sup>. The residue was finally purified by column chromatography using PE:AcOEt (1:1) then AcOEt as solvent gradient to afford a yellow semisolid that was recrystallised from a DCM to yield the title compound as yellow needles (382 mg, 41%).

**Chemical Formula:** C<sub>18</sub>H<sub>18</sub>N<sub>2</sub>O<sub>3</sub>

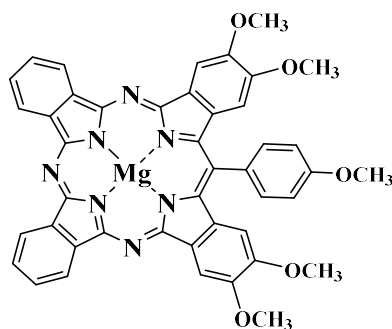
**Mp** 220-223°C

**<sup>1</sup>H-NMR** (500 MHz, Chloroform-*d*) δ 7.99 (d, *J* = 8.8 Hz, 2H), 7.23 (s, 1H), 7.02 (s, 1H), 6.93 (d, *J* = 8.8 Hz, 2H), 6.59 (s, 1H), 4.02 (s, 3H), 3.94 (s, 3H), 3.83 (s, 3H).

**<sup>13</sup>C-NMR** (126 MHz, CDCl<sub>3</sub>) δ 164.33, 159.24, 151.66, 149.56, 143.65, 136.40, 131.70, 129.25, 122.84, 114.92, 114.27, 102.18, 102.08, 56.48, 56.39, 55.45.

**MS** (MALDI-TOF): *m/z* = 310.98 [M]<sup>+</sup> (100%).

**UV-vis** λ<sub>max</sub> (nm) (ε (dm<sup>3</sup>.mol<sup>-1</sup>.cm<sup>-1</sup>)) = 362 (2.15·10<sup>4</sup>).

**3.4.1 p-(OMe)<sub>4</sub>-MgTBTAP-(4-MeO-Ph) 161**

At 220°C, in an oil bath, a suspension of phthalonitrile **8** (255 mg, 2 mmol, 5eq), MgBr<sub>2</sub> (110 mg, 0.6 mmol, 1.5eq), and DABCO (67.5 mg, 0.6 mmol, 1.5eq) and dimethoxy-aminoisoindoline **157** (124 mg, 0.4 mmol, 1eq) in dry diglyme (2 ml) was heated for 1.5 h under an argon atmosphere. Then, the solvent was removed under an argon stream while cooling. A 1:1 mixture of DCM:MeOH (20 ml) was added and the mixture sonicated. The solvents were removed under vacuum and the crude purified by two consecutive flash chromatography columns. First, using DCM→DCM:Et<sub>3</sub>N (20:1)→DCM:THF:Et<sub>3</sub>N (10:4:1) as eluent, the fractions collected according to their colours. Only the green fraction was subjected to the second column using PE:THF:MeOH (10:3:1) as eluent. Recrystallisation from acetone and ethanol gave the title compound as green crystals, (9.2 mg, 6%).

**Chemical Formula:** C<sub>44</sub>H<sub>31</sub>MgN<sub>7</sub>O<sub>5</sub>

**Mp** > 300 °C

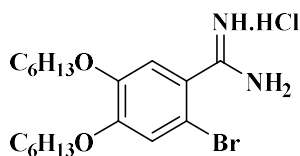
**<sup>1</sup>H-NMR** (500 MHz, THF-*d*<sub>8</sub>) δ 9.55-9.52 (m, 4H), 9.06 (s, 2H), 8.17-8.18 (m, 4H), 8.10 (d, *J* = 8.1 Hz, 2H), 7.61 (d, *J* = 8.1 Hz, 2H), 6.84 (s, 2H), 4.31 (s, 6H), 4.14 (s, 3H), 3.77 (s, 6H).

**<sup>13</sup>C-NMR** (126 MHz, THF-*d*<sub>8</sub>) δ 161.92, 155.24, 152.78, 152.56, 151.39, 151.26, 143.77, 140.89, 140.76, 136.22, 134.82, 134.32, 134.19, 129.48, 129.32, 125.00, 123.66, 123.45, 115.62, 107.83, 104.91, 56.54, 56.24, 55.86.

**MS** (MALDI-TOF): *m/z* = 761.82 [M]<sup>+</sup> (100%)

UV-vis  $\lambda_{\max}$  (nm) ( $\epsilon$  ( $\text{dm}^3 \cdot \text{mol}^{-1} \cdot \text{cm}^{-1}$ )) = 673 ( $1.64 \cdot 10^5$ ), 650 ( $9.82 \cdot 10^4$ ), 596 ( $2.84 \cdot 10^4$ ), 446 ( $3.10 \cdot 10^4$ ), 395 ( $9.29 \cdot 10^4$ ).

### 2-Bromo-4,5-bis(hexyloxy)-benzamidinium hydrochloride **162**



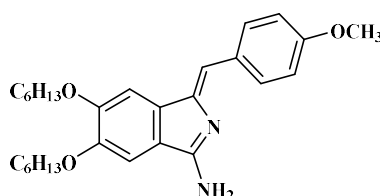
Following the method reported by Dalai<sup>49</sup>, a solution of 2-bromo,4,5-bis(hexyloxy)-benzonitrile **125** (4.16 g, 10.88 mmol) in dry THF (3 ml) was added to a solution of  $\text{LiN}(\text{SiMe}_3)_2$  in anhydrous THF (1 M, 12 ml, 11.97 mmol, 1.1eq). The reaction mixture was stirred at room temperature for 4 h. A 5N HCl solution in iso-propanol (15 ml) was added to the cooled mixture. The crude reaction mixture was left to stir at room temperature overnight. The precipitate was filtered off and washed with diethyl ether to give the title compound as colorless crystals (3.9 g, 82%).

**Mp** 158.9-160 °C

<sup>1</sup>H-NMR (500 MHz, MeOH-*d*<sub>4</sub>)  $\delta$  7.27 (s, 1H), 7.14 (s, 1H), 4.07- 4.02 (m, 4H), 1.83-1.78 (m, 4H), 1.54-1.48 (m, 4H), 1.39-1.35 (m, 8H), 0.94-0.91 (m, 6H).

<sup>13</sup>C-NMR (125.7 MHz, MeOH-*d*<sub>4</sub>)  $\delta$  168.04, 153.80, 150.00, 124.18, 118.66, 115.18, 111.88, 70.70, 70.57, 32.69, 30.21, 30.10, 26.86, 26.82, 23.70, 14.39.

### (*Z*)-5,6-bis(hexyloxy)-1-[(4-methoxy)benzylidene]-1*H*-isoindol-3-amine **164**<sup>48</sup>



A mixture of 2-bromo-4,5-bis(hexyloxy)-benzamidinium hydrochloride **162** (1.31 g, 3 mmol), BINAP (102 mg, 0.165 mmol, 0.055eq) and  $\text{PdCl}_2(\text{MeCN})_2$  (39 mg, 0.15 mmol, 0.05eq) was sealed in a microwave vessel with a magnetic bar and then purged

and refilled with N<sub>2</sub> thrice. Then, 4-ethynylanisole (0.467 ml, 0.476 g, 3.6 mmol, 1.2eq) and DBU (1.12 ml, 1.14 g, 7.5 mmol, 2.5eq) in dry DMF (12 ml) was added. The mixture was stirred under N<sub>2</sub> for 5 min to give a clear yellow solution with a white solid. Finally, the mixture was irradiated in a microwave reactor at 120°C for 1 h. After cooling, ethyl acetate (50 ml) was added and the mixture washed with a saturated solution of NaHCO<sub>3</sub> (75 ml) thrice. The organic layer was dried (MgSO<sub>4</sub>), filtered and concentrated. The residue was finally purified by column chromatography using PE:AcOEt (1:1) then AcOEt as solvent gradient to afford a yellow semisolid that was recrystallized from a DCM:Petroleum ether (1:1) to yield the title compound as yellow needles (450 mg, 32%).

**Chemical Formula:** C<sub>28</sub>H<sub>38</sub>N<sub>2</sub>O<sub>3</sub>

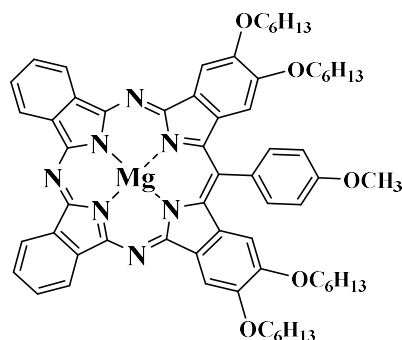
**Mp** 147- 150 °C

**<sup>1</sup>H-NMR** (500 MHz, Chloroform-d) δ 8.00 (d, *J*= 8.8 Hz, 2H), 7.22 (s, 1H), 6.95 – 6.87 (m, 3H), 6.55 (s, 1H), 4.11 (t, *J*= 6.6 Hz, 2H), 3.99 (t, *J*= 6.6 Hz, 2H), 3.82 (s, 3H), 1.91– 1.81 (m, 4H), 1.54- 1.46 (m, 4H), 1.38 – 1.33 (m, 8H), 0.94– 0.85 (m, 6H).

**<sup>13</sup>C-NMR** (125.7 MHz, CDCl<sub>3</sub>, 298K) δ (ppm)= 164.95, 158.94, 151.51, 149.36, 145.31, 136.89, 131.65, 129.81, 123.54 114.13, 113.51, 104.19, 104.10, 69.87, 69.52, 55.41, 31.73, 29.38, 29.34, 25.87, 25.85, 22.75, 14.16.

**MS** (MALDI-TOF): *m/z* = 451.41[M]<sup>+</sup> (100%)

**UV-vis** λ<sub>max</sub> (nm) (ε (dm<sup>3</sup>.mol<sup>-1</sup>.cm<sup>-1</sup>)) = 356 (1.76·10<sup>4</sup>).

3.4.2 p-(OC<sub>6</sub>H<sub>13</sub>)<sub>4</sub>-MgTBTAP-(4-MeO-Ph) 166

A suspension of phthalonitrile (255 mg, 2 mmol), MgBr<sub>2</sub> (110 mg, 0.6 mmol, 1.5eq), dihexyloxy-aminoisoindoline 164 (180 mg, 0.4 mmol) and DABCO (67.5 mg, 0.6 mmol, 1.5eq) in dry diglyme (2 ml) was heated at 220°C, in an oil bath, for 1.5 h under an argon atmosphere. Then, the solvent was removed under an argon stream while cooling. A 1:1 mixture of DCM:MeOH (20 ml) was added and the mixture sonicated. The solvents were removed under vacuum and the crude purified by two consecutive flash chromatography columns. First, using DCM→DCM:Et<sub>3</sub>N (20:1)→DCM:THF:Et<sub>3</sub>N (10:4:1) as eluent, the fractions collected according to their colours. Only the green fraction was subjected to the second column using PE:THF:MeOH (10:3:1) as eluent. Recrystallisation from acetone and Ethanol gave the title compound as purple crystals (62 mg, 30%).

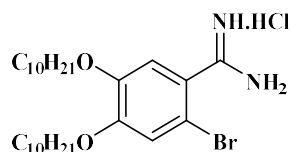
**Chemical Formula:** C<sub>64</sub>H<sub>71</sub>MgN<sub>7</sub>O<sub>5</sub>

**Mp** 159.2 °C

**<sup>1</sup>H-NMR** (500 MHz, THF-*d*<sub>8</sub>) δ 9.54- 9.51 (m, 4H), 9.04 (s, 2H), 8.16- 8.14 (m, 4H), 8.08 (d, *J* = 8.5 Hz, 2H), 7.60 (d, *J* = 8.5 Hz, 2H), 6.84 (s, 2H), 4.54 (t, *J* = 6.5 Hz, 4H), 4.18 (s, 3H), 3.91 (t, *J* = 6.5 Hz, 4H), 2.11-2.01 (m, 4H), 1.96-1.86 (m, 4H), 1.67- 1.63 (m, 4H), 1.54-1.56 (m, 4H), 1.53-1.45 (m, 16H), 1.05- 1.00 (m, 12H).

**MS** (MALDI-TOF): *m/z* = 1041.98 [M]<sup>+</sup> (100%)

**UV-vis** λ<sub>max</sub> (nm) (ε (dm<sup>3</sup>.mol<sup>-1</sup>.cm<sup>-1</sup>)) = 675 (1.00·10<sup>6</sup>), 652 (5.82·10<sup>5</sup>), 597 (1.53·10<sup>5</sup>), 446 (1.57·10<sup>5</sup>), 396 (5.15·10<sup>5</sup>).

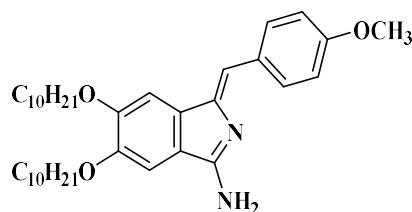
**2-Bromo-4,5-bis(decyloxy)-benzamidinium hydrochloride 163**

Following the method reported by Dalai<sup>49</sup>, a solution of 2-bromo-4,5-bis(decyloxy)-benzamidinium **130** (6.77g, 13.96 mmol) in dry THF (3 ml) was added to a solution of LiN(SiMe<sub>3</sub>)<sub>2</sub> in anhydrous THF (1 M, 15 ml, 15 mmol, 1.1eq). The reaction mixture was stirred at room temperature for 4 h. A 5 N HCl solution in isopropanol (15 ml) was added to the cooled mixture. The crude reaction mixture was left to stir at room temperature overnight. The precipitate was filtered off and washed with diethyl ether to give the title compound as colorless crystals (4.68 g, 61%).

**Mp** 159- 161 °C

<sup>1</sup>H-NMR (500 MHz, MeOH-*d*<sub>4</sub>, 298K) δ (ppm) = 7.27 (s, 1H), 7.15 (s, 1H), 4.07- 4.02 (m, 4H), 1.84- 1.78 (m, 4H), 1.54- 1.48 (m, 4H), 1.40- 1.31 (m, 24H), 0.92- 0.89 (m, 6H).

<sup>13</sup>C-NMR (125.7 MHz, MeOH-*d*<sub>4</sub>, 298K) δ (ppm) = 168.04, 153.82, 150.01, 124.18, 118.68, 115.21, 111.89, 70.71, 70.57, 33.11, 30.83, 30.82, 30.73, 30.52, 30.50, 30.28, 30.16, 27.24, 27.20, 23.77, 14.47.

**(Z)-5,6-bis(decyloxy)-1-[(4-methoxy)benzylidene]-1H-indolizine-3-amine 165**<sup>48</sup>

A mixture of 2-bromo-4,5-bis(decyloxy)-benzamidinium hydrochloride **163** (1.6 g, 3 mmol), BINAP (102 mg, 0.165 mmol, 0.055eq) and PdCl<sub>2</sub>(MeCN)<sub>2</sub> (39 mg, 0.15 mmol, 0.05eq) was sealed in a microwave vessel with a magnetic bar and then purged and refilled with N<sub>2</sub> thrice. Then, 4-ethynylanisole (0.467 ml, 0.476 g, 3.6 mmol,

1.2eq) and DBU (1.12 ml, 1.14 g, 7.5 mmol, 2.5eq) in dry DMF (12 ml) was added. The mixture was stirred under N<sub>2</sub> for 5 min to give a clear yellow solution with a white solid. Finally, the mixture was irradiated in a microwave reactor at 120°C for 1 h. After cooling, ethyl acetate (50 ml) was added and the mixture washed with a saturated solution of NaHCO<sub>3</sub> (3x75 ml). The organic layer was dried (MgSO<sub>4</sub>), filtered and concentrated. The residue was finally purified by column chromatography using PE:AcOEt (1:1) then AcOEt as solvent gradient to afford a yellow semisolid that was recrystallized from a DCM:Petroleum ether (1:1) to yield the title compound **165** as yellow needles (510 mg, 30%).

**Chemical Formula:** C<sub>36</sub>H<sub>54</sub>N<sub>2</sub>O<sub>3</sub>

**Mp** 136.6 °C

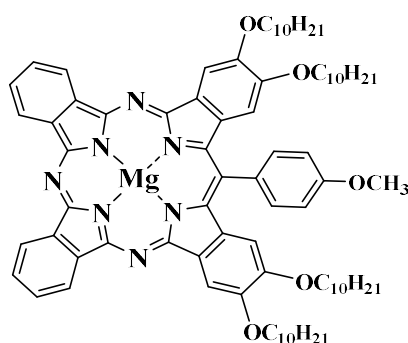
**<sup>1</sup>H-NMR** (500 MHz, CDCl<sub>3</sub>) δ 7.95 (d, 2H, *J*= 8.8 Hz), 7.20 (s, 1H), 7.03 (s, 1H), 6.92 (d, 2H, *J*= 8.8 Hz), 6.55 (s, 1H), 4.10 (t, 2H, *J*= 6.6 Hz), 4.00 (t, 2H, *J*= 6.6 Hz), 3.82 (s, 3H, OCH<sub>3</sub>), 1.95- 1.75 (m, 4H), 1.58- 1.41 (m, 4H), 1.39- 1.27 (m, 24H), 0.96- 0.87 (m, 6H).

**<sup>13</sup>C-NMR** (101 MHz, CDCl<sub>3</sub>) δ 164.61, 159.09, 151.87, 149.54, 143.87, 136.40, 131.60, 129.39, 122.91, 114.22, 113.48, 104.41, 104.05, 69.87, 69.54, 55.41, 32.06, 29.78, 29.74, 29.59, 29.57, 29.50, 29.41, 29.37, 26.20, 22.83, 14.26.

**MS** (MALDI-TOF): *m/z* = 563.24 [M]<sup>+</sup> (100%)

**UV-vis** λ<sub>max</sub> (nm) (ε (dm<sup>3</sup>.mol<sup>-1</sup>.cm<sup>-1</sup>)) = 356 (3.11·10<sup>4</sup>).

### 3.4.3 p-(OC<sub>10</sub>H<sub>21</sub>)<sub>4</sub>-MgTBTAP-(4-MeO-Ph) **167**



A suspension of phthalonitrile **8** (255 mg, 2 mmol), MgBr<sub>2</sub> (110 mg, 0.6 mmol, 1.5eq), didecyloxy-aminoisindoline **165** (225 mg, 0.4 mmol) and DABCO (67.5 mg, 0.6 mmol, 1.5eq) in dry diglyme (2 ml) was heated at 220°C, in an oil bath, for 1.5 h under an argon atmosphere. Then, the solvent was removed under an argon stream while cooling. A 1:1 mixture of DCM:MeOH (20 ml) was added and the mixture sonicated. The solvents were removed under vacuum and the crude purified by two consecutive flash chromatography columns. First, using DCM→DCM:Et<sub>3</sub>N (20:1)→DCM:THF:Et<sub>3</sub>N (10:4:1) as eluent, the fractions collected according to their colours. Only the green fraction was subjected to the second column using PE:THF:MeOH (10:3:1) as eluent. Recrystallisation from acetone and Ethanol gave the title compound as green crystals (9.3 mg, 4%).

**Chemical Formula:** C<sub>30</sub>H<sub>103</sub>MgN<sub>7</sub>O<sub>5</sub>

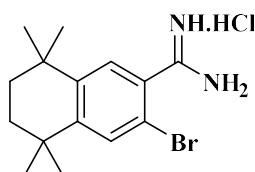
**Mp** 189.8 °C

**<sup>1</sup>H-NMR** (500 MHz, THF-*d*<sub>8</sub>) δ 9.57- 9.45 (m, 4H), 9.03 (s, 2H), 8.19- 8.11 (m, 4H), 8.08 (d, *J* = 8.5 Hz, 2H), 7.60 (d, *J* = 8.5 Hz, 2H), 6.83 (s, 2H), 4.53 (t, *J* = 6.5 Hz, 4H), 4.18 (s, 3H, OCH<sub>3</sub>), 3.91 (t, *J* = 6.5 Hz, 4H), 2.12- 2.01 (m, 4H), 1.93- 1.87 (m, 4H), 1.68 – 1.19 (m, 56H), 0.95- 0.90 (m, 12H).

**MS** (MALDI-TOF): *m/z* = 1266.55 [M]<sup>+</sup> (100%)

**UV-vis** λ<sub>max</sub> (nm) (ε (dm<sup>3</sup>.mol<sup>-1</sup>.cm<sup>-1</sup>)) = 675 (2.64·10<sup>5</sup>), 652 (1.56·10<sup>5</sup>), 597 (4.47·10<sup>4</sup>), 447 (4.73·10<sup>4</sup>), 396 (1.46·10<sup>5</sup>).

**6-Bromo-1,1,4,4-tetramethyl-1,2,3,4-tetrahydronaphthalene-7-imidamide hydrochloride 170**



Following the method reported in literature, a solution of 2-bromobenzonitrile **141** (1.43 g, 4.89 mmol) in dry THF (1.0 mL) was added to a solution of LiN(SiMe<sub>3</sub>)<sub>2</sub> in

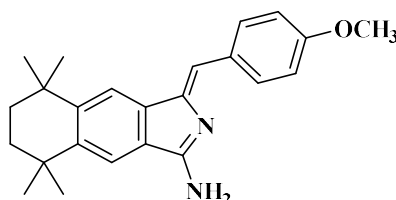
anhydrous THF (1 M, 5.38 mL, 5.38 mmol, 1.1eq) and the reaction mixture was stirred at room temperature for 4 h. A 5N HCl solution in isopropanol (15 mL) was added to the cooled mixture. The crude reaction mixture was left to stir at room temperature overnight. The precipitated product was filtered off, washed with diethyl ether and finally recrystallised from Et<sub>2</sub>O and MeOH to yield the title compound as colorless crystals<sup>49</sup>, (1.23 g, 77%).

**Mp** 153-155 °C

**<sup>1</sup>H-NMR** (500 MHz, Methanol-*d*<sub>4</sub>) δ 7.70 (s, 1H), 7.56 (s, 1H), 1.75 (s, 4H), 1.33 (s, 6H), 1.31 (s, 6H).

**<sup>13</sup>C-NMR** (126 MHz, MeOD) δ 168.28, 152.68, 152.66, 146.72, 132.82, 130.23, 129.37, 117.45, 35.72, 35.56, 35.52, 35.35, 31.80, 31.79.

**(Z)-1-[(4-methoxybenzylidene)]-5,5,8,8-tetramethyl-5H,6H,7H,8H-benzo[f]isoindol-3-amine 171**



A mixture of 2-bromobenzimidamide hydrochloride **170** (1.0 g, 3 mmol), BINAP (102 mg, 0.165 mmol, 0.055eq) and PdCl<sub>2</sub>(MeCN)<sub>2</sub> (39 mg, 0.15 mmol, 0.05eq) was sealed in a microwave vessel with a magnetic bar and then purged and refilled with N<sub>2</sub> thrice. Then, 4-ethynylanisole (0.467 ml, 0.476 g, 1.2eq) and DBU (1.12 ml, 1.14 g, 2.5eq) in dry DMF (12 ml) was added. The mixture was stirred under N<sub>2</sub> for 5 min to give a clear yellow solution with a white solid. Finally, the mixture was irradiated in a microwave reactor at 120°C for 1 h. After cooling, 50 ml of ethyl acetate was added and the mixture washed with a saturated solution of NaHCO<sub>3</sub> (75 ml) thrice. The organic layer was dried (MgSO<sub>4</sub>), filtered and concentrated<sup>48</sup>. The residue was finally purified by column chromatography using PE:AcOEt (1:1) then AcOEt as solvent

gradient to afford a yellow semisolid that was recrystallized from a DCM:Petroleum ether (1:1) to yield the title compound as yellow needles (400 mg, 36%).

**Chemical Formula:** C<sub>24</sub>H<sub>28</sub>N<sub>2</sub>O

**Mp** 202- 205 °C

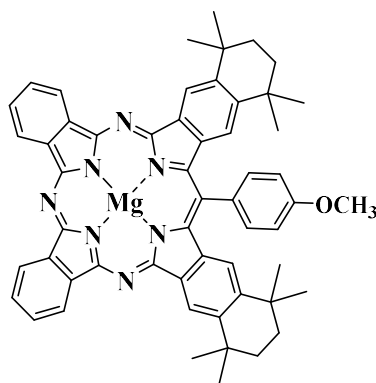
**<sup>1</sup>H-NMR** (500 MHz, Chloroform-*d*) δ 8.04 (d, *J* = 8.6 Hz, 2H), 7.70 (s, 1H), 7.41 (s, 1H), 6.93 (d, *J* = 8.6 Hz, 2H), 6.67 (s, 1H), 3.83 (s, 3H, OCH<sub>3</sub>), 1.74 (s, 4H), 1.38 (s, 6H), 1.33 (s, 6H).

**<sup>13</sup>C-NMR** (126 MHz, CDCl<sub>3</sub>) δ 164.73, 158.93, 147.05, 145.27, 144.74, 140.24, 131.74, 129.85, 128.65, 117.66, 117.13, 114.13, 113.76, 55.43, 35.19, 35.17, 35.13, 34.97, 32.38, 32.28.

**MS** (MALDI-TOF): *m/z* = 362.20 [M]<sup>+</sup> (100%)

**UV-vis** λ<sub>max</sub> (nm) (ε (dm<sup>3</sup>.mol<sup>-1</sup>.cm<sup>-1</sup>)) = 372 (2.28·10<sup>4</sup>).

#### 3.4.4 (Tetramethyl-tetralino)<sub>2</sub>-MgTBTAP-(4-OMe-Ph) 173



A suspension of phthalonitrile **8** (154 mg, 1.2 mmol, 3eq) and MgBr<sub>2</sub> (110 mg, 0.6 mmol, 1.5eq) in dry diglyme (0.5 ml) was stirred for 10 min at 220 °C, in a preheated mantle, under an argon atmosphere. A solution of aminoisoindoline **171** (144 mg, 0.4 mmol), phthalonitrile **8** (101 mg, 0.8 mmol) and DABCO (67.5 mg, 0.6 mmol, 1.5eq) in dry diglyme (1.5 ml) was added to the mixture. The reaction was heated for 1.5 h at

220 °C under an argon atmosphere. Then, the solvent was removed under an argon stream while cooling. A 1:1 mixture of DCM:MeOH (20 ml) was added and the mixture sonicated. The solvents were removed under vacuum and the crude was purified by two consecutive flash chromatography columns. First, using DCM→DCM:Et<sub>3</sub>N (20:1)→DCM:THF:Et<sub>3</sub>N (10:4:1) as eluent, the fractions collected according to their colours. Only the green fraction was subjected to the second column using PE:THF:MeOH (10:3:1) as eluent. Recrystallisation from acetone and Ethanol gave the title compound as purple crystals (16 mg, 10%).

**Chemical Formula:** C<sub>56</sub>H<sub>51</sub>MgN<sub>7</sub>O

**Mp** > 300 °C

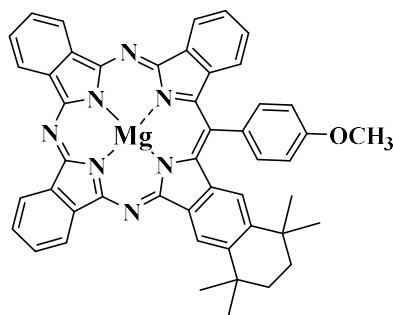
**<sup>1</sup>H-NMR** <sup>1</sup>H NMR (500 MHz, THF-*d*<sub>8</sub>) δ 9.57 (s, 2H), 9.53 (m, 4H), 8.18- 8.11 (m, 4H), 8.08 (d, *J* = 8.4 Hz, 2H), 7.62 (d, *J* = 8.4 Hz, 2H), 7.39 (s, 2H), 4.21 (s, 3H, OCH<sub>3</sub>), 1.81 (s, 8H), 1.37 (s, 24H).

**<sup>13</sup>C NMR** (126 MHz, THF) δ 162.07, 157.31, 154.85, 152.82, 145.40, 144.62, 140.89, 140.81, 139.37, 139.02, 138.64, 134.59, 134.35, 129.45, 129.34, 127.04, 125.78, 124.79, 123.69, 120.98, 115.72, 56.40, 36.66, 36.64, 36.30, 36.16, 33.16, 33.13.

**MS** (MALDI-TOF): *m/z* = 862.42 [M]<sup>+</sup> (100%)

**UV-vis** λ<sub>max</sub> (nm) (ε (dm<sup>3</sup>.mol<sup>-1</sup>.cm<sup>-1</sup>)) = 680 (1.20·10<sup>3</sup>), 656 (6.56·10<sup>2</sup>), 600 (1.79·10<sup>2</sup>), 449 (1.65·10<sup>2</sup>), 398 (4.07·10<sup>2</sup>).

### 3.4.5 (Tetramethyl-tetralino)-MgTBTAP-(4-OMe-Ph) 172



This compound was isolated from the previous reaction as side product (5 mg, 2%).

**Chemical Formula:** C<sub>48</sub>H<sub>37</sub>MgN<sub>7</sub>O

**Mp** > 300 °C

**<sup>1</sup>H-NMR** <sup>1</sup>H NMR (500 MHz, THF-*d*<sub>8</sub>) δ 9.60 (d, *J* = 7.5 Hz, 1H), 9.57 (s, 1H), 9.55-9.53 (m, 4H), 8.18- 8.16 (m, 4H), 8.06 (d, *J* = 8.4 Hz, 2H), 7.92 (t, *J* = 6.9 Hz, 1H), 7.62 (t, *J* = 6.9 Hz, 1H), 7.57 (d, *J* = 8.4 Hz, 2H), 7.43 (d, *J* = 8.0 Hz, 1H), 7.21 (s, 1H), 4.21 (s, 3H, OCH<sub>3</sub>), 1.80 (s, 4H), 1.37 (s, 12H).

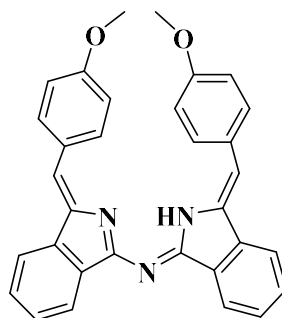
**<sup>13</sup>C-NMR** (126 MHz, THF) δ 161.97, 155.84, 153.55, 152.87, 152.17, 145.59, 145.43, 144.58, 143.60, 141.16, 141.06, 140.84, 140.33, 139.47, 138.54, 136.28, 134.36, 129.76, 129.62, 129.49, 128.02, 127.32, 125.90, 125.61, 124.79, 123.78, 123.57, 120.99, 115.59, 56.24, 36.69, 36.61, 36.34, 36.16, 33.14, 33.11.

**MS** (MALDI-TOF): *m/z* = 751.96 [M]<sup>+</sup> (100%)

**UV-vis** λ<sub>max</sub> (nm) (ε (dm<sup>3</sup>·mol<sup>-1</sup>·cm<sup>-1</sup>)) = 677 (6.11·10<sup>3</sup>), 653 (3.61·10<sup>3</sup>), 599 (8.91·10<sup>2</sup>), 447 (8.91·10<sup>2</sup>), 398 (2.26·10<sup>3</sup>).

### 3.5 Aza-dipyrromethene series (self-condensation dimers)

#### Aza-dipyrromethene (self-condensation dimer) 70a



A solution of aminoisoindoline **68a** (100 mg, 0.4 mmol) in toluene (2 mL) was heated at 120 °C for 2h under a N<sub>2</sub> atmosphere, and the solvent was allowed to slowly evaporate during the process. After cooling, the residue was purified by column chromatography using DCM and then DCM/MeOH (50:1) as the eluent to afford a red compound that was recrystallized from DCM and washed twice with MeOH to yield the product as red crystals<sup>137</sup>, (84 mg, 87%).

**Chemical Formula:** C<sub>32</sub>H<sub>25</sub>N<sub>3</sub>O<sub>2</sub>

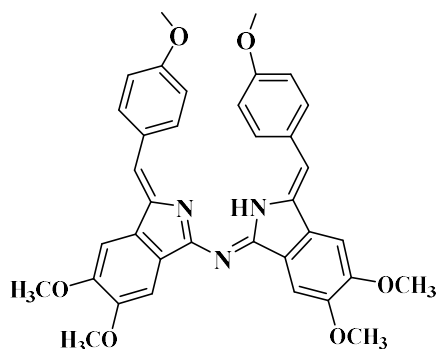
**Mp** 203-205 °C (lit. 203-204 °C)<sup>137</sup>

**<sup>1</sup>H-NMR** (500 MHz, Methylene Chloride-*d*<sub>2</sub>) δ (ppm)= 12.98 (s, 1H, N-H), 8.06 (d, *J* = 7.5 Hz, 2H), 7.87 (d, *J* = 8.6 Hz, 4H), 7.84 (d, *J* = 7.6 Hz, 2H), 7.56 (td, *J* = 7.4, 1.1 Hz, 2H), 7.51 (td, *J* = 7.4, 1.1 Hz, 2H), 6.83 (s, 2H), 6.63 (d, *J* = 8.6 Hz, 4H, H-d), 3.70 (s, 6H, OCH<sub>3</sub>).

**<sup>13</sup>C-NMR** (126 MHz, CD<sub>2</sub>Cl<sub>2</sub>) δ (ppm)= 166.06, 159.77, 140.61, 140.31, 135.08, 131.70, 130.55, 128.96, 128.50, 122.56, 119.83, 115.17, 114.6, 55.54.

**MS** (MALDI-TOF): *m/z* = 483.7 [M]<sup>+</sup> (100%)

**UV-vis** λ<sub>max</sub> (nm) (ε (dm<sup>3</sup>.mol<sup>-1</sup>.cm<sup>-1</sup>)) = 488 (2.06·10<sup>4</sup>)

**Aza-dipyrromethene (self-condensation dimer) 159**

A solution of dimethoxyaminoisoindoline **157** (250 mg, 0.414 mmol) in dry diglyme (5 mL) was heated at 220 °C under a N<sub>2</sub> atmosphere and monitored by TLC. After cooling, water (50 mL) was added, and the mixture was stirred for 15 min. The solid was filtered off, dissolved in DCM, dried (MgSO<sub>4</sub>), filtered, and concentrated<sup>137</sup>. The residue was purified by column chromatography using petroleum ether/DCM (1:1→1:2) and then neat DCM as the eluent to afford a red compound that was recrystallised from DCM and washed twice with MeOH to yield the product as red needles (38 mg, 30%).

**Chemical Formula:** C<sub>36</sub>H<sub>33</sub>N<sub>3</sub>O<sub>6</sub>

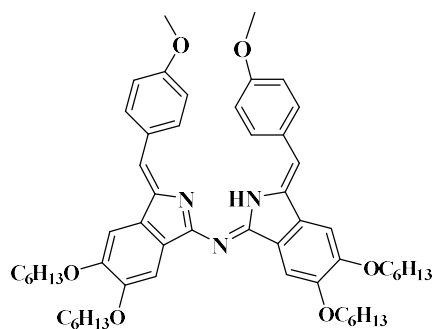
**Mp** 280-284°C

**<sup>1</sup>H-NMR** (500 MHz, CD<sub>2</sub>Cl<sub>2</sub>-d<sub>2</sub>): δ 12.80 ((s, 1H, N-H ), 7.83 (d, *J* = 8.2 Hz, 4H), 7.50 (s, 2H), 7.25 (s, 2H), 6.66 (s, 2H), 6.62 (d, *J* = 8.2 Hz, 4H), 3.99 (s, 12H), 3.69 (s, 6H).

**<sup>13</sup>C-NMR** (126 MHz, CD<sub>2</sub>Cl<sub>2</sub>) δ 166.14, 159.53, 152.59, 150.93, 140.76, 134.05, 131.49, 129.19, 127.93, 115.14, 113.49, 104.10, 102.15, 56.74, 56.66, 55.51.

**MS** (MALDI-TOF): *m/z* = 605.89 [M]<sup>+</sup> (100%)

**UV-vis** λ<sub>max</sub> (nm) (ε (dm<sup>3</sup>.mol<sup>-1</sup>.cm<sup>-1</sup>)) = 484 (1.63·10<sup>4</sup>)

**Aza-dipyrromethene (self-condensation dimer) 168**

A solution of dihexyloxyaminoisoidoline **164** (366 mg, 0.414mmol) in dry diglyme (5 mL) was heated at 220 °C under a N<sub>2</sub> atmosphere and monitored by TLC. After cooling water (50 mL) was added, and the mixture was stirred for 15 min. The solid was filtered off, dissolved in DCM, dried (MgSO<sub>4</sub>), filtered, and concentrated<sup>137</sup>. The residue was purified by column chromatography using PE/DCM (5:1→3:1) and then neat DCM as the eluent to afford a red compound that was recrystallised from DCM and washed twice with MeOH to yield the product as red needles (90 mg, 49%).

**Chemical Formula:** C<sub>56</sub>H<sub>73</sub>N<sub>3</sub>O<sub>6</sub>

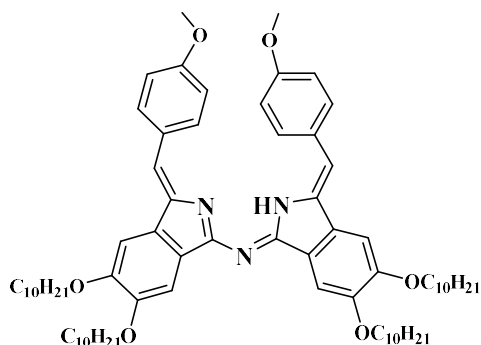
**Mp** 112 °C

**<sup>1</sup>H-NMR** (500 MHz, Methylene Chloride-*d*<sub>2</sub>) δ 12.78 (s, 1H, N-H), 7.83 (d, *J* = 8.8 Hz, 4H), 7.50 (s, 2H), 7.27 (s, 2H), 6.65 (s, 2H), 6.61 (d, *J* = 8.8 Hz, 4H), 4.16-4.12 (m, 8H), 3.69 (s, 6H, OCH<sub>3</sub>), 1.91- 1.85 (m, 8H), 1.56- 1.51 (m, 8H), 1.42- 1.36 (m, 16H), 0.95- 0.92 (m, 12H).

**<sup>13</sup>C-NMR** (126 MHz, CD<sub>2</sub>Cl<sub>2</sub>) δ 166.30, 159.48, 152.49, 150.87, 140.92, 134.00, 131.43, 129.28, 128.05, 115.12, 113.13, 105.73, 103.90, 69.97, 55.52, 32.18, 29.86, 29.81, 26.31, 23.21, 14.39.

**MS** (MALDI-TOF): *m/z* = 884.39 [M]<sup>+</sup> (100%)

**UV-vis** λ<sub>max</sub> (nm) (ε (dm<sup>3</sup>.mol<sup>-1</sup>.cm<sup>-1</sup>)) = 476 (1.51·10<sup>4</sup>).

**Aza-dipyrromethene (self-condensation dimer) 169**

A solution of didecyloxyaminoisindoline **165** (233 mg, 0.414 mmol) in dry diglyme (5 mL) was heated at 220 °C under a N<sub>2</sub> atmosphere and monitored by TLC. After cooling water (50 mL) was added, and the mixture was stirred for 15 min. The solid was filtered off, dissolved in DCM, dried (MgSO<sub>4</sub>), filtered, and concentrated<sup>137</sup>. The residue was purified by column chromatography using PE/DCM (5:1→3:1) and then neat DCM as the eluent to afford a red compound that was recrystallised from DCM and washed twice with MeOH to yield the product as red needles (98 mg, 43%).

**Chemical Formula:** C<sub>72</sub>H<sub>105</sub>N<sub>3</sub>O<sub>6</sub>

**Mp** 90 °C

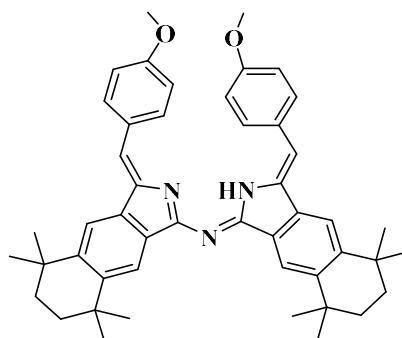
**<sup>1</sup>H-NMR** (500 MHz, Methylene Chloride-*d*<sub>2</sub>) δ 12.78 (s, 1H, N-H), 7.83 (d, *J* = 8.8 Hz, 4H), 7.52 (s, 2H), 7.26 (s, 2H), 6.64 (s, 2H), 6.61 (d, *J* = 8.8 Hz, 4H), 4.13- 4.10 (m, 8H), 3.69 (s, 6H, OCH<sub>3</sub>), 1.91- 1.83 (m, 8H), 1.57- 1.48 (m, 8H), 1.42- 1.29 (m, 48H), 0.90- 0.88 (m, 12H).

**<sup>13</sup>C-NMR** (126 MHz, CD<sub>2</sub>Cl<sub>2</sub>) δ 166.32, 159.46, 152.47, 150.88, 140.93, 133.99, 131.44, 129.31, 128.07, 115.12, 113.12, 105.77, 103.92, 69.98, 69.94, 55.51, 32.52, 30.25, 30.21, 30.19, 30.04, 30.03, 29.96, 29.93, 29.87, 26.67, 26.66, 23.29, 14.47.

**MS** (MALDI-TOF): *m/z* = 1106.60 [M]<sup>+</sup> (100%)

**UV-vis** λ<sub>max</sub> (nm) (ε (dm<sup>3</sup>.mol<sup>-1</sup>.cm<sup>-1</sup>)) = 446 (1.51·10<sup>4</sup>).

### Aza-dipyrromethene (self-condensation dimer) 174



A solution of Tetramethyl aminoisoidoline **171** (149 mg, 0.414 mmol) in dry diglyme (5 mL) was heated at 220 °C under a N<sub>2</sub> atmosphere and monitored by TLC. After cooling water (50 mL) was added, and the mixture was stirred for 15 min. The solid was filtered off, dissolved in DCM, dried (MgSO<sub>4</sub>), filtered, and concentrated<sup>137</sup>. The residue was purified by column chromatography using PE/DCM (5:1→3:1) and then neat DCM as the eluent to afford a red compound that was recrystallised from DCM and washed twice with MeOH to yield the product as red needles (89 mg, 61%).

**Chemical Formula:** C<sub>48</sub>H<sub>53</sub>N<sub>3</sub>O<sub>2</sub>

**Mp** 82 °C

**<sup>1</sup>H-NMR** (500 MHz, Methylene Chloride-*d*<sub>2</sub>) δ 13.02 (s, 1H, N-H), 8.04 (s, 2H), 7.84 (d, *J* = 8.7 Hz, 4H), 7.79 (s, 2H), 6.77 (s, 2H), 6.61 (d, *J* = 8.7 Hz, 4H), 3.69 (s, 6H, OCH<sub>3</sub>), 1.79 (s, 8H), 1.45 (s, 12H), 1.42 (s, 12H).

**<sup>13</sup>C-NMR** (126 MHz, CD<sub>2</sub>Cl<sub>2</sub>) δ 166.43, 159.46, 148.57, 146.58, 140.74, 137.71, 132.85, 131.42, 129.24, 120.54, 117.88, 115.10, 113.01, 55.52, 35.67, 35.64, 35.57, 35.55, 32.54, 32.50.

**MS** (MALDI-TOF): *m/z* = 704.41 [M]<sup>+</sup> (100%)

**UV-vis** λ<sub>max</sub> (nm) (ε (dm<sup>3</sup>.mol<sup>-1</sup>.cm<sup>-1</sup>)) = 476 (1.41·10<sup>4</sup>)

### 3.6 Bibliography

- (1) Dolphin, D. *The Porphyrins; Structure and Synthesis*; Academic Press New York San Francisco London, 1978; Vol. I.
- (2) McKeown, N. B. *Phthalocyanine Materials: Synthesis, Structure and Function*; Cambridge University Press, 1998.
- (3) Waring, D. R. Heterocyclic Dyes and Pigments. In *Comprehensive Heterocyclic Chemistry*; Elsevier Inc.: Oxford, 1984; pp 317–346.
- (4) Milaeva, E. R.; Speier, G.; Lever, A. B. P.; Leznoff, C. C. *The Phthalocyanines, Properties and Applications*; Wiley, 1992.
- (5) Leznoff, C. C. *Phthalocyanines: Properties and Applications*; VCH publishers, 1989; Vol. 1–4.
- (6) MacK, J.; Sosa-Vargas, L.; Coles, S. J.; Tizzard, G. J.; Chambrier, I.; Cammidge, A. N.; Cook, M. J.; Kobayashi, N. *Inorg. Chem.* **2012**, *51* (23), 12820–12833.
- (7) Moos, G. . Nomenclature of Tetrapyrroles. *Pure Appl. Chem.* **1987**, *56* (6), 779–832.
- (8) Cammidge, A. N.; Chambrier, I.; Cook, M. J.; Sosa-Vargas, L. In *Handbook of Porphyrin Science*; 2012; pp 331–404.
- (9) Linstead, R. P.; Dent, C. E.; Lowe, A. R. *J. Chem. Soc.* **1934**, 1033–1039.
- (10) Barrett, P. A.; Linstead, R. P.; Tvey, G. A. P. *J. Chem. Soc.* **1939**, 1809–1820.
- (11) Fischer, H.; Friedrich, W. *Justus Liebigs Ann. Chem.* **1936**, *523* (1), 154–164.
- (12) Fischer, H.; Haberland, H.; Müller, A. *Justus Liebigs Ann. Chem.* **1936**, *521* (1), 122–128.
- (13) Helberger, H. J. *Justus Liebigs Ann. Chem.* **1937**, *529* (1), 205–218.

- (14) Helberger, J. H.; von Rebay, A. *Justus Liebigs Ann. Chem.* **1937**, 531 (1), 279–287.
- (15) Barrett, P. A.; Linstead, R. P.; Rundall, F. G.; Tuey, G. A. P. *J. Chem. Soc.* **1940**, 1079–1092.
- (16) Dent, C. E. *J. Chem. Soc.* **1938**, 1–6.
- (17) Troll, D. R.; De Meutter, S. K.; Kaletta, B. *Eur. Pat. Appl.* **1991**, EP 0428214 A1.
- (18) Kaletta, B.; Rolf, M.; Wolf, W.; Terrell, D. R. *United States Pat.* **1992**, US 005162518.
- (19) Kachura, T. F.; Mashenkov, V. A.; Solov'ev, K. N.; Shkirman, S. F. *Cd. Izv. Akad. Nauk BSSR, Ser. Kim. Navuk* **1969**, 1, 65–72.
- (20) Ziegler, K.; Colonius, H. *Justus Liebigs Ann. Chem.* **1930**, 479 (1), 135–149.
- (21) Gilman, H.; Kirby, R. H. *J. Am. Chem. Soc.* **1933**, 55 (3), 1265–1270.
- (22) Kopranchikov, V. N.; Makarova, E. A.; Dashkevich, S. N. *Khimiya Geterotsiklicheskikh Soedin.* **1985**, 10, 1372–1377.
- (23) Makarova, E. A.; Kopranchikov, V. N.; Shevtsov, V. K.; Luk'yanets, E. A. *Khimiya Geterotsiklicheskikh Soedin.* **1989**, 10, 1385–1390.
- (24) Godfrey, M. R.; Newcomb, T. P.; Hoffman, B. M.; Ibers, J. A. *J. Am. Chem. Soc.* **1990**, 112 (20), 7260–7269.
- (25) Antunes, E. M.; Nyokong, T. *J. Porphyr. Phthalocyanines* **2009**, 13 (01), 153–160.
- (26) Dandliker, W. B.; Hsu, M. L. *Eur. Pat. Appl.* **1991**, EP 0528991 A1.
- (27) Dandliker, W. B.; Hsu, M. L. *United States Pat.* **1999**, US 005919922 A.

- (28) Leznoff, C. C.; McKeown, N. B. *J. Org. Chem.* **1990**, *55*, 2186–2190.
- (29) Ivanova, Y. B.; Churakhina, Y. I.; Semeikin, A. S.; Mamardashvili, N. Z. *Russ. J. Gen. Chem.* **2009**, *79* (4), 833–838.
- (30) Karasev, V. V.; Sheinin, V. B.; Berezin, B. D.; Perfilev, V. A. *Zhurnal Obs. Khimii.* **1991**, *61* (10), 2344–2348.
- (31) Tse, Y.-H.; Goel, A.; Hu, M.; Lever, A. B. P.; Leznoff, C. C.; Van Lier, J. E. *Can. J. Chem.* **1993**, *71* (5), 742–753.
- (32) Galanin, N. E.; Shaposhnikov, G. P. *Russ. J. Gen. Chem.* **2007**, *77* (11), 1951–1954.
- (33) Galanin, N. E.; Yakubov, L. A.; Shaposhnikov, G. P. *Russ. J. Gen. Chem.* **2007**, *77* (8), 1448–1454.
- (34) Yakubov, L. A.; Galanin, N. E.; Shaposhnikov, G. P.; Lebedeva, N. S.; Mal'kova, E. A. *Russ. J. Gen. Chem.* **2008**, *78* (6), 1255–1259.
- (35) Galanin, N. E.; Kudrik, E. V.; Shaposhnikov, G. P. *Russ. Chem. Bull.* **2008**, *57* (8), 1595–1610.
- (36) Galanin, N. E.; Kudrik, E. V.; Shaposhnikov, G. P. *Russ. J. Org. Chem.* **2002**, *38* (8), 1200–1203.
- (37) Galanin, N. E.; Kudrik, E. V.; Shaposhnikov, G. P. *Russ. J. Gen. Chem.* **2005**, *75* (November), 651–655.
- (38) Galanin, N. E.; Yakubov, L. A.; Kudrik, E. V.; Shaposhnikov, G. P. *Russ. J. Gen. Chem.* **2008**, *78* (7), 1436–1440.
- (39) Galanin, N. E.; Kudrik, E. V.; Shaposhnikov, G. P. *Russ. J. Gen. Chem.* **2004**, *74* (2), 282–285.
- (40) Kalashnikov, V. V.; Pushkarev, V. E.; Tomilova, L. G. A. *Mendeleev Commun.* **2011**, *21* (2), 92–93.

- (41) Kalashnikov, V. V.; Tomilova, L. G. *Macroheterocycles* **2011**, *4* (3), 209–210.
- (42) Borisov, S. M.; Zenkl, G.; Klimant, I. *ACS Appl. Mater. Interfaces*. **2010**, *2* (2), 366–374.
- (43) Pushkarev, V. E.; Kalashnikov, V. V.; Trashin, S. A.; Borisova, N. E.; Tomilova, L. G.; Zefirov, N. S. *Dalt. Trans.* **2013**, *42* (34), 12083–12086.
- (44) Cammidge, A. N.; Cook, M. J.; Hughes, D. L.; Nekelson, F.; Rahman, M. A Remarkable. *Chem. Commun.* **2005**, No. 7, 930–932.
- (45) Cammidge, A. N.; Chambrier, I.; Cook, M. J.; Hughes, D. L.; Rahman, M.; Sosa-Vargas, L. *Chem. Eur. J.* **2011**, *17* (11), 3136–3146.
- (46) Fujii, A.; Itani, H.; Watanabe, K.; Dao, Q. D.; Sosa-Vargas, L.; Shimizu, Y.; Ozaki, M. *Mol. Cryst. Liq. Cryst.* **2017**, *653* (1), 22–26.
- (47) Díaz-Moscoso, A.; Tizzard, G. J.; Coles, S. J.; Cammidge, A. N. *Angew. Chemie - Int. Ed.* **2013**, *52* (41), 10784–10787.
- (48) Hellal, M.; Cuny, G. D. *Tetrahedron Lett.* **2011**, *52* (42), 5508–5511.
- (49) Dalai, S.; Belov, V. N.; Nizamov, S.; Rauch, K.; Finsinger, D.; De Meijere, A. *European J. Org. Chem.* **2006**, No. 12, 2753–2765.
- (50) Alharbi, N.; Díaz-Moscoso, A.; Tizzard, G. J.; Coles, S. J.; Cook, M. J.; Cammidge, A. N. *Tetrahedron*. **2014**, *70* (40), 7370–7379.
- (51) Alharbi, N.; Tizzard, G. J.; Coles, S. J.; Cook, M. J.; Cammidge, A. N. *Tetrahedron*. **2015**, *71* (39), 7227–7232.
- (52) Cammidge, A. N.; Chambrier, I.; Cook, M. J.; Langner, E. H. G.; Rahman, M.; Swarts, J. C. *J. Porphyr. Phthalocyanines*. **2011**, *15* (9–10), 890–897.
- (53) Khelevina, O. G.; Berezin, B. D.; Petrov, O. A.; Glazunov, A. V. *Koord. Khimiya*. **1990**, *16* (8), 1047–1052.

- (54) Renzoni, G. E.; Schindele, D. C.; Theodore, L. J.; Leznoff, C. C.; Fearon, K. L.; Pepich, B. V. *World Intellect. Prop. Organ.* **1990**, WO 9002747A1.
- (55) Renzoni, G. E.; Schindele, D. C.; Theodore, L. J.; Leznoff, C. C.; Fearon, K. L.; Pepich, B. V. *United States Pat.* **1992**, US 005135717 A.
- (56) Silver, J.; Rickwood, K. R.; Ahmet, M. T. *United States Pat.* **1995**, US 005451674 A.
- (57) Silver, J.; Rickwood, K. R.; Ahmet, M. T. *World Intellect. Prop. Organ.* **1991**, WO 91/07659A1.
- (58) Silver, J.; Rickwood, K. R.; Ahmet, M. T. *World Intellect. Prop. Organ.* **1991**, WO 91/07658.
- (59) Zvezdina, S. V.; Mamardashvili, N. Z. *Russ. J. Coord. Chem.* **2011**, 37 (7), 495–500.
- (60) Breusova, M. O.; Pushkarev, V. E.; Tomilova, L. G. *Russ. Chem. Bull.* **2007**, 56 (7), 1456–1460.
- (61) Dent, C. E. *UK Pat.* **1938**, GB P. 494738 A.
- (62) Yaqub, S. N. *Eur. Pat. Appl.* **1979**, EP 0003149 A2.
- (63) Horst, J.; Kaletta, B. *Ger. Pat.* **1990**, DE P. 3902053 A1.
- (64) Gouterman, M. *The Porphyrins, Vol. III*; Dolphin, D., Ed.; (Academic Press, New York), 1978.
- (65) Solovev, K. N.; Mashenkov, V. A.; Kachura, T. F. *Opt. Spectrosc.* **1969**, 27, 24.
- (66) Kobayashi, N. *Synthesis and Spectroscopic Properties of Phthalocyanine Analogues*; Kadish, K. M., Smith, K. M., Guillard, R. B., Eds.; Academic Press: Amsterdam, 2003.
- (67) Mack, J.; Kobayashi, N.; Leznoff, C. C.; Stillman, M. J. *Inorg. Chem.* **1997**, 36 (24), 5624–5634.
- (68) Solov'ev, K. N.; Mashenkov, V. A.; Kachura, T. F. *Opt. Spectrosk* **1969**, 27, 50–60.

- (69) Fu, Y.; Forman, M.; Leznoff, C. C.; Lever, A. B. P. *J. Phys. Chem.* **1994**, *98* (36), 8985–8991.
- (70) Van As, A.; Joubert, C. C.; Buitendach, B. E.; Erasmus, E.; Conradie, J.; Cammidge, A. N.; Chambrier, I.; Cook, M. J.; Swarts, J. C. *Inorg. Chem.* **2015**, *54* (11), 5329–5341.
- (71) Niwa, Y.; Kobayashi, H.; Tsuchiya, T. *Inorg. Chem.* **1974**, *13* (12), 2891–2896.
- (72) Mack, J.; Stillman, M. J.; Kobayashi, N. *Coord. Chem. Rev.* **2007**, *251* (3–4), 429–453.
- (73) Michl, J. *J. Am. Chem. Soc.* **1978**, *100* (22), 6801–6811.
- (74) Alberto, M. E.; De Simone, B. C.; Mazzone, G.; Marino, T.; Russo, N. *Dye. Pigment.* **2015**, *120*, 335–339.
- (75) Theisen, R. F.; Huang, L.; Fleetham, T.; Adams, J. B.; Li, J. *J. Chem. Phys.* **2015**, *142* (9).
- (76) Woodward, I. *J. Chem. Soc.* **1940**, 601–603.
- (77) Kalashnikov, V. V.; Pushkarev, V. E.; Starikova, Z. A.; Tomilova, L. G. *Dye. Pigment.* **2014**, *105*, 216–222.
- (78) Sosa-Vargas, L. PhD thesis, University of East Anglia. **2011**.
- (79) Bahadur, B. *Mol. Cryst. Liq. Cryst.* **1984**, *109* (1), 37–41.
- (80) Cook, M. J.; Daniel, M. F.; Harrison, K. J.; McKeown, N. .; Thomson, A. J. *J. Chem. soc. chem. commun.* **1987**, 1086–1088.
- (81) Cherodian, A. S.; Davies, A. N.; Richardson, R. M.; Cook, M. J.; McKeown, N. B.; Thomson, A. J.; Feijoo, J.; Ungar, G.; Harrison, J. *Mol. Cryst. Liq. Cryst.* **1991**, *196* (1), 103–114.
- (82) Garland, A. D.; Chambrier, I.; Cammidge, A. N.; Cook, M. J. *Tetrahedron.* **2015**, *71* (39), 7310–7314.

- (83) McKeown, N. B.; Leznoff, C. C.; Richardson, R. M.; Cherodian, A. S. *Mol. Cryst. Liq. Cryst.* **1992**, *213* (1), 91–98.
- (84) Corsellis, E. A.; Coles, H. J.; McKeown, N. B.; Weber, P.; Guillon, D.; Skoulios, A. *Liq. Cryst.* **1997**, *23* (4), 475–479.
- (85) Nakagawa, D.; Nakano, C.; Ohmori, M.; Itani, H.; Shimizu, Y.; Fujii, A.; Ozaki, M. *Org. Electron.* **2017**, *44*, 67–73.
- (86) Kitagawa, T.; Fujisaki, M.; Nagano, S.; Tohnai, N.; Fujii, A.; Ozaki, M. *Appl. Phys. Express.* **2019**, *12* (5).
- (87) Ohmori, M.; Nakano, C.; Fujii, A.; Shimizu, Y.; Ozaki, M. *J. Cryst. Growth.* **2017**, *468* (August 2016), 804–809.
- (88) O'Neill, M.; Kelly, S. M. *Adv. Mater.* **2011**, *23* (5), 566–584.
- (89) Hohnholz, D.; Steinbrecher, S.; Hanack, M. *J. Mol. Struct.* **2000**, *521* (1–3), 231–237.
- (90) Walter, M. G.; Rudine, A. B.; Wamser, C. C. *J. Porphyr. Phthalocyanines.* **2010**, *14* (09), 759–792.
- (91) Melville, O. A.; Lessard, B. H.; Bender, T. P. *ACS Appl. Mater. Interfaces.* **2015**, *7* (24), 13105–13118.
- (92) Valkova, L. A.; Shabyshev, L. S.; Borovkov, N. Y.; Feigin, L. A.; Rustichelli, F. *J. Incl. Phenom.* **1999**, *35* (1–2), 243–249.
- (93) Valkova, L. A.; Glibin, A. S.; Koifman, O. I. *Macroheterocycles.* **2011**, *4* (3), 222–226.
- (94) Chaure, N. B.; Cammidge, A. N.; Chambrier, I.; Cook, M. J.; Ray, A. K. *ACS J. Solid State Sci. Technol.* **2015**, *4* (4), P3086–P3090.
- (95) Jimenez Tejada, J. A.; Lopez Varo, P.; Cammidge, A. N.; Chambrier, I.; Cook, M. J.; Chaure, N. B.; Ray, A. K. *IEEE Trans. Electron Devices* **2017**, *64* (6), 2629–2634.

- (96) Dao, Q.-D.; Uno, T.; Ohmori, M.; Watanabe, K.; Itani, H.; Fujii, A.; Shimizu, Y.; Ozaki, M. *J. Phys. D. Appl. Phys.* **2015**, *48* (38).
- (97) Dao, Q.-D.; Sosa-Vargas, L.; Higashi, T.; Ohmori, M.; Itani, H.; Fujii, A.; Shimizu, Y.; Ozaki, M. *Org. Electron.* **2015**, *23*, 44–52.
- (98) Gao, F.; Yang, C. L.; Wang, M. S.; Ma, X. G.; Liu, W. W. *Spectrochim. Acta - Part A Mol. Biomol. Spectrosc.* **2018**, *195*, 176–183.
- (99) Kaletta, B.; Rolf, M.; Wolf, W.; Terrell, D. R. *United States Pat.* **1992**, US 005162518 A.
- (100) Dandliker, W. B.; Hsu, M. L. *World Intellect. Prop. Organ.* **1991**, WO 91/18007 A1.
- (101) Schnatterer, A.; Fiege, H.; Neumann, K. H. *United States Pat.* **1992**, US 005130493A.
- (102) Ogiso, A.; Inoue, S.; Nishimoto, T.; Tsukahara, H.; Misawa, T.; Koike, T.; Mihara, N.; Murayama, S.; Nara, R. *United States Pat.* **2005**, US 6,969,764 B2.
- (103) Tamada, S.; Iwamura, T.; Sabi, Y.; Oyamada, M.; Yamamoto, M.; Koike, T.; Misawa, T.; Ogiso, A.; Nara, R.; Tokuhiro, J. *United States Pat. Appl. Publ.* **2006**, US 2006/0088786 A1.
- (104) Terrell, D. R.; De Meutter, S. K.; Kaletta, B. *United States Pat.* **1992**, US 005134048 A.
- (105) Li, J.; Wang, Z. *United States Pat. Appl. Publ.* **2012**, US 2012/0108806 A1.
- (106) Li, J.; Wang, Z. *United States Pat. Appl. Publ.* **2014**, US 2014/0332121 A1.
- (107) Heeney, M. J.; Al-Raqa, S. A.; Auger, A.; Burnham, P. M.; Cammidge, A. N.; Chambrier, I.; Cook, M. J. *J. Porphy. Phthalocyanines.* **2013**, *17* (8–9), 649–664.
- (108) Ellis, G. P.; Romney-Alexander, T. M. *Chem. Rev.* **1987**, *87* (4), 779–794.

- (109) Drechsler, U.; Hanack, M. *Synlett* . **1998**, No. 11, 1207–1208.
- (110) Nesi, R.; Turchi, S.; Giomi, D.; Corsi, C. *Tetrahedron*. **1998**, 54 (36), 10851–10856.
- (111) Farooq, O. *Synthesis (Stuttg)*. **1994**, 1994 (10), 1035–1036.
- (112) Drager, A. S.; O'Brien, D. F. *J. Org. Chem.* **2000**, 65 (7), 2257–2260.
- (113) Negishi, E.; King, A. O.; Okukado, N. *J. Org. Chem.* **1977**, 42 (10), 1821–1823.
- (114) Sonogashira, K. *J. Organomet. Chem.* **2002**, 653 (1–2), 46–49.
- (115) Miyaura, N.; Suzuki, A. *Chem. Rev.* **1995**, 95 (7), 2457–2483.
- (116) Tamao, K.; Sumitani, K.; Kiso, Y.; Zembayashi, M.; Fujioka, A.; Kodama, S.; Nakajima, I.; Minato, A.; Kumada, M. *Bulletin of the Chemical Society of Japan*. 1976, pp 1958–1969.
- (117) Terekhov, D. S.; Nolan, K. J. M.; McArthur, C. R.; Leznoff, C. C. *J. Org. Chem.* **1996**, 61 (9), 3034–3040.
- (118) Sosa-Vargas, L. X.; Chambrier, I.; Macdonald, C. J.; Coles, S. J.; Tizzard, G. J.; Cammidge, A. N.; Cook, M. J. *J. Porphyr. Phthalocyanines*. **2013**, 17 (6–7), 511–521.
- (119) Nemykina, V. N.; Lukyanets, E. A. *Arkivoc*. **2010**, 2010 (1), 136–208.
- (120) Boden, N.; Bushby, R. J.; Cammidge, A. N. *J. Am. Chem. Soc.* **1995**, 117 (3), 924–927.
- (121) Cammidge, A. N.; Gopee, H. *J. Mater. Chem.* **2001**, 11 (11), 2773–2783.
- (122) Wenderski, T.; Light, K. M.; Ogrin, D.; Bott, S. G.; Harlan, C. J. *Tetrahedron Lett.* **2004**, 45 (37), 6851–6853.
- (123) Metz, J.; Schneider, O.; Hanack, M. *Inorg. Chem.* **1984**, 23 (8), 1065–1071.

- (124) Youssef, T. E. *Polyhedron*. **2010**, 29 (7), 1776–1783.
- (125) Wöhrle, D.; Schnurpfeil, G.; Knothe, G. *Dye. Pigment*. **1992**, 18 (2), 91–102.
- (126) Metz, J.; Schneider, O.; Hanack, M. *Inorg. Chem*. **1984**, 23 (8), 1065–1071.
- (127) Sauer, T.; Wegner, G. *Mol. Cryst. Liq. Cryst. Inc. Nonlinear Opt*. **1988**, 162 (2), 97–118.
- (128) Koptyaev, A. I.; Galanin, N. E.; Shaposhnikov, G. P. *Russ. J. Gen. Chem*. **2016**, 86 (4), 854–858.
- (129) Platonova, Y. B.; Volov, A. N.; Tomilova, L. G. *J. Catal*. **2019**, 373, 222–227.
- (130) Lamei, N.; Foroumadi, A.; Emami, S.; Amini, M.; Shafiee, A. *Chin. J. Chem*. **2010**, 28, 1951–1956.
- (131) Bruson, H. A.; Kroeger, J. W. *J. Am. Chem. Soc*. **1940**, 62 (1), 36–44.
- (132) Ashton, P. R.; Girreser, U.; Giuffrida, D.; Stoddart, J. F.; Kohnke, F. H.; Mathias, J. P.; Raymo, F. M.; Slawin, A. M. Z.; Williams, D. J.; Kohnke, F. H.; et al. *J. Am. Chem. Soc*. **1993**, 115 (13), 5422–5429.
- (133) Hanack, M. , Haisch, P. , Lehmann, H. and Subramanian, L. R. *Synthesis (Stuttg)*. **1993**, 387–390.
- (134) Abou-Elkhair, R. A. I.; Hassan, A. E. A.; Boykin, D. W.; Wilson, W. D. *Org. Lett*. **2016**, 18 (18), 4714–4717.
- (135) Wood, T. E.; Thompson, A. Advances in the Chemistry of Dipyrins and Their Complexes. *Chem. Rev*. **2007**, 107 (5), 1831–1861.
- (136) Mckeown, G. R.; Manion, J. G.; Lough, A. J.; Seferos, D. S. *Chem. Commun*. **2018**, 54 (64), 8893–8896.
- (137) Díaz-Moscoso, A.; Emond, E.; Hughes, D. L.; Tizzard, G. J.; Coles, S. J.; Cammidge, A. N. *J. Org. Chem*. **2014**, 79 (18), 8932–8936.
- (138) Senevirathna, W.; Liao, J.; Mao, Z.; Gu, J.; Porter, M.; Wang, C.; Fernando,

- R.; Sauv , G. *J. Mater. Chem. A* **2015**, *3* (8), 4203–4214.
- (139) Peji , S.; Thomsen, A. M.; Etheridge, F. S.; Fernando, R.; Wang, C.; Sauv , G. *J. Mater. Chem. C* **2018**, *6* (15), 3990–3998.
- (140) Remiro-Buenama ana, S.; D az-Moscoso, A.; Hughes, D. L.; Bochmann, M.; Tizzard, G. J.; Coles, S. J.; Cammidge, A. N. *Angew. Chemie - Int. Ed.* **2015**, *54* (26), 7510–7514.
- (141) Buenama ana, S. R. PhD thesis, University of East Anglia. **2015**.
- (142) Hurley, T. J.; Robinson, M. A.; Trotz, S. I. *Inorg. Chem.* **1967**, *6* (2), 389–392.
- (143) Borodkin, V. F. *Russ. J. Appl. Chem.* **1958**, *31*, 803.
- (144) Donaldson, L. R.; Wallace, S.; Haigh, D.; Patton, E. E.; Hulme, A. N. *Org. Biomol. Chem.* **2011**, *9* (7), 2233–2239.
- (145) Mohr, B.; Enkelmann, V.; Wegner, G. *J. Org. Chem.* **1994**, *59* (3), 635–638.
- (146) Sleven, J.; G rller-Walrand, C.; Binnemans, K. *Mater. Sci. Eng. C* **2001**, *18* (1–2), 229–238.
- (147) Bruson, H. A.; Kroeger, J. W. *J. Am. Chem. Soc.* **1940**, *62* (1), 36–44.
- (148) Rose, I.; Bezzu, C. G.; Carta, M.; Comesan -G ndara, B.; Lasseguette, E.; Ferrari, M. C.; Bernardo, P.; Clarizia, G.; Fuoco, A.; Jansen, J. C.; et al. *Nat. Mater.* **2017**, *16* (9), 932–937.
- (149) Mikhalenko, S. A.; Solov'Eva, L. I.; Luk'Yanets, E. A. *J. Gen. Chem. USSR.* **1988**, *58*, 2618–2619.

### 3.7 Appendix

#### Crystal data and structure refinement for 1-Br,2-C(NH<sub>2</sub>)<sub>2</sub>,4,5-(OMe)<sub>2</sub>-benzene, Cl, H<sub>2</sub>O (156)

---

<b>Identification code</b>	<b>156 (Figure 2.19)</b>
Elemental formula	C <sub>9</sub> H <sub>12</sub> Br N <sub>2</sub> O <sub>2</sub> , Cl, H <sub>2</sub> O
Formula weight	313.58
Crystal system, space group	Triclinic, P -1 (no. 2)
Unit cell dimensions	a = 7.86437(16) Å    α = 78.3964(18) ° b = 8.22233(16) Å    β = 76.7837(18) ° c = 9.9670(2) Å    γ = 82.7698(16) °
Volume	612.45(3) Å <sup>3</sup>
Z, Calculated density	2, 1.700 Mg/m <sup>3</sup>
F(000)	316
Absorption coefficient	6.569 mm <sup>-1</sup>
Temperature	100.01(10) K
Wavelength	1.54184 Å
Crystal colour, shape	colourless prism
Crystal size	0.115 x 0.09 x 0.05 mm
Crystal mounting:	on a small loop, in oil, fixed in cold N <sub>2</sub> stream
On the diffractometer:	
Theta range for data collection	4.632 to 72.496 °
Limiting indices	-9<=h<=9, -10<=k<=9, -12<=l<=12
Completeness to theta = 67.684	100.0 %
Absorption correction	Semi-empirical from equivalents
Max. and min. transmission	1.00000 and 0.52074
Reflections collected (not including absences)	16222
No. of unique reflections	2424 [R(int) for equivalents = 0.032]
No. of 'observed' reflections (I > 2σ <sub>I</sub> )	2422

Structure determined by: dual methods, in SHELXT

Refinement: Full-matrix least-squares on  $F^2$ , in SHELXL

Data / restraints / parameters 2424 / 0 / 193

Goodness-of-fit on  $F^2$  1.108

Final R indices ('observed' data)  $R_1 = 0.021$ ,  $wR_2 = 0.054$

Final R indices (all data)  $R_1 = 0.021$ ,  $wR_2 = 0.054$

Reflections weighted:

$w = [\sigma^2(\text{Fo}^2) + (0.0277\text{P})^2 + 0.5283\text{P}]^{-1}$  where  $\text{P} = (\text{Fo}^2 + 2\text{Fc}^2) / 3$

Extinction coefficient n/a

Largest diff. peak and hole 0.30 and -0.61 e.Å<sup>-3</sup>

Location of largest difference peak near Br(1)

**Table 1. Atomic coordinates (  $\times 10^5$  ) and equivalent isotropic displacement parameters (Å<sup>2</sup>  $\times 10^4$  ). U(eq) is defined as one third of the trace of the orthogonalized  $U_{ij}$  tensor. E.s.ds are in parentheses.**

	x	y	z	U(eq)
Br(1)	44769(2)	21885(2)	41663(2)	129.9(8)
C(1)	28850(20)	36970(20)	51482(17)	98(3)
C(2)	19590(20)	31953(19)	65028(17)	100(3)
C(21)	21230(20)	14680(20)	73009(17)	104(3)
N(21)	16320(20)	2227(18)	68809(16)	137(3)
N(22)	27280(20)	12546(19)	84527(15)	143(3)
C(3)	8450(20)	43850(20)	71915(16)	105(3)
C(4)	6550(20)	60230(20)	65237(16)	95(3)
O(4)	-4143(16)	72573(14)	70880(12)	124(2)
C(41)	-15310(20)	67550(20)	84324(18)	152(3)
C(5)	16330(20)	65078(19)	51533(17)	98(3)
O(5)	13917(15)	81557(14)	45890(12)	115(2)
C(51)	24710(20)	86910(20)	32286(18)	142(3)
C(6)	27460(20)	53470(20)	44742(16)	110(3)
O(9)	44745(18)	38836(17)	87241(13)	160(3)
Cl	74591(5)	26347(5)	104486(4)	146.5(10)

**Table 2. Molecular dimensions. Bond lengths are in Ångstroms angles in degrees. E.s.ds are in parentheses.**

Br(1)-C(1)	1.8974(16)	C(21)-N(22)	1.313(2)
C(1)-C(2)	1.387(2)	N(21)-H(21A)	0.84(2)
C(1)-C(6)	1.391(2)	N(21)-H(21B)	0.86(3)
C(2)-C(3)	1.406(2)	N(22)-H(22A)	0.83(2)
C(2)-C(21)	1.488(2)	N(22)-H(22B)	0.90(3)
C(21)-N(21)	1.311(2)	C(3)-C(4)	1.383(2)

C(4)-O(4)	1.361(2)	C(5)-C(6)	1.383(2)
C(4)-C(5)	1.412(2)	O(5)-C(51)	1.442(2)
O(4)-C(41)	1.438(2)	C(51)-H(51)	0.97(2)
C(41)-H(41)	0.95(2)	C(51)-H(52)	0.96(2)
C(41)-H(42)	0.98(2)	C(51)-H(53)	0.94(3)
C(41)-H(43)	0.96(2)	O(9)-H(91)	0.80(3)
C(5)-O(5)	1.3659(19)	O(9)-H(92)	0.81(3)
C(2)-C(1)-C(6)	121.31(15)	C(4)-O(4)-C(41)	116.09(12)
C(2)-C(1)-Br(1)	121.60(12)	O(4)-C(41)-H(41)	110.6(14)
C(6)-C(1)-Br(1)	117.03(12)	O(4)-C(41)-H(42)	110.9(13)
C(1)-C(2)-C(3)	118.86(14)	H(41)-C(41)-H(42)	108.9(18)
C(1)-C(2)-C(21)	123.69(15)	O(4)-C(41)-H(43)	107.0(14)
C(3)-C(2)-C(21)	117.41(14)	H(41)-C(41)-H(43)	108.0(19)
N(21)-C(21)-N(22)	121.76(15)	H(42)-C(41)-H(43)	111.4(18)
N(21)-C(21)-C(2)	120.75(15)	O(5)-C(5)-C(6)	124.35(14)
N(22)-C(21)-C(2)	117.46(15)	O(5)-C(5)-C(4)	115.41(14)
C(21)-N(21)-H(21A)	120.3(15)	C(6)-C(5)-C(4)	120.24(14)
C(21)-N(21)-H(21B)	120.2(16)	C(5)-O(5)-C(51)	115.95(13)
H(21A)-N(21)-H(21B)	119(2)	O(5)-C(51)-H(51)	112.5(14)
C(21)-N(22)-H(22A)	117.8(15)	O(5)-C(51)-H(52)	111.8(14)
C(21)-N(22)-H(22B)	119.1(17)	H(51)-C(51)-H(52)	106.5(19)
H(22A)-N(22)-H(22B)	122(2)	O(5)-C(51)-H(53)	104.0(14)
C(4)-C(3)-C(2)	120.58(15)	H(51)-C(51)-H(53)	108(2)
O(4)-C(4)-C(3)	125.06(14)	H(52)-C(51)-H(53)	114.3(19)
O(4)-C(4)-C(5)	115.45(14)	C(5)-C(6)-C(1)	119.49(15)
C(3)-C(4)-C(5)	119.49(15)	H(91)-O(9)-H(92)	108(3)

**Table 3. Anisotropic displacement parameters ( $\text{\AA}^2 \times 10^4$ ) for the expression:  $\exp \{-2\pi^2(h^2a^{*2}U_{11} + \dots + 2hka^*b^*U_{12})\}$ . E.s.ds are in parentheses.**

	$U_{11}$	$U_{22}$	$U_{33}$	$U_{23}$	$U_{13}$	$U_{12}$
Br(1)	142.6(11)	87.7(10)	148.5(11)	-28.3(7)	-16.9(7)	17.8(7)
C(1)	104(7)	89(7)	113(7)	-24(6)	-40(6)	-6(6)
C(2)	120(8)	68(7)	119(7)	3(6)	-52(6)	-13(6)
C(21)	93(7)	92(8)	110(7)	-2(6)	-5(6)	1(6)
N(21)	194(8)	78(7)	149(7)	3(6)	-74(6)	-16(5)
N(22)	221(8)	76(7)	148(7)	15(6)	-94(6)	-26(6)
C(3)	124(8)	97(8)	94(7)	6(6)	-30(6)	-32(6)
C(4)	107(7)	76(7)	111(7)	-25(6)	-39(6)	1(6)
O(4)	164(6)	66(5)	113(5)	0(4)	9(5)	2(4)
C(41)	197(9)	97(8)	120(8)	8(6)	19(7)	3(7)
C(5)	134(8)	54(7)	111(7)	21(6)	-61(6)	-15(6)
O(5)	158(6)	61(5)	105(5)	21(4)	-17(4)	-8(4)
C(51)	189(9)	93(8)	107(8)	41(6)	-6(6)	-22(6)
C(6)	125(8)	108(8)	98(7)	0(6)	-34(6)	-20(6)
O(9)	200(7)	122(6)	174(6)	-30(5)	-70(5)	-10(5)
C1	200(2)	78(2)	150(2)	25.4(14)	-57.0(15)	-3.2(14)

**Table 4. Hydrogen coordinates ( $\times 10^4$ ) and isotropic displacement parameters ( $\text{\AA}^2 \times 10^3$ ). The phenyl ring hydrogen atoms were included in idealised positions with  $U(\text{iso})$ 's set at  $1.2 \cdot U(\text{eq})$  or, for the methyl group hydrogen atoms,  $1.5 \cdot U(\text{eq})$  of the parent carbon atoms. All remaining hydrogen atoms were located in difference maps and were refined freely and isotropically.**

	x	y	z	$U(\text{iso})$
H(3)	229	4069	8104	13
H(6)	3395	5668	3574	13
H(21A)	1180(30)	390(30)	6180(20)	15(5)
H(21B)	1710(30)	-770(30)	7360(30)	24(6)

H(22A)	3140(30)	2060(30)	8620(20)	16(5)
H(22B)	2810(30)	230(30)	8960(30)	31(6)
H(41)	-2230(30)	5910(30)	8390(20)	17(5)
H(42)	-840(30)	6340(30)	9150(20)	13(5)
H(43)	-2300(30)	7710(30)	8650(20)	18(5)
H(51)	3710(30)	8450(30)	3220(20)	21(6)
H(52)	2230(30)	8150(30)	2530(20)	17(5)
H(53)	2230(30)	9850(30)	3060(20)	21(6)
H(91)	5180(40)	3630(40)	9210(30)	41(8)
H(92)	3990(40)	4790(40)	8860(30)	30(7)

**Table 5. Torsion angles, in degrees. E.s.ds are in parentheses.**

C(6)-C(1)-C(2)-C(3)	0.8(2)	C(3)-C(4)-O(4)-C(41)	-5.7(2)
Br(1)-C(1)-C(2)-C(3)	177.84(12)	C(5)-C(4)-O(4)-C(41)	174.78(14)
C(6)-C(1)-C(2)-C(21)	-176.85(15)	O(4)-C(4)-C(5)-O(5)	0.9(2)
Br(1)-C(1)-C(2)-C(21)	0.1(2)	C(3)-C(4)-C(5)-O(5)	-178.58(14)
C(1)-C(2)-C(21)-N(21)	-64.6(2)	O(4)-C(4)-C(5)-C(6)	-179.22(14)
C(3)-C(2)-C(21)-N(21)	117.63(18)	C(3)-C(4)-C(5)-C(6)	1.3(2)
C(1)-C(2)-C(21)-N(22)	117.20(18)	C(6)-C(5)-O(5)-C(51)	-3.9(2)
C(3)-C(2)-C(21)-N(22)	-60.5(2)	C(4)-C(5)-O(5)-C(51)	175.93(14)
C(1)-C(2)-C(3)-C(4)	0.9(2)	O(5)-C(5)-C(6)-C(1)	-179.76(14)
C(21)-C(2)-C(3)-C(4)	178.72(15)	C(4)-C(5)-C(6)-C(1)	0.4(2)
C(2)-C(3)-C(4)-O(4)	178.62(15)	C(2)-C(1)-C(6)-C(5)	-1.5(2)
C(2)-C(3)-C(4)-C(5)	-1.9(2)	Br(1)-C(1)-C(6)-C(5)	-178.61(12)

**Table 6. Hydrogen bonds, in Ångstroms and degrees.**

D-H...A	d(D-H)	d(H...A)	d(D...A)	<(DHA)
C(6)-H(6)...O(9)#2	0.93	2.50	3.419(2)	169.8
N(21)-H(21B)...Cl#3	0.86(3)	2.57(3)	3.3236(16)	147(2)
N(22)-H(22A)...O(9)	0.83(2)	1.97(3)	2.790(2)	170(2)
N(22)-H(22B)...Cl#3	0.90(3)	2.33(3)	3.1755(15)	156(2)
O(9)-H(91)...Cl	0.80(3)	2.38(3)	3.1696(14)	173(3)
O(9)-H(92)...Cl#4	0.81(3)	2.43(3)	3.2354(14)	173(2)

Symmetry transformations used to generate equivalent atoms:

#1 : x-1, y, z      #2 : 1-x, 1-y, 1-z      #3 : 1-x, -y, 2-z

#4 : 1-x, 1-y, 2-z

### Crystal structure analysis of 1-Br,2-C(NH<sub>2</sub>)<sub>2</sub>,4,5-(OMe)<sub>2</sub>-benzene, Cl, H<sub>2</sub>O (156)

*Crystal data:* C<sub>9</sub>H<sub>12</sub>BrN<sub>2</sub>O<sub>2</sub>, Cl, H<sub>2</sub>O, M = 313.58. Triclinic, space group P-1 (no. 2), a = 7.86437(16), b = 8.22233(16), c = 9.9670(2) Å, α = 78.3964(18), β = 76.7837(18), γ = 82.7698(16) °, V = 612.45(3) Å<sup>3</sup>. Z = 2, D<sub>c</sub> = 1.700 g cm<sup>-3</sup>, F(000) = 316, T = 100.01(10) K, μ(Cu-Kα) = 65.7 cm<sup>-1</sup>, λ(Cu-Kα) = 1.54184 Å.

The crystal was a colourless prism, ca 0.05 x 0.09 x 0.115 mm, mounted in oil on a small loop and fixed in the cold nitrogen stream on a Rigaku Oxford Diffraction XtaLAB Synergy diffractometer, equipped with Cu-Kα radiation, HyPix detector and

mirror monochromator. Intensity data were measured by thin-slice  $\omega$ -scans. Total no. of reflections recorded, to  $\theta_{\max} = 72.5^\circ$ , was 16222 of which 2424 were unique ( $R_{\text{int}} = 0.032$ ); 2422 were 'observed' with  $I > 2\sigma_I$ .

Data were processed using the CrysAlisPro-CCD and -RED (1) programs. The structure was determined by the intrinsic phasing routines in the SHELXT program (2A) and refined by full-matrix least-squares methods, on  $F^2$ 's, in SHELXL (2B). The non-hydrogen atoms were refined with anisotropic thermal parameters. The phenyl ring hydrogen atoms were included in idealised positions and their Uiso values were set to ride on the Ueq values of the parent carbon atoms. The remaining hydrogen atoms were located in a difference map and were refined freely and isotropically. At the conclusion of the refinement,  $wR_2 = 0.054$  and  $R_1 = 0.021$  (2B) for all 2424 reflections weighted  $w = [\sigma^2(F_o^2) + (0.0277 P)^2 + 0.5283 P]^{-1}$  with  $P = (F_o^2 + 2F_c^2)/3$ .

In the final difference map, the highest peak (*ca*  $0.3 \text{ e}\text{\AA}^{-3}$ ) was near Br(1).

Scattering factors for neutral atoms were taken from reference (3). Computer programs used in this analysis have been noted above, and were run through WinGX (4) on a Dell Optiplex 780 PC at the University of East Anglia.

## References

1. Programs CrysAlisPro, Rigaku Oxford Diffraction Ltd., Abingdon, UK (2018).
2. G. M. Sheldrick, Programs for crystal structure determination (SHELXT), *Acta Cryst.* (2015) **A71**, 3-8, and refinement (SHELXL), *Acta Cryst.* (2008) **A64**, 112-122 and (2015) **C71**, 3-8.
3. '*International Tables for X-ray Crystallography*', Kluwer Academic Publishers, Dordrecht (1992). Vol. C, pp. 500, 219 and 193.
4. L. J. Farrugia, *J. Appl. Cryst.* (2012) **45**, 849–854.

## Legends for Figures

- Figure 1. View of a molecule of 1-Br,2-C(NH<sub>2</sub>)<sub>2</sub>,4,5-(OMe)<sub>2</sub>-benzene, Cl, H<sub>2</sub>O indicating the atom numbering scheme and the major hydrogen bonds. Thermal ellipsoids are drawn at the 50% probability level.
- Figure 2. View of the packing of moieties. Molecules are linked through N-H...O(water) and N-H...Cl and O-H...Cl hydrogen bonds in paired-chains parallel to the *b* axis.

## Notes on the structure

The principal moiety in this crystal is a 1-Br,2-C(NH<sub>2</sub>)<sub>2</sub>,4,5-(OMe)<sub>2</sub>-benzene cation, with the positive charge distributed through the H<sub>2</sub>N-C-NH<sub>2</sub> group; all the hydrogen atoms in this group were located in a difference map and were refined freely and isotropically. The C(2)-

C(21) bond appears to be a normal single bond and the two C-N bonds are both rather short and equivalent at 1.312(2)Å.

The crystal contains, in addition to the cation, a chloride anion and a water molecule.

The bromine substituent, the two methoxy groups and the carbon atom of the diamino-methyl group, all lie on or very close to the plane of the phenyl ring. The C(NH<sub>2</sub>)<sub>2</sub> group forms a separate plane, rotated 62.8(1)° from the phenyl group plane.

All the amino and water hydrogen atoms are involved in hydrogen bonds that link the moieties; the stronger bonds link the cations, through the chloride and water units, in paired chains (ladder-like) parallel to the *b*-axis, while weaker bonds, through the methoxy groups, connect the ladders to form hydrogen-bonded sheets.

The cations overlap in pairs about centres of symmetry; the two phenyl rings are *ca* 3.4 Å apart. Outside these pairs, there is off-set pairing about further symmetry centres so that C(1)-C(6) bonds are *ca* 3.6 Å apart.

**Crystal data and structure refinement for (MeO)<sub>2</sub>-C<sub>8</sub>H<sub>2</sub>N-NH<sub>2</sub>,=CH-C<sub>6</sub>H<sub>4</sub>-OMe (157)**

---

<b>Identification code</b>	<b>157 (Figure 2.20)</b>
Elemental formula	C18 H18 N2 O3
Formula weight	310.34
Crystal system, space group	Orthorhombic, Pna2 <sub>1</sub> (no. 33)
Unit cell dimensions	a = 8.06974(5) Å    α = 90 ° b = 10.85362(6) Å    β = 90 ° c = 17.48441(9) Å    γ = 90 °
Volume	1531.386(15) Å <sup>3</sup>
Z, Calculated density	4, 1.346 Mg/m <sup>3</sup>
F(000)	656
Absorption coefficient	0.754 mm <sup>-1</sup>
Temperature	100.01(10) K
Wavelength	1.54184 Å
Crystal colour, shape	yellow plate
Crystal size	0.15 x 0.13 x 0.055 mm
Crystal mounting:	on a small loop, in oil, fixed in cold N <sub>2</sub> stream
On the diffractometer:	
Theta range for data collection	4.796 to 72.488 °
Limiting indices	-9<=h<=9, -13<=k<=13, -21<=l<=21
Completeness to theta = 67.684	100.0 %
Absorption correction	Semi-empirical from equivalents
Max. and min. transmission	1.00000 and 0.55757
Reflections collected (not including absences)	55632
No. of unique reflections	3033 [R(int) for equivalents = 0.070]
No. of 'observed' reflections (I > 2σ <sub>I</sub> )	3018
Structure determined by:	dual methods, in SHELXT
Refinement:	Full-matrix least-squares on F <sup>2</sup> , in SHELXL

Data / restraints / parameters 3033 / 1 / 219

Goodness-of-fit on  $F^2$  1.049

Final R indices ('observed' data)  $R_1 = 0.027$ ,  $wR_2 = 0.074$

Final R indices (all data)  $R_1 = 0.028$ ,  $wR_2 = 0.075$

Reflections weighted:  $w = [\sigma^2(F_o^2) + (0.0491P)^2 + 0.2402P]^{-1}$  where  $P = (F_o^2 + 2F_c^2) / 3$

Absolute structure parameter 0.02(5)

Extinction coefficient n/a

Largest diff. peak and hole 0.19 and -0.14 e.Å<sup>-3</sup>

Location of largest difference peak near H(14b)

**Table 1. Atomic coordinates ( $\times 10^5$ ) and equivalent isotropic displacement parameters ( $\text{\AA}^2 \times 10^4$ ).  $U(\text{eq})$  is defined as one third of the trace of the orthogonalized  $U_{ij}$  tensor. E.s.ds are in parentheses.**

	x	y	z	$U(\text{eq})$
C(1)	60360(20)	41427(16)	48621(10)	207(3)
C(2)	49780(20)	50844(17)	46252(10)	212(3)
C(3)	54690(20)	58909(18)	40433(10)	232(4)
C(4)	70270(20)	57309(18)	37208(10)	246(4)
O(4)	76876(17)	64567(14)	31604(8)	318(3)
C(41)	66250(30)	73650(20)	28310(12)	379(5)
C(5)	80930(20)	47610(18)	39684(10)	232(4)
O(5)	96021(17)	47304(13)	36202(8)	291(3)
C(51)	106150(20)	36728(18)	37633(11)	285(4)
C(6)	75970(20)	39577(17)	45378(11)	226(4)
C(7)	51540(20)	35001(16)	54759(10)	215(3)
N(7)	57410(20)	25263(17)	58630(10)	271(4)
N(8)	36860(18)	39843(13)	56135(9)	228(3)
C(9)	35010(20)	50058(16)	51186(11)	210(3)
C(10)	21840(20)	57799(16)	51320(11)	221(3)
C(11)	7910(20)	57670(15)	56666(10)	208(4)
C(12)	8670(20)	51966(16)	63897(11)	216(4)
C(13)	-4980(20)	51711(16)	68695(10)	219(4)
C(14)	-19810(20)	57272(16)	66508(11)	222(4)
O(14)	-32490(16)	56349(12)	71692(7)	268(3)
C(141)	-47570(20)	62620(20)	69928(12)	293(4)
C(15)	-20780(20)	63439(17)	59541(10)	234(4)
C(16)	-6930(20)	63620(16)	54759(10)	222(4)

**Table 2. Molecular dimensions. Bond lengths are in Ångstroms, angles in degrees. E.s.ds are in parentheses.**

C (1) -C (2)	1.395 (3)	N (7) -H (7A)	0.87 (3)
C (1) -C (6)	1.396 (2)	N (7) -H (7B)	0.89 (3)
C (1) -C (7)	1.465 (2)	N (8) -C (9)	1.414 (2)
C (2) -C (3)	1.399 (3)	C (9) -C (10)	1.355 (2)
C (2) -C (9)	1.474 (2)	C (10) -C (11)	1.462 (2)
C (3) -C (4)	1.389 (3)	C (11) -C (16)	1.401 (2)
C (4) -O (4)	1.366 (2)	C (11) -C (12)	1.409 (3)
C (4) -C (5)	1.427 (3)	C (12) -C (13)	1.385 (2)
O (4) -C (41)	1.428 (2)	C (13) -C (14)	1.394 (3)
C (5) -O (5)	1.362 (2)	C (14) -O (14)	1.371 (2)
C (5) -C (6)	1.382 (3)	C (14) -C (15)	1.392 (3)
O (5) -C (51)	1.431 (2)	O (14) -C (141)	1.428 (2)
C (7) -N (8)	1.318 (2)	C (15) -C (16)	1.396 (3)
C (7) -N (7)	1.341 (3)		
C (2) -C (1) -C (6)	122.50 (16)	C (7) -N (7) -H (7A)	117.2 (19)
C (2) -C (1) -C (7)	105.58 (15)	C (7) -N (7) -H (7B)	124.3 (19)
C (6) -C (1) -C (7)	131.91 (17)	H (7A) -N (7) -H (7B)	118 (3)
C (1) -C (2) -C (3)	120.06 (17)	C (7) -N (8) -C (9)	107.21 (15)
C (1) -C (2) -C (9)	106.21 (15)	C (10) -C (9) -N (8)	123.94 (16)
C (3) -C (2) -C (9)	133.68 (17)	C (10) -C (9) -C (2)	127.49 (17)
C (4) -C (3) -C (2)	118.24 (17)	N (8) -C (9) -C (2)	108.54 (15)
O (4) -C (4) -C (3)	124.93 (17)	C (9) -C (10) -C (11)	127.46 (17)
O (4) -C (4) -C (5)	114.07 (16)	C (16) -C (11) -C (12)	116.94 (16)
C (3) -C (4) -C (5)	120.99 (17)	C (16) -C (11) -C (10)	120.05 (16)
C (4) -O (4) -C (41)	116.95 (15)	C (12) -C (11) -C (10)	123.00 (16)
O (5) -C (5) -C (6)	124.42 (17)	C (13) -C (12) -C (11)	121.20 (16)
O (5) -C (5) -C (4)	114.93 (16)	C (12) -C (13) -C (14)	120.53 (16)
C (6) -C (5) -C (4)	120.62 (17)	O (14) -C (14) -C (15)	124.86 (16)
C (5) -O (5) -C (51)	116.88 (15)	O (14) -C (14) -C (13)	115.34 (16)
C (5) -C (6) -C (1)	117.58 (17)	C (15) -C (14) -C (13)	119.78 (16)
N (8) -C (7) -N (7)	122.64 (17)	C (14) -O (14) -C (141)	117.29 (15)
N (8) -C (7) -C (1)	112.39 (16)	C (14) -C (15) -C (16)	119.05 (16)
N (7) -C (7) -C (1)	124.97 (17)	C (15) -C (16) -C (11)	122.38 (16)

**Table 3. Anisotropic displacement parameters ( $\text{\AA}^2 \times 10^4$ ) for the expression:  $\exp \{-2\pi^2(h^2a^*U_{11} + \dots + 2hka^*b^*U_{12})\}$  E.s.ds are in parentheses.**

	$U_{11}$	$U_{22}$	$U_{33}$	$U_{23}$	$U_{13}$	$U_{12}$
C (1)	212 (8)	193 (8)	215 (8)	-10 (6)	0 (7)	-9 (6)
C (2)	202 (7)	221 (8)	212 (8)	-23 (6)	0 (7)	-10 (6)
C (3)	227 (9)	257 (9)	212 (9)	18 (7)	4 (6)	26 (7)
C (4)	252 (9)	278 (9)	207 (8)	23 (7)	29 (7)	10 (7)
O (4)	272 (7)	370 (8)	312 (7)	145 (6)	89 (5)	80 (6)
C (41)	332 (11)	462 (13)	343 (11)	192 (10)	66 (8)	114 (9)
C (5)	199 (8)	277 (9)	219 (8)	16 (7)	22 (6)	18 (7)
O (5)	239 (7)	329 (7)	306 (7)	93 (6)	84 (5)	77 (6)
C (51)	244 (9)	329 (10)	283 (10)	37 (8)	51 (7)	71 (7)
C (6)	230 (8)	221 (8)	229 (8)	-6 (7)	10 (7)	9 (7)
C (7)	214 (8)	195 (8)	237 (8)	-14 (7)	15 (7)	-8 (6)
N (7)	247 (9)	247 (8)	320 (8)	64 (6)	91 (6)	50 (6)
N (8)	209 (7)	192 (6)	284 (8)	4 (6)	33 (6)	2 (5)
C (9)	212 (8)	210 (8)	208 (8)	-4 (7)	3 (6)	-22 (7)
C (10)	220 (8)	210 (8)	233 (8)	4 (6)	0 (7)	-17 (6)
C (11)	211 (8)	175 (8)	237 (9)	-31 (6)	6 (7)	-11 (6)
C (12)	208 (8)	184 (8)	256 (8)	-29 (7)	-11 (7)	11 (6)
C (13)	255 (9)	197 (8)	205 (8)	-4 (6)	0 (6)	-1 (7)
C (14)	213 (8)	216 (8)	239 (8)	-49 (7)	32 (7)	-16 (6)
O (14)	221 (6)	317 (7)	267 (6)	20 (6)	49 (5)	26 (5)
C (141)	203 (8)	348 (10)	328 (10)	-27 (8)	25 (8)	18 (7)
C (15)	198 (8)	233 (9)	270 (9)	-33 (7)	-27 (7)	28 (6)
C (16)	226 (8)	213 (8)	226 (8)	1 (7)	-6 (7)	3 (6)

**Table 4. Hydrogen coordinates ( $\times 10^4$ ) and isotropic displacement parameters ( $\text{\AA}^2 \times 10^3$ ). The amino hydrogen atoms were located in a difference map and were refined freely. The remaining hydrogen atoms were included in idealised positions with  $U(\text{iso})$ 's set at  $1.2 \cdot U(\text{eq})$  or, for the methyl group hydrogen atoms,  $1.5 \cdot U(\text{eq})$  of the parent carbon atoms.**

	x	y	z	U(iso)
H(3)	4770	6517	3877	28
H(41A)	5671	6971	2613	57
H(41B)	7213	7804	2439	57
H(41C)	6276	7933	3220	57
H(51A)	10900	3643	4296	43
H(51B)	11608	3725	3463	43
H(51C)	10017	2940	3627	43
H(6)	8279	3317	4699	27
H(10)	2164	6389	4758	27
H(12)	1851	4831	6548	26
H(13)	-425	4780	7342	26
H(14A)	-4544	7129	6946	44
H(14B)	-5547	6125	7395	44
H(14C)	-5194	5955	6519	44
H(15)	-3052	6738	5809	28
H(16)	-758	6784	5014	27
H(7A)	5090 (40)	2190 (30)	6201 (17)	41 (7)
H(7B)	6680 (40)	2130 (30)	5748 (16)	40 (7)

**Table 5. Torsion angles, in degrees. E.s.ds are in parentheses.**

C(6)-C(1)-C(2)-C(3)	-0.2(3)	N(7)-C(7)-N(8)-C(9)	178.41(17)
C(7)-C(1)-C(2)-C(3)	179.19(16)	C(1)-C(7)-N(8)-C(9)	-1.7(2)
C(6)-C(1)-C(2)-C(9)	-177.86(16)	C(7)-N(8)-C(9)-C(10)	-175.60(17)
C(7)-C(1)-C(2)-C(9)	1.55(19)	C(7)-N(8)-C(9)-C(2)	2.63(19)
C(1)-C(2)-C(3)-C(4)	-0.6(3)	C(1)-C(2)-C(9)-C(10)	175.54(18)
C(9)-C(2)-C(3)-C(4)	176.24(18)	C(3)-C(2)-C(9)-C(10)	-1.6(3)
C(2)-C(3)-C(4)-O(4)	-178.70(18)	C(1)-C(2)-C(9)-N(8)	-2.60(19)
C(2)-C(3)-C(4)-C(5)	0.8(3)	C(3)-C(2)-C(9)-N(8)	-179.8(2)
C(3)-C(4)-O(4)-C(41)	-6.7(3)	N(8)-C(9)-C(10)-C(11)	3.9(3)
C(5)-C(4)-O(4)-C(41)	173.75(18)	C(2)-C(9)-C(10)-C(11)	-174.02(17)
O(4)-C(4)-C(5)-O(5)	1.3(2)	C(9)-C(10)-C(11)-C(16)	-160.50(18)
C(3)-C(4)-C(5)-O(5)	-178.22(17)	C(9)-C(10)-C(11)-C(12)	20.9(3)
O(4)-C(4)-C(5)-C(6)	179.43(18)	C(16)-C(11)-C(12)-C(13)	3.4(2)
C(3)-C(4)-C(5)-C(6)	-0.1(3)	C(10)-C(11)-C(12)-C(13)	-177.93(16)
C(6)-C(5)-O(5)-C(51)	11.1(3)	C(11)-C(12)-C(13)-C(14)	-0.9(3)
C(4)-C(5)-O(5)-C(51)	-170.87(17)	C(12)-C(13)-C(14)-O(14)	179.51(16)
O(5)-C(5)-C(6)-C(1)	177.20(17)	C(12)-C(13)-C(14)-C(15)	-1.8(3)
C(4)-C(5)-C(6)-C(1)	-0.7(3)	C(15)-C(14)-O(14)-C(141)	-2.7(3)
C(2)-C(1)-C(6)-C(5)	0.9(3)	C(13)-C(14)-O(14)-C(141)	175.85(16)
C(7)-C(1)-C(6)-C(5)	-178.35(18)	O(14)-C(14)-C(15)-C(16)	-179.65(16)
C(2)-C(1)-C(7)-N(8)	0.0(2)	C(13)-C(14)-C(15)-C(16)	1.8(3)
C(6)-C(1)-C(7)-N(8)	179.37(19)	C(14)-C(15)-C(16)-C(11)	0.9(3)
C(2)-C(1)-C(7)-N(7)	179.95(17)	C(12)-C(11)-C(16)-C(15)	-3.4(3)
C(6)-C(1)-C(7)-N(7)	-0.7(3)	C(10)-C(11)-C(16)-C(15)	177.86(16)

**Table 6. Hydrogen bonds, in Ångstroms and degrees.**

D-H...A	d(D-H)	d(H...A)	d(D...A)	<(DHA)
---------	--------	----------	----------	--------

N(7)-H(7B)...N(8)#1	0.89(3)	2.04(3)	2.920(2)	170(3)
C(13)-H(13)...O(5)#2	0.93	2.39	3.147(2)	138.2

Symmetry transformations used to generate equivalent atoms:

#1 :  $\frac{1}{2}+x, \frac{1}{2}-y, z$  #2 :  $1-x, 1-y, \frac{1}{2}+z$

### Crystal structure analysis of (MeO)<sub>2</sub>-C<sub>8</sub>H<sub>2</sub>N-NH<sub>2</sub>=CH-C<sub>6</sub>H<sub>4</sub>-OMe (157)

*Crystal data:* C<sub>18</sub>H<sub>18</sub>N<sub>2</sub>O<sub>3</sub>, M = 310.34. Orthorhombic, space group Pna2<sub>1</sub> (no. 33), a = 8.06974(5), b = 10.85362(6), c = 17.48441(9) Å, V = 1531.385(15) Å<sup>3</sup>. Z = 4, D<sub>c</sub> = 1.346 g cm<sup>-3</sup>, F(000) = 656, T = 100.01(10) K, μ(Cu-Kα) = 7.54 cm<sup>-1</sup>, λ(Cu-Kα) = 1.54184 Å.

The crystal was a yellow plate, *ca* 0.055 x 0.13 x 0.15 mm, mounted on a small loop and fixed in the cold nitrogen stream on a Rigaku Oxford Diffraction XtaLAB Synergy diffractometer, equipped with Cu-Kα radiation, HyPix detector and mirror monochromator. Intensity data were measured by thin-slice ω-scans. Total no. of reflections recorded, to θ<sub>max</sub> = 72.5°, was 55632 of which 3033 were unique (R<sub>int</sub> = 0.070); 3018 were 'observed' with I > 2σ<sub>I</sub>.

Data were processed using the CrysAlisPro-CCD and -RED (1) programs. The structure was determined by the intrinsic phasing routines in the SHELXT program (2A) and refined by full-matrix least-squares methods, on F<sup>2</sup>'s, in SHELXL (2B). The non-hydrogen atoms were refined with anisotropic thermal parameters. The hydrogen atoms on N(7) were located in a difference map and refined freely. The remaining hydrogen atoms were included in idealised positions and their U<sub>iso</sub> values were set to ride on the U<sub>eq</sub> values of the parent carbon atoms. At the conclusion of the refinement, wR<sub>2</sub> = 0.075 and R<sub>1</sub> = 0.028 (2B) for all 3033 reflections weighted w = [σ<sup>2</sup>(F<sub>o</sub><sup>2</sup>) + (0.0491 P)<sup>2</sup> + 0.2402 P]<sup>-1</sup> with P = (F<sub>o</sub><sup>2</sup> + 2F<sub>c</sub><sup>2</sup>)/3. The absolute structure (Flack) parameter refined to 0.02(5), and the diagrams show the correct configuration.

In the final difference map, the highest peak (*ca* 0.2 eÅ<sup>-3</sup>) was near H(14b).

Scattering factors for neutral atoms were taken from reference (3). Computer programs used in this analysis have been noted above, and were run through WinGX (4) on a Dell Optiplex 780 PC at the University of East Anglia.

### References

1. Programs CrysAlisPro, Rigaku Oxford Diffraction Ltd., Abingdon, UK (2018).
2. G. M. Sheldrick, Programs for crystal structure determination (SHELXT), *Acta Cryst.* (2015) A71, 3-8, and refinement (SHELXL), *Acta Cryst.* (2008) A64, 112-122 and (2015) C71, 3-8.
3. 'International Tables for X-ray Crystallography', Kluwer Academic Publishers, Dordrecht (1992). Vol. C, pp. 500, 219 and 193.

4. L. J. Farrugia, *J. Appl. Cryst.* (2012) **45**, 849–854.

### Legends for Figures

View of a molecule of (MeO)<sub>2</sub>-C<sub>8</sub>H<sub>2</sub>N-NH<sub>2</sub>,=CH-C<sub>6</sub>H<sub>4</sub>-OMe, indicating the atom numbering scheme. Thermal ellipsoids are drawn at the 50% probability level.

View of the packing of molecules, along the *b* axis. Molecules are linked through N-H...N hydrogen bonds in chains parallel to the *a* axis.

### Notes on the structure

The molecule comprises two planar units, *viz* the isoindole nine-membered group and the phenyl ring of C(41-46). These rings are linked at C(10) and the torsion angle of C(9)-C(10)-C(11)-C(12) is 20.9(3)°. The three methoxy groups lie close to the plane of the adjoining aromatic rings.

Molecules are linked in chains parallel to the *a* axis through N(7)-H(7b)...N(8') hydrogen bonds. The second hydrogen of the N(7) amino group is not involved in any hydrogen bond formation but has a close contact, H(7a)...C(12) at 2.69 Å, on to the face of the phenyl ring. We note a 'weak hydrogen bond' between C(13)-H(13) and a neighbouring O(5) atom, where the H...O distance is 2.39 Å.

**Crystal data and structure refinement for [Mg {porph-(OMe)<sub>4</sub>,C-C<sub>6</sub>H<sub>4</sub>OMe} },OHEt],  
ca 2H<sub>2</sub>O (161)**

---

Identification code	161 (Figure 2.23)
Elemental formula	C <sub>46</sub> H <sub>37</sub> Mg N <sub>7</sub> O <sub>6</sub> , ca C <sub>0.5</sub> H <sub>2</sub> O <sub>2</sub>
Formula weight	842.15
Crystal system, space group	Orthorhombic, Pbca (no. 61)
Unit cell dimensions	a = 18.7395(8) Å    α = 90 ° b = 16.9239(4) Å    β = 90 ° c = 25.4014(7) Å    γ = 90 °
Volume	8055.9(5) Å <sup>3</sup>
Z, Calculated density	8, 1.389 Mg/m <sup>3</sup>
F(000)	3520
Absorption coefficient	0.935 mm <sup>-1</sup>
Temperature	100.01(10) K
Wavelength	1.54184 Å
Crystal colour, shape	dark red plate
Crystal size	0.11 x 0.08 x 0.03 mm
Crystal mounting:	on a small loop, in oil, fixed in cold N <sub>2</sub> stream
On the diffractometer:	
Theta range for data collection	7.759 to 64.998 °
Limiting indices	-22<=h<=22, -19<=k<=18, -29<=l<=29
Completeness to theta = 64.999	99.7 %
Absorption correction	Semi-empirical from equivalents
Max. and min. transmission	1.00000 and 0.75698
Reflections collected (not including absences)	207908
No. of unique reflections	6821 [R(int) for equivalents = 0.097]
No. of 'observed' reflections (I > 2σ <sub>I</sub> )	5675
Structure determined by:	dual methods, in SHELXT
Refinement:	Full-matrix least-squares on F <sup>2</sup> , in SHELXL
Data / restraints / parameters	6821 / 0 / 579
Goodness-of-fit on F <sup>2</sup>	1.059
Final R indices ('observed' data)	R <sub>1</sub> = 0.082, wR <sub>2</sub> = 0.213
Final R indices (all data)	R <sub>1</sub> = 0.094, wR <sub>2</sub> = 0.219
Reflections weighted:	w = [σ <sup>2</sup> (Fo <sup>2</sup> ) + (0.0929P) <sup>2</sup> + 19.498P] <sup>-1</sup> where P = (Fo <sup>2</sup> + 2Fc <sup>2</sup> ) / 3
Extinction coefficient	n/a
Largest diff. peak and hole	1.07 and -0.61 e.Å <sup>-3</sup>
Location of largest difference peak	near H(91a)

---

**Table 1. Atomic coordinates (  $\times 10^5$ ) and equivalent isotropic displacement parameters ( $\text{\AA}^2 \times 10^4$ ).  $U(\text{eq})$  is defined as one third of the trace of the orthogonalized  $U_{ij}$  tensor. E.s.ds are in parentheses.**

	x	y	z	U (eq)	S.o.f. #
Mg	57650 (8)	65886 (7)	36665 (5)	428 (4)	
N(1)	51909 (19)	55460 (18)	36734 (12)	440 (8)	
C(2)	53280 (20)	48790 (20)	39694 (15)	423 (9)	
C(3)	48880 (20)	42220 (20)	37606 (15)	430 (9)	
C(4)	47970 (20)	34170 (20)	38854 (16)	453 (9)	
C(5)	43280 (20)	29800 (20)	35871 (17)	480 (10)	
O(5)	41861 (18)	21946 (16)	36676 (12)	549 (8)	
C(51)	45160 (30)	18210 (30)	41093 (19)	644 (13)	
C(6)	39490 (30)	33180 (20)	31619 (18)	513 (10)	
O(6)	35143 (18)	27990 (17)	28990 (12)	575 (8)	
C(61)	30880 (30)	31130 (30)	24832 (18)	578 (12)	
C(7)	40260 (20)	41000 (20)	30400 (17)	482 (10)	
C(8)	44990 (20)	45430 (20)	33442 (16)	463 (10)	
C(9)	47010 (20)	53620 (20)	32996 (16)	455 (10)	
N(10)	44190 (20)	58271 (19)	29219 (13)	473 (8)	
N(11)	49970 (20)	70509 (18)	31706 (12)	445 (8)	
C(12)	45580 (20)	65920 (20)	28691 (15)	458 (10)	
C(13)	42080 (20)	70830 (20)	24686 (16)	462 (10)	
C(14)	37340 (30)	69080 (30)	20696 (16)	504 (10)	
C(15)	34870 (30)	75400 (30)	17715 (17)	520 (11)	
C(16)	36940 (30)	83120 (30)	18778 (17)	521 (11)	
C(17)	41670 (20)	84870 (20)	22721 (16)	479 (10)	
C(18)	44320 (20)	78560 (20)	25692 (15)	445 (10)	
C(19)	49300 (20)	78160 (20)	30072 (15)	449 (10)	
N(20)	52330 (20)	84601 (19)	32198 (13)	466 (8)	
N(21)	59003 (19)	77589 (18)	38913 (13)	434 (8)	
N(22)	56710 (20)	84210 (20)	36320 (16)	448 (10)	
C(23)	59670 (20)	91260 (20)	38840 (16)	446 (9)	
C(24)	58990 (30)	99380 (20)	37788 (17)	492 (10)	
C(25)	62410 (30)	104560 (20)	41134 (17)	500 (11)	
C(26)	66410 (20)	101890 (20)	45425 (17)	488 (10)	
C(27)	67010 (20)	93860 (20)	46503 (16)	449 (9)	
C(28)	63620 (20)	88630 (20)	43133 (16)	445 (10)	
C(29)	63030 (20)	79990 (20)	43108 (15)	413 (9)	
N(30)	65862 (19)	75545 (17)	46868 (12)	419 (8)	
N(31)	61530 (19)	62643 (18)	43930 (12)	413 (8)	
C(32)	65070 (20)	67660 (20)	47231 (15)	407 (9)	
C(33)	67850 (20)	63330 (20)	51661 (15)	408 (9)	
C(34)	71840 (20)	66010 (20)	55903 (15)	450 (10)	
C(35)	74020 (30)	60660 (20)	59597 (16)	494 (11)	
O(35)	78210 (20)	62301 (16)	63829 (12)	623 (9)	
C(351)	80100 (30)	70400 (20)	64555 (18)	578 (12)	
C(36)	72000 (30)	52520 (20)	59069 (16)	529 (11)	
O(36)	74460 (20)	47937 (17)	63052 (13)	726 (11)	
C(361)	72600 (40)	39750 (30)	62900 (20)	762 (18)	
C(37)	67980 (20)	49940 (20)	54905 (15)	461 (10)	
C(38)	65900 (20)	55480 (20)	50998 (15)	418 (9)	
C(39)	61800 (20)	55160 (20)	46067 (15)	406 (9)	
C(40)	58140 (20)	48560 (20)	43917 (15)	411 (9)	
C(41)	59350 (20)	40660 (20)	46475 (14)	403 (9)	
C(42)	65200 (20)	36090 (20)	45052 (15)	410 (9)	
C(43)	66030 (20)	28480 (20)	47032 (15)	438 (9)	
C(44)	60950 (20)	25370 (20)	50414 (15)	433 (9)	
O(44)	62014 (17)	17655 (16)	51894 (11)	521 (7)	
C(441)	56490 (30)	13900 (30)	54825 (19)	588 (12)	
C(45)	55300 (20)	29980 (20)	52091 (15)	446 (10)	
C(46)	54610 (20)	37630 (20)	50089 (16)	448 (10)	
O(9)	65678 (17)	62832 (16)	31723 (12)	503 (7)	
C(91)	71120 (30)	56950 (40)	33170 (20)	884 (19)	
C(92)	74030 (40)	52240 (40)	28700 (30)	1040 (20)	
O(71)	62020 (30)	61430 (20)	21984 (14)	848 (14)	
O(72)	58980 (30)	48170 (30)	16436 (16)	853 (12)	

C(71) 57890(80) 56430(90) 20420(60) 930(40)\* 0.5

# - site occupancy, if different from 1.

\* - U(iso) ( $\text{\AA}^2 \times 10^4$ )

**Table 2. Molecular dimensions. Bond lengths are in Ångstroms, angles in degrees. E.s.ds are in parentheses.**

Mg-O(9)	2.026(3)	Mg-N(1)	2.067(4)
Mg-N(31)	2.058(3)	Mg-N(21)	2.077(3)
Mg-N(11)	2.066(4)		
O(9)-Mg-N(31)	103.01(14)	N(11)-Mg-N(1)	88.05(14)
O(9)-Mg-N(11)	103.64(14)	O(9)-Mg-N(21)	108.84(14)
N(31)-Mg-N(11)	153.34(15)	N(31)-Mg-N(21)	87.98(13)
O(9)-Mg-N(1)	100.02(14)	N(11)-Mg-N(21)	83.77(14)
N(31)-Mg-N(1)	87.05(13)	N(1)-Mg-N(21)	151.10(15)
N(1)-C(9)	1.357(5)	C(24)-C(25)	1.379(6)
N(1)-C(2)	1.380(5)	C(25)-C(26)	1.399(6)
C(2)-C(40)	1.408(6)	C(26)-C(27)	1.390(6)
C(2)-C(3)	1.482(5)	C(27)-C(28)	1.386(6)
C(3)-C(8)	1.395(6)	C(28)-C(29)	1.467(5)
C(3)-C(4)	1.408(5)	C(29)-N(30)	1.327(5)
C(4)-C(5)	1.377(6)	N(30)-C(32)	1.346(5)
C(5)-O(5)	1.370(5)	N(31)-C(32)	1.365(5)
C(5)-C(6)	1.414(6)	N(31)-C(39)	1.379(5)
O(5)-C(51)	1.429(5)	C(32)-C(33)	1.440(5)
C(6)-C(7)	1.366(6)	C(33)-C(34)	1.387(6)
C(6)-O(6)	1.372(5)	C(33)-C(38)	1.389(5)
O(6)-C(61)	1.426(5)	C(34)-C(35)	1.367(6)
C(7)-C(8)	1.395(6)	C(35)-O(35)	1.359(5)
C(8)-C(9)	1.441(6)	C(35)-C(36)	1.436(6)
C(9)-N(10)	1.348(5)	O(35)-C(351)	1.428(5)
N(10)-C(12)	1.327(5)	C(36)-O(36)	1.356(5)
N(11)-C(19)	1.366(5)	C(36)-C(37)	1.369(6)
N(11)-C(12)	1.367(5)	O(36)-C(361)	1.429(5)
C(12)-C(13)	1.468(6)	C(37)-C(38)	1.420(5)
C(13)-C(14)	1.380(6)	C(38)-C(39)	1.470(5)
C(13)-C(18)	1.399(6)	C(39)-C(40)	1.421(5)
C(14)-C(15)	1.390(6)	C(40)-C(41)	1.503(5)
C(15)-C(16)	1.390(6)	C(41)-C(46)	1.378(6)
C(16)-C(17)	1.370(6)	C(41)-C(42)	1.390(6)
C(17)-C(18)	1.398(6)	C(42)-C(43)	1.390(5)
C(18)-C(19)	1.453(6)	C(43)-C(44)	1.386(6)
C(19)-N(20)	1.342(5)	C(44)-O(44)	1.373(5)
N(20)-N(22)	1.333(5)	C(44)-C(45)	1.381(6)
N(21)-C(29)	1.367(5)	O(44)-C(441)	1.425(5)
N(21)-N(22)	1.369(5)	C(45)-C(46)	1.397(6)
N(22)-C(23)	1.462(6)	O(9)-C(91)	1.471(7)
C(23)-C(28)	1.391(6)	O(9)-H(90)	1.08(8)
C(23)-C(24)	1.406(5)	C(91)-C(92)	1.490(8)
C(9)-N(1)-C(2)	108.6(3)	C(5)-O(5)-C(51)	117.5(3)
C(9)-N(1)-Mg	122.8(3)	C(7)-C(6)-O(6)	124.9(4)
C(2)-N(1)-Mg	127.3(3)	C(7)-C(6)-C(5)	120.8(4)
N(1)-C(2)-C(40)	123.9(3)	O(6)-C(6)-C(5)	114.2(4)
N(1)-C(2)-C(3)	108.4(3)	C(6)-O(6)-C(61)	117.0(3)
C(40)-C(2)-C(3)	127.7(3)	C(6)-C(7)-C(8)	117.5(4)
C(8)-C(3)-C(4)	118.9(4)	C(7)-C(8)-C(3)	122.9(4)
C(8)-C(3)-C(2)	105.6(3)	C(7)-C(8)-C(9)	129.8(4)
C(4)-C(3)-C(2)	135.5(4)	C(3)-C(8)-C(9)	107.3(4)
C(5)-C(4)-C(3)	118.3(4)	N(10)-C(9)-N(1)	129.0(4)
O(5)-C(5)-C(4)	124.3(4)	N(10)-C(9)-C(8)	121.0(4)
O(5)-C(5)-C(6)	114.2(4)	N(1)-C(9)-C(8)	110.1(3)
C(4)-C(5)-C(6)	121.5(4)	C(12)-N(10)-C(9)	124.4(4)

C (19) -N (11) -C (12)	108.2 (3)	C (32) -N (31) -Mg	123.8 (2)
C (19) -N (11) -Mg	127.5 (3)	C (39) -N (31) -Mg	127.7 (3)
C (12) -N (11) -Mg	123.1 (3)	N (30) -C (32) -N (31)	128.9 (4)
N (10) -C (12) -N (11)	128.0 (4)	N (30) -C (32) -C (33)	121.1 (3)
N (10) -C (12) -C (13)	122.3 (4)	N (31) -C (32) -C (33)	109.9 (3)
N (11) -C (12) -C (13)	109.6 (3)	C (34) -C (33) -C (38)	123.3 (4)
C (14) -C (13) -C (18)	121.9 (4)	C (34) -C (33) -C (32)	129.5 (3)
C (14) -C (13) -C (12)	132.5 (4)	C (38) -C (33) -C (32)	107.2 (3)
C (18) -C (13) -C (12)	105.6 (4)	C (35) -C (34) -C (33)	118.5 (4)
C (13) -C (14) -C (15)	116.7 (4)	O (35) -C (35) -C (34)	125.5 (4)
C (16) -C (15) -C (14)	121.6 (4)	O (35) -C (35) -C (36)	115.0 (3)
C (17) -C (16) -C (15)	121.8 (4)	C (34) -C (35) -C (36)	119.5 (4)
C (16) -C (17) -C (18)	117.4 (4)	C (35) -O (35) -C (351)	116.2 (3)
C (17) -C (18) -C (13)	120.6 (4)	O (36) -C (36) -C (37)	125.5 (4)
C (17) -C (18) -C (19)	132.6 (4)	O (36) -C (36) -C (35)	112.9 (4)
C (13) -C (18) -C (19)	106.8 (3)	C (37) -C (36) -C (35)	121.6 (4)
N (20) -C (19) -N (11)	127.5 (4)	C (36) -O (36) -C (361)	116.8 (4)
N (20) -C (19) -C (18)	122.8 (3)	C (36) -C (37) -C (38)	118.7 (4)
N (11) -C (19) -C (18)	109.7 (3)	C (33) -C (38) -C (37)	118.4 (4)
N (22) -N (20) -C (19)	122.5 (3)	C (33) -C (38) -C (39)	106.0 (3)
C (29) -N (21) -N (22)	107.8 (3)	C (37) -C (38) -C (39)	135.6 (4)
C (29) -N (21) -Mg	124.4 (2)	N (31) -C (39) -C (40)	123.6 (4)
N (22) -N (21) -Mg	127.6 (3)	N (31) -C (39) -C (38)	108.7 (3)
N (20) -N (22) -N (21)	127.8 (4)	C (40) -C (39) -C (38)	127.5 (3)
N (20) -N (22) -C (23)	122.5 (4)	C (2) -C (40) -C (39)	125.7 (3)
N (21) -N (22) -C (23)	109.8 (3)	C (2) -C (40) -C (41)	116.9 (3)
C (28) -C (23) -C (24)	120.6 (4)	C (39) -C (40) -C (41)	117.4 (3)
C (28) -C (23) -N (22)	106.5 (3)	C (46) -C (41) -C (42)	118.4 (4)
C (24) -C (23) -N (22)	132.8 (4)	C (46) -C (41) -C (40)	121.4 (4)
C (25) -C (24) -C (23)	117.6 (4)	C (42) -C (41) -C (40)	120.1 (4)
C (24) -C (25) -C (26)	121.6 (4)	C (41) -C (42) -C (43)	120.6 (4)
C (27) -C (26) -C (25)	120.9 (4)	C (44) -C (43) -C (42)	120.0 (4)
C (28) -C (27) -C (26)	117.7 (4)	O (44) -C (44) -C (45)	124.3 (4)
C (27) -C (28) -C (23)	121.7 (4)	O (44) -C (44) -C (43)	115.5 (4)
C (27) -C (28) -C (29)	132.4 (4)	C (45) -C (44) -C (43)	120.2 (4)
C (23) -C (28) -C (29)	105.9 (4)	C (44) -O (44) -C (441)	117.5 (3)
N (30) -C (29) -N (21)	127.9 (3)	C (44) -C (45) -C (46)	118.8 (4)
N (30) -C (29) -C (28)	122.1 (4)	C (41) -C (46) -C (45)	121.8 (4)
N (21) -C (29) -C (28)	110.0 (3)	C (91) -O (9) -Mg	122.2 (3)
C (29) -N (30) -C (32)	124.6 (3)	O (9) -C (91) -C (92)	115.2 (5)
C (32) -N (31) -C (39)	108.1 (3)		
O (71) -C (71)	1.214 (15)	C (71) -O (71) -H (71)	105 (6)
O (71) -H (71)	1.05 (11)	C (71) -O (72) -H (72)	114 (8)
O (72) . . . C (71)	1.738 (16)	O (71) -C (71) -O (72)	132.5 (11)
O (72) -H (72)	1.15 (16)		

**Table 3. Anisotropic displacement parameters ( $\text{\AA}^2 \times 10^4$ ) for the expression:  $\exp \{-2n^2(h^2a^*U_{11} + \dots + 2hka^*b^*U_{12})\}$  E.s.ds are in parentheses.**

	$U_{11}$	$U_{22}$	$U_{33}$	$U_{23}$	$U_{13}$	$U_{12}$
Mg	672 (9)	239 (6)	372 (7)	-10 (5)	-25 (6)	13 (6)
N (1)	660 (20)	270 (16)	392 (17)	-2 (13)	-43 (16)	21 (15)
C (2)	640 (30)	226 (18)	400 (20)	-55 (15)	43 (19)	19 (17)
C (3)	620 (30)	258 (19)	410 (20)	-59 (16)	9 (19)	17 (17)
C (4)	610 (30)	330 (20)	420 (20)	-19 (17)	2 (19)	25 (18)
C (5)	680 (30)	270 (20)	480 (20)	-29 (17)	-10 (20)	11 (19)
O (5)	820 (20)	281 (14)	545 (17)	-4 (13)	-129 (16)	-25 (14)
C (51)	920 (40)	360 (20)	650 (30)	50 (20)	-170 (30)	-40 (20)
C (6)	640 (30)	370 (20)	530 (20)	-82 (19)	-70 (20)	-10 (20)
O (6)	760 (20)	329 (15)	635 (19)	-38 (14)	-193 (16)	-14 (14)
C (61)	740 (30)	470 (30)	530 (20)	-50 (20)	-150 (20)	-10 (20)
C (7)	680 (30)	330 (20)	440 (20)	-15 (17)	-50 (20)	34 (19)
C (8)	640 (30)	340 (20)	420 (20)	-44 (17)	-17 (19)	31 (19)
C (9)	690 (30)	253 (19)	430 (20)	-36 (16)	0 (20)	25 (18)
N (10)	720 (20)	273 (17)	425 (18)	-14 (14)	-63 (17)	42 (16)
N (11)	680 (20)	279 (17)	371 (17)	-2 (13)	-22 (16)	15 (15)
C (12)	690 (30)	290 (20)	390 (20)	-18 (16)	-10 (20)	50 (19)

C(13)	670(30)	350(20)	370(20)	-13(17)	30(19)	74(19)
C(14)	720(30)	370(20)	420(20)	-4(18)	0(20)	40(20)
C(15)	710(30)	460(20)	390(20)	17(18)	-30(20)	30(20)
C(16)	760(30)	390(20)	410(20)	85(18)	-20(20)	50(20)
C(17)	700(30)	340(20)	390(20)	58(17)	20(20)	2(19)
C(18)	660(30)	320(20)	350(20)	10(16)	55(19)	10(18)
C(19)	670(30)	300(20)	370(20)	16(16)	43(19)	46(18)
N(20)	710(20)	284(17)	407(18)	10(14)	-9(17)	-20(16)
N(21)	670(20)	240(16)	393(17)	48(13)	-12(16)	-7(15)
N(22)	650(30)	300(20)	400(20)	31(16)	5(19)	-2(18)
C(23)	650(30)	262(19)	430(20)	16(16)	20(20)	-9(18)
C(24)	700(30)	290(20)	490(20)	70(18)	10(20)	15(19)
C(25)	710(30)	194(19)	600(30)	37(18)	20(20)	-8(18)
C(26)	660(30)	270(20)	540(20)	-49(18)	10(20)	-27(18)
C(27)	610(30)	280(20)	460(20)	-9(17)	14(19)	-8(18)
C(28)	630(30)	252(19)	450(20)	9(16)	30(20)	-7(18)
C(29)	610(20)	222(19)	410(20)	-11(16)	-9(18)	7(17)
N(30)	650(20)	201(15)	410(17)	-20(13)	-11(16)	0(14)
N(31)	610(20)	240(16)	385(17)	-4(13)	10(15)	20(14)
C(32)	580(20)	268(19)	370(20)	-27(15)	4(18)	-7(17)
C(33)	620(20)	212(18)	390(20)	-18(15)	19(18)	20(17)
C(34)	690(30)	229(19)	430(20)	-30(16)	-30(20)	-9(18)
C(35)	810(30)	260(20)	420(20)	-35(16)	-120(20)	36(19)
O(35)	1050(30)	282(15)	542(18)	-14(13)	-307(18)	0(16)
C(351)	930(30)	270(20)	530(20)	-69(18)	-230(30)	-20(20)
C(36)	880(30)	280(20)	420(20)	54(17)	-110(20)	10(20)
O(36)	1340(30)	240(15)	593(19)	82(13)	-390(20)	-36(17)
C(361)	1450(50)	240(20)	600(30)	70(20)	-300(30)	-40(30)
C(37)	760(30)	206(18)	410(20)	15(16)	0(20)	-2(18)
C(38)	610(20)	272(19)	372(19)	-42(16)	24(18)	12(17)
C(39)	570(20)	261(19)	380(20)	-12(15)	27(18)	29(17)
C(40)	600(20)	260(19)	367(19)	-35(15)	44(18)	29(17)
C(41)	610(20)	260(19)	334(19)	-51(15)	-13(18)	4(17)
C(42)	610(20)	274(19)	351(19)	-12(15)	15(18)	0(17)
C(43)	600(20)	320(20)	390(20)	-9(16)	-11(19)	55(18)
C(44)	690(30)	242(18)	370(20)	-7(15)	-39(19)	22(18)
O(44)	760(20)	294(14)	511(16)	109(12)	64(15)	77(14)
C(441)	830(30)	350(20)	580(30)	140(20)	120(20)	40(20)
C(45)	660(30)	270(20)	400(20)	-27(16)	67(19)	-27(18)
C(46)	620(30)	270(20)	450(20)	-84(17)	30(20)	32(18)
O(9)	720(20)	353(15)	431(16)	3(12)	40(15)	39(14)
C(91)	850(40)	1240(60)	560(30)	80(30)	90(30)	170(40)
C(92)	1050(50)	600(40)	1460(60)	-360(40)	-150(50)	170(30)
O(71)	1720(40)	364(18)	465(19)	-43(15)	-200(20)	80(20)
O(72)	1090(30)	790(30)	680(20)	0(20)	80(20)	230(20)

**Table 4. Hydrogen coordinates ( $\times 10^4$ ) and isotropic displacement parameters ( $\text{\AA}^2 \times 10^3$ ). Hydrogen atoms involved hydrogen bonds were located in difference maps and were refined isotropically and freely. All remaining hydrogen atoms were included in idealised positions with  $U(\text{iso})$ 's set at  $1.2 \cdot U(\text{eq})$  or, for the methyl group hydrogen atoms,  $1.5 \cdot U(\text{eq})$  of the parent carbon atoms.**

	x	y	z	U(iso)	S.o.f.#
H(4)	5047	3188	4162	54	
H(51A)	4376	1276	4122	97	
H(51B)	5026	1855	4075	97	
H(51C)	4370	2081	4427	97	
H(61A)	2808	2697	2330	87	
H(61B)	2777	3513	2621	87	
H(61C)	3392	3339	2219	87	
H(7)	3773	4328	2764	58	
H(14)	3587	6392	2003	60	
H(15)	3175	7444	1494	62	
H(16)	3507	8720	1676	63	
H(17)	4306	9004	2340	57	
H(24)	5634	10119	3494	59	

H(25)	6204	10996	4052	60	
H(26)	6870	10553	4759	59	
H(27)	6961	9206	4939	54	
H(34)	7299	7134	5623	54	
H(35A)	8304	7091	6763	87	
H(35B)	8268	7225	6153	87	
H(35C)	7585	7350	6499	87	
H(36A)	7462	3711	6589	114	
H(36B)	6750	3922	6297	114	
H(36C)	7443	3742	5972	114	
H(37)	6664	4466	5464	55	
H(42)	6860	3813	4275	49	
H(43)	6999	2548	4609	53	
H(44A)	5787	856	5561	88	
H(44B)	5571	1673	5805	88	
H(44C)	5217	1386	5279	88	
H(45)	5202	2802	5451	53	
H(46)	5083	4076	5123	54	
H(91A)	6906	5334	3571	106	
H(91B)	7504	5966	3488	106	
H(92A)	7752	4858	2999	156	
H(92B)	7022	4939	2703	156	
H(92C)	7622	5573	2619	156	
H(90)	6410 (40)	6180 (50)	2770 (30)	140 (30)	
H(71)	6160 (50)	6610 (60)	1930 (40)	190 (40)	
H(72)	6450 (80)	4780 (90)	1440 (60)	130 (50)	0.5
H(73)	4720 (100)	9180 (100)	3320 (70)	170 (60)	0.5

# - site occupancy, if different from 1.

**Table 5. Torsion angles, in degrees. E.s.ds are in parentheses.**

C(9)-N(1)-C(2)-C(40)	179.7(4)	C(3)-C(8)-C(9)-N(10)	178.8(4)
Mg-N(1)-C(2)-C(40)	12.3(6)	C(7)-C(8)-C(9)-N(1)	-178.8(4)
C(9)-N(1)-C(2)-C(3)	0.3(5)	C(3)-C(8)-C(9)-N(1)	-0.4(5)
Mg-N(1)-C(2)-C(3)	-167.1(3)	N(1)-C(9)-N(10)-C(12)	-3.7(7)
N(1)-C(2)-C(3)-C(8)	-0.5(5)	C(8)-C(9)-N(10)-C(12)	177.3(4)
C(40)-C(2)-C(3)-C(8)	-179.9(4)	C(9)-N(10)-C(12)-N(11)	0.2(7)
N(1)-C(2)-C(3)-C(4)	179.2(5)	C(9)-N(10)-C(12)-C(13)	-176.6(4)
C(40)-C(2)-C(3)-C(4)	-0.2(8)	C(19)-N(11)-C(12)-N(10)	-174.3(4)
C(8)-C(3)-C(4)-C(5)	0.4(6)	Mg-N(11)-C(12)-N(10)	17.2(6)
C(2)-C(3)-C(4)-C(5)	-179.3(4)	C(19)-N(11)-C(12)-C(13)	2.8(5)
C(3)-C(4)-C(5)-O(5)	-179.7(4)	Mg-N(11)-C(12)-C(13)	-165.7(3)
C(3)-C(4)-C(5)-C(6)	0.7(6)	N(10)-C(12)-C(13)-C(14)	-3.9(8)
C(4)-C(5)-O(5)-C(51)	3.9(7)	N(11)-C(12)-C(13)-C(14)	178.8(4)
C(6)-C(5)-O(5)-C(51)	-176.4(4)	N(10)-C(12)-C(13)-C(18)	174.1(4)
O(5)-C(5)-C(6)-C(7)	178.8(4)	N(11)-C(12)-C(13)-C(18)	-3.2(5)
C(4)-C(5)-C(6)-C(7)	-1.4(7)	C(18)-C(13)-C(14)-C(15)	-0.2(6)
O(5)-C(5)-C(6)-O(6)	-0.9(6)	C(12)-C(13)-C(14)-C(15)	177.6(4)
C(4)-C(5)-C(6)-O(6)	178.8(4)	C(13)-C(14)-C(15)-C(16)	-1.4(7)
C(7)-C(6)-O(6)-C(61)	-3.0(7)	C(14)-C(15)-C(16)-C(17)	1.7(7)
C(5)-C(6)-O(6)-C(61)	176.7(4)	C(15)-C(16)-C(17)-C(18)	-0.4(7)
O(6)-C(6)-C(7)-C(8)	-179.2(4)	C(16)-C(17)-C(18)-C(13)	-1.1(6)
C(5)-C(6)-C(7)-C(8)	1.1(7)	C(16)-C(17)-C(18)-C(19)	180.0(4)
C(6)-C(7)-C(8)-C(3)	0.0(7)	C(14)-C(13)-C(18)-C(17)	1.5(7)
C(6)-C(7)-C(8)-C(9)	178.2(5)	C(12)-C(13)-C(18)-C(17)	-176.8(4)
C(4)-C(3)-C(8)-C(7)	-0.7(6)	C(14)-C(13)-C(18)-C(19)	-179.4(4)
C(2)-C(3)-C(8)-C(7)	179.1(4)	C(12)-C(13)-C(18)-C(19)	2.3(5)
C(4)-C(3)-C(8)-C(9)	-179.3(4)	C(12)-N(11)-C(19)-N(20)	175.5(4)
C(2)-C(3)-C(8)-C(9)	0.5(5)	Mg-N(11)-C(19)-N(20)	-16.7(6)
C(2)-N(1)-C(9)-N(10)	-179.1(4)	C(12)-N(11)-C(19)-C(18)	-1.3(5)
Mg-N(1)-C(9)-N(10)	-11.0(6)	Mg-N(11)-C(19)-C(18)	166.5(3)
C(2)-N(1)-C(9)-C(8)	0.0(5)	C(17)-C(18)-C(19)-N(20)	1.2(7)
Mg-N(1)-C(9)-C(8)	168.1(3)	C(13)-C(18)-C(19)-N(20)	-177.7(4)
C(7)-C(8)-C(9)-N(10)	0.4(7)	C(17)-C(18)-C(19)-N(11)	178.2(4)

C(13)-C(18)-C(19)-N(11)	-0.8(5)	C(36)-C(35)-O(35)-C(351)	-177.9(4)
N(11)-C(19)-N(20)-N(22)	1.4(7)	O(35)-C(35)-C(36)-O(36)	2.2(6)
C(18)-C(19)-N(20)-N(22)	177.9(4)	C(34)-C(35)-C(36)-O(36)	-179.1(4)
C(19)-N(20)-N(22)-N(21)	2.2(7)	O(35)-C(35)-C(36)-C(37)	-177.8(4)
C(19)-N(20)-N(22)-C(23)	-176.1(4)	C(34)-C(35)-C(36)-C(37)	0.8(7)
C(29)-N(21)-N(22)-N(20)	-175.9(4)	C(37)-C(36)-O(36)-C(361)	-0.9(8)
Mg-N(21)-N(22)-N(20)	9.8(7)	C(35)-C(36)-O(36)-C(361)	179.0(5)
C(29)-N(21)-N(22)-C(23)	2.6(5)	O(36)-C(36)-C(37)-C(38)	-179.0(5)
Mg-N(21)-N(22)-C(23)	-171.8(3)	C(35)-C(36)-C(37)-C(38)	1.0(7)
N(20)-N(22)-C(23)-C(28)	176.7(4)	C(34)-C(33)-C(38)-C(37)	1.1(6)
N(21)-N(22)-C(23)-C(28)	-1.9(5)	C(32)-C(33)-C(38)-C(37)	-179.5(4)
N(20)-N(22)-C(23)-C(24)	-1.1(8)	C(34)-C(33)-C(38)-C(39)	-179.8(4)
N(21)-N(22)-C(23)-C(24)	-179.7(5)	C(32)-C(33)-C(38)-C(39)	-0.5(5)
C(28)-C(23)-C(24)-C(25)	0.3(7)	C(36)-C(37)-C(38)-C(33)	-2.0(6)
N(22)-C(23)-C(24)-C(25)	177.9(5)	C(36)-C(37)-C(38)-C(39)	179.3(5)
C(23)-C(24)-C(25)-C(26)	0.1(7)	C(32)-N(31)-C(39)-C(40)	174.3(4)
C(24)-C(25)-C(26)-C(27)	-0.8(7)	Mg-N(31)-C(39)-C(40)	-12.5(6)
C(25)-C(26)-C(27)-C(28)	1.1(7)	C(32)-N(31)-C(39)-C(38)	-1.0(4)
C(26)-C(27)-C(28)-C(23)	-0.7(6)	Mg-N(31)-C(39)-C(38)	172.1(3)
C(26)-C(27)-C(28)-C(29)	-178.8(4)	C(33)-C(38)-C(39)-N(31)	0.9(5)
C(24)-C(23)-C(28)-C(27)	0.0(7)	C(37)-C(38)-C(39)-N(31)	179.8(5)
N(22)-C(23)-C(28)-C(27)	-178.2(4)	C(33)-C(38)-C(39)-C(40)	-174.2(4)
C(24)-C(23)-C(28)-C(29)	178.6(4)	C(37)-C(38)-C(39)-C(40)	4.6(8)
N(22)-C(23)-C(28)-C(29)	0.4(5)	N(1)-C(2)-C(40)-C(39)	6.3(6)
N(22)-N(21)-C(29)-N(30)	174.8(4)	C(3)-C(2)-C(40)-C(39)	-174.5(4)
Mg-N(21)-C(29)-N(30)	-10.5(6)	N(1)-C(2)-C(40)-C(41)	-175.9(4)
N(22)-N(21)-C(29)-C(28)	-2.3(5)	C(3)-C(2)-C(40)-C(41)	3.4(6)
Mg-N(21)-C(29)-C(28)	172.3(3)	N(31)-C(39)-C(40)-C(2)	-6.2(6)
C(27)-C(28)-C(29)-N(30)	2.1(8)	C(38)-C(39)-C(40)-C(2)	168.3(4)
C(23)-C(28)-C(29)-N(30)	-176.2(4)	N(31)-C(39)-C(40)-C(41)	175.9(4)
C(27)-C(28)-C(29)-N(21)	179.5(4)	C(38)-C(39)-C(40)-C(41)	-9.6(6)
C(23)-C(28)-C(29)-N(21)	1.2(5)	C(2)-C(40)-C(41)-C(46)	-79.7(5)
N(21)-C(29)-N(30)-C(32)	-1.6(7)	C(39)-C(40)-C(41)-C(46)	98.3(5)
C(28)-C(29)-N(30)-C(32)	175.3(4)	C(2)-C(40)-C(41)-C(42)	97.5(5)
C(29)-N(30)-C(32)-N(31)	1.9(7)	C(39)-C(40)-C(41)-C(42)	-84.5(5)
C(29)-N(30)-C(32)-C(33)	-175.1(4)	C(46)-C(41)-C(42)-C(43)	3.2(6)
C(39)-N(31)-C(32)-N(30)	-176.5(4)	C(40)-C(41)-C(42)-C(43)	-174.1(4)
Mg-N(31)-C(32)-N(30)	10.1(6)	C(41)-C(42)-C(43)-C(44)	0.7(6)
C(39)-N(31)-C(32)-C(33)	0.8(5)	C(42)-C(43)-C(44)-O(44)	176.1(4)
Mg-N(31)-C(32)-C(33)	-172.7(3)	C(42)-C(43)-C(44)-C(45)	-4.2(6)
N(30)-C(32)-C(33)-C(34)	-3.4(7)	C(45)-C(44)-O(44)-C(441)	7.9(6)
N(31)-C(32)-C(33)-C(34)	179.1(4)	C(43)-C(44)-O(44)-C(441)	-172.4(4)
N(30)-C(32)-C(33)-C(38)	177.3(4)	O(44)-C(44)-C(45)-C(46)	-176.8(4)
N(31)-C(32)-C(33)-C(38)	-0.1(5)	C(43)-C(44)-C(45)-C(46)	3.6(6)
C(38)-C(33)-C(34)-C(35)	0.7(7)	C(42)-C(41)-C(46)-C(45)	-3.8(6)
C(32)-C(33)-C(34)-C(35)	-178.5(4)	C(40)-C(41)-C(46)-C(45)	173.5(4)
C(33)-C(34)-C(35)-O(35)	176.8(4)	C(44)-C(45)-C(46)-C(41)	0.5(6)
C(33)-C(34)-C(35)-C(36)	-1.7(7)		
C(34)-C(35)-O(35)-C(351)	3.6(7)	Mg-O(9)-C(91)-C(92)	148.6(5)

**Table 6. Hydrogen bonds, in Ångstroms and degrees.**

D-H...A	d(D-H)	d(H...A)	d(D...A)	<(DHA)
O(9)-H(90)...O(71)	1.08(8)	1.50(8)	2.578(4)	173(7)
O(71)-H(71)...O(5)#3	1.05(11)	1.92(11)	2.921(5)	158(9)
O(71)-H(71)...O(6)#3	1.05(11)	2.15(10)	2.863(5)	123(8)
O(72)-H(72)...O(35)#4	1.15(16)	2.19(15)	3.057(5)	129(10)
O(72)-H(72)...O(36)#4	1.15(16)	2.23(16)	3.287(6)	152(11)

Symmetry transformations used to generate equivalent atoms:  
 #3 : 1-x, ½+y, z-½      #4 : 1½-x, 1-y, z-½

## Crystal structure analysis of [Mg {porph-(OMe)<sub>4</sub>C-C<sub>6</sub>H<sub>4</sub>OMe}], OH<sub>2</sub>Et], ca 2H<sub>2</sub>O (161)

*Crystal data:* C<sub>46</sub>H<sub>37</sub>MgN<sub>7</sub>O<sub>6</sub>, ca 2(H<sub>2</sub>O), M = 842.15. Orthorhombic, space group Pbc<sub>a</sub> (no. 61), a = 18.7395(8), b = 16.9239(4), c = 25.4014(7) Å, V = 8055.9(5) Å<sup>3</sup>. Z = 8, D<sub>c</sub> = 1.389 g cm<sup>-3</sup>, F(000) = 3520, T = 100.01(10) K, μ(Cu-Kα) = 9.35 cm<sup>-1</sup>, λ(Cu-Kα) = 1.54184 Å.

The crystal was a dark red plate, ca 0.03 x 0.08 x 0.11 mm; it was mounted in oil on a small loop and fixed in the cold nitrogen stream on a Rigaku Oxford Diffraction XtaLAB Synergy diffractometer, equipped with Cu-Kα radiation, HyPix detector and mirror monochromator. Intensity data were measured by thin-slice ω-scans. Total no. of reflections recorded, to θ<sub>max</sub> = 65°, was 207908 of which 6821 were unique (R<sub>int</sub> = 0.097); 5675 were 'observed' with I > 2σ<sub>I</sub>.

Data were processed using the CrysAlisPro-CCD and -RED (1) programs. The structure was determined by the intrinsic phasing routines in the SHELXT program (2A) and refined by full-matrix least-squares methods, on F<sup>2</sup>'s, in SHELXL (2B). The structure comprises the magnesium complex and approximately two solvent (water) molecules. The non-hydrogen atoms were refined with anisotropic thermal parameters. Hydrogen atoms in the solvent region and located in difference maps were refined freely. The remaining hydrogen atoms were included in idealised positions and their U<sub>iso</sub> values were set to ride on the U<sub>eq</sub> values of the parent carbon atoms. At the conclusion of the refinement, wR<sub>2</sub> = 0.219 and R<sub>1</sub> = 0.094 (2B) for all 6821 reflections weighted  $w = [\sigma^2(F_o^2) + (0.0929 P)^2 + 19.50 P]^{-1}$  with  $P = (F_o^2 + 2F_c^2)/3$ .

In the final difference map, the highest peak (ca 1.1 eÅ<sup>-3</sup>) was near H(91a) of the ethanol ligand.

Scattering factors for neutral atoms were taken from reference (3). Computer programs used in this analysis have been noted above, and were run through WinGX (4) on a Dell Optiplex 780 PC at the University of East Anglia.

## References

1. Programs CrysAlisPro, Rigaku Oxford Diffraction Ltd., Abingdon, UK (2018).
2. G. M. Sheldrick, Programs for crystal structure determination (SHELXT), *Acta Cryst.* (2015) **A71**, 3-8, and refinement (SHELXL), *Acta Cryst.* (2008) **A64**, 112-122 and (2015) **C71**, 3-8.
3. 'International Tables for X-ray Crystallography', Kluwer Academic Publishers, Dordrecht (1992). Vol. C, pp. 500, 219 and 193.
4. L. J. Farrugia, *J. Appl. Cryst.* (2012) **45**, 849–854.

## Legends for Figures

Figure 1. View of a molecule of [Mg {porph-(OMe)<sub>4</sub>,C-C<sub>6</sub>H<sub>4</sub>OMe}], ca 2H<sub>2</sub>O, indicating the atom numbering scheme. Thermal ellipsoids are drawn at the 40% probability level.

Figure 2. A similar view, showing the intermolecular hydrogen bonding.

## Notes on the structure

The magnesium is coordinated at the centre of the porphyrin ligand, and removed 0.495(2) Å from the mean-plane of the four coordinating N atoms; it is also bound to an ethanol molecule, forming a square pyramidal pattern. This is all well-resolved and reliable. Then the hydroxyl group of the EtOH ligand is hydrogen bonded to an oxygen atom (probably) of a solvent/water molecule and that has further hydrogen bonds to a second water molecule which is linked by more hydrogen bonds to two further Mg-porphyrin molecules. There is some uncertainty and/or disorder about all the hydrogen atoms and the hydrogen bonds in this water/solvent region - I am assuming the solvent molecules are water molecules, although there is one site of electron density here that refines best as 'half-a-carbon' atom, C(71).

On the opposite side of the Mg-Porph system, a centrosymmetrically related molecule lies with the C(3-8) and C(33-38) rings of one molecule overlapping the C(33'-39') and C(3'-8') rings of the opposing molecule.

The methoxyphenyl group is linked to the porphyrin ring through the carbon atom C(40) which replaces one of the normal porphyrin bridging N atoms. The phenyl ring is almost perpendicular to the general porphyrin ring plane. H(4) and H(37), which are on adjacent benzo groups, have close H... $\pi$  contacts with this ring; H(4) is 2.49 Å from C(46) and 2.55 Å from C(41), and H(37) is 2.57 Å from C(41). H(45) and H(46) of the phenyl ring are directed towards the underside of the centrosymmetrically related Mg-porph group, with short H... $\pi$  distances of H(45)...Mg' at 3.06 Å, and ...N(21') at 2.82 Å, and H(46)...C(39') at 2.56 Å and ...N(31') at 2.69 Å; we note also the short contact of H(44b)...C(22') at 2.74 Å.

**Crystal data and structure refinement for (C<sub>24</sub>H<sub>26</sub>N<sub>2</sub>O)-N=(C<sub>24</sub>H<sub>27</sub>N<sub>2</sub>O) (174)**

---

<b>Identification code</b>	<b>174 (Figure 2.30)</b>
Elemental formula	C <sub>48</sub> H <sub>53</sub> N <sub>3</sub> O <sub>2</sub>
Formula weight	703.93
Crystal system, space group	Monoclinic, P 2 <sub>1</sub> /c (no. 14)
Unit cell dimensions	a = 19.59378(19) Å    α = 90.0 ° b = 16.33724(13) Å    β = 96.1282(9) ° c = 12.15503(11) Å    γ = 90.0 °
Volume	3868.69(6) Å <sup>3</sup>
Z, Calculated density	4, 1.209 Mg/m <sup>3</sup>
F(000)	1512
Absorption coefficient	0.566 mm <sup>-1</sup>
Temperature	100.01(10) K
Wavelength	1.54184 Å
Crystal colour, shape	orange-red prism
Crystal size	0.20 x 0.17 x 0.09 mm
Crystal mounting:	on a small loop, in oil, fixed in cold N <sub>2</sub> stream
On the diffractometer:	
Theta range for data collection	3.531 to 74.989 °
Limiting indices	-20<=h<=24, -20<=k<=20, -15<=l<=15
Completeness to theta = 67.684	100.0 %
Absorption correction	Semi-empirical from equivalents
Max. and min. transmission	1.00000 and 0.72080
Reflections collected (not including absences)	115389
No. of unique reflections	7950 [R(int) for equivalents = 0.036]
No. of 'observed' reflections (I > 2σ <sub>I</sub> )	7469
Structure determined by:	dual methods, in SHELXT
Refinement:	Full-matrix least-squares on F <sup>2</sup> , in SHELXL
Data / restraints / parameters	7950 / 0 / 488
Goodness-of-fit on F <sup>2</sup>	1.034
Final R indices ('observed' data)	R <sub>1</sub> = 0.052, wR <sub>2</sub> = 0.127
Final R indices (all data)	R <sub>1</sub> = 0.054, wR <sub>2</sub> = 0.128
Reflections weighted:	w = [σ <sup>2</sup> (F <sub>o</sub> <sup>2</sup> ) + (0.0552P) <sup>2</sup> + 3.017P] <sup>-1</sup> where P = (F <sub>o</sub> <sup>2</sup> + 2F <sub>c</sub> <sup>2</sup> ) / 3
Extinction coefficient	n/a
Largest diff. peak and hole	0.86 and -0.68 e.Å <sup>-3</sup>
Location of largest difference peak	near H(92a)

---

Table 1. Atomic coordinates ( $\times 10^5$ ) and equivalent isotropic displacement parameters ( $\text{\AA}^2 \times 10^4$ ).  $U(\text{eq})$  is defined as one third of the trace of the orthogonalized  $U_{ij}$  tensor. E.s.ds are in parentheses.

	x	y	z	U(eq)	S.o.f.#
N(1)	24972 (6)	52980 (8)	55870 (10)	211 (2)	
C(1)	29739 (7)	56667 (9)	49985 (11)	201 (3)	
N(2)	28873 (6)	58481 (7)	39315 (10)	215 (3)	
C(3)	34882 (7)	62496 (9)	36774 (12)	205 (3)	
C(4)	46643 (7)	65030 (9)	48896 (12)	221 (3)	
C(5)	50211 (7)	63738 (9)	59371 (12)	222 (3)	
C(6)	46810 (7)	60160 (9)	67886 (12)	218 (3)	
C(7)	39897 (7)	57882 (9)	65624 (12)	214 (3)	
C(8)	36535 (7)	59091 (8)	55180 (12)	202 (3)	
C(9)	39850 (7)	62642 (8)	46773 (12)	206 (3)	
C(10)	57727 (8)	66488 (10)	61270 (14)	281 (3)	
C(101)	57832 (9)	75792 (11)	63058 (18)	414 (4)	
C(102)	61633 (8)	64466 (12)	51308 (16)	374 (4)	
C(11)	61449 (8)	62078 (13)	71350 (15)	381 (4)	
C(12)	57441 (9)	62404 (13)	81287 (15)	393 (4)	
C(13)	50479 (8)	58043 (10)	79311 (13)	272 (3)	
C(131)	51471 (10)	48712 (11)	79843 (15)	390 (4)	
C(132)	46244 (8)	60673 (11)	88579 (13)	313 (4)	
C(20)	35888 (7)	65630 (9)	26751 (12)	213 (3)	
C(21)	31360 (7)	65610 (8)	16429 (12)	209 (3)	
C(22)	34008 (8)	68013 (10)	6725 (13)	254 (3)	
C(23)	30118 (8)	67794 (10)	-3534 (12)	257 (3)	
C(24)	23347 (8)	65178 (9)	-4190 (12)	224 (3)	
C(25)	20478 (7)	63143 (9)	5476 (12)	234 (3)	
C(26)	24392 (7)	63313 (9)	15575 (12)	222 (3)	
O(27)	19104 (5)	64368 (7)	-13813 (9)	276 (2)	
C(28)	21765 (9)	66750 (11)	-23814 (13)	320 (4)	
C(31)	20427 (7)	48125 (8)	50654 (11)	192 (3)	
N(32)	20228 (6)	45291 (7)	40041 (10)	205 (2)	
C(33)	15079 (7)	39393 (9)	37490 (12)	206 (3)	
C(34)	5375 (7)	35110 (9)	49319 (12)	212 (3)	
C(35)	2618 (7)	36255 (8)	59367 (12)	200 (3)	
C(36)	5883 (7)	41659 (8)	67388 (11)	194 (3)	
C(37)	11931 (7)	45606 (9)	65276 (12)	203 (3)	
C(38)	14571 (7)	44386 (8)	55286 (11)	190 (3)	
C(39)	11292 (7)	39192 (8)	47249 (11)	198 (3)	
C(40)	-3960 (7)	31555 (9)	61112 (13)	249 (3)	
C(401)	-2983 (9)	22424 (11)	59140 (20)	447 (5)	
C(402)	-9841 (10)	34510 (14)	53090 (20)	605 (7)	
C(41)	-5192 (11)	31751 (14)	73565 (18)	285 (7)	0.748 (6)
C(42)	-4120 (11)	39817 (16)	78521 (18)	567 (6)	0.748 (6)
C(91)	-7690 (30)	36120 (40)	69900 (50)	220 (17) *	0.252 (6)
C(92)	-4120 (11)	39817 (16)	78521 (18)	567 (6)	0.252 (6)
C(43)	2997 (7)	43493 (9)	78361 (12)	232 (3)	
C(431)	2299 (12)	52734 (12)	79889 (18)	487 (5)	
C(432)	7890 (10)	40203 (15)	87897 (14)	474 (5)	
C(50)	14180 (8)	34732 (9)	28331 (12)	227 (3)	
C(51)	17898 (7)	35115 (9)	18623 (12)	219 (3)	
C(52)	18712 (8)	27979 (9)	12389 (13)	264 (3)	
C(53)	21959 (8)	28176 (10)	2896 (14)	286 (3)	
C(54)	24454 (8)	35551 (10)	-865 (13)	253 (3)	
C(55)	23892 (8)	42635 (9)	5232 (12)	242 (3)	
C(56)	20568 (8)	42369 (9)	14749 (12)	235 (3)	
O(57)	27104 (6)	35212 (7)	-10829 (10)	353 (3)	
C(58)	29405 (10)	42669 (11)	-15223 (16)	393 (4)	

# - site occupancy, if different from 1.

\* -  $U(\text{iso})$  ( $\text{\AA}^2 \times 10^4$ )

**Table 2. Molecular dimensions. Bond lengths are in Ångstroms, angles in degrees. E.s.ds are in parentheses.**

N(1)-C(1)	1.3747(18)	N(1)-C(31)	1.3051(18)
C(1)-N(2)	1.3235(18)	C(31)-N(32)	1.3672(18)
C(1)-C(8)	1.4660(19)	C(31)-C(38)	1.4645(19)
N(2)-C(3)	1.4106(18)	N(32)-C(33)	1.4055(18)
		N(32)-H(32)	0.89(2)
C(3)-C(20)	1.355(2)	C(33)-C(50)	1.345(2)
C(3)-C(9)	1.474(2)	C(33)-C(39)	1.4652(19)
C(4)-C(9)	1.385(2)	C(34)-C(39)	1.384(2)
C(4)-C(5)	1.402(2)	C(34)-C(35)	1.400(2)
C(5)-C(6)	1.416(2)	C(35)-C(36)	1.416(2)
C(5)-C(10)	1.533(2)	C(35)-C(40)	1.5343(19)
C(6)-C(7)	1.403(2)	C(36)-C(37)	1.397(2)
C(6)-C(13)	1.533(2)	C(36)-C(43)	1.5328(19)
C(7)-C(8)	1.381(2)	C(37)-C(38)	1.3841(19)
C(8)-C(9)	1.394(2)	C(38)-C(39)	1.3976(19)
C(10)-C(101)	1.535(2)	C(40)-C(402)	1.507(2)
C(10)-C(102)	1.536(2)	C(40)-C(401)	1.526(2)
C(10)-C(11)	1.537(2)	C(40)-C(91)	1.548(6)
C(11)-C(12)	1.510(2)	C(40)-C(41)	1.558(3)
C(12)-C(13)	1.535(2)	C(41)-C(42)	1.455(3)
C(13)-C(132)	1.530(2)	C(42)-C(43)	1.520(2)
C(13)-C(131)	1.537(2)	C(91)-C(92)	1.340(6)
C(20)-C(21)	1.457(2)	C(92)-C(43)	1.520(2)
C(21)-C(22)	1.395(2)	C(43)-C(432)	1.521(2)
C(21)-C(26)	1.409(2)	C(43)-C(431)	1.529(2)
C(22)-C(23)	1.391(2)	C(50)-C(51)	1.453(2)
C(23)-C(24)	1.388(2)	C(51)-C(56)	1.397(2)
C(24)-O(27)	1.3673(18)	C(51)-C(52)	1.409(2)
C(24)-C(25)	1.396(2)	C(52)-C(53)	1.376(2)
C(25)-C(26)	1.376(2)	C(53)-C(54)	1.396(2)
O(27)-C(28)	1.4270(18)	C(54)-O(57)	1.3688(18)
		C(54)-C(55)	1.385(2)
		C(55)-C(56)	1.387(2)
		O(57)-C(58)	1.423(2)
C(31)-N(1)-C(1)	118.67(12)	C(34)-C(35)-C(40)	117.51(13)
N(2)-C(1)-N(1)	125.79(13)	C(36)-C(35)-C(40)	122.77(13)
N(2)-C(1)-C(8)	112.16(12)	C(37)-C(36)-C(35)	119.41(13)
N(1)-C(1)-C(8)	122.05(12)	C(37)-C(36)-C(43)	117.96(12)
C(1)-N(2)-C(3)	107.22(12)	C(35)-C(36)-C(43)	122.63(12)
C(20)-C(3)-N(2)	125.28(13)	C(38)-C(37)-C(36)	119.91(13)
C(20)-C(3)-C(9)	126.05(13)	C(37)-C(38)-C(39)	120.91(13)
N(2)-C(3)-C(9)	108.67(12)	C(37)-C(38)-C(31)	131.20(13)
C(9)-C(4)-C(5)	120.21(13)	C(39)-C(38)-C(31)	107.77(12)
C(4)-C(5)-C(6)	119.89(13)	C(34)-C(39)-C(38)	119.81(13)
C(4)-C(5)-C(10)	118.06(13)	C(5)-C(10)-C(101)	108.04(13)
C(6)-C(5)-C(10)	122.03(13)	C(5)-C(10)-C(102)	111.69(13)
C(7)-C(6)-C(5)	119.08(13)	C(101)-C(10)-C(102)	108.92(15)
C(7)-C(6)-C(13)	117.84(13)	C(5)-C(10)-C(11)	110.43(13)
C(5)-C(6)-C(13)	122.92(13)	C(101)-C(10)-C(11)	110.69(15)
C(8)-C(7)-C(6)	119.87(13)	C(102)-C(10)-C(11)	107.08(14)
C(7)-C(8)-C(9)	121.30(13)	C(12)-C(11)-C(10)	112.21(14)
C(7)-C(8)-C(1)	132.82(13)	C(11)-C(12)-C(13)	112.81(15)
C(9)-C(8)-C(1)	105.63(12)	C(132)-C(13)-C(6)	111.39(13)
C(4)-C(9)-C(8)	119.63(13)	C(132)-C(13)-C(12)	107.28(14)
C(4)-C(9)-C(3)	134.04(13)	C(6)-C(13)-C(12)	111.09(13)
C(8)-C(9)-C(3)	106.22(12)	C(132)-C(13)-C(131)	108.88(14)
		C(6)-C(13)-C(131)	107.87(13)
N(1)-C(31)-N(32)	127.84(13)	C(12)-C(13)-C(131)	110.33(15)
N(1)-C(31)-C(38)	126.06(13)	C(3)-C(20)-C(21)	129.76(13)
N(32)-C(31)-C(38)	106.07(12)	C(22)-C(21)-C(26)	117.24(13)
C(31)-N(32)-C(33)	112.83(12)	C(22)-C(21)-C(20)	118.70(13)
C(31)-N(32)-H(32)	120.0(12)	C(26)-C(21)-C(20)	124.06(13)
C(33)-N(32)-H(32)	127.2(12)	C(23)-C(22)-C(21)	122.23(14)
C(50)-C(33)-N(32)	126.75(13)	C(24)-C(23)-C(22)	119.24(13)
C(50)-C(33)-C(39)	128.66(13)	O(27)-C(24)-C(23)	124.70(13)
N(32)-C(33)-C(39)	104.50(12)	O(27)-C(24)-C(25)	115.74(13)
C(39)-C(34)-C(35)	120.21(13)	C(23)-C(24)-C(25)	119.56(14)
C(34)-C(35)-C(36)	119.72(13)	C(26)-C(25)-C(24)	120.65(13)

C(25)-C(26)-C(21)	120.95(13)	C(92)-C(43)-C(431)	107.13(16)
C(24)-O(27)-C(28)	117.27(12)	C(42)-C(43)-C(431)	107.13(16)
C(38)-C(39)-C(33)	108.52(12)	C(432)-C(43)-C(431)	108.27(16)
C(34)-C(39)-C(33)	131.65(13)	C(92)-C(43)-C(36)	110.98(13)
C(402)-C(40)-C(401)	108.15(16)	C(42)-C(43)-C(36)	110.98(13)
C(402)-C(40)-C(35)	110.23(13)	C(432)-C(43)-C(36)	109.44(13)
C(401)-C(40)-C(35)	110.25(13)	C(431)-C(43)-C(36)	110.17(13)
C(402)-C(40)-C(91)	84.7(3)	C(33)-C(50)-C(51)	127.97(13)
C(401)-C(40)-C(91)	131.0(3)	C(56)-C(51)-C(52)	116.92(14)
C(35)-C(40)-C(91)	108.6(2)	C(56)-C(51)-C(50)	123.26(13)
C(402)-C(40)-C(41)	115.76(17)	C(52)-C(51)-C(50)	119.77(13)
C(401)-C(40)-C(41)	102.00(15)	C(53)-C(52)-C(51)	121.37(14)
C(35)-C(40)-C(41)	110.09(13)	C(52)-C(53)-C(54)	120.29(14)
C(42)-C(41)-C(40)	112.97(17)	O(57)-C(54)-C(55)	124.52(14)
C(41)-C(42)-C(43)	116.41(18)	O(57)-C(54)-C(53)	115.73(14)
C(92)-C(91)-C(40)	120.7(4)	C(55)-C(54)-C(53)	119.70(14)
C(91)-C(92)-C(43)	124.8(3)	C(54)-C(55)-C(56)	119.43(14)
C(92)-C(43)-C(432)	110.79(17)	C(55)-C(56)-C(51)	122.24(14)
C(42)-C(43)-C(432)	110.79(17)	C(54)-O(57)-C(58)	117.57(13)

**Table 3. Anisotropic displacement parameters ( $\text{\AA}^2 \times 10^4$ ) for the expression:  $\exp \{-2\pi^2(h^2a^*U_{11} + \dots + 2hka^*b^*U_{12})\}$  E.s.ds are in parentheses.**

	U <sub>11</sub>	U <sub>22</sub>	U <sub>33</sub>	U <sub>23</sub>	U <sub>13</sub>	U <sub>12</sub>
N(1)	181(6)	247(6)	206(6)	-7(5)	30(4)	-45(5)
C(1)	186(7)	209(7)	212(7)	-21(5)	40(5)	-17(5)
N(2)	201(6)	232(6)	215(6)	-1(5)	40(5)	-39(5)
C(3)	179(7)	201(7)	241(7)	-19(5)	44(5)	-15(5)
C(4)	203(7)	198(7)	269(7)	7(5)	60(6)	-18(5)
C(5)	174(7)	203(7)	290(7)	-9(6)	32(6)	-4(5)
C(6)	202(7)	209(7)	243(7)	-18(5)	22(5)	5(5)
C(7)	206(7)	216(7)	225(7)	-7(5)	47(5)	-16(5)
C(8)	186(7)	190(6)	235(7)	-27(5)	44(5)	-23(5)
C(9)	196(7)	188(6)	237(7)	-9(5)	39(5)	-3(5)
C(10)	171(7)	316(8)	351(8)	31(7)	12(6)	-30(6)
C(101)	276(9)	348(9)	605(12)	-33(8)	-18(8)	-105(7)
C(102)	188(8)	494(11)	449(10)	59(8)	76(7)	-6(7)
C(11)	177(7)	558(11)	399(10)	82(8)	-7(7)	-8(7)
C(12)	229(8)	606(12)	326(9)	48(8)	-52(7)	-51(8)
C(13)	213(7)	338(8)	262(7)	19(6)	5(6)	11(6)
C(131)	416(10)	385(10)	371(9)	106(8)	52(8)	140(8)
C(132)	278(8)	407(9)	248(8)	-26(7)	3(6)	-28(7)
C(20)	180(7)	201(7)	266(7)	2(5)	53(5)	-14(5)
C(21)	209(7)	185(6)	240(7)	13(5)	51(5)	4(5)
C(22)	195(7)	294(8)	279(8)	47(6)	58(6)	-26(6)
C(23)	245(7)	294(8)	244(7)	58(6)	81(6)	7(6)
C(24)	224(7)	207(7)	240(7)	19(5)	26(6)	35(5)
C(25)	178(7)	241(7)	287(7)	28(6)	50(6)	-1(5)
C(26)	216(7)	213(7)	246(7)	25(5)	67(5)	9(5)
O(27)	246(5)	356(6)	225(5)	45(4)	22(4)	-7(4)
C(28)	318(8)	413(9)	232(7)	50(7)	41(6)	6(7)
C(31)	182(6)	206(7)	188(6)	10(5)	19(5)	-1(5)
N(32)	188(6)	231(6)	199(6)	-15(5)	36(5)	-44(5)
C(33)	188(7)	201(7)	229(7)	14(5)	20(5)	-17(5)
C(34)	201(7)	192(6)	241(7)	-8(5)	5(5)	-26(5)
C(35)	163(6)	183(6)	255(7)	26(5)	22(5)	5(5)
C(36)	183(6)	184(6)	215(7)	33(5)	23(5)	22(5)
C(37)	195(7)	199(6)	210(7)	7(5)	6(5)	-8(5)
C(38)	173(6)	183(6)	213(7)	21(5)	12(5)	-4(5)
C(39)	191(7)	192(6)	212(7)	11(5)	20(5)	-1(5)
C(40)	185(7)	263(7)	303(8)	-17(6)	48(6)	-50(6)
C(401)	276(9)	271(9)	796(14)	126(9)	69(9)	-64(7)
C(402)	221(9)	538(13)	1009(19)	418(13)	-155(10)	-105(8)
C(41)	255(11)	316(12)	299(11)	7(9)	93(8)	-71(9)
C(42)	474(12)	806(16)	470(11)	-248(11)	272(10)	-359(11)
C(92)	474(12)	806(16)	470(11)	-248(11)	272(10)	-359(11)
C(43)	206(7)	259(7)	239(7)	-6(6)	57(6)	-15(6)
C(431)	672(14)	327(9)	526(12)	-7(8)	352(11)	102(9)
C(432)	426(11)	776(15)	222(8)	32(9)	38(7)	161(10)

C(50)	216(7)	211(7)	253(7)	-3(5)	10(6)	-37(5)
C(51)	182(7)	234(7)	236(7)	-24(5)	-6(5)	-19(5)
C(52)	255(7)	228(7)	316(8)	-36(6)	58(6)	-42(6)
C(53)	286(8)	242(7)	345(8)	-71(6)	97(6)	-9(6)
C(54)	204(7)	292(8)	270(7)	-6(6)	63(6)	23(6)
C(55)	221(7)	240(7)	263(7)	17(6)	18(6)	-3(6)
C(56)	252(7)	219(7)	229(7)	-19(6)	3(6)	6(6)
O(57)	409(7)	325(6)	365(6)	-15(5)	217(5)	15(5)
C(58)	444(10)	367(9)	400(10)	64(8)	200(8)	26(8)

**Table 4. Hydrogen coordinates ( $\times 10^4$ ) and isotropic displacement parameters ( $\text{\AA}^2 \times 10^3$ ). The amino hydrogen atom, H(32), was located in a difference map and was refined freely and isotropically. All remaining hydrogen atoms were included in idealised positions with U(iso)'s set at  $1.2 \times U(\text{eq})$  or, for the methyl group hydrogen atoms  $1.5 \times U(\text{eq})$  of the parent carbon atoms.**

	x	y	z	U(iso)	S.o.f.#
H(4)	4885	6750	4335	27	
H(7)	3759	5556	7115	26	
H(10A)	6250	7765	6427	62	
H(10B)	5556	7844	5663	62	
H(10C)	5550	7710	6939	62	
H(10D)	6631	6627	5277	56	
H(10E)	6154	5866	5007	56	
H(10F)	5949	6721	4485	56	
H(11A)	6219	5640	6945	46	
H(11B)	6591	6459	7323	46	
H(12A)	5669	6808	8316	47	
H(12B)	6014	5988	8754	47	
H(13A)	5412	4700	7405	58	
H(13B)	5384	4724	8689	58	
H(13C)	4707	4607	7892	58	
H(13D)	4866	5927	9561	47	
H(13E)	4552	6648	8822	47	
H(13F)	4189	5792	8772	47	
H(20)	4011	6818	2641	26	
H(22)	3853	6982	713	30	
H(23)	3203	6938	-988	31	
H(25)	1588	6166	509	28	
H(26)	2241	6189	2193	27	
H(28A)	1833	6590	-2995	48	
H(28B)	2301	7243	-2340	48	
H(28C)	2574	6352	-2481	48	
H(34)	322	3159	4402	25	
H(37)	1418	4905	7057	24	
H(40A)	-271	2147	5140	67	
H(40B)	-680	1945	6147	67	
H(40C)	118	2061	6330	67	
H(40D)	-1054	4025	5420	91	
H(40E)	-879	3359	4565	91	
H(40F)	-1393	3157	5431	91	
H(41A)	-986	3001	7427	34	0.748(6)
H(41B)	-211	2789	7760	34	0.748(6)
H(42A)	-512	3950	8616	68	0.748(6)
H(42B)	-742	4355	7471	68	0.748(6)
H(91A)	-1058	4026	6603	26	0.252(6)
H(91B)	-1073	3221	7288	26	0.252(6)
H(92A)	-375	3586	8451	68	0.252(6)
H(92B)	-702	4420	8074	68	0.252(6)
H(43A)	671	5527	7983	73	
H(43B)	-81	5492	7397	73	
H(43C)	55	5381	8683	73	
H(43D)	1235	4260	8765	71	
H(43E)	619	4158	9479	71	
H(43F)	822	3436	8728	71	
H(50)	1076	3078	2820	27	
H(52)	1702	2303	1474	32	
H(53)	2249	2337	-103	34	

H(55)	2573	4753	297	29
H(56)	2010	4718	1868	28
H(58A)	3113	4162	-2218	59
H(58B)	2565	4645	-1630	59
H(58C)	3299	4497	-1015	59
H(32)	2327(10)	4708(12)	3566(16)	30(5)

# - site occupancy, if different from 1.

**Table 5. Torsion angles, in degrees. E.s.ds are in parentheses.**

C(31)-N(1)-C(1)-N(2)	27.7(2)	C(24)-C(25)-C(26)-C(21)	0.6(2)
C(31)-N(1)-C(1)-C(8)	-152.57(14)	C(22)-C(21)-C(26)-C(25)	2.6(2)
N(1)-C(1)-N(2)-C(3)	177.51(13)	C(20)-C(21)-C(26)-C(25)	-177.51(14)
C(8)-C(1)-N(2)-C(3)	-2.24(16)	C(23)-C(24)-O(27)-C(28)	-3.0(2)
C(1)-N(2)-C(3)-C(20)	-177.16(14)	C(25)-C(24)-O(27)-C(28)	177.22(13)
C(1)-N(2)-C(3)-C(9)	3.26(16)	C(1)-N(1)-C(31)-N(32)	9.0(2)
C(9)-C(4)-C(5)-C(6)	-1.5(2)	C(1)-N(1)-C(31)-C(38)	-173.16(13)
C(9)-C(4)-C(5)-C(10)	179.92(13)	N(1)-C(31)-N(32)-C(33)	172.84(14)
C(4)-C(5)-C(6)-C(7)	0.7(2)	C(38)-C(31)-N(32)-C(33)	-5.30(16)
C(10)-C(5)-C(6)-C(7)	179.15(13)	C(31)-N(32)-C(33)-C(50)	-170.70(14)
C(4)-C(5)-C(6)-C(13)	175.90(14)	C(31)-N(32)-C(33)-C(39)	5.98(16)
C(10)-C(5)-C(6)-C(13)	-5.6(2)	C(39)-C(34)-C(35)-C(36)	0.5(2)
C(5)-C(6)-C(7)-C(8)	0.5(2)	C(39)-C(34)-C(35)-C(40)	179.88(13)
C(13)-C(6)-C(7)-C(8)	-175.02(13)	C(34)-C(35)-C(36)-C(37)	-1.8(2)
C(6)-C(7)-C(8)-C(9)	-0.7(2)	C(40)-C(35)-C(36)-C(37)	178.84(13)
C(6)-C(7)-C(8)-C(1)	172.69(15)	C(34)-C(35)-C(36)-C(43)	177.36(13)
N(2)-C(1)-C(8)-C(7)	-173.87(15)	C(40)-C(35)-C(36)-C(43)	-2.0(2)
N(1)-C(1)-C(8)-C(7)	6.4(2)	C(35)-C(36)-C(37)-C(38)	1.8(2)
N(2)-C(1)-C(8)-C(9)	0.30(16)	C(43)-C(36)-C(37)-C(38)	-177.41(12)
N(1)-C(1)-C(8)-C(9)	-179.46(13)	C(36)-C(37)-C(38)-C(39)	-0.4(2)
C(5)-C(4)-C(9)-C(8)	1.3(2)	C(36)-C(37)-C(38)-C(31)	175.00(14)
C(5)-C(4)-C(9)-C(3)	-174.47(15)	N(1)-C(31)-C(38)-C(37)	8.2(2)
C(7)-C(8)-C(9)-C(4)	-0.1(2)	N(32)-C(31)-C(38)-C(37)	-173.56(14)
C(1)-C(8)-C(9)-C(4)	-175.13(13)	N(1)-C(31)-C(38)-C(39)	-175.85(14)
C(7)-C(8)-C(9)-C(3)	176.68(13)	N(32)-C(31)-C(38)-C(39)	2.33(15)
C(1)-C(8)-C(9)-C(3)	1.68(15)	C(35)-C(34)-C(39)-C(38)	0.9(2)
C(20)-C(3)-C(9)-C(4)	-6.5(3)	C(35)-C(34)-C(39)-C(33)	-177.27(14)
N(2)-C(3)-C(9)-C(4)	173.07(15)	C(37)-C(38)-C(39)-C(34)	-0.9(2)
C(20)-C(3)-C(9)-C(8)	177.35(14)	C(31)-C(38)-C(39)-C(34)	-177.29(13)
N(2)-C(3)-C(9)-C(8)	-3.07(16)	C(37)-C(38)-C(39)-C(33)	177.65(12)
C(4)-C(5)-C(10)-C(101)	78.43(18)	C(31)-C(38)-C(39)-C(33)	1.24(15)
C(6)-C(5)-C(10)-C(101)	-100.09(17)	C(50)-C(33)-C(39)-C(34)	-9.3(3)
C(4)-C(5)-C(10)-C(102)	-41.35(19)	N(32)-C(33)-C(39)-C(34)	174.08(15)
C(6)-C(5)-C(10)-C(102)	140.13(15)	C(50)-C(33)-C(39)-C(38)	172.37(15)
C(4)-C(5)-C(10)-C(11)	-160.38(14)	N(32)-C(33)-C(39)-C(38)	-4.23(15)
C(6)-C(5)-C(10)-C(11)	21.1(2)	C(34)-C(35)-C(40)-C(402)	-65.8(2)
C(5)-C(10)-C(11)-C(12)	-48.6(2)	C(36)-C(35)-C(40)-C(402)	113.64(19)
C(101)-C(10)-C(11)-C(12)	71.03(19)	C(34)-C(35)-C(40)-C(401)	53.56(19)
C(102)-C(10)-C(11)-C(12)	-170.37(15)	C(36)-C(35)-C(40)-C(401)	-127.03(16)
C(10)-C(11)-C(12)-C(13)	62.7(2)	C(34)-C(35)-C(40)-C(91)	-156.9(3)
C(7)-C(6)-C(13)-C(132)	-49.08(19)	C(36)-C(35)-C(40)-C(91)	22.5(3)
C(5)-C(6)-C(13)-C(132)	135.62(15)	C(34)-C(35)-C(40)-C(41)	165.33(15)
C(7)-C(6)-C(13)-C(12)	-168.61(14)	C(36)-C(35)-C(40)-C(41)	-15.3(2)
C(5)-C(6)-C(13)-C(12)	16.1(2)	C(402)-C(40)-C(41)-C(42)	-81.3(2)
C(7)-C(6)-C(13)-C(131)	70.35(17)	C(401)-C(40)-C(41)-C(42)	161.55(18)
C(5)-C(6)-C(13)-C(131)	-104.95(17)	C(35)-C(40)-C(41)-C(42)	44.5(2)
C(11)-C(12)-C(13)-C(132)	-165.62(15)	C(40)-C(41)-C(42)-C(43)	-59.8(3)
C(11)-C(12)-C(13)-C(6)	-43.7(2)	C(402)-C(40)-C(91)-C(92)	-145.9(5)
C(11)-C(12)-C(13)-C(131)	75.92(19)	C(401)-C(40)-C(91)-C(92)	104.7(5)
N(2)-C(3)-C(20)-C(21)	-1.0(2)	C(35)-C(40)-C(91)-C(92)	-36.3(6)
C(9)-C(3)-C(20)-C(21)	178.55(14)	C(40)-C(91)-C(92)-C(43)	30.0(7)
C(3)-C(20)-C(21)-C(22)	-169.23(15)	C(91)-C(92)-C(43)-C(432)	-127.6(4)
C(3)-C(20)-C(21)-C(26)	10.9(2)	C(91)-C(92)-C(43)-C(431)	114.5(4)
C(26)-C(21)-C(22)-C(23)	-3.2(2)	C(91)-C(92)-C(43)-C(36)	-5.8(5)
C(20)-C(21)-C(22)-C(23)	176.88(14)	C(41)-C(42)-C(43)-C(432)	-82.4(2)
C(21)-C(22)-C(23)-C(24)	0.6(2)	C(41)-C(42)-C(43)-C(431)	159.7(2)
C(22)-C(23)-C(24)-O(27)	-177.12(14)	C(41)-C(42)-C(43)-C(36)	39.4(3)
C(22)-C(23)-C(24)-C(25)	2.6(2)	C(37)-C(36)-C(43)-C(92)	170.83(16)
O(27)-C(24)-C(25)-C(26)	176.53(13)	C(35)-C(36)-C(43)-C(92)	-8.3(2)
C(23)-C(24)-C(25)-C(26)	-3.3(2)	C(37)-C(36)-C(43)-C(42)	170.83(16)

C(35)-C(36)-C(43)-C(42)	-8.3(2)
C(37)-C(36)-C(43)-C(432)	-66.59(18)
C(35)-C(36)-C(43)-C(432)	114.27(17)
C(37)-C(36)-C(43)-C(431)	52.34(19)
C(35)-C(36)-C(43)-C(431)	-126.80(16)
N(32)-C(33)-C(50)-C(51)	-5.4(3)
C(39)-C(33)-C(50)-C(51)	178.71(14)
C(33)-C(50)-C(51)-C(56)	-31.9(2)
C(33)-C(50)-C(51)-C(52)	150.59(16)
C(56)-C(51)-C(52)-C(53)	-0.3(2)
C(50)-C(51)-C(52)-C(53)	177.33(14)
C(51)-C(52)-C(53)-C(54)	-0.9(2)
C(52)-C(53)-C(54)-O(57)	-174.98(14)
C(52)-C(53)-C(54)-C(55)	2.5(2)
O(57)-C(54)-C(55)-C(56)	174.34(14)
C(53)-C(54)-C(55)-C(56)	-2.9(2)
C(54)-C(55)-C(56)-C(51)	1.8(2)
C(52)-C(51)-C(56)-C(55)	-0.1(2)
C(50)-C(51)-C(56)-C(55)	-177.68(14)
C(55)-C(54)-O(57)-C(58)	-0.3(2)
C(53)-C(54)-O(57)-C(58)	177.08(15)

---

**Table 6. Hydrogen bond, in Ångstroms and degrees.**

D-H...A	d(D-H)	d(H...A)	d(D...A)	<(DHA)
N(32)-H(32)...N(2)	0.89(2)	2.183(19)	2.7482(17)	120.8(15)

**Crystal structure analysis of (C<sub>24</sub>H<sub>26</sub>N<sub>2</sub>O)-N=(C<sub>24</sub>H<sub>27</sub>N<sub>2</sub>O) (174)**

*Crystal data:* C<sub>48</sub>H<sub>53</sub>N<sub>3</sub>O<sub>2</sub>, M = 703.93. Monoclinic, space group P2<sub>1</sub>/c (no. 14), a = 19.59378(19), b = 16.33724(13), c = 12.15503(11) Å, β = 96.1282(9) °, V = 3868.69(6) Å<sup>3</sup>. Z = 4, D<sub>c</sub> = 1.209 g cm<sup>-3</sup>, F(000) = 1512, T = 100.01(10) K, μ(Cu-Kα) = 5.66 cm<sup>-1</sup>, λ(Cu-Kα) = 1.54184 Å.

The crystal was an orange-red prism, *ca* 0.20 x 0.17 x 0.09 mm, and was mounted, in oil, on a small loop and fixed in the cold nitrogen stream on a Rigaku Oxford Diffraction XtaLAB Synergy diffractometer, equipped with Cu-Kα radiation, HyPix detector and mirror monochromator. Intensity data were measured by thin-slice ω-scans. Total no. of reflections recorded, to θ<sub>max</sub> = 75.0°, was 115389 of which 7950 were unique (R<sub>int</sub> = 0.036); 7469 were 'observed' with I > 2σ<sub>I</sub>.

Data were processed using the CrysAlisPro-CCD and -RED (1) programs. The structure was determined by the intrinsic phasing routines in the SHELXT program (2A) and refined by full-matrix least-squares methods, on F<sup>2</sup>'s, in SHELXL (2B). The non-hydrogen atoms (except for C(91) in a disordered group) were refined with anisotropic thermal parameters. The hydrogen atom on N(22) was located in a difference map and was refined isotropically and freely. The remaining hydrogen atoms were included in idealised positions and their U<sub>iso</sub> values were set to ride on the U<sub>eq</sub> values of the parent carbon atoms. At the conclusion of the refinement, wR<sub>2</sub> = 0.128 and R<sub>1</sub> = 0.054 (2B) for all 7950 reflections weighted w = [σ<sup>2</sup>(F<sub>o</sub><sup>2</sup>) + (0.0552 P)<sup>2</sup> + 3.017 P]<sup>-1</sup> with P = (F<sub>o</sub><sup>2</sup> + 2F<sub>c</sub><sup>2</sup>)/3.

In the final difference map, the highest peak (*ca* 0.85 eÅ<sup>-3</sup>) was near H(92a) in the disordered region.

Scattering factors for neutral atoms were taken from reference (3). Computer programs used in this analysis have been noted above, and were run through WinGX (4) on a Dell Optiplex 780 PC at the University of East Anglia.

**References**

1. Programs CrysAlisPro, Rigaku Oxford Diffraction Ltd., Abingdon, UK (2018).
2. G. M. Sheldrick, Programs for crystal structure determination (SHELXT), *Acta Cryst.* (2015) **A71**, 3-8, and refinement (SHELXL), *Acta Cryst.* (2008) **A64**, 112-122 and (2015) **C71**, 3-8.
3. *International Tables for X-ray Crystallography*, Kluwer Academic Publishers, Dordrecht (1992). Vol. C, pp. 500, 219 and 193.
4. L. J. Farrugia, *J. Appl. Cryst.* (2012) **45**, 849–854.

**Legends for Figures**

Figure 1. View of a molecule of  $(C_{24}H_{26}N_2O)-N=(C_{24}H_{27}N_2O)$  indicating the atom numbering scheme. Thermal ellipsoids are drawn at the 50% probability level.

Figure 2. Other views of the molecule.

### Notes on the structure

Above the line of C(50)...C(20) in Figure 1, there is pseudo-twofold symmetry in the molecule about the vertical line through N(1). Below the C(20)...C(50) line, there is considerable diversion from this symmetry; in particular, we note that whereas the torsion angle for C(3)-C(20)-C(21)-C(26) is  $10.9^\circ$ , the angle C(33)-C(50)-C(51)-C(56) is  $-31.9^\circ$ . [In BUDUR5, the pseudosymmetry is extended further through the molecule and the corresponding angles are  $27.2$  and  $29.7^\circ$ ].

The hydrogen atom H(32) of the hydrogen bond was located clearly in a difference map and was refined freely, isotropically and satisfactorily. The bond distances and angles in the chain between N(2) and N(32) are in agreement with the arrangement of single- and double-bonds of the formula, with double-bond distances of  $1.3235(18)$  and  $1.3051(18)$  for C(1)-N(2) and N(1)-C(31) respectively.

In this crystal, there is no  $\pi$ -stacking of aromatic rings; most of the shorter intermolecular contacts are of the C-H... $\pi$  type.